THERMODYNAMIC STUDIES OF DISORDER IN INORGANIC CRYSTALLINE SOLIDS

A thesis submitted for the degree of

Doctor of Philosophy

M. Jowess, M.A.

New College, Oxford

Michaelmas Term, 1978

Acknowledgment

The work described in this thesis was performed in the Inorganic Chemistry Laboratory under the supervision of Dr L.A.K. Staveley. I should like to thank Dr Staveley for his advice, help, and encouragement.

SYMBOLS, ETC. IN THIS THESIS

With a few exceptions, symbols, signs, units and their abbreviations, and conventions follow Symbols, Signs, and Abbreviations Recommended for British Scientific Publications, Royal Society, London (1969). Values for physical constants and conversion factors were taken from the same source. The following additional comments may be helpful:-

Temperatures expressed in K are absolute temperatures T. Temperatures expressed in °C (° for short) are Celsius temperatures t given approximately by the equation $t/^{\circ}C = T/K - 273$.

For T_F, T_A, T_{MID}, ΔT, and $\bar{C}$ in relation to calorimetry, see pages 15 to 16 and 78.

S is used both for entropy and for the spin angular momentum quantum number of atoms or ions. The sign $\rightarrow$ above a symbol indicates that the quantity is a vector quantity, and $\hat{}$ indicates the quantum-mechanical operator. Thus $\hat{\vec{S}}$ is the quantum-mechanical operator for spin angular momentum.

The subscript m (e.g. H_m, S_m, and $C_{p,m}$) indicates that the quantity is a molar quantity. Specific quantities (quantities per unit mass) are indicated by the use of the lower case, e.g. c_p.

L is used for the Avogadro constant, R for the gas constant, and k for the Boltzmann constant ($R = Lk$).

Energies on a molecular scale are frequently expressed in K k (i.e. approximately 1.381×10^{-23} J).

J is used both for the exchange integral and for the joule.

mmHg and cmHg (equal approximately tc $13.60 \times 981 \times 10^{-2}$ Nm^{-2} and $13.60 \times 981 \times 10^{-1}$ Nm^{-2} respectively) are frequently used for pressures.

Å is used for 10^{-10} m.

Oe is used for $10^{3} (4\pi)^{-1}$ A m^{-1}.*

---

*This conversion factor is not given in the above reference - instead see C.A. Coulson, Electricity, corrected reprint of fifth edition, at pages 244 and 246, Oliver and Boyd, Edinburgh and London (1965).

TABLE OF CONTENTS

CHAPTER 1: INTRODUCTION

Section 1-1: subject of the present work

Changes of entropy accompanying changes of temperature at constant pressure can be calculated from the heat capacity at constant pressure over the temperature range concerned. Thus the molar entropy change ΔS_m as a substance is heated from thermodynamic temperature T_1 to thermodynamic temperature T_2 at constant pressure is given by the equation

$$\Delta S_m = \int_{T_1}^{T_2} (C_{p,m}/T)\, dT \qquad \text{eq. 1-1}$$

in which $C_{p,m}$ is the molar heat capacity at constant pressure. Entropy is well known to be a measure of the "disorder" of a system. The measurement of heat capacities at constant pressure is an important method of studying disorder, and is the principal subject of the work described in this thesis.

The major part of the experimental work consisted of the design and construction, and the subsequent use, of a low-temperature calorimeter for the measurement of the heat capacities of solids at constant pressure. The operating range of the calorimeter was from about 1.5 K to about 84 K. Measurements of molar heat capacity at constant pressure were made at temperatures within this range for each of three crystalline solids. These three solids were bis(adiponitrile)copper(I) nitrate (Chapter 3); tetramethylammonium trichloromanganate(II), also known as tetramethylammonium manganese chloride or TMMC (Chapter 4); and metal-free phthalocyanine (Chapter 5). In each case, more-or-less

complementary investigations were carried out in other calorimeters in this laboratory, either by the author or by other workers. These complementary investigations included measurements of $C_{p,m}$ to higher temperatures than 84 K (in the cases of bis(adiponitrile)copper(I) nitrate and TMNC) and measurements of $C_{p,m}$ on related compounds (in the case of metal-free phthalocyanine). Both the results obtained in the new calorimeter and those obtained in the other calorimeters will be discussed in the respective later chapters.

The purpose of these heat capacity measurements was to study disorder in the various crystalline solids, as revealed by heat capacity "anomalies". (In studies of a different type, heat capacity measurements have been used to investigate disorder through the calculation of "residual entropies" in those solids which do not tend towards complete order as they are cooled towards 0 K; but residual entropies are not the concern of the present work.) Therefore, in Sections 1-2 and 1-3 the nature and cause of heat capacity anomalies in crystalline solids will be discussed in general terms. Detailed discussion of the particular solids experimentally studied will be deferred until the respective later chapters.

Section 1-2: vibrational and anomalous contributions to heat capacities of crystalline solids

A valuable theoretical approach to the heat capacity of simple solids (e.g. KCl) is to identify the molar heat capacity with the excitation of 3zL simple harmonic oscillators each having a fixed frequency corresponding to a normal vibrational mode of the system (zL being the number of particles per mole, e.g. z = 2 for KCl). Following Einstein's well-known treatment of the simple harmonic oscillator, the molar heat capacity is calculated as the sum of 3zL contributions each of which rises, from 0 at 0 K, monotonically with

T towards an asymptotically-approached limit of k at high T. It follows that, regardless of what the frequencies of the normal modes actually are, the molar heat-capacity will rise, from 0 at 0 K, monotonically with T towards an asymptotically-approached limit of 3zR at high T. One plot of this type is shown (dashed lines) in Figure 1-1(i).

This approach is strictly valid for $C_{p,m}$ (the heat capacity which is most conveniently measured) only if the coefficient of thermal expansion is zero. Coefficients of thermal expansion tend towards 0 as T tends towards 0, and therefore the approach is especially useful at low temperatures. For many simple solids such as KCl, $C_{p,m}$ at high temperatures exceeds 3zR; but $C_{p,m}$ is still observed to approach 0 as T approaches 0, and to rise monotonically with T - see the continuous line in Figure 1-1(i) for one plot of this type.

The particularly simple plots of Figure 1-1(i) are in fact what would be expected with a rather simple distribution of normal mode frequencies (this distribution being commonly referred to as the "frequency spectrum" in view of the large number of modes). Such a simple distribution is assumed, for example, in the Debye model according to which the 3zL modes correspond to the 3zL lowest-frequency modes of a continuous isotropic elastic medium; this model gives

$$C_{V,m} = 3zRf(T/\Theta_D) \qquad \text{eq. 1-2}$$

where Θ_D is the "Debye temperature" characteristic of the particular solid and f is a universal function for all solids.

A more complex plot is shown in Figure 1-1(ii). The heat capacity rises monotonically (i.e. there is no maximum) but there are additional points of inflexion in the plot. Such plots are not necessarily inconsistent with a purely vibrational origin for the heat capacity, for they may reflect merely a more complex frequency spectrum

FIGURE 1-1

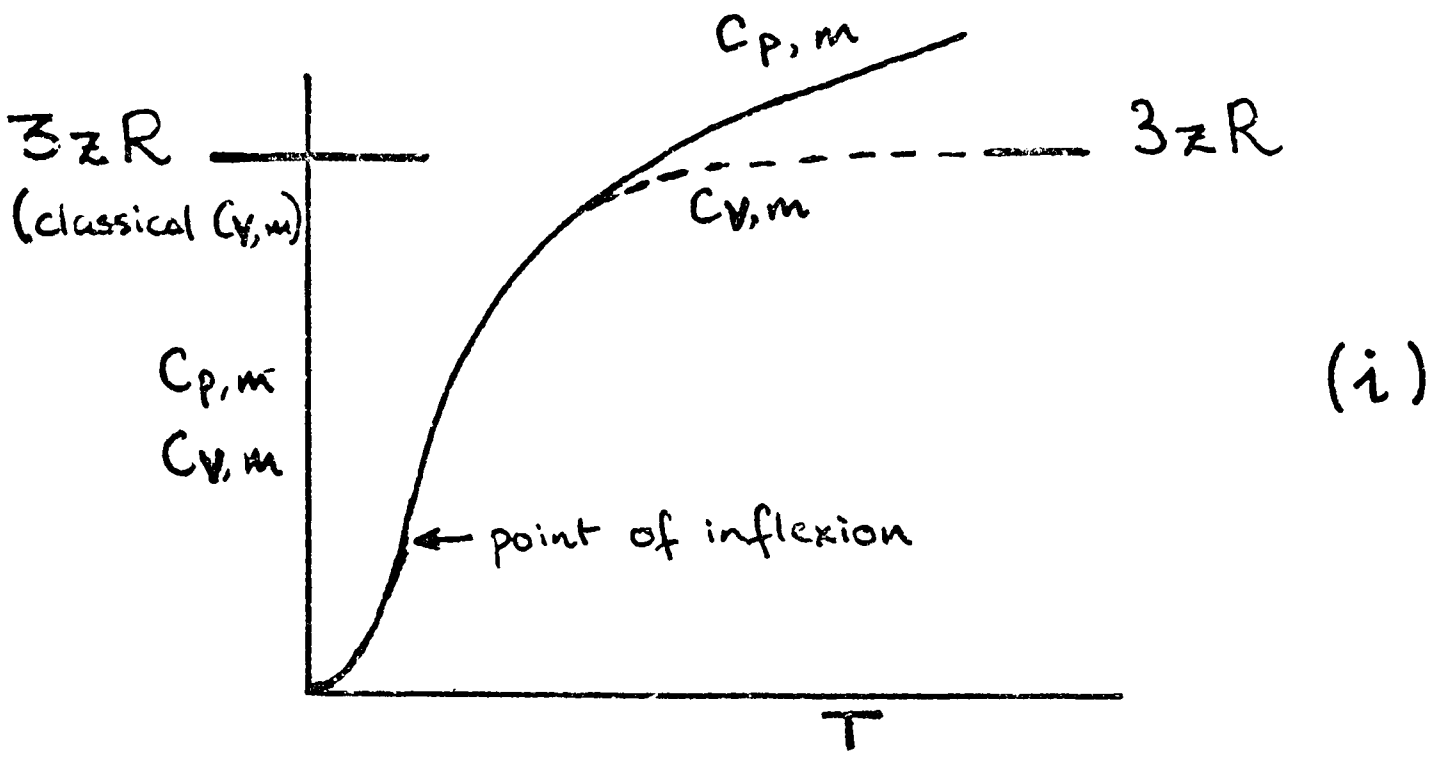

(i)

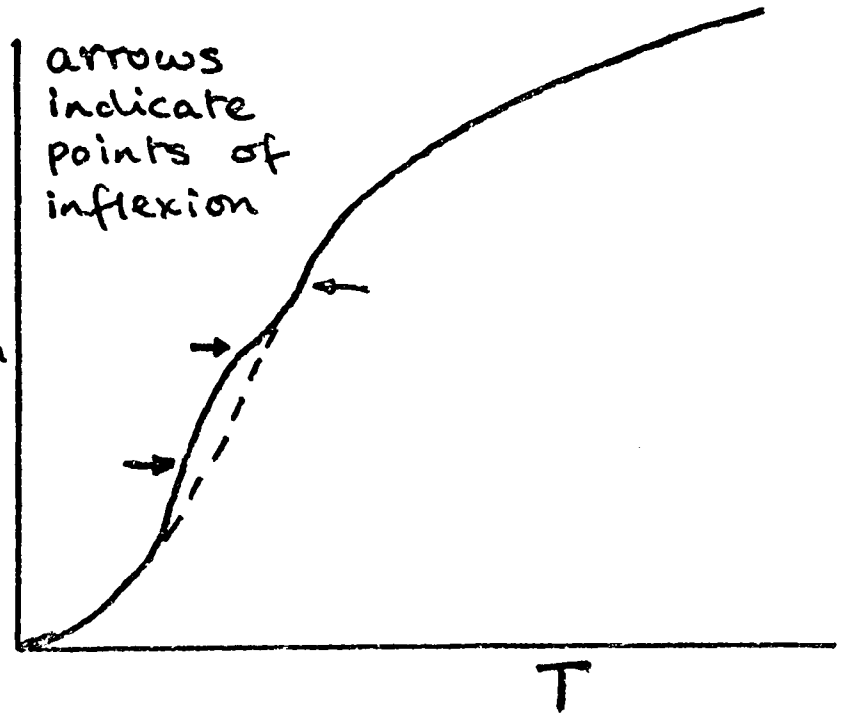

(ii)

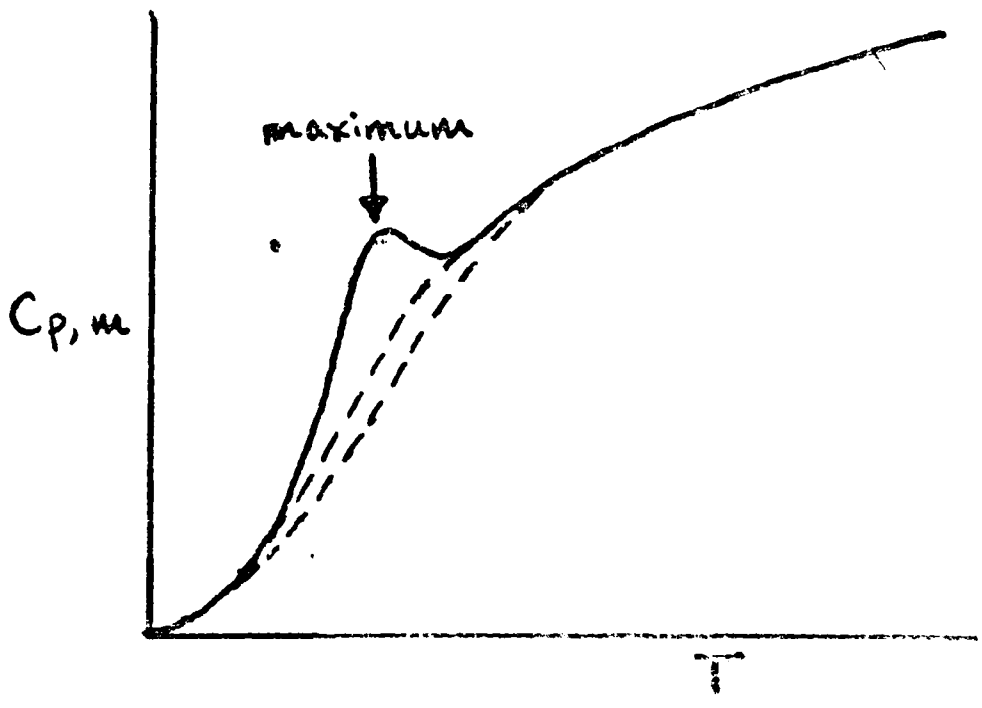

(iii)

than does the plot of Figure 1-1(i). Such more complex frequency spectra can reasonably be expected to arise in at least some of the solids that are markedly anisotropic and/or contain polyatomic species.

It is a conventional exercise to attempt (in the event with variable success) to discern in measured heat capacities any contributions which are not vibrational in origin. Implicit in this approach is the assumption that the total heat capacity can, approximately at least, be expressed as a sum of vibrational and various non-vibrational contributions. Such additional contributions often reflect effects of considerable importance; and therein lies the value of the exercise. Thus, the heat capacity of metals is found to include a contribution from the conduction electrons; this contribution rises in proportion to T and is most significant, as a proportion of the total heat capacity, at low temperatures. A second type of additional contribution is the anomalous contribution with which the present work is especially concerned; by "anomalous contribution" is meant one which (in contrast with a vibrational or electronic contribution) passes through a maximum at some temperature. A solid of which the heat capacity includes such a contribution is said to display a heat capacity anomaly.* Some of the effects giving rise to anomalies will be discussed in Section 1-3.

It is clear that the heat capacity shown in Figure 1-1(iii) (which passes through a maximum) must include an anomalous contribution. A priori, without knowledge of the frequency spectrum of the solid, it is not possible to estimate the vibrational contribution or, therefore, the anomalous contribution by difference; either of the two dashed curves in Figure 1-1(iii), or various other curves,

*There is some variation in the way the terms "anomaly", "anomalous" are defined. For instance, Gopal (1966) would reserve the term "anomaly" for unexplained heat capacity features; however, such a definition certainly contravenes popular usage (e.g. of "Schottky anomaly").

might represent the vibrational contribution. Likewise, an observed heat capacity plot such as that in Figure 1-1(ii) might conceivably indicate not a complex frequency spectrum as previously discussed but the presence of an anomalous contribution, for example that cut off by the dashed line.

These difficulties would be resolved (at least at such low temperatures that $C_{p,m} \approx C_{V,m}$) if the Debye equation 1-2, or *any* equation involving a small number of parameters, were quantitatively reliable. The heat capacity could then be fitted to the equation over some range of temperature where the anomalous contribution was negligible, the parameters (e.g. Θ_D) could be evaluated, and the vibrational heat capacity could be extrapolated into the anomalous region. However, even purely vibrational heat capacities are found not to follow the Debye equation over large temperature ranges; this is so, not only for highly anisotropic solids or those containing polyatomic species (as one would expect in any case), but also for such "fine-grained" and isotropic solids as KCl (see Dekker, 1958). It follows that, unless it is used with caution, the Debye theory will lead one to the conclusion that practically any heat capacity is anomalous. (Indeed, Gopal (1966) relates that many spurious Schottky anomalies were "found" in this way, ca 1930.)

The Debye model is generally more reliable at low temperatures (e.g. below 10 K). The reason for this is presumably that at low temperatures only the lowest-frequency modes of the lattice contribute significantly to the heat capacity; therefore, since these frequencies correspond to wavelengths greatly in excess of the nearest interatomic distances, they are fairly close to those calculated on the basis of a continuous medium. At low temperatures, equation 1-2 can often be usefully applied in the low-temperature limit form -

$$C_{p,m} \approx C_{V,m} \propto T^3 \qquad \text{eq. 1-3}$$

With this exception, analytical methods of separating the total heat capacity into contributions are of limited use.* In some cases, it suffices to draw a more-or-less freehand curve such as one of those given in Figure 1-1(iii). The more pronounced is a heat capacity maximum (in particular, the sharper is the whole anomaly), the more likely is this procedure to be reliable. (In the limiting case of a first-order phase transition, see Figure 1-2(a), the whole anomaly occurs at a single temperature. $C_{p,m}$ is infinite at that temperature and there is a latent heat, and the problem vanishes altogether.) This was the procedure used for estimating the anomalous heat capacity in bis(adiponitrile)copper(I) nitrate, where two heat capacity maxima were observed.

A more satisfactory procedure is to estimate the vibrational heat capacity from the heat capacity of a related substance or mixture of substances which is not expected to display an anomalous heat capacity. Thus, for example, an anomaly may be dependent on magnetic interactions between particular paramagnetic ions (see Section 1-3); in that case an isomorphous or nearly isomorphous compound in which the paramagnetic ions are replaced by non-magnetic ions of similar mass may well have a similar frequency spectrum, and therefore a total heat capacity closely approximating to the vibrational contribution in the magnetic isomorph. In the analysis of the heat capacities of TMMC (Chapter 4) and of copper and nickel phthalocyanines (Chapter 5), comparisons of this general type were made.

Section 1-3: some effects giving rise to anomalous heat capacity contributions in crystalline solids

There are various systems which are expected, on theoretical grounds, to display anomalous heat capacities. Moreover, the effects

*A recent, remarkable further exception to this conventional wisdom is discussed in Section 4-4d.

FIGURE 1-2

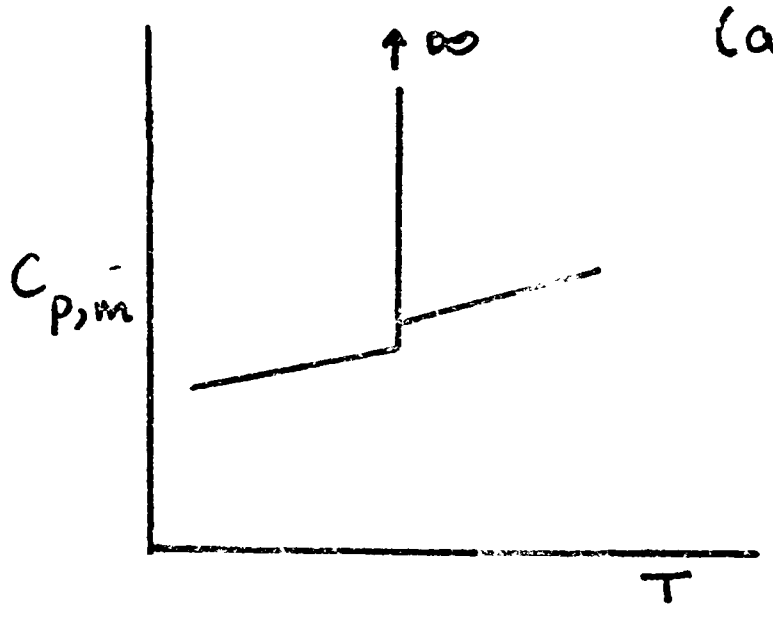

H discontinuous; ΔH at discontinuity is latent heat

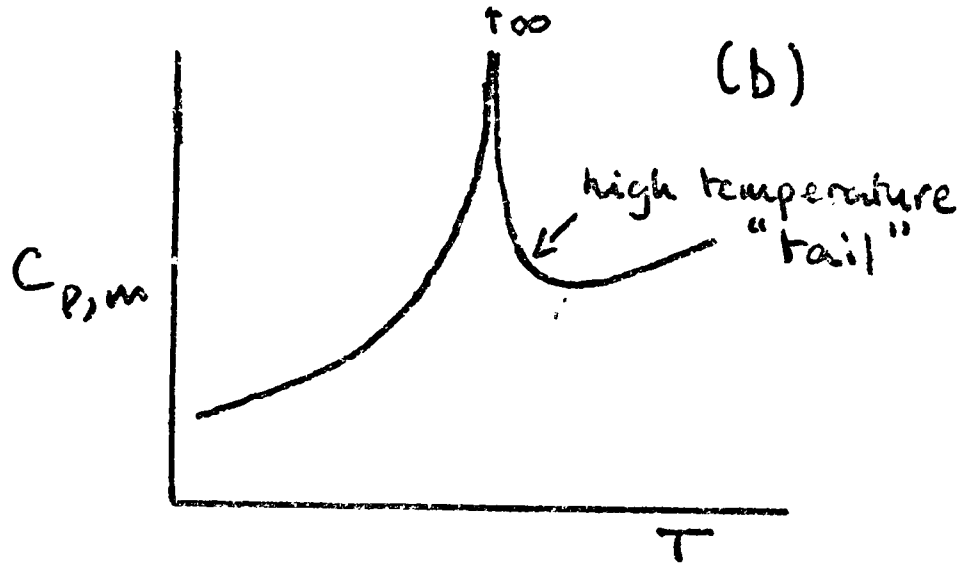

$C_{p,m}$ discontinuous but not H

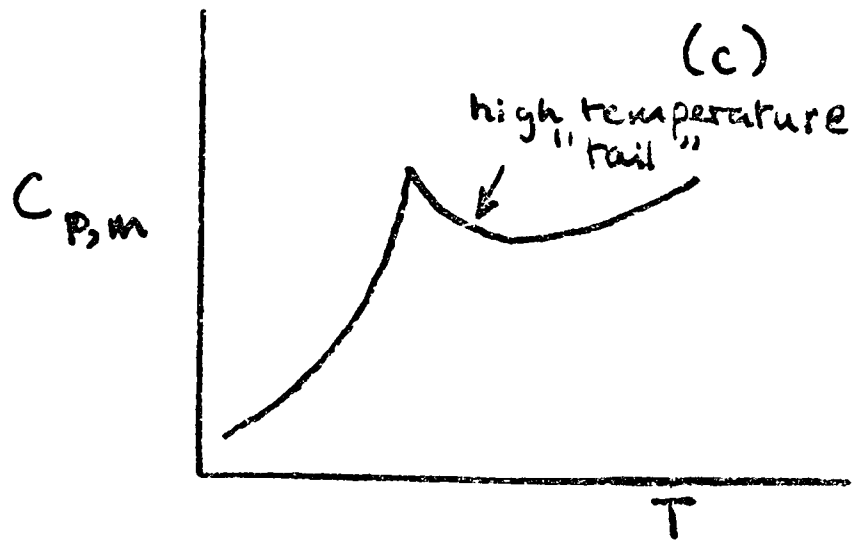

$dC_{p,m}/dT$ discontinuous

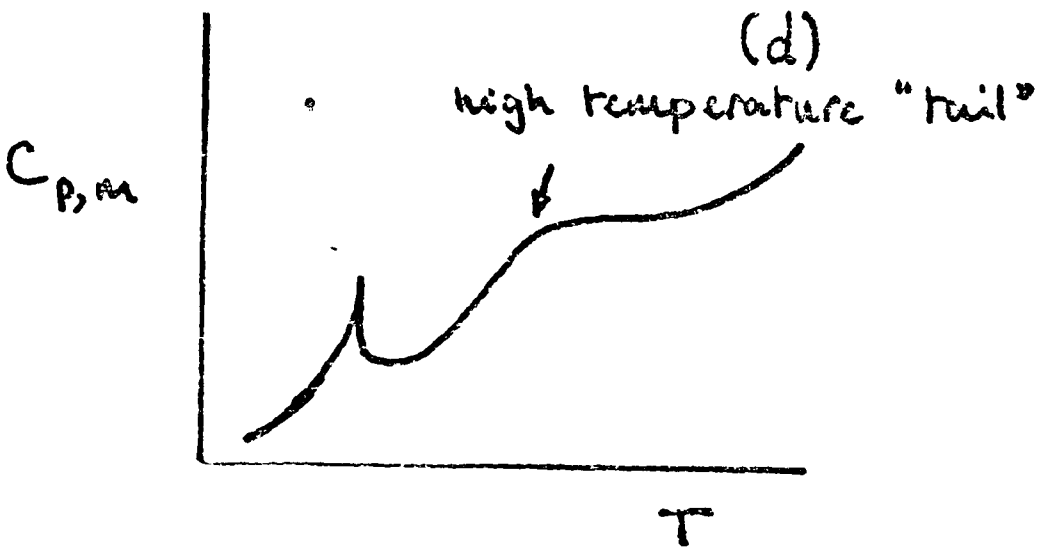

$dC_{p,m}/dT$ discontinuous

arising in these systems can often be investigated by non-calorimetric methods, for example by X-ray crystallography, by magnetic resonance, or by magnetic susceptibility measurements. (TMMC (Chapter 4) is a case in which an exceptionally large amount of additional information was available.)

It has been found that the various effects can be more or less successfully correlated with the heat capacity anomalies observed, in particular with the overall heat capacity - temperature plot and with the anomalous entropy gain over the whole anomaly. This anomalous entropy gain is estimated by the steps of (a) estimating, as discussed in Section 1-2, the anomalous heat capacity contribution over the entire temperature range for which it is significant, and (b) applying equation 1-1 to just the anomalous contribution with integration over this temperature range.

According to a simple statistical-mechanical treatment, one system which must have a heat capacity passing through a maximum is an assembly of mutually independent stationary ions, each having a ground electronic state of degeneracy g_0 and an excited electronic state of degeneracy g_1 of an energy higher by E. The heat capacity of a mole of such ions approaches 0 as T approaches 0 (when all ions will be in the ground state) and also approaches 0 at high T (when $g_0L/(g_0 + g_1)$ ions will be in the ground state and $g_1L/(g_0 + g_1)$ ions will be in the excited state); the necessary intermediate absorption of energy involves a heat capacity maximum.

In a real system, the ions are not stationary, but undergo vibrational motion (as will the other species in the system). However, the vibrational and electronic changesoccurring as the temperature is raised will be more or less independent, and the electronic change will be responsible for a more or less separable anomalous contribution

to the total heat capacity. The anomaly is known as a Schottky anomaly, and one arises for instance in iron(III) methylammonium sulphate (the anomaly being associated with the iron(III) ions - see Rosenberg, 1963). Insofar as the ions undergo excitation in a truly independent manner, the form of the anomalous contribution - temperature plot (which can be calculated simply by application of the Boltzmann principle) will be rather a smooth one, and in particular there will be at no temperature any discontinuity in the heat capacity or in the derivatives of the heat capacity with respect to T.

This smoothness can make Schottky anomalies difficult to detect, especially at higher temperatures when the vibrational heat capacity is large; for example the contribution might affect the overall heat capacity plot only to the degree shown in Figure 1-1(ii). Unless a comparison heat capacity is measured (e.g. of an isomorphous compound with a different ion) or there is further evidence (e.g. from electron paramagnetic resonance), the question of whether a Schottky anomaly occurs at all may well be unanswerable.

If, however, the anomalous heat capacity contribution and anomalous entropy gain can be estimated, then the anomalous entropy gain should be equal to that calculated from the well-known equation $S = k \ln W$. For one mole of ions, the anomalous entropy gain is simply

$$\Delta S_{m,\text{Schottky}} = R \ln \frac{g_0 + g_1}{g_0} \qquad \text{eq. 1-4}$$

For the case where $g_0 = g_1$,

$$\Delta S_{m,\text{Schottky}} = R \ln 2 = 5.76 \text{ J K}^{-1} \text{ mol}^{-1}.$$

Physical systems containing hindered rotators also display anomalous heat capacities. At low temperatures these rotators (polyatomic ions or molecules) undergo libration in the crystal field, and

at high temperatures almost free rotation. At some intermediate temperature depending on the barrier to rotation, the heat capacity contribution from this effect passes through a maximum (see Rushbrooke, 1949). Again, insofar as the rotators are mutually independent, the anomalous heat capacity contribution - temperature plot will be rather smooth, without discontinuities of any order. An anomaly of this general type has been observed, for example, in $(NH_4)_2\ SnCl_6$, wherein the hindered rotators are the ammonium ions (see Staveley, 1961).

However, altogether sharper anomalous heat capacities can arise (but do not necessarily arise) in systems where the change occurring can <u>not</u> be described in terms of changes in independent microscopic units; indeed, a discontinuity in the anomalous heat capacity contribution or in its derivatives with respect to temperature may arise. In such cases the change must be described in terms of a large number of microscopic units mutually linked by interactions of an appropriate kind (see Temperley, 1956*). Since heat capacities are in practice measured as averages over a finite temperature range (and for other reasons), the precise identification of a discontinuity is a matter of some practical difficulty; but the various sorts of discontinuities observed are broadly represented in Figure 1-2.

Where the change, such as that from rhombic to monoclinic sulphur at 95.5°C, involves a rather substantial rearrangement of the relative positions of the molecules, it occurs isothermally - i.e. there is a first-order phase transition (Figure 1-2(a)). If, as in the sulphur case, each of the two phases is ordered structurally,

---

*Temperley observes <u>inter alia</u> that the discontinuity corresponds to a partition function (or derivative thereof) which is, for practical purposes, a non-convergent summation by virtue of the large number of units involved.

the anomalous entropy gain (simply $\Delta H_{m,tr}/T_{tr}$) corresponds to the vibrational entropy change resulting from the change in the frequency spectrum. Such changes are usually small; for the transition in **sulphur** $\Delta S_{m,tr} = 1.1\ J\ K^{-1}\ mol^{-1}$ = R ln 1.14 (calculated from the information in Kubaschewski et al, 1967).

In other cases, the $C_{p,m}$ - T plot indicates that the change is gradual in the sense that the anomalous heat capacity contribution is significant over a considerable temperature range, but there is still a discontinuity in $C_{p,m}$ or one of its derivatives with respect to T (Figures 1-2(b) to (d)). These transitions are commonly called "λ-transitions" because of a resemblance of the plot to a capital λ.*

One effect which can give rise to a λ-transition is the change from an antiferromagnetic to a paramagnetic state in transition metal compounds such as $MnCl_2$. If the paramagnetic ion involved has "spin-only" magnetism then at high temperatures each ionic magnetic moment can take up with equal probability $(2S_i + 1)$ orientations. where S_i is the spin of the ion. For T = 0, each moment can take up only one orientation. Therefore the total anomalous entropy change expected is, for a mole of ions,

$$\Delta S_{m,mag} = R \ln (2S_i + 1) \qquad \text{eq. 1-5}$$

A simple explanation of why this system gives rise to an anomalous heat capacity with a discontinuity is that, as the temperature is raised, each magnetic moment which takes up an orientation contrary to the **ordered arrangement** renders a similar disorientation of adjacent ions more favourable as the temperature is raised further.

---

*As with "anomaly" itself, there are variations in the usage of "λ-anomaly" or "λ-transition". Pippard (1964) adopts a narrower definition of "λ-anomaly" than is used here; but that definition seems not to be in general use.

The discontinuity indicates when this process takes on a catastrophic character. λ-transitions (and first-order transitions) are said to be "cooperative" because the change is self-helping.

The heat capacity discontinuity is found to occur at a temperature in the vicinity of the Néel temperature as determined by magnetic susceptibility measurements, i.e. with the change from the antiferromagnetic state to the paramagnetic state. In the antiferromagnetic state there exists long-range order in the crystal - that is to say, mutually remote ions have significantly correlated magnetic moments. Below the Néel temperature the long-range order breaks down progressively more rapidly with increasing temperature. In the paramagnetic state, this long-range order is non-existent, but there must still exist short-range order - that is to say, correlation between the moments of nearby ions. It is the progressive breakdown of short-range order which accounts for the high-temperature "tail" marked in Figures 1-2(b) to (d).

It is found that the greater part of the anomalous entropy gain $R \ln (2S_i + 1)$ is gained below the temperature of the discontinuity in antiferromagnetic solids where the magnetic ions form a three-dimensional network with interactions of rather similar magnitude between an ion and each of its neighbours. If, however, the interactions of an ion with each of its neighbours are of very different magnitudes, the proportion is generally less. In some systems, the paramagnetic ions are arranged in linear chains and nearest-neighbour ions within the chains mutually interact more strongly than nearest-neighbour ions in adjacent chains; characteristically, these systems give $C_{p,m}$ - T plots as shown in Figure 1-2(d). A related point of considerable theoretical significance is that an isolated linear chain of magnetic moments can have no long-range order at any finite temperature; the

heat capacity curve of such a system would be "all tail" - rather like Figure 1-2(d) without the λ-anomaly.

Domb and Miedema (1964) have reviewed theoretical and experimental work on magnetic transitions.

Very roughly analogous discontinuities arise in the heat capacities of some nitrates (and of other compounds containing polyatomic species), the interactions responsible for long-range ordering of the nitrate ions at low temperatures being not the exchange and other interactions which cause magnetic ordering but, instead, simple electrostatic interactions or the interactions of the type which are represented by, for example, the Lennard-Jones equation. If in the high-temperature limit each nitrate ion takes up with equal probability one of n orientations in the crystal, and only one orientation is permitted in the low-temperature limit, then the entropy gain associated with the change is, for a mole of ions,

$$\Delta S_{m,orient} = R \ln n \qquad \text{eq. 1-6}$$

There are other effects that give rise to anomalous heat capacity contributions in solids; but these are not of particular concern in the present work, with the exception of a type of positional ordering (see Section 5-4d) that is conceptually similar to orientational ordering.

CHAPTER 2: CONSTRUCTION AND OPERATION OF A NEW LOW-TEMPERATURE CALORIMETER

Section 2-1: general principles of heat capacity determination

In this laboratory, over the last fifteen years, several calorimeters have been constructed for the purpose of measuring the molar heat capacities of solids as a function of temperature. In all of these calorimeters (including that which the author has constructed), the calorimetric sample is contained in a vessel that is equipped with an electrical heater and a thermometer. The heat capacity is determined both of the empty vessel and of the vessel loaded with sample. Subtraction of the former heat capacity from the latter gives, at any given temperature, the heat capacity of the sample, from which the molar heat capacity of the sample may be calculated if the amount of sample is known. It is, of course, desirable that the proportion of the total heat capacity measured due to the sample should be as high as possible.

Further, all the calorimeters have been designed for operation by the widely-used method of intermittent electrical heating (the term used by Hill, 1961). According to this method an individual determination consists of temperature measurements with the thermometer before and after a measured time period of electrical heating at a measured power dissipation.

In an idealised experiment in which the entire transfer of energy between the vessel and its contents (if any) and the outside world is confined to the process of electrical heating, interpretation of the results is simple. A steady temperature T_F will be observed on the thermometer before the heating period, and the temperature after the

heating period will gradually approach a constant value T_A after the heating period. If during the heating period the power at time t is represented by P(t), the mean heat capacity of the vessel and its contents (if any) over the temperature range T_F to T_A is given by

$$\overline{C}(T_F, T_A) = \int_{\text{heating period}} P(t)\, dt \,/\, (T_A - T_F) \qquad \text{eq. 2-1}$$

Provided that the initial and final states are indeed equilibrium states, then any inaccuracy in the values of $\overline{C}(T_F, T_A)$ obtained can derive only from experimental inaccuracy in the power, time, or temperature measurements, and will not depend (directly at least) on the form of P(t) or on the equilibrium time.

However, the latter two factors become significant in a real experiment, where heat exchange between the vessel and its environment is a serious consideration. This heat exchange can be kept down by ensuring that the equilibrium time is short (and therefore the total duration of the determination). To achieve short equilibrium times, the vessel is made of a highly conductive metal, and an exchange medium (usually, but not always, a gas) is used within the vessel to maintain thermal contact between the vessel and the sample.

Further, the calorimeter is designed on the one hand so as to keep down the rate of heat exchange between the vessel and its environment, and on the other so as to control (and therefore permit correction for) whatever heat exchange nevertheless takes place. This is achieved by the use of a "shield" surrounding the vessel. The space between the "shield" and the vessel is usually evacuated to reduce gas conductance, and the materials forming the members connecting the shield and vessel (electrical leads, supports) are chosen for low thermal conductance, insofar as this is consistent with their prime function (electrical conduction, mechanical support).

The shield temperature is normally controlled in one of two ways during the determination. Either the shield is maintained at constant temperature (isoperibolic operation), or its temperature is controlled to follow that of the vessel (adiabatic operation). In isoperibolic operation, the temperature of the shield may be maintained, for example, by direct or indirect contact with a boiling liquid, or by the controlled use of a heater, the temperature being monitored with a suitable thermometer. In adiabatic operation, a pair of thermocouples is commonly used to monitor the temperature difference between shield and vessel, and suitable adjustments are made in the power supplied to a heater on the shield so as to maintain at least approximately equal shield and vessel temperatures.

The results of a real determination by the method of intermittent electrical heating consist of a series of temperature measurements (showing the "drift" of temperature with time) both before and after the heating period, and also power measurements during the heating period. With both isoperibolic and adiabatic shield operation, it is normal to maintain the power to the vessel, P(t), roughly constant during the heating period, and to correct for heat exchange during the determination by extrapolating both the fore and the after temperature drifts to the time mid-point of the heating period. These extrapolations respectively furnish T_F and T_A for use in equation 2-1. The after drift generally becomes linear only some time (the "equilibrium time", q.v.) after the end of heating, and it is this portion of the after drift that is extrapolated. For such a procedure to be strictly valid, various conditions must be met which cannot be generally guaranteed; therefore errors, including systematic errors, may result, which are often larger in magnitude than the errors resulting from inaccuracies in the measurements of temperature and energy input.

Generally speaking, this correction procedure is less valid with adiabatic operation than with isoperibolic operation; but on the other hand, the total magnitude of the correction for heat exchange is usually less with adiabatic shield operation.

With isoperibolic shield operation, the shield temperature employed has to be changed periodically, after every few determinations, so as to avoid excessively high drift rates. Adiabatic operation has the considerable advantage that a continuous run of determinations is possible, the after drift of one determination serving as the fore drift of the next.

Both systems of shield operation are employed in the new calorimeter (see Sections 2-2 to 2-9).

The design of a calorimeter is highly dependent on the temperature range over which it is to be operated, since the relative heat capacities and thermal conductances of the various possible component parts vary enormously with temperature, as do the principal likely mechanisms of heat transfer (e.g. conduction through solids, conduction through gases, or radiation).. In addition the choice of thermometry, both for the measurements of the vessel temperature and for shield control, depends on the temperature range. The new calorimeter is peculiar in that its operating range is very wide (from 1.4 - 1.5 K to above 80 K), and therefore has to be operated in a variety of different manners depending on the particular temperature.

Section 2-2: the purpose of the new calorimeter

At the time of writing, this laboratory possesses two other calorimeters suitable for the measurement of heat capacities of solids, namely that constructed by Linford (1967) and that constructed by Worswick (1972). The former may be used from about 10 K to about 300 K.

The latter may be used from about 80 K to about 500 K.

The main purpose of the new calorimeter constructed in the course of the present work was to complement the Linford and Worswick calorimeters by permitting specific heat measurements to be made at temperatures lower than are possible with the Linford calorimeter and to provide more precise measurements than are possible with the Linford calorimeter at the lower end of its range. By the use of both the new calorimeter and one of the high temperature calorimeters, the molar heat capacities of bis(adiponitrile)copper(I) nitrate and of TMMC were in fact determined over very wide temperature ranges (see Chapters 3 and 4).

Clay (1965) had previously constructed in this laboratory a calorimeter for similar purposes, and the present calorimeter was constructed to supersede that calorimeter. The Clay calorimeter was operated from 2 K to 4.2 K with pumped liquid helium as a refrigerant, the liquid helium being (in normal practice) pumped in a glass dewar; from 4.2 K to 20 K with liquid helium as a refrigerant, the shield being isoperibolically controlled at 4.2 K; and from 20 K to 84 K with liquid hydrogen as a refrigerant, the shield being controlled adiabatically. The thermometer on the vessel was a germanium resistance thermometer calibrated over the overall range, and the accuracy of the heat capacity measurements indicated that the calibration was substantially correct.

In the construction of the new calorimeter, it was found possible to reuse some of the parts of the Clay calorimeter - the platinum-iridium shell of the sample-containing vessel, the germanium resistance thermometer (after further calibration by the National Physical Laboratory), and the jaws of the thermal switch - ; but the rest of the apparatus (cryostat, electrical circuitry, and vacuum lines) were

replaced. The new construction was intended to provide a calorimeter in which the following objectives (not in order of importance) would be achieved: -

1. In the interests of safety, the use of liquid hydrogen as a refrigerant would be avoided, while liquid helium consumption would be kept at an economically low level.
2. Pumping on liquid helium in a glass dewar (again somewhat hazardous) would be avoided by the use of a separate liquid helium-4 pot of adequate size.
3. Temperatures of about 1.4 - 1.5 K would be achieved by pumping on liquid helium-4.
4. Helium-3 would be used (once objective 3 was achieved) to obtain temperatures of 1 K or below.
5. Measurements of heat capacity should be possible with reasonable accuracy up to 84 K (the limit of calibration of the germanium resistance thermometer, which is in any case very insensitive above this temperature).
6. Isoperibolic operation with shield temperatures between 4 K and 20 K should be possible.
7. It should be possible to use pumped liquid nitrogen (again, <u>not</u> pumped in a glass dewar) to permit work below the normal nitrogen boiling point (in fact down to 48 K) without the use of liquid helium. (This proved to be a most convenient feature of the apparatus.)

All of these objectives were achieved except for 4. The apparatus developed a leak in the helium-3 pot during the early low-temperature runs, and it was impossible to fix this leak without essentially dismantling the cryostat. The achievement of objective 3 constituted, at the time, a record low temperature in the Inorganic

Chemistry Laboratory.

The calorimeter is a complicated one, and its success was entirely dependent on attention during its design and operation to a large number of points which are dealt with in the subsequent Sections 2-3 to 2-9.

Section 2-3: the overall scheme of the cryostat

With the objectives indicated in the previous section in mind, the cryostat shown schematically in Figure 2-1 was designed and constructed. (See also Plates 2-I to 2-VI.) In Figure 2-1, for the sake of clarity, the various pumping tubes (which in fact simultaneously serve as mechanical supports for the central assembly of the cryostat) are shown only schematically by arrows. It is to be understood that the three spaces labelled outermost space, intermediate space, and innermost space, as well as the helium-4/nitrogen pot and the helium-3 pot each have a pumping tube, the helium-4 pot being also connected by a tube to a needle valve on the outermost lid for the admission of refrigerant liquid from the monax dewar.

In the following description of the overall scheme of the cryostat, underlining indicates the first mention of a feature labelled in Figure 2-1.

The central assembly of the cryostat comprises three concentric cylindrical chambers. The innermost chamber serves as a calorimetric shield, the sample-containing vessel being suspended within this chamber on four thin nylon threads (for low thermal conductivity). This chamber is enclosed by an intermediate chamber, which is in turn enclosed by an outermost chamber, the outer wall of which is directly immersed in the refrigerant (contained in the monax dewar) when the calorimeter is in use. Either liquid helium or liquid nitrogen can

FIGURE 2-1

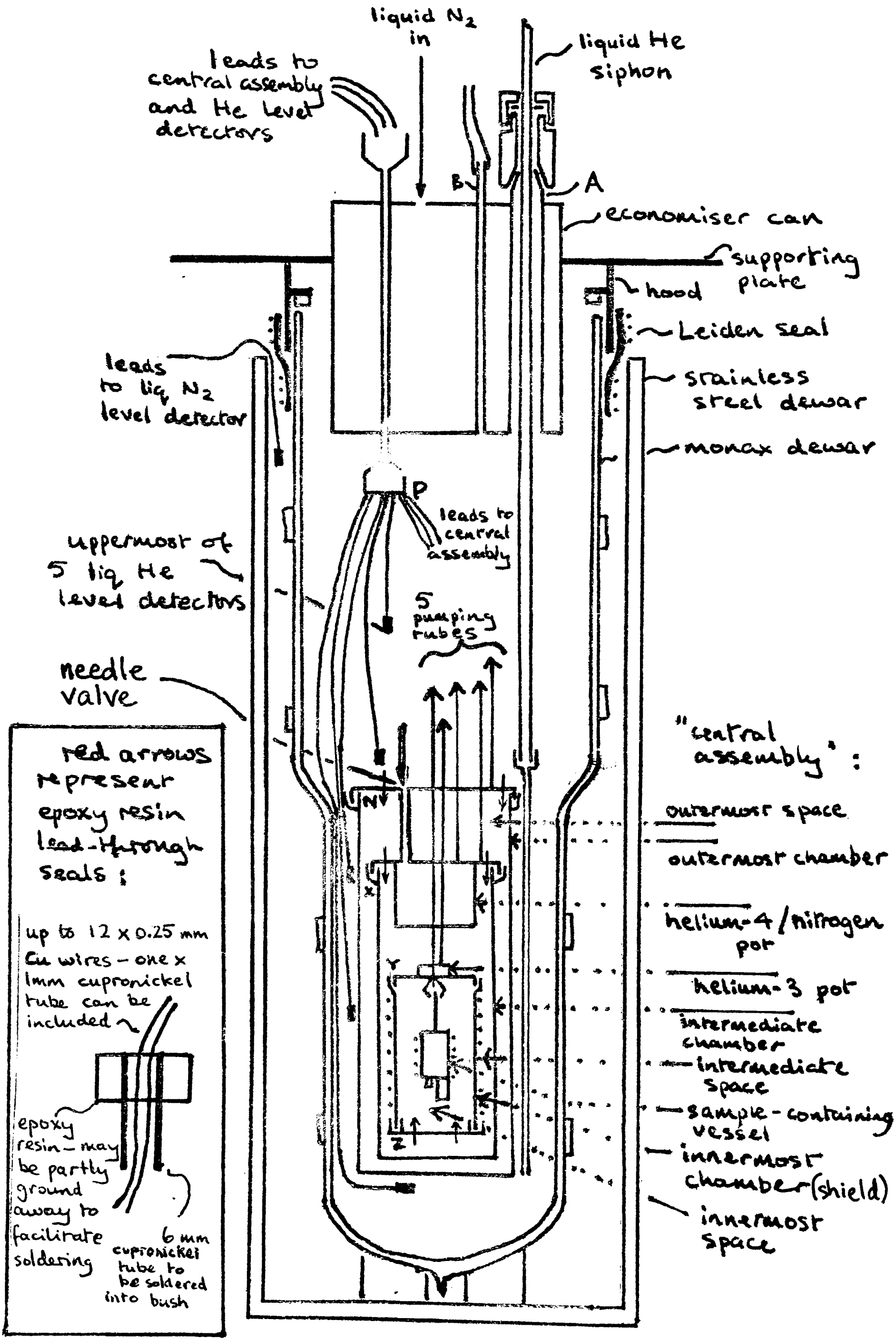
liquid N_2 in
leads to central assembly and He level detectors
liquid He siphon
B
A
economiser can
supporting plate
hood
Leiden seal
leads to liq N_2 level detector
stainless steel dewar
monax dewar
P
leads to central assembly
uppermost of 5 liq He level detectors
5 pumping tubes
needle valve
N
x
Y
Z
"central assembly":
outermost space
outermost chamber
helium-4/nitrogen pot
helium-3 pot
intermediate chamber
intermediate space
sample-containing vessel
innermost chamber (shield)
innermost space
red arrows represent epoxy resin lead-through seals:
up to 12 x 0.25 mm Cu wires – one x 1mm cupronickel tube can be included
epoxy resin – may be partly ground away to facilitate soldering
6 mm cupronickel tube to be soldered into bush

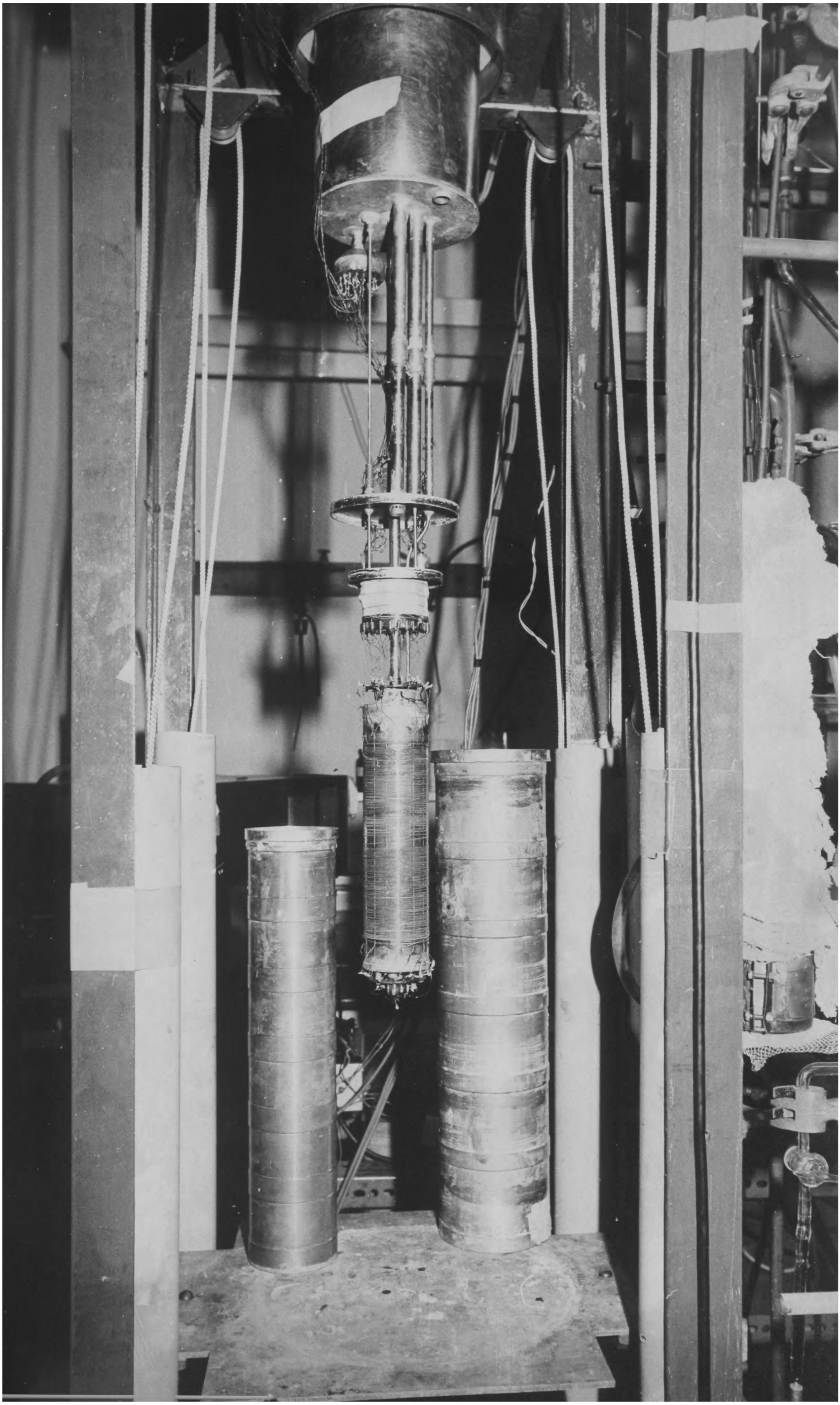

PLATE
2-II

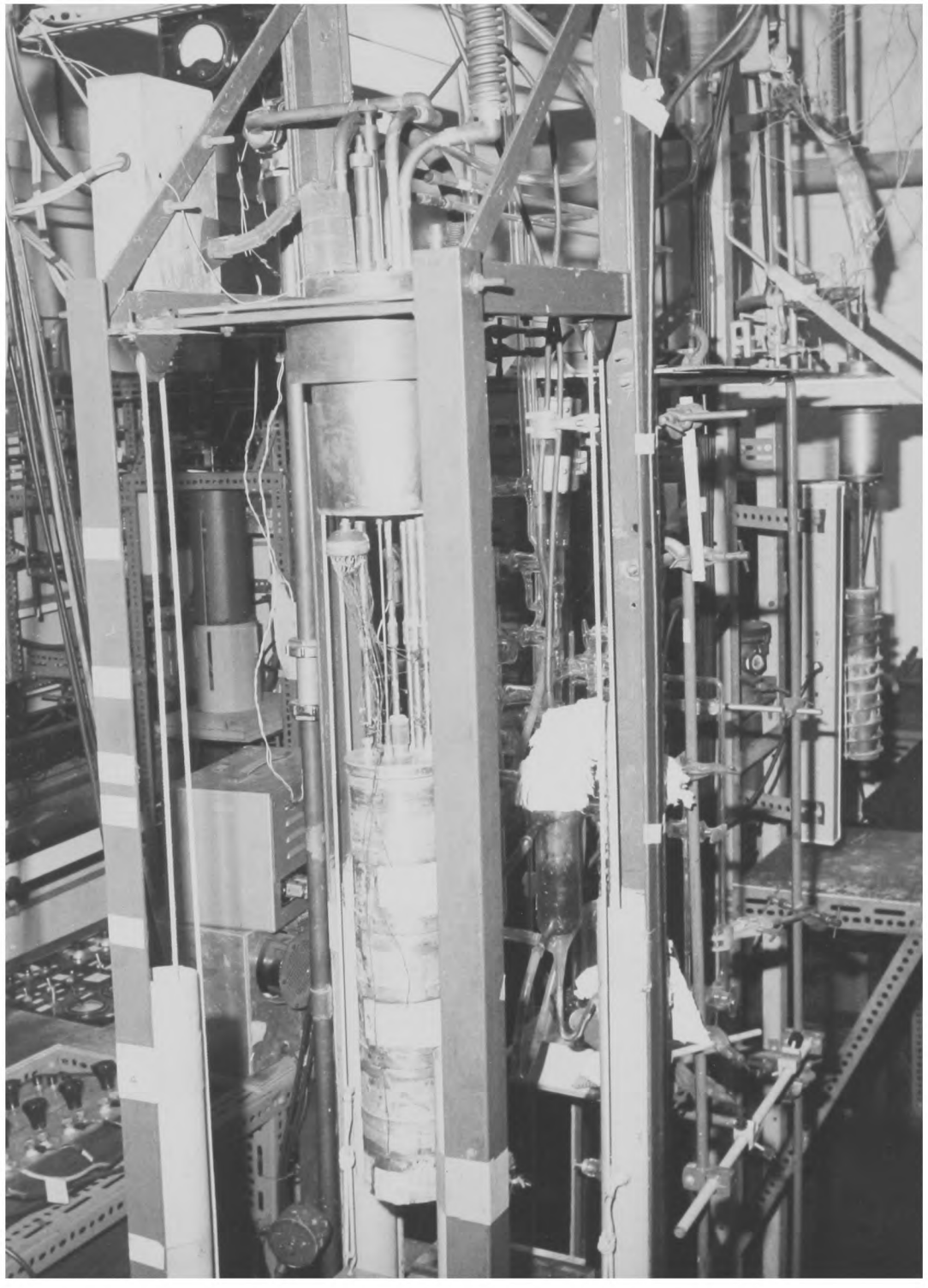

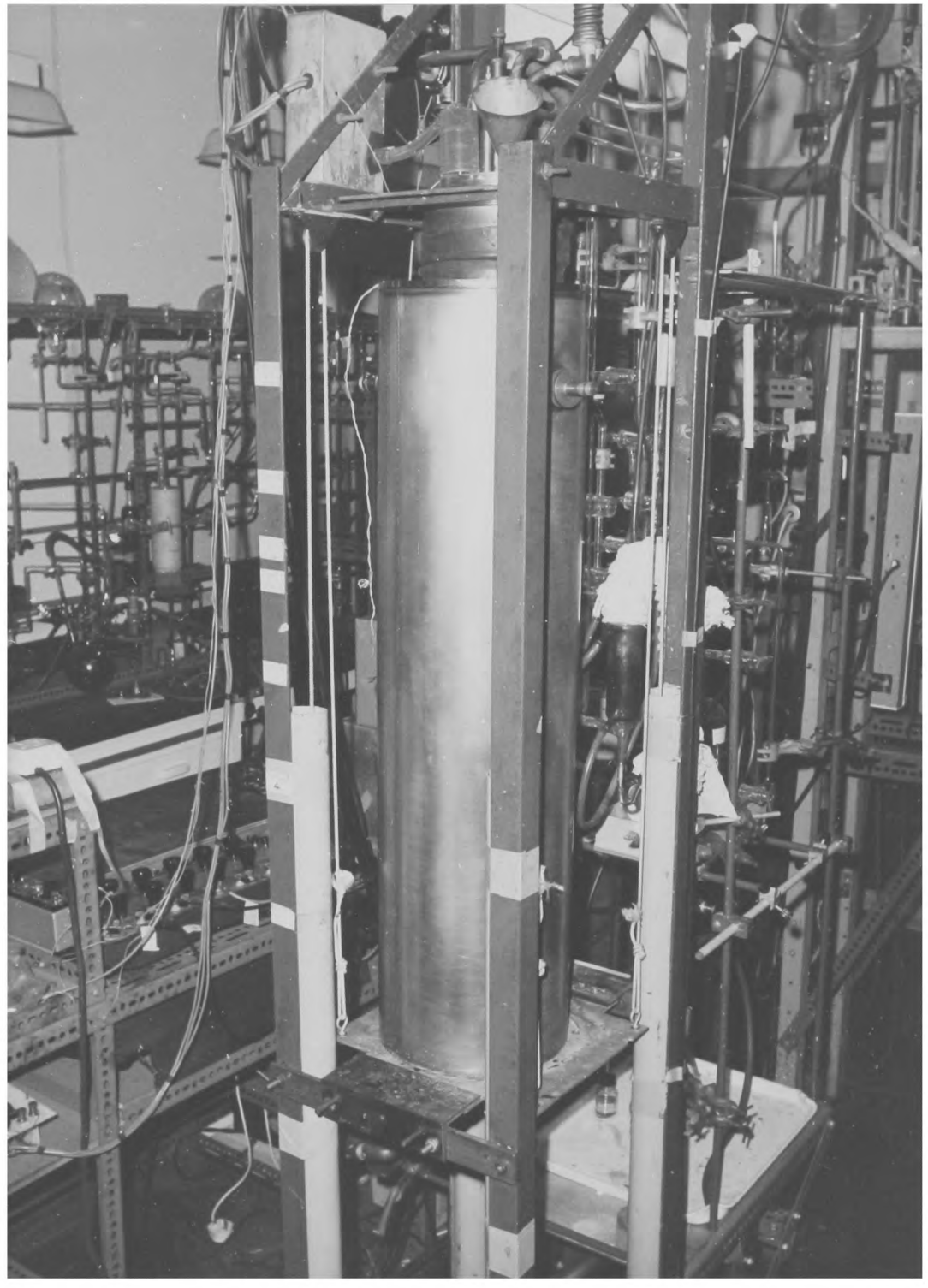

PLATE
2-III

PLATE 2-IV

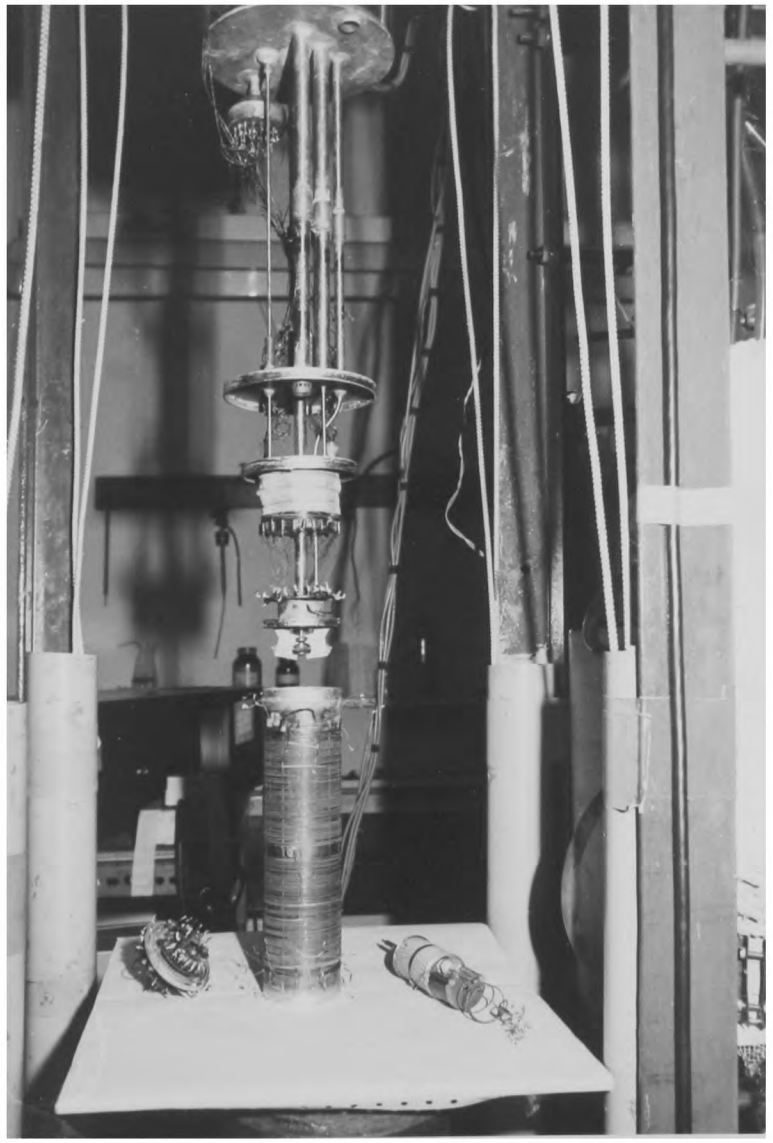

PLATE 2-V

PLATE 2-VI

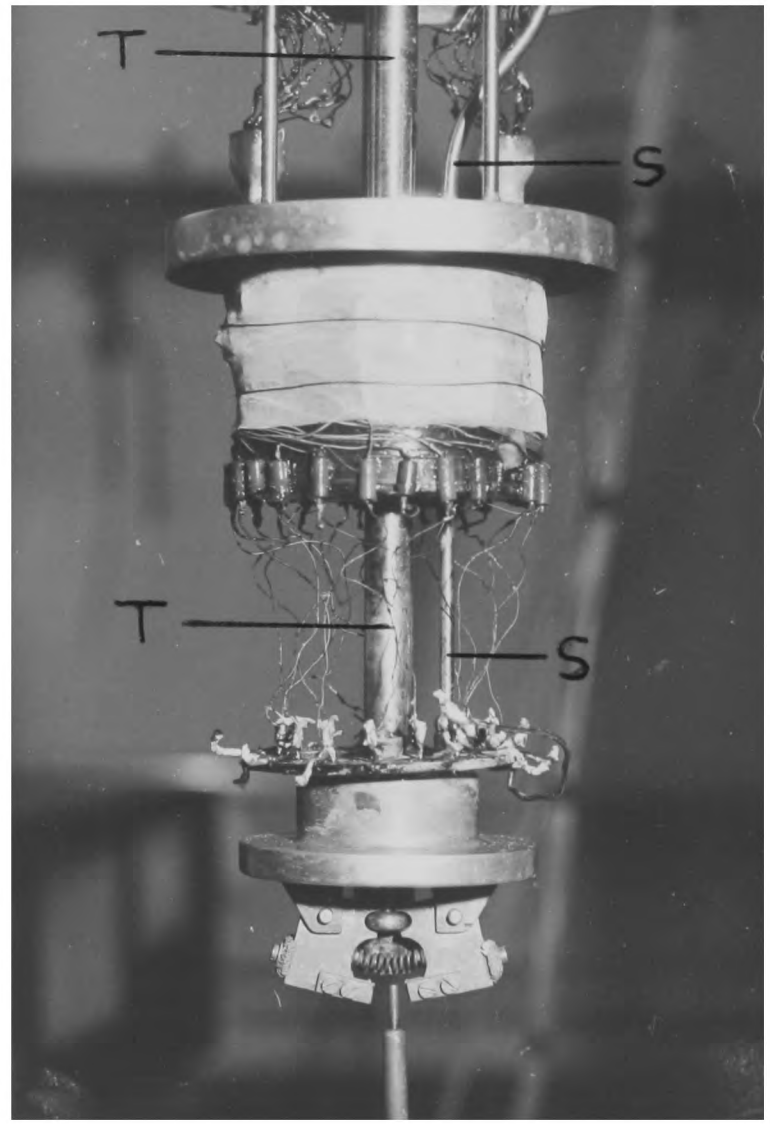

be used as the refrigerant in the monax dewar. The spaces between the compartments (labelled, respectively, innermost, intermediate, and outermost spaces) are bridged only by members of low thermal conductance (e.g. thin-walled stainless steel pumping tubes and narrow gauge manganin wires), and each of the three spaces can be evacuated independently of the other two. The walls of the chambers are constructed of copper for high thermal conductivity.

Accordingly, in operation, it is possible to maintain temperature differences between the chambers while each chamber is substantially at uniform temperature. Temperature differences between adjacent chambers may be equalised by the admission of helium exchange gas into the outermost space or intermediate space. To allow temperature differences between chambers to be created, the intermediate chamber is provided with the helium-4 / nitrogen pot in which the respective refrigerant (admitted via the needle valve from the monax dewar, as already mentioned) may be pumped, and the innermost chamber is provided both with a helium-3 pot (smaller than the helium-4 / nitrogen pot) and an electrical shield heater.

The central assembly is demountable by low-temperature soldered joints at N, X, Y, and Z to allow insertion and removal of the sample-containing vessel between runs on different samples. Plates 2-IV, 2-I, and 2-II (in that order) show the assembly of the parts.

Thermal contact between the sample-containing vessel and the innermost chamber may be established or broken by means of a mechanical thermal switch (on the inside of the top lid of the innermost chamber) consisting of jaws closing on a copper spike on the vessel (see Plates 2-V and 2-VI). (Exchange gas would be generally unsuitable for this purpose below about 10 K; see Section 2-9a for further comment on this point.)

The innermost chamber, in addition to the shield heater and the helium-3 pot, carries a carbon resistance thermometer (for isoperibolic shield operation below 20 K) and a manganin-constantan thermocouple linked via constantan with another on the sample vessel (for adiabatic shield operation above 20 K).

The sample-containing vessel also carries a germanium resistence thermometer and a heater. The body of the vessel (constructed largely of platinum-iridium with some copper) is connected by an indicator wire which allows an electrical check to be made on the position of the jaws. The leads from the vessel to the distribution board on the inside of the bottom lid of the innermost compartment are of narrow gauge manganin (except for one narrow gauge constantan thermocouple wire), for low thermal conductance.

The central assembly is suspended by the various pumping tubes from the economiser can, through which all the tubes and leads pass, and which is filled with liquid nitrogen during operation. (This reduces consumption of liquid helium in the monax dewar, and when liquid nitrogen is being used in that dewar, it eliminates varying thermal e.m.f.s at the soldered junctions at P in Figure 2-1.) The economiser can is fixed in a supporting plate, which is in turn bolted to a rigid frame (see Plate 2-III).

The monax dewar is contained within a stainless steel dewar. The two dewars can be raised up around the assembled cryostat on a hoist (see Plate 2-III). The stainless steel dewar contains liquid nitrogen when liquid helium is being used in the monax dewar, to keep down helium consumption, but is empty when liquid nitrogen is being used in the monax dewar. A gas tight seal between the monax dewar and the hood around the economiser can can be made with a Leiden seal of rubber. Refrigerant can be introduced through tube A in the

economiser can, which tube is large enough to take a helium siphon. Gas from evaporating refrigerant can escape through tube B.

Liquid helium level detectors are provided at various levels in the monax dewar, and a liquid nitrogen level detector in the stainless steel dewar.

The electrical leads to the central assembly pass from compartment to compartment, as required, as indicated schematically by the red arrows in Figure 2-1. The electrical connections between the mutually vacuum-tight compartments were achieved by the use, for the first time in this laboratory, of epoxy resin lead-through seals (see inset to Figure 2-1) soldered into bushes at the appropriate places.

These seals were supplied by Thor Cryogenics Ltd of Berinsfield, Oxfordshire, and were found, in accordance with the suppliers' claims, to be absolutely leak-tight even when subjected to repeated rapid cooling and heating.

Because of the use of these seals, it was readily possible to ensure that leads passing from one compartment to another were thermally anchored at or near the temperature of the respective compartments at either end; this is highly desirable so as to minimise heat leaks during operation at the lowest temperatures and excessive thermoelectric e.m.f.s. Thus, referring once more to Figure 2-1, the leads from P downwards are cooled directly by the refrigerant or else (if the refrigerant level in the monax dewar is too low) by rising cold gas from the refrigerant, before they pass through the lid of the outermost chamber; and thermal anchoring on the inner two chambers is readily provided on the outer cylindrical surfaces of the helium-4 / nitrogen pot and the innermost chamber respectively (see Sections 2-6 and 2-7 for details).

Arranging for such effective thermal anchoring would have been extremely difficult if reliable low-temperature lead-through seals had not been available; for in this case it would have been necessary to introduce all the leads into the pumping tubes at the top of the cryostat (e.g. via a black wax seal).

In each of the following Sections 2-4 to 2-8, a part of the cryostat will be described together with any associated electrical circuitry or vacuum lines, and some information on operational procedure and performance will be given as appropriate. This will be followed in Section 2-9a by an account of an entire calorimetric run; it may be helpful at the present stage for the reader to refer briefly to one particular part of that section, namely to Figure 2-13 (b) to (g), which shows a typical scheme according to which calorimetric measurements are made over the 1.4 K - 84 K temperature range, and how the three vacuum spaces, two pumping pots, and shield heater are to be used.

Section 2-4: the germanium resistance thermometer

The thermometer carried on the sample-containing vessel of the calorimeter is a germanium resistance thermometer. Since such thermometers were first described (Kunzler et al, 1957), they have passed into common use at temperatures from those obtainable with pumped He^3 up to liquid nitrogen temperatures. The thermometers are of high cost (the thermometer used in the present calorimeter cost $220 in 1963), but have excellent reproducibility ($\pm$ 0.1 mK according to Edlow and Plumb, 1961), both when maintained for days at a fixed temperature and when recycled from liquid helium temperatures to room temperature and back again.

Temperature dependence of thermometer resistance; calibration

The thermometer used was a CG-1 model, bought in 1963 from Radiation Research Corporation of Westbury, Long Island, New York. It comprises a slice of doped germanium sealed, together with helium gas, in a platinum can 8.5 mm long by 2.5 mm diameter, in the one end of which is a glass-metal seal through which four wires from the germanium slice pass. The slice is machined into such a shape that resistance measurements on the germanium can be made which are substantially independent of contact resistances (which may not be reproducible). The shape is not specified by the manufacturers, but a typical shape is shown in the inset of Figure 2-4; the voltage drop measured across RO when a particular current passes through PB is substantially unaffected by the contact resistances. The manufacturers claimed a reproducibility of $\pm$ 0.5 mK for the thermometer.

The resistance of the thermometer is (to the nearest ohm) 10 Ω at 80 K, 34 Ω at 40 K, 98 Ω at 25 K, 192 Ω at 14 K, 407 Ω at 4.2 K, 1330 Ω at 2.0 K, and 2540 Ω at 1.5 K (see Figure 2-2). The author observed (at first with considerable alarm) the previously unremarked fact that the resistance measured at room temperature is greater than that measured at 80 K. At a room temperature of 17.5°C, the resistance at a current of 100 μA was measured as 14.0 Ω.

The thermometer had been calibrated in this laboratory from 2 K to 84 K by R.M. Clay (1965), partly in collaboration with C.E. Dyball (1966). Then R.S. Rusby (1971) calibrated the thermometer from 0.49 K to 4.25 K, in the National Physical Laboratory. Because Rusby's measuring apparatus was superior to that used by Clay, and because Rusby used lower thermometer currents (important because of self-heating, discussed later in this Section), the Rusby calibration was preferred to the Clay calibration where the two calibrations overlapped.

FIGURE 2-2

R is resistance of germanium thermometer at temperature T

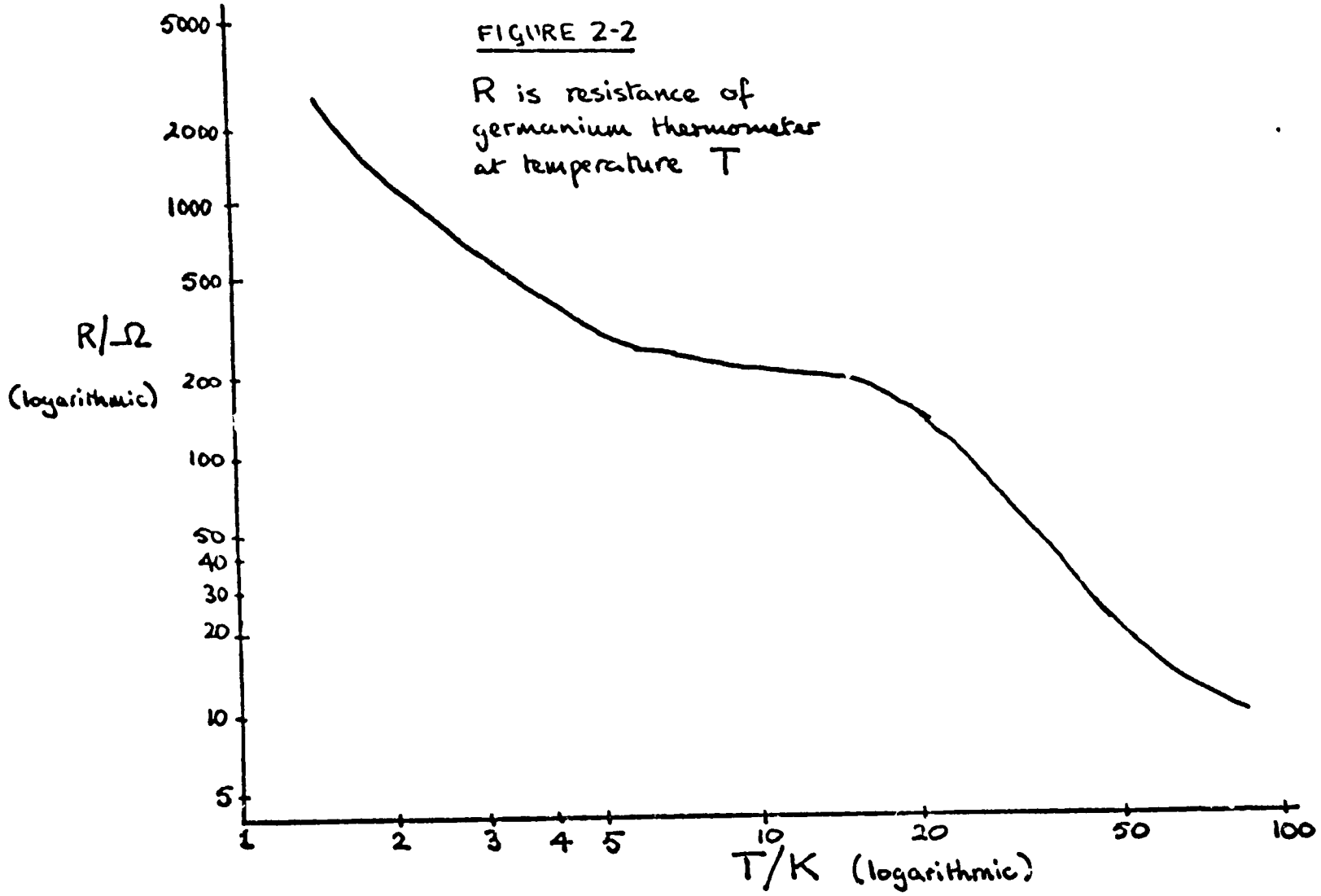

FIGURE 2-3

error is the likely error in measurement of a constant temperature T

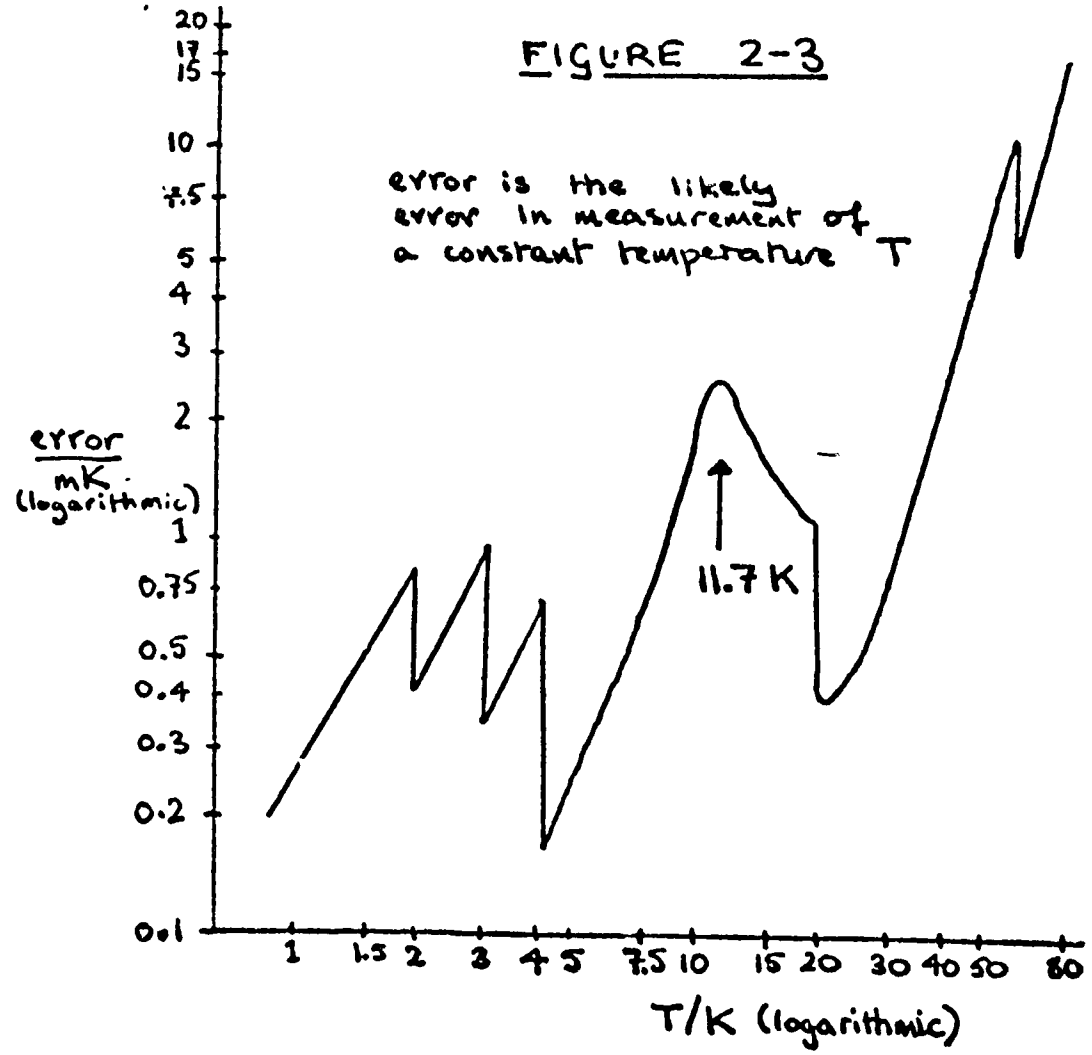

Table 2-1

No	smoothed function	fit to experimental points (i.e. deviations to be applied)	range of use	calibrations (all by d.c. potentiometer)
(1)	$\frac{T}{K} = \frac{a_0}{2} + \sum_{k=1}^{8} a_k \cos(k \cos^{-1} X)$ where $x = A \ln(\frac{R}{\Omega}) + B$	|deviation| $\lesssim$ 0.0033 K at all temperatures in range of use	$\frac{R}{\Omega} \geq 402.0$ ($\frac{T}{K} < 4.237$)	Rusby (1971) by comparison with NPL-calibrated Ge resistance thermometer (T_{62} He^3 scale < 2.2 K, T_{58} He^4 scale > 2.2 K) Thermometer current: - 1μA. Measurements from 0.49 K to 4.24 K
(2)	$\frac{T}{K} = \frac{\ln (R/\Omega)}{(A + B \ln (R/\Omega))^2}$	|deviation| $\lesssim$ 0.032 K at all temperatures in range of use	$402.0 \geq \frac{R}{\Omega} > 334.64$ ($4.237 \leq \frac{T}{K} < 5.022$)	Clay (1965) by He^4 vapour pressure from 2 K to 4.21 K, (T_{58} He^4 scale), He^4 gas thermometry from 4.21 K to 20 K. Clay and Dyball (see Dyball, 1966) by comparison with NPL calibrated Pt resistance thermometer (NPL - 1961 scale), >20 K. Thermometer currents:- 10 μA < 4.21 K 20 μA from 4.21 K to 20 K 50 μA from 20 K to 60 K 100 μA from 60 K to 84 K
(3)	$\log_{10}\frac{R}{\Omega} = a_0 + \sum_{k=1}^{6} a_k (\frac{T}{K})^{-k}$	|deviation| $\lesssim$ 0.22 K at all temperatures in range of use	$334.64 \geq \frac{R}{\Omega} > 154.36$ ($5.022 \leq \frac{T}{K} < 19.010$)	
(4)	$\ln \frac{R}{\Omega} = a_0 + \sum_{k=1}^{6} a_k (\frac{T}{K})^{-k}$	|deviation| $\lesssim$ 0.04 K from 19.01 K to 60 K; deviation $\lesssim$ 0.15 K from 60 K to 84 K	$\frac{R}{\Omega} \leq 154.36$ ($\frac{T}{K} \geq 19.010$ K) used up to 84 K	

Temperatures above 14 K obtained from functions and deviation plots were converted to IPTS-68 using "Measurement Science in the NPL", March 1969.

Table 2-2

Function No	1	2	3	4
A	+0. 349 200 223 6	-2. 389 917	-	-
B	-3. 093 614 774 1	+0. 596 793	-	-
a_0	+3. 185 471	-	-0. 168 99	+1. 936 508
a_1	-1. 578 944	-	+110. 332	$-6.\ 482\ 571 \times 10^{+1}$
a_2	+0. 644 254	-	-2019. 70	$+1.\ 190\ 292 \times 10^{+4}$
a_3	-0. 253 566	-	+19222. 5	$-4.\ 171\ 286 \times 10^{+5}$
a_4	+0. 101 246	-	-99 189. 3	$+7.\ 507\ 719 \times 10^{+6}$
a_5	-0. 036 501	-	+264 341	$-7.\ 462\ 432 \times 10^{+7}$
a_6	+0. 020 980	-	-285 173	$+3.\ 239\ 957 \times 10^{+8}$
a_7	-0. 002 496	-	-	-
a_8	+0.006 804	-	-	-

The results of these calibrations are expressed as a series of four functions (1) to (4) relating thermometer resistance and temperature, each function being used over a particular temperature range, and each function being used in combination with a deviation plot (smoothed by hand). Details of these functions are given in Tables 2-1 and 2-2.

The link-up between functions (2), (3), and (4), taken with their respective deviation plots, is practically perfect because of the way in which Clay and Dyball treated their results.

However, it was necessary to check on the link-up between functions (1) and (2), taken with their respective deviation plots, since these functions were derived by independent workers. At the changeover thermometer resistance of 402.0 Ω, function (1) with its deviation plot gave T = 4.235(1) K, and function (2) with its respective deviation plot gave 4.236(7) K. dT/dR at 402.0 Ω derived from functions (1) and (2) with their respective deviation plots were 8.98 mK Ω^{-1} and 9.03 mK Ω^{-1} respectively.

Self-heating

Because of the poor thermal conductivity of germanium, the resistance recorded on a germanium resistance thermometer for a given ambient temperature is significantly dependent on the power dissipated in the thermometer, because of self-heating (see, for example, P. Lindenfeld, 1962).

It is therefore necessary to select thermometer currents so that this self-heating effect is not substantial, while reasonably accurate resistance measurements are still possible. In the present work, the current used was varied with the temperature according to the following schedule: -

temperature	thermometer current
from 1.4 K to 2 K	1 μA
from 2 K to 3 K	2 μA
from 3 K to 4.2 K	5 μA
from 4.2 K to 20 K	20 μA
from 20 K to 60 K	50 μA
from 60 K to 84 K	100 μA

The currents in the above schedule correspond to those used in the various calibrations (see Table 2-1, right-hand column), except that Rusby used a current of 1 μA from 2 K to 4.2 K. Higher currents than this were used in the present work simply because the measuring apparatus was rather less sensitive than that used by Rusby.

The effect of self-heating was estimated in the course of the calorimetric runs. This was done by following the same "drift" first at lower current and then at higher current, and extrapolating the two sets of measurements to the time when the current was changed. It was found that the apparent temperature increased by less than 2 mK when the current was changed from 1 μA to 2 μA at about 2 K, from 2 μA to 5 μA at about 3 K, from 5 μA to 20 μA at about 4.2 K, or from 20 μA to 50 μA at about 20 K. When the current was changed from 50 μA to 100 μA at about 60 K, the apparent change in temperature was less than 4 mK.

It appears from these results that no unacceptable inaccuracy is caused by the choice of current.

Measuring circuit

The present author, like Clay, Dyball, and Rusby, measured the thermometer resistance by the well-known d.c. potentiometric method. The circuit is shown in Figure 2-4. The appropriate thermometer current is selected by using potentiometer P and selector switch S, and the potential drops across the thermometer and a 10 kΩ standard resistor can be measured at E and D on a precision potentiometer, a preamplifier and galvanometer being used for null detection. Switch X

FIGURE 2-4

(germanium thermometer circuit)

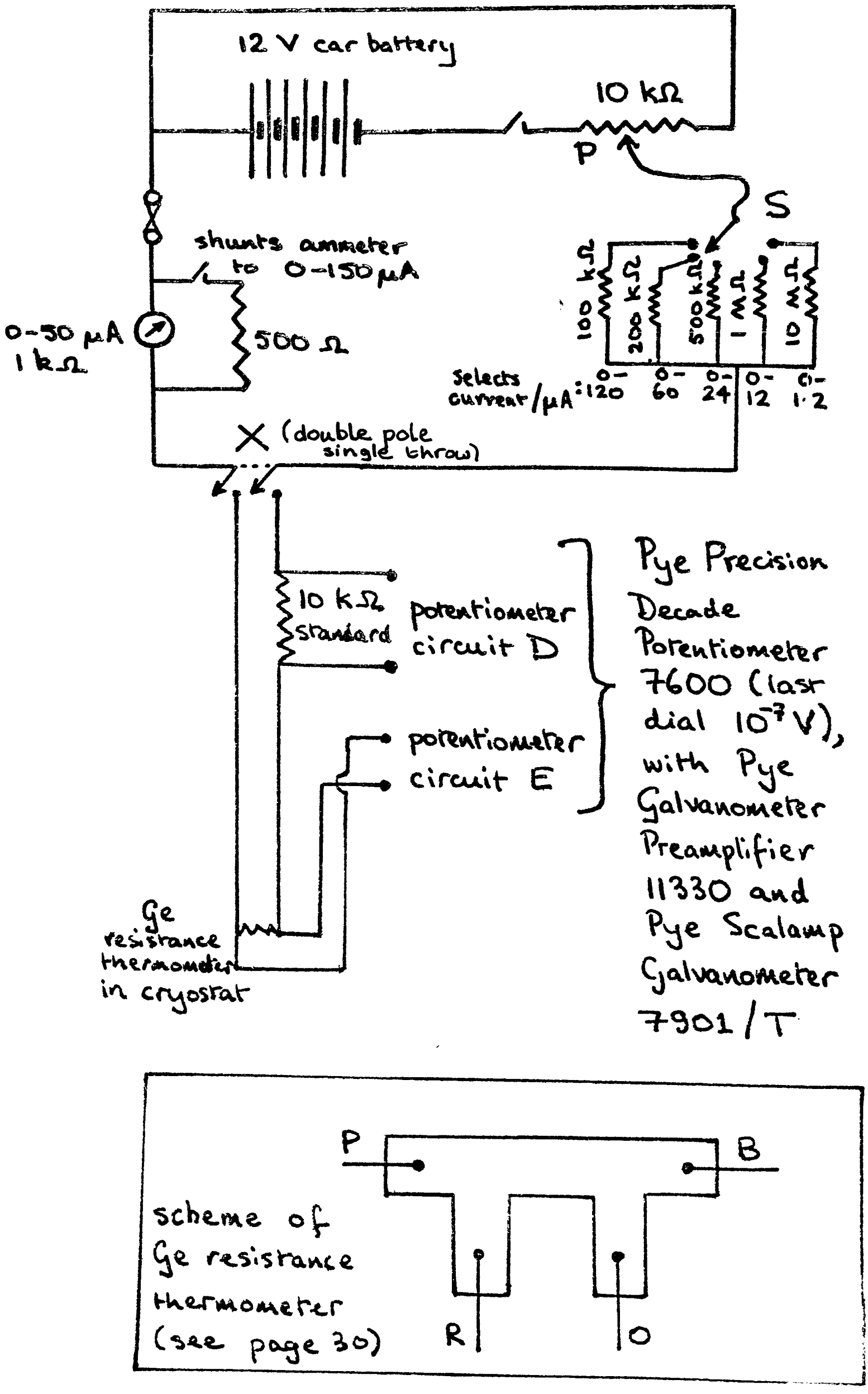

scheme of Ge resistance thermometer (see page 30)

allows the current to be switched off so that the "thermals" across the thermometer and the 10 kΩ standard resistor can be measured. The thermometer resistance is given by the resistance of the standard resistor (corrected for ambient temperature) x the ratio of the potential drops across E and D (corrected for "thermals").

(The "thermals" include not only genuine thermoelectric e.m.f.s in the circuit but also the spurious e.m.f. generated in the preamplifier when an open circuit (galvanometer key not depressed) is replaced by a closed circuit of low resistance itself generating no e.m.f.)

Crude calculations indicated that the likely error in temperature measurement with this circuitry was as plotted in Figure 2-3. The maximum at 11.7 K corresponds to the point of inflexion in Figure 2-2, while the discontinuities correspond to the changes in current used.

A 12 V car battery is used to provide a steady source of power for the thermometer, while the potentiometer is powered by two 2 V accumulators. Such power supplies were preferred to power packs since they guarantee that ac ripple is absent.

Normally, such ac ripple is unimportant in measurements by the dc potentiometric method. In the present case, however, even an ac ripple small in absolute terms could lead to an inaccurate determination of temperature (especially below 4.2 K) through self-heating, q.v.

Ambler and Plumb (1960) have noted that rf pickup in the leads to a germanium resistance thermometer will have the same self-heating effect. Accordingly, the leads to the thermometer were carefully screened, the screening being earthed - as, in fact, were all the leads, as a matter of course. Some check on rf pickup was made with

an oscilloscope connected across the terminals of the 10 kΩ standard resistor while a 1 μA current was passed through the thermometer. No signal was detected in the range from 50 Hz to 16 MHz on an oscilloscope capable of detecting signals as small as 5 mV (equivalent to 0.5 μA through the thermometer).

Section 2-5: the sample-containing vessel

The sample-containing vessel is shown in Plate 2-V (page 25).

The major part of the vessel comprises essentially a platinum-iridium tube 5 cm long by $2\frac{1}{2}$ cm diameter capped at both ends with platinum-iridium disks.

Platinum-iridium is not the ideal material for a low-temperature calorimeter vessel insofar as it has a much higher specific heat capacity at low temperatures than does copper. However, it has the merit of greater chemical inertness to a wide range of inorganic compounds. Clay had considerable trouble with copper calorimeter vessels, even when they were internally gold-plated, because of corrosion by the copper(II) compounds with which he was working (see Dyball, 1966a).

Attached through holes drilled in the flanges formed where the platinum tube and disks join are four nylon threads, pseudo-tetrahedrally disposed, by which the vessel is suspended within the shield. At the end of each thread is a loop for hooking over the adjusters set in the shield (see Section 2-6). Nylon threads of 0.22 mm diameter and about 14 mm overall length are used.

To the one end disk of the sample vessel there is soldered a hollow copper spike, on which the jaws of the thermal switch can be closed when the cryostat is assembled. Plate 2-VI shows a close-up of the jaws with the sample-containing vessel held manually in position.

Loading with sample; note on indium solder

In the other end disk of the vessel there is a filling port of about 5 mm internal diameter, through which the sample is introduced and removed. The port is surrounded by a gutter which takes a cap with a small central (~1 mm diameter) hole. Once the vessel has been filled with sample, a length of silver tube is soldered (with electrical solder) onto the cap to communicate with the small central hole. The cap with silver tube is then soldered into the gutter with indium solder (49% Bi, 15% Sn, 18% Pb, 18% In, m.p. 58° - see Catalano and Stout, 1955), and the vessel is evacuated and then filled with exchange gas (see below) via the silver tube. The vessel is then sealed off by flattening the silver tube, cutting the silver tube in the flattened region, and applying a cautionary blob of solder at the cut end. (The vessel shown in Plate 2-V has been filled and sealed off in this way.) The pressure of exchange gas employed is noted, and at various stages in the filling procedure just described weighings are made, with some care - in particular, the vessel is allowed to cool down and readsorb surface moisture after soldering operations. (The calculation of the set of molar heat capacities for a given charge of sample involves corrections involving the amounts of silver, solders, and exchange gas used - see Section 2-9d.)

Exchange gas in vessel

It is known that when He^4 is used as an exchange gas "at temperatures less than 10 K, particularly with powdered samples, adsorption of helium may result in complete loss of thermal contact, or the change in adsorption with temperature may cause a spurious heat effect" (McCullough and Scott, 1968).

Accordingly, in the present work, from about 7 to 15 mmHg of He^3 (measured at room temperature) was introduced into the sample-

containing vessel to maintain thermal contact between the vessel and the sample, following Colwell et al (1969), who reported that 10^2 N m^{-2} (0.75 mmHg) of the He^3 maintained thermal contact with rare earth trihalide samples down to 1 K, 10^3 N m^{-2} (7.5 mmHg) down to 0.3 K. Satisfactory equilibrium times were obtained in fact with bis(adiponitrile)copper(I) nitrate (Chapter 3) and tetramethylammonium manganese chloride (Chapter 4). Equilibrium times were less satisfactory with metal-free phthalocyanine (Chapter 5), even above 4.2 K, but the reasons for this are obscure.

Electrical heater on vessel

In order to minimise the amount of heat generated in the leads to the heater on the vessel for any given power dissipation in the heater, the heater was wound to a very high resistance (about 1900 Ω). (The zig-zag patterning in Plate 2-V is the heater winding.) In order to achieve such a high resistance on such a small vessel, a remarkable alloy called Karma (British Driver Harris Trade Mark, Ni 76%, Cr 20%, remainder Fe, Al) was used. This has over $2\frac{1}{2}$ times the resistivity of manganin or constantan at room temperature (Furakawa et al, 1964). The present heater was non-inductively wound onto the tubular part of the vessel in 43 SWG fibre-glass-coated Karma, and secured and insulated with GE 7031 varnish.

In Figure 2-5 is plotted the heater resistance as a function of temperature, as determined in the course of calorimetric runs. Figure 2-5 confirms the further observation of Furakawa et al that down to 10 K the resistivity of Karma is many times less sensitive to temperature than is manganin or constantan. This makes for much greater ease and precision in the measurement of heater power in calorimetric work, in which the temperature of the heater during use is commonly changing at a rate of from 0.1 to 1 K min^{-1}. Below 15 K, and more

FIGURE 2-5

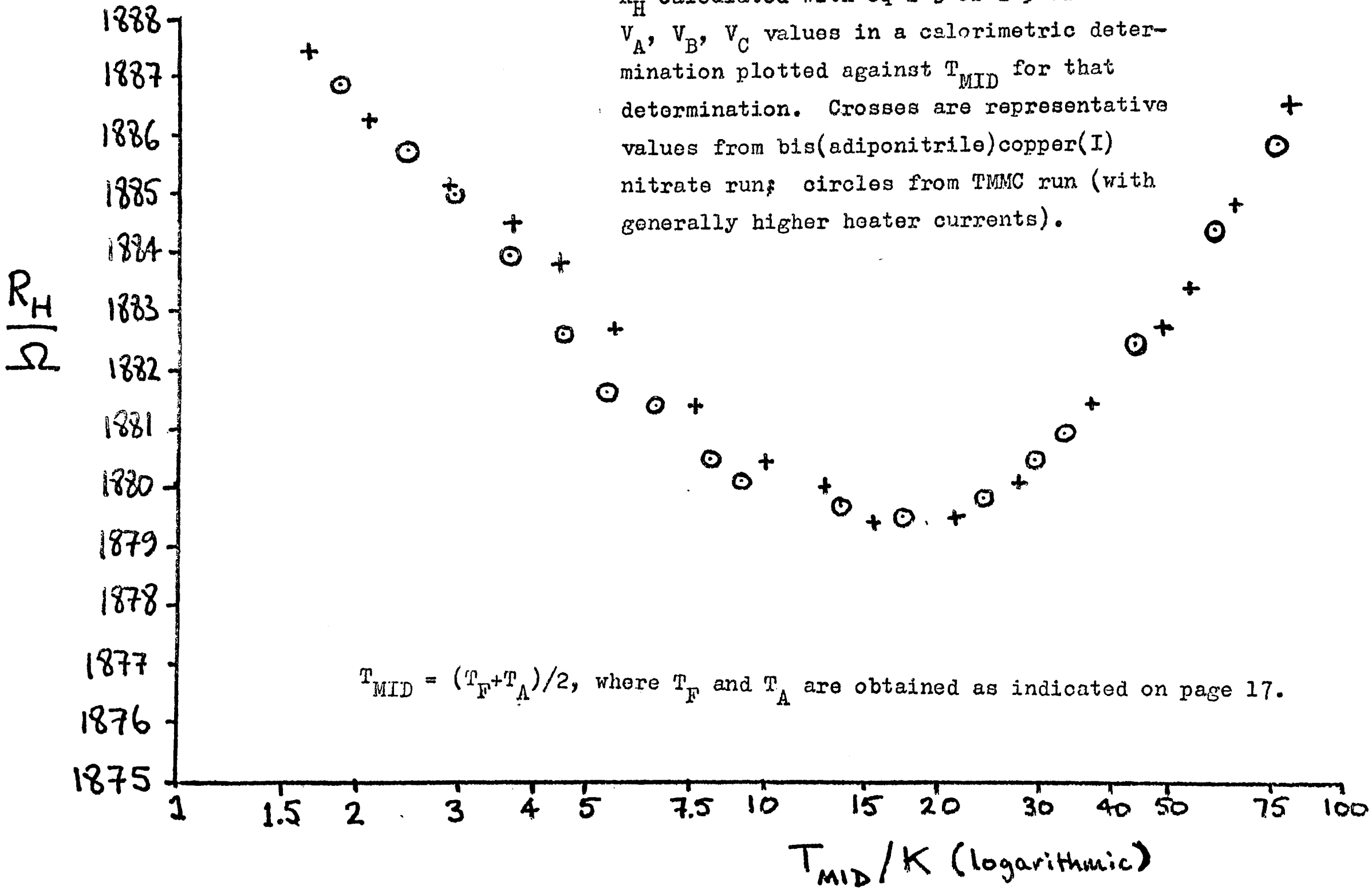

R_H calculated with eq 2-3 or 2-5 from mean V_A, V_B, V_C values in a calorimetric determination plotted against T_{MID} for that determination. Crosses are representative values from bis(adiponitrile)copper(I) nitrate run; circles from TMMC run (with generally higher heater currents).

$T_{MID} = (T_F+T_A)/2$, where T_F and T_A are obtained as indicated on page 17.

markedly below 10 K (the lower limit of Furakawa et al's work), the heater resistance was observed to increase with decreasing temperature, and apparently was somewhat dependent on the heater current.

Electrical connections on vessel; note on thermal-free solder

A piece of copper foil is screwed onto a lug half-way along the length of the platinum-iridium tube (as shown in profile in Plate 2-V). The manganin - constantan thermocouple for adiabatic shield operation is fixed to the foil without electrical contact by Araldite, and a separate manganin wire (forming part of the "indicator circuit", see later) is soldered onto the foil so as to be in electrical contact with the vessel.

Adjacent to the filling port in Plate 2-V the cable of leads from the vessel is seen emerging from a copper-foil protective hood, the purpose of which is to protect the various leads, and also, especially, the germanium resistance thermometer from mechanical damage during handling. Figure 2-6a shows the arrangement below this hood, and Figure 2-6b the way in which the hood is fixed onto the vessel.

As shown in Figure 2-6a, the thermocouple, indicator circuit, and heater leads pass over the edge of the platinum-iridium disk into the space enclosed by the hood. The germanium resistance thermometer is fitted in a copper block with a central hole, and Apiezon T grease provides good thermal contact between the block and the thermometer. All the leads (2 thermocouple, 1 indicator, 4 thermometer, 2 heater, and also 1 spare) are varnished with GE 7031 varnish about a hollow copper anchoring post, 8 mm in diameter, before they are bound together to form the cable. The post serves two functions: firstly, it secures the cable so that tension on the cable cannot damage the individual very thin leads to the thermometer, etc.; and secondly, it thermally anchors the leads to the vessel. The second function is particularly

FIGURE 2-6a

(~3x FS)

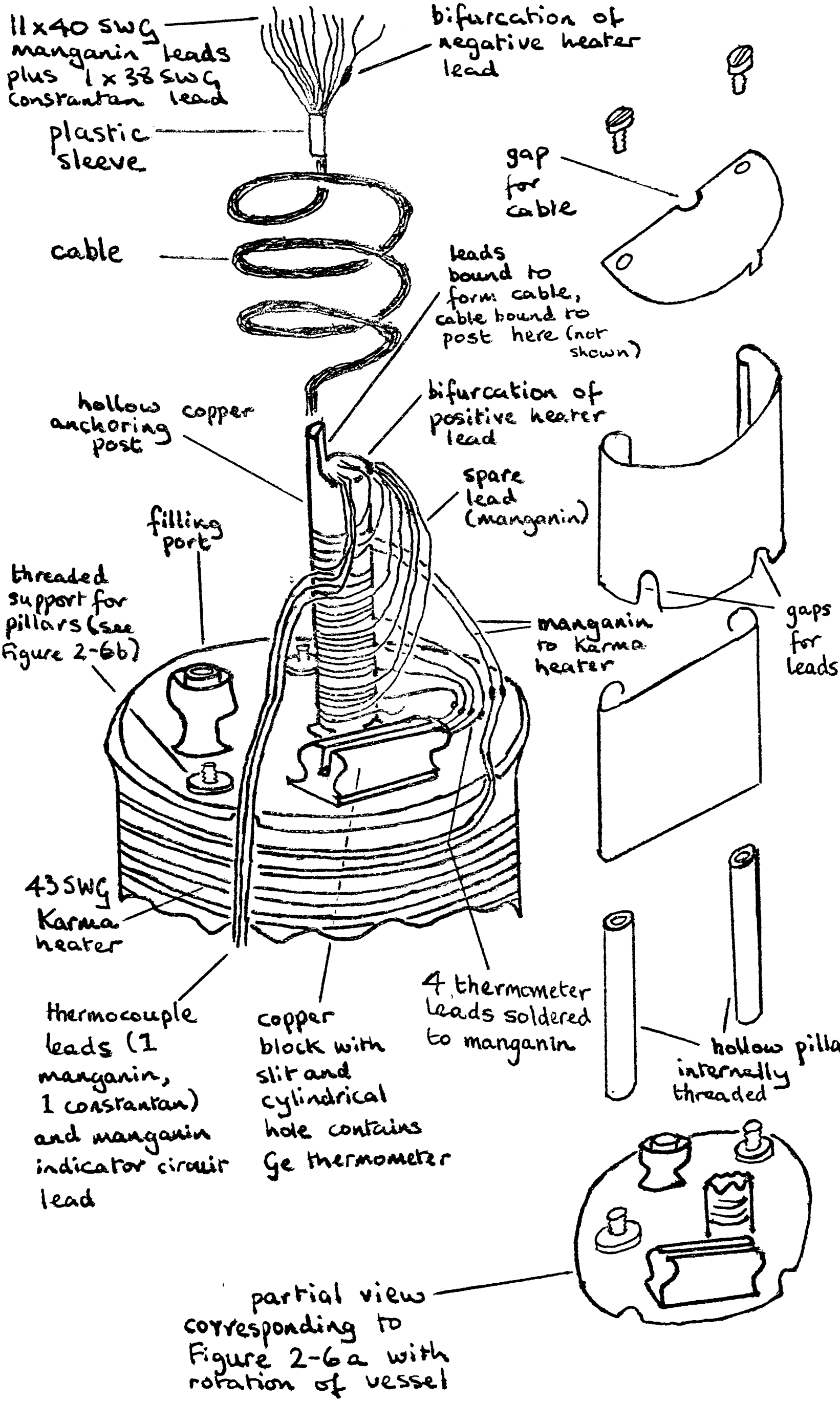

FIGURE 2-6b

partial view corresponding to Figure 2-6a with rotation of vessel

important for the leads to the thermometer, which could otherwise be very significantly locally heated or cooled by conduction along the leads when the shield is at a substantially different temperature from the vessel; therefore, following Colwell (1969), approximately 10 cm of each thermometer lead was wrapped about the post.

The construction of the various parts of the hood and of the anchoring post was so light that their total contribution to the heat capacity of the empty vessel was calculated to be only a few per cent at any temperature.

The cable of leads from the vessel is in the form of a springy spiral (to maximise the thermal conduction path length for a given shield-vessel distance), and all the leads are 40 SWG manganin except the 38 SWG constantan thermocouple wire. In higher-temperature calorimeters (e.g. the "Linford" calorimeter, q.v.) the cable from vessel to shield generally comprises mainly copper leads. For low-temperature work, the use of copper in such situations is to be avoided, since thermal conductivities generally fall with temperature less quickly than heat capacities, so that higher standards of thermal insulation must be adopted. The thermal conductivity of copper in the 1 - 20 K region as reported by Chemical Rubber Company (1974) is of the order of 10^4 greater than that of manganin or constantan; accordingly even a single copper lead in the cable would have a very serious effect on the "drifts" of the vessel (especially below 4 K). It was for this reason that a manganin-constantan thermocouple was preferred to the more usual manganin-copper thermocouple (in any case, the thermoelectric powers of the two thermocouples are of the same general magnitude and sign).

The end of the cable remote from the vessel has a plastic sleeve which allows the cable to be secured by means of a screw at the bottom

cap of the shield (see Section 2-6).

All the soldered electrical connections on the vessel - and throughout the cryostat - are made with thermal-free solder (70.44% Cd, 29.56% Sn, see White, 1968). This solder has a low thermoelectric force with respect to copper, Karma, and manganin, and accordingly its use should avoid the generation of large thermal e.m.f.s by temperature gradients across soldered junctions involving wires of these materials.

It will be seen from Figure 2-6a that the two heater leads bifurcate, the one at the vessel end of the cable and the other at the shield end of the cable (compare West and Ginnings, 1958). This arrangement makes an automatic correction for the heat generated in the leads, at least partially (see the following sub-section).

Power circuit for vessel heater

The power circuit for the heater on the vessel is shown in Figure 2-7, in which the essential components and also various lead resistances r_1, r_2, and r_3 are indicated.

Operation of switch Z sends power to the vessel heater and at the same time starts an electronic timer. When Z is in the off position a variable dummy heater is substituted for the real load so as to maintain circuit stability between vessel heating periods. After each heating period in a calorimetric run, the dummy is adjusted to give the same current (measured on the potentiometer) as was observed towards the end of the heating period with the real heater.

Over the temperature range from 1.4 to 84 K there is an enormous variation in heat capacities and therefore in the heating powers needed. The control in heating power is achieved by adjusting the power unit output voltage, the 0 - 20 kΩ resistance box, and the "low/high power" switch Y. The potentiometer cannot directly measure

FIGURE 2-7
(vessel heater circuit)

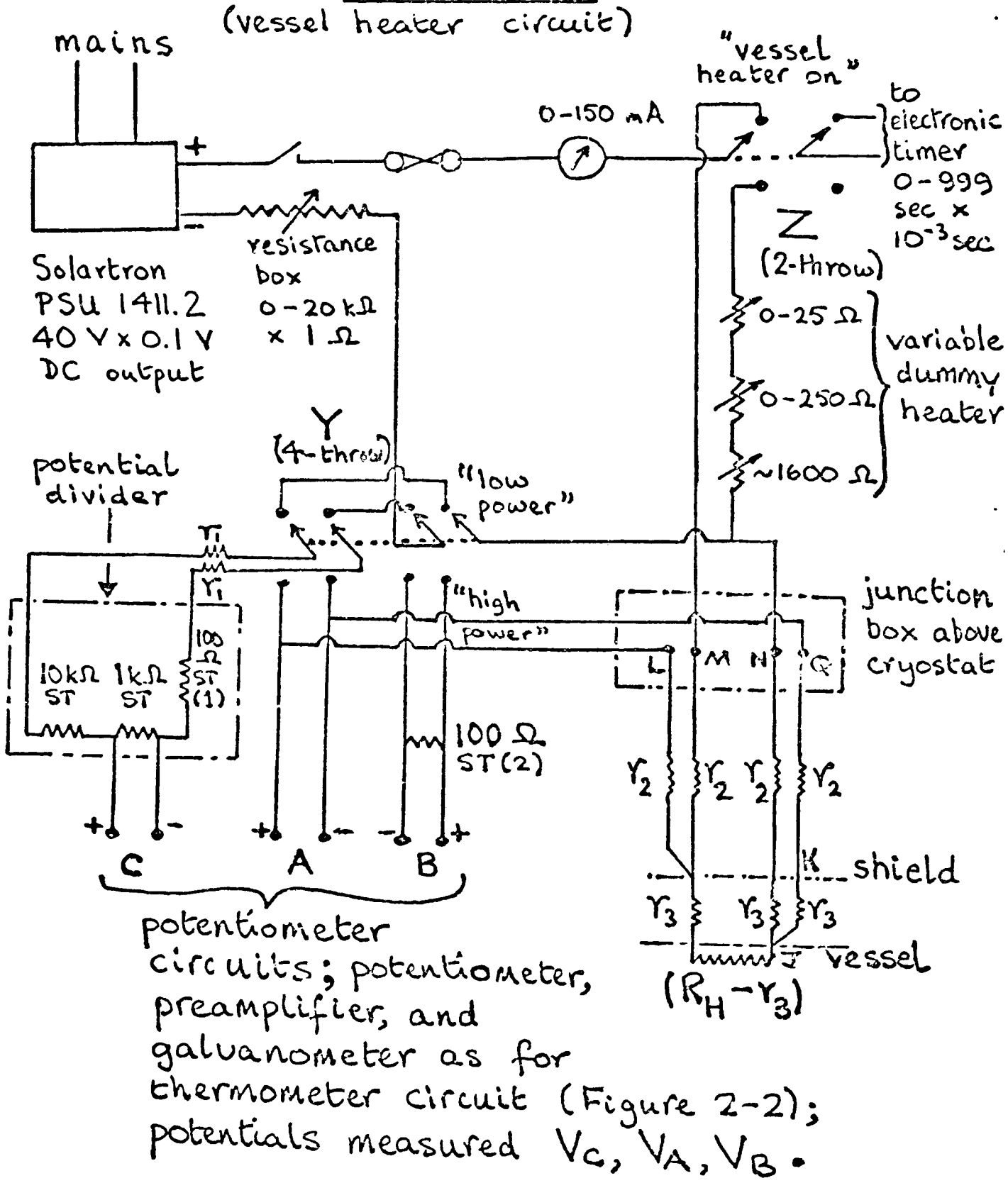

R_H is resistance of heater as plotted in Figure 2-5;

r_1s are lead resistances (marked positions notional) from potential divider to L, Q when Y is in high power position;

r_2s are lead resistances from junction box to shield;

r_3s are lead resistances from shield to vessel.

Values used:

$$2r_1 = 0.65\ \Omega$$

$$\frac{(2r_2+r_3)}{\Omega} = 18.0 + \frac{1.68}{90} \times \frac{T_{MID}}{K}$$

$$\frac{r_3}{\Omega} = \frac{8.69(T_{MID}-20) + 8.18(90-T_{MID})}{70}$$

} equations 2-2 precision 0.1 Ω approx.

$T_{MID} = (T_F+T_A)/2$, where T_F and T_A are obtained as indicated on page 17.

potentials of more than 2 V, and in the "high power" setting, the voltage drop across the heater is divided on the potential divider. In the "low power" setting, the potential divider serves as a series resistance, the 1 kΩ resistance in it being used to measure the heater current, while the potential drop across the heater is measured directly. The high to low change is generally made in the 8 - 16 K temperature range.

On the low power setting, the heater resistance R_H is given by

$$R_H = V_A \times \left(\frac{V_C}{R_{1k\Omega ST}}\right)^{-1} \qquad \text{eq. 2-3}$$

and, if it is assumed that any heat generated in the leads r_3 goes equally to vessel and shield, the heater power P is given simply by

$$P = V_A \times \frac{V_C}{R_{1k\Omega ST}} \qquad \text{eq. 2-4}$$

On the high power setting, the heater resistance is given by

$$R_H = \frac{V_C \times (R_{10k\Omega ST} + R_{1k\Omega ST} + R_{100\Omega ST(1)} + 2r_1 + 2r_2 + r_3)/R_{1k\Omega ST}}{(V_B/R_{100\Omega ST(2)} - V_C/R_{1k\Omega ST})} \qquad \text{eq. 2-5}$$

The heater power is given by

$$P = \frac{V_C \times (R_{10k\Omega ST} + R_{1k\Omega ST} + R_{100\Omega ST(1)} + 2r_1 + 2r_2 + r_3)}{R_{1k\Omega ST}} \times$$

$$\left(\frac{V_B}{R_{100\Omega ST(2)}} - \frac{V_C}{R_{1000\Omega ST}}\right) + \frac{r_3}{2}\left(\frac{V_C}{R_{1000\Omega ST}}\right)^2 \qquad \text{eq. 2-6}$$

The latter term in the last equation accounts for the heat generated in lead JK of the divider circuit between the vessel and the shield. The values of $2r_1$, $2r_2 + r_3$, and r_3 used in equation 2-6 are obtained from equations 2-2 (page 46, below Figure 2-7); equations 2-2 were derived from measurements with an Avcmeter or an Advance Multimeter (these measurements being of adequate accuracy

having regard to the smallness of the terms in question in equation 2-6).

Indicator circuit

The indicator wire which provides electrical contact with the vessel serves in a simple indicator circuit (Figure 2-8) which is used to check whether the jaws are open or closed. This circuit helps the operator to guard against possible sticking of the jaws and also against excessive tightening of the jaws.

Section 2-6: the shield cylinder and the bottom cap of the innermost chamber

The innermost chamber, as has already been seen in Figure 2-1 (page 22) and in Plates 2-IV (page 25) and 2-I (page 23) is formed from three parts, demountable at joints Y and Z in Figure 2-1. The three parts are an upper lid, carrying the helium-3 pot and the jaws of the thermal switch; a cylindrical portion (hereinafter called the shield cylinder); and a bottom cap. The latter two parts are particularly described in this Section.

Once the vessel has been loaded and sealed as described in Section 2-5, it must be suspended and enclosed within the innermost chamber by means of its pseudo-tetrahedrally disposed nylon loops, and wired up electrically. The steps of this operation are illustrated in Figure 2-10, which constitutes a partly exploded view of the fully assembled chamber. In the following discussion, underlining indicates the first mention of a feature labelled in Figure 2-10.

The first step of the operation illustrated in Figure 2-10 is the suspension of the vessel by its upper two nylon loops from screw adjusters tightening against supports set in an annular plate, the central hole of which leaves the vessel's spike free. The male part

FIGURE 2-8

(indicator circuit)

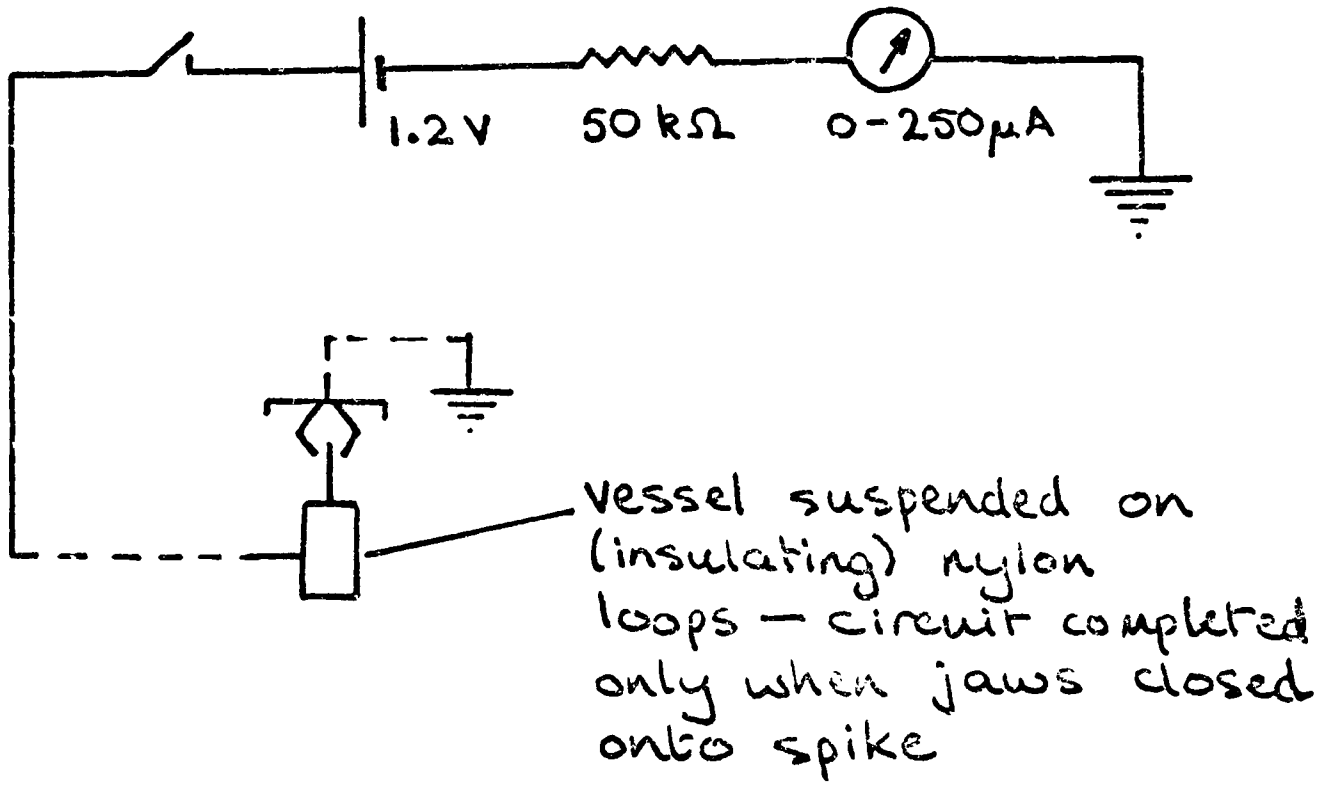

FIGURE 2-9

(shield heater circuit)

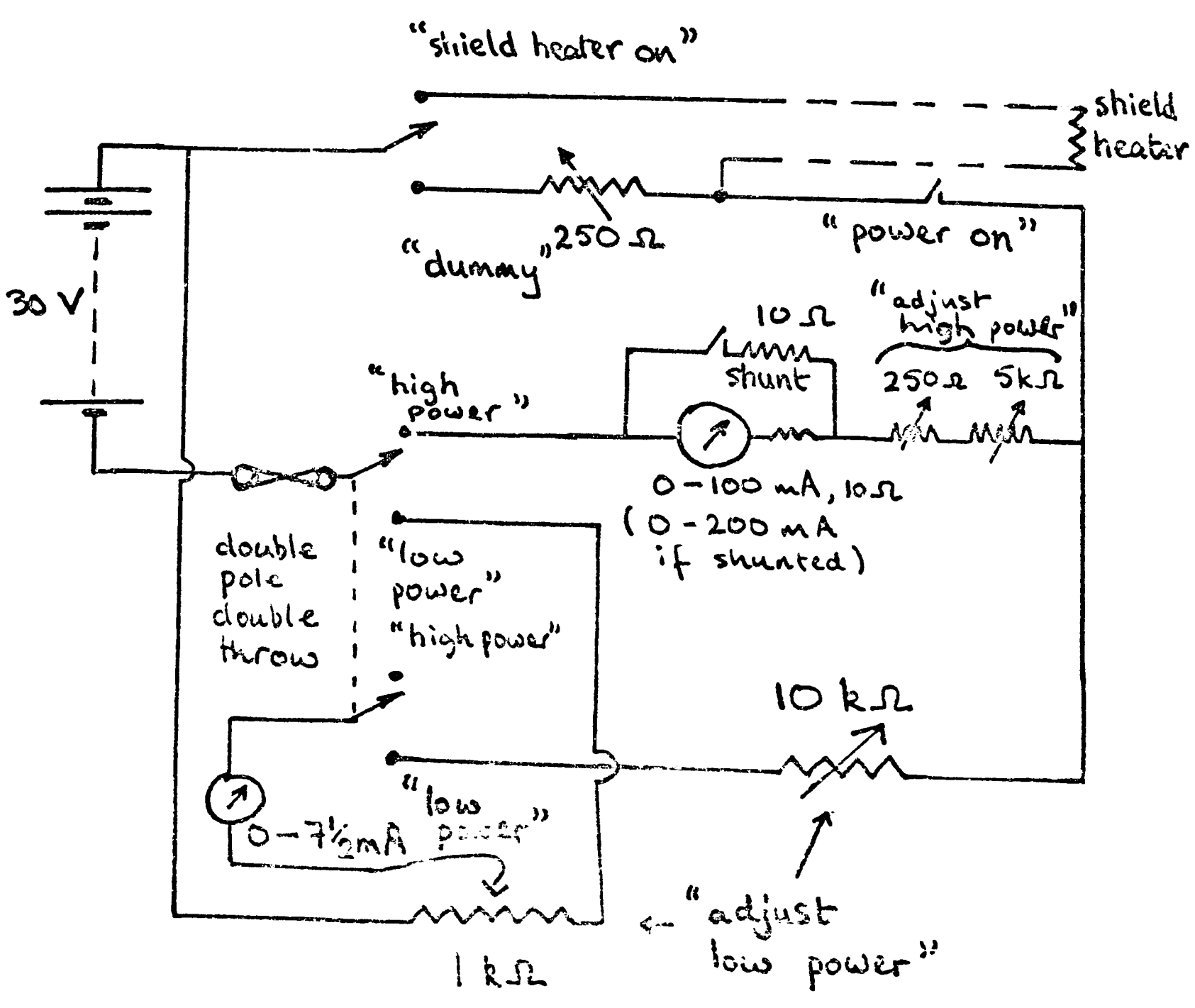

Figure 2-10

Engineering sketch (not to scale); both views exploded; both views in section except for sample-containing vessel; supports for distribution boards not shown; most leads and grooves not shown

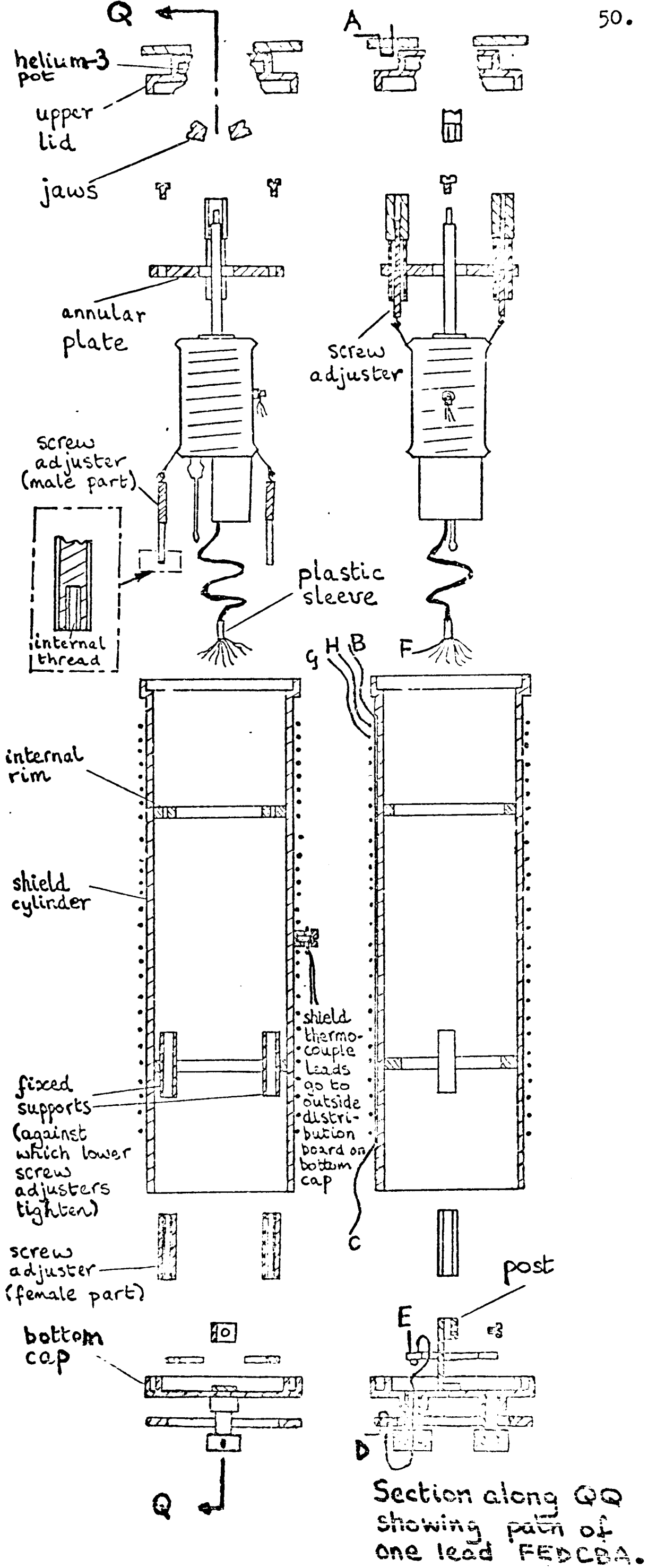

of each of two further screw adjusters is suspended from each of the lower two nylon loops. Then the plate with pendant vessel is lowered onto an internal rim in the shield cylinder, the male parts of the lower screw adjusters being guided at the same time through fixed supports set in the shield cylinder. For this guiding, use is made of long metal rods threaded at the end and screwed temporarily into the internal thread in each of the male parts. The plate is then screwed down onto the internal rim, and all four adjusters are tightened with a special tool, care being taken to maintain the spike centrally. See Section 2-9a under the sub-heading "Vibration" for some comment on the desirable tensioning of the adjusters.

The next step is to bring up the bottom cap, screw-clamp the plastic sleeve of the cable to the post on the inside of the cap, and make electrical connections such as F to E to the distribution board on the inside of the cap (with thermal-free solder). Vacuum-tight connections through the cap via epoxy lead-through seals (see pages 28 to 29) are permanent, such as E to D (D being on a distribution board on the outside of the cap).

Then, indium-soldered vacuum-tight joints are made between the cap and the shield cylinder and between the shield cylinder and the upper lid; and further soldering of leads such as D to C and B to A (this scheme being modified somewhat in the case of the thermocouple circuit - see Figure 2-11) makes all the necessary electrical connections from the vessel as far as a distribution board on top of the helium-3 pot, from which board all connections to the outside world are permanent. The shield heater leads G, H are connected to this board at the same time.

* * *

It is to be noted that wires such as BC (consisting of 36 SWG

fibre-glass-covered copper) pass in grooves beneath the shield heater for thermal anchoring; this can be plainly seen also in Plate 2-I (page 23).

* * *

The shield heater is non-inductively wound in 32 SWG manganin to a room temperature resistance of 200 Ω, and is powered by the circuit shown in Figure 2-9 (page 49). As with the vessel heater circuit, two ranges of power are provided, since a wide range of currents are necessary, both because of the wide temperature range over which the apparatus was used and because, even at a single temperature, currents during a "drift" will be substantially less than during a heating period.

Section 2-7: the remainder of the central assembly

The remainder of the central assembly (as defined in Section 2-3 and as shown in Figure 2-1 on page 22) comprises the fixed part of the cryostat from the lid of the outermost chamber to the lid of the innermost chamber and also the removable cans of the outer two chambers. The essential functions of the various parts have been described in Section 2-3; more detailed comments on various features follow.

* * *

It was previously noted (page 26) that the pumping tubes passing between the chambers are of stainless steel for low thermal conductance. However, it will be seen by comparing Plate 2-VI (page 25) with Figure 2-1 that the pumping tube for the helium-3 pot (S in the Plate) passes <u>through</u> the helium-4/nitrogen pot, and that the pumping tube for the innermost space (T in the Plate) passes <u>through</u> both the helium-4/nitrogen and the helium-3 pot. This achieves

excellent thermal anchoring of the tubes; but since the pots are of copper the materials of these tubes change over to copper where they pass through the pots, so as to avoid excessive strain when the cryostat is cooled.

Thermal switch

The thermal switch, clearly shown in Plate 2-VI, is operated by a wire attached to the inside of a metal bellows in the centre of the top lid (see Plate 2-II, page 24). This wire runs in the pumping tube for the innermost space. The thermal switch is generally similar to that used by Manchester (1959). Referring to Plate 2-VI, the two copper jaws of the thermal switch are pivoted in copper brackets soldered onto the bottom side of the lid of the innermost space. A spring between the jaws keeps the jaws apart until the wire from the bellows is moved upwards. The wire from the bellows, on being raised, moves an ovoid-shaped member (shown about 5 mm above the spring in Plate 2-VI) which engages with both jaws. Good thermal contact between the jaws and the lid is provided by copper braid screwed onto each jaw and fastened onto a solid copper pillar soldered to the lid (these features are almost completely hidden behind the jaws in Plate 2-VI). The surfaces of the jaws engageable with the spike of the vessel are concave so as to engage with as large an area of the cylindrical spike as possible, and are coated with indium metal (which according to Manchester should further improve the conductance of the switch).

* * *

Each of the pumping tubes reaching the lid of the outermost chamber is "baffled" so that any radiation reaching this level down the tubes is absorbed and does not reach the inner two chambers. In the case of the tube to the outermost space, the baffle is in the

form of a copper "hat" with holes in the cylindrical sides, positioned on the underside of the lid (see Plate 2-I, page 23). The pumping tubes to the helium-4/nitrogen pot and the helium-3 pot, which pass through the lid, have internal baffles of a somewhat modified form. The pumping tube to the innermost space follows a zig-zag path at this point anyway, where it connects with the bellows of the thermal switch, so that no extra measure was necessary in that case.

Helium-3 pot and helium-4/nitrogen pot and their operation

The helium-3 pot has a total internal volume of 5 cm^3. As already mentioned, this pot developed a leak and was not used; but it was calculated that the evaporation of 5 cm^3 of liquid He^3 would have been adequate to bring the temperature of shield and vessel (containing any likely sample) from 1.4 - 1.5 K down to 1 K provided that heat leaks from the intermediate chamber to the innermost chamber were not large.

The volume of the helium-4/nitrogen pot is about 70 cm^3. The size of this pot was chosen to be generally in line with that used by other workers in comparable calorimeters; Manchester (1959) used a pot of about 180 cm^3 capacity, Leadbetter and Wycherly (1970) a pot of 130 cm^3 capacity, and Craig et al (1965) a pot of 40 cm^3 capacity.

In view of the large volume of liquid helium involved, introduction of the liquid from the helium-containing monax dewar is preferred over introduction by condensing gas under pressure; in the present apparatus this is effected by the needle valve in the lid of the outermost chamber. The procedure of condensing helium gas would require the use of 54 litres of helium gas at ordinary temperature and pressure to fill the pot, and would be time-consuming. Further, even if

the gas were precooled to 80 K before being passed into the helium-4/nitrogen pot, about 1.4 l of the liquid helium in the dewar would be boiled off.

It is worthy of note, however, that the volume chosen for the helium-4/nitrogen pot is far greater than can be justified by a simple calculation of the quantity of liquid helium which must be evaporated to cool the intermediate and innermost chambers (including the vessel containing the sample) to 1.4 - 1.5 K and then to maintain this temperature for, say, 8 hours against the thermal conduction along the tubes and leads from the lid of the outermost chamber to the lid of the intermediate chamber. The reason for this discrepancy is apparently that two other heat leaks are involved: (1) the conduction through the helium exchange gas remaining within the outermost chamber, which is put into the space when the apparatus is being cooled down and which cannot then be easily pumped away; and (2), potentially very important. the conduction of heat along a film of superfluid helium (the λ-point of He^4 is at 2.17 K) in the tubes down to the helium-4/nitrogen pot. It has long been known that effect (2) can be minimised by constricting the tube to the helium-4 pot (Blaisse et al (1939)); in the present calorimeter, the two tubes from the lid of the outermost chamber into the pot were chosen to have an internal diameter of 2 mm.

From the lid of the outermost chamber upwards, however, it is desirable to make the tube to the pot as wide as possible for maximum pumping rates. Thus the tube diameter is 9.6 mm up to above the economiser can, while still wider tubes (1") are used from the economiser can to the pump, a single-stage 100 l/min rotary pump. A manometer is provided in the line to monitor the pressure, and a ball valve is provided for throttling the pumping.

The needle valve comprises a stainless steel needle (angle at tip of 13°) moveable vertically, with no rotary motion, onto a phosphor-bronze seat. A copper sleeve, about 15 mm high (with an inlet hole in the lower portion) protects the seat, to some extent, from mechanical damage.

* * *

The pumping lines to the three main spaces (outermost, intermediate, and innermost) are connected to a single large vacuum line, so that each space can, if desired, be pumped by one of two fast single-stage diffusion pumps with liquid nitrogen traps, each with a Penning gauge, and backed by the same three-stage diffusion pump and rotary pump. Backing volumes are provided for the fast diffusion pumps so that each can function for a time while the three-stage diffusion pump and rotary pump are being used to rough out helium from either of the other two spaces. In practice, two fast diffusion pumps (rather than three) prove to be adequate, simply because it is never necessary to pump all three spaces independently at the same time with fast diffusion pumps.

Shield control - carbon resistance thermometer and thermocouple circuit

The carbon resistance thermometer used for shield control was an Allen-Bradley radio resistor. Although very cheap, these resistors are useful as low-temperature thermometers below the N_2 b.p. provided that high stability to thermal recycling is not essential (as in the present case). The resistors can be obtained from Oxford Instrument Company Limited, Osney Mead, Oxford OX2 0DX.

The resistor (47 Ω, 1/4 W) is Araldited onto the lid of the innermost chamber, next to the outer wall of the He^3 pot (at the side not visible in Plate 2-VI) and two leads from this resistor are connected to the distribution board on top of the helium-3 pot, whence

they pass to the outside world (see next sub-section). A pair of dummy leads join together at the same level, having also come in from outside the cryostat. The four leads (see Figure 2-11) are connected to a simple home-made Wheatstone bridge which is used to measure the resistance of the Allen-Bradley resistor. The galvanometer of the Wheatstone bridge circuit also serves as the detector for the signal from the thermocouples on the vessel and shield (also see Figure 2-11).

The thermocouple circuit is used for adiabatic operation above 20 K, and the carbon resistor for isoperibolic operation over the 4.2 K - 20 K range. In addition, over the entire working range of the calorimeter, the carbon resistance thermometer is useful for the approximate checking of the shield temperature.

The temperature variations of the resistances of the two 47 Ω, 1/4 W resistors used (one was damaged and had to be replaced) were roughly similar. The one had, very approximately, resistances of 47 Ω at 300 K, 75 Ω at 51 K, 95 Ω at 25 K, 160 Ω at 10 K, 420 Ω at 4.4 K, and 5000 Ω at 1.4 K. This variation is generally in line with that observed by Goodall (1965) for similar resistors, except that he provides no value at a temperature as low as 1.4 K.

* * *

From the distribution board on top of the He^3 pot (through which the vessel heater, shield heater, indicator, thermocouple, and carbon resistance thermometer circuits pass) 40 SWG manganin wires pass to the bottom of the helium-4 pot, where they are soldered to 38 SWG copper wires wrapped around the cylindrical part of the pot for thermal anchoring and secured and insulated with GE 7031 varnish. In Plate 2-VI the pieces of plastic sleeving covering the soldered joints are visible, but the wires wound around the pot are concealed by protective nylon

FIGURE 2-11

(carbon resistance thermometer and thermocouple circuit)

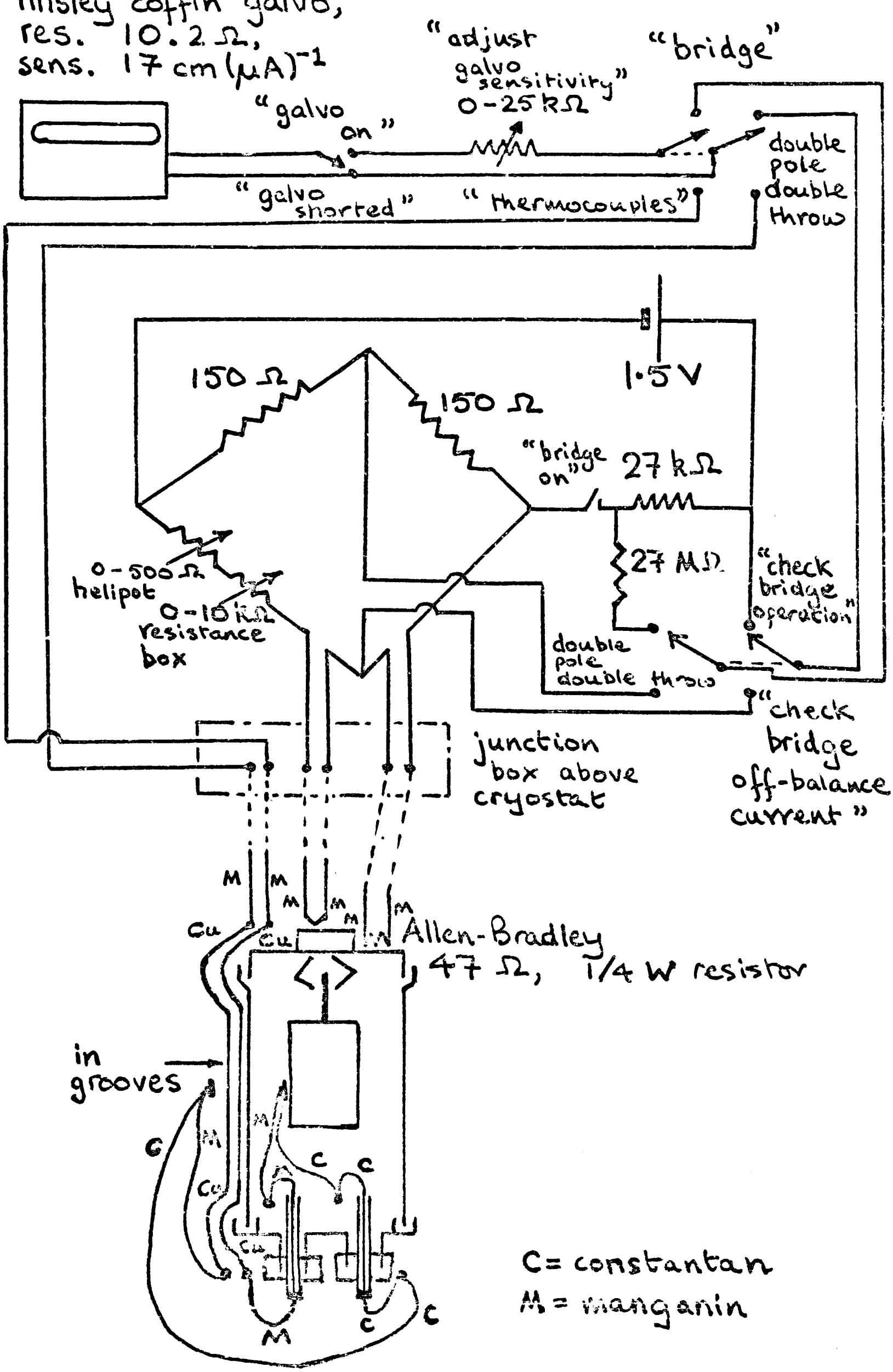

Total resistance of thermocouple circuit approx. 10 Ω ±0.1 Ω
Sum of lead resistances to Allen-Bradley resistor approx. 10 Ω.

gauze.

These copper wires now connect to the copper wires passing through the epoxy-resin lead-through seals in the lid of the intermediate chamber. 40 SWG manganin wires connect the upper side of these lead-through seals to the lower side of the lead-through seals in the lid of the outermost chamber.

* * *

Cans of intermediate and outermost chambers - further comments on the assembly of the cryostat for a run

The cans which form, with the respective lids, the intermediate and outermost chambers (see Plate 2-I and Figure 2-1) are made of copper. Inevitably the cylindrical walls of these cans provide a substantial part of the total mass of the part of the assembled cryostat which is immersed in liquid helium, and accordingly account for a substantial part of the helium boiled off when this part of the cryostat is cooled from 77 K to 4.2 K. The wall thickness was therefore made as thin (0.8 mm) as seemed safe (nevertheless this is thinner than would be safe for long unsupported tubes of these diameters), while ribs were provided along the length of the cans for extra reinforcement. (See Sanders and Windenberg (1931) for a discussion of the elastic collapse of tubes supported at the ends and/or by ribs.) The outermost can is externally covered with a thin layer of tin-lead solder, to provide some protection against corrosion.

Once the innermost chamber has been assembled and the electrical connections have been made as described in Section 2-6 (i.e. assembly has reached the point shown in Plate 2-I), the two cans are indium - soldered on (see Plate 2-II). During the assembly of the cryostat for each run, leak testing with a helium leak-detector and also

electrical testing is performed at every stage, the former, where possible, after cooling the cryostat in liquid nitrogen to guard against low-temperature leaks. In the present work, it was universally found that these precautions were time-saving in the long run, especially since newly-sprung leaks were not confined to the temporary indium-soldered joints. Even leaks in the permanent "ordinary"-soldered joints could be readily sealed with experience; but the leak in the helium-3 pot, at a silver-soldered joint, could not.

Section 2-8: the remainder of the cryostat - liquid helium level detectors, economiser can, dewars, hoist, liquid nitrogen level detectors

Once the assembly of the calorimeter has reached the point described in the last section (all chambers assembled and electrical and leak testing complete), three liquid helium level detectors are positioned on the outside of the outermost can by tying them with silk thread, covering them with cigarette paper, and securing the paper with a little varnish (see Plate 2-II). These liquid helium level detectors, and also the two detectors permanently positioned between the economiser can and the lid of the outermost chamber, consist of 47 Ω, 1/4 W Allen-Bradley resistors wound round with 25 Ω heaters of 43 SWG fibre-glass-covered Karma, secured by varnish.

The external circuitry for the use of the detectors is contained in a portable box (just visible near the bottom left-hand corner of Plate 2-III), which is connected to the junction box above the cryostat by a long flexible lead. The entire circuit is shown in Figure 2-12. In order to check whether a detector is in liquid helium, a potential of about 0.1 V (adjusted by potentiometer A with switch G in "set volts" position) is applied to the resistor. At 4.2 K the current is typically 170 μA, regardless of whether the resistor is

FIGURE 2-12

(liquid He and - inset - liquid N_2 level detectors)

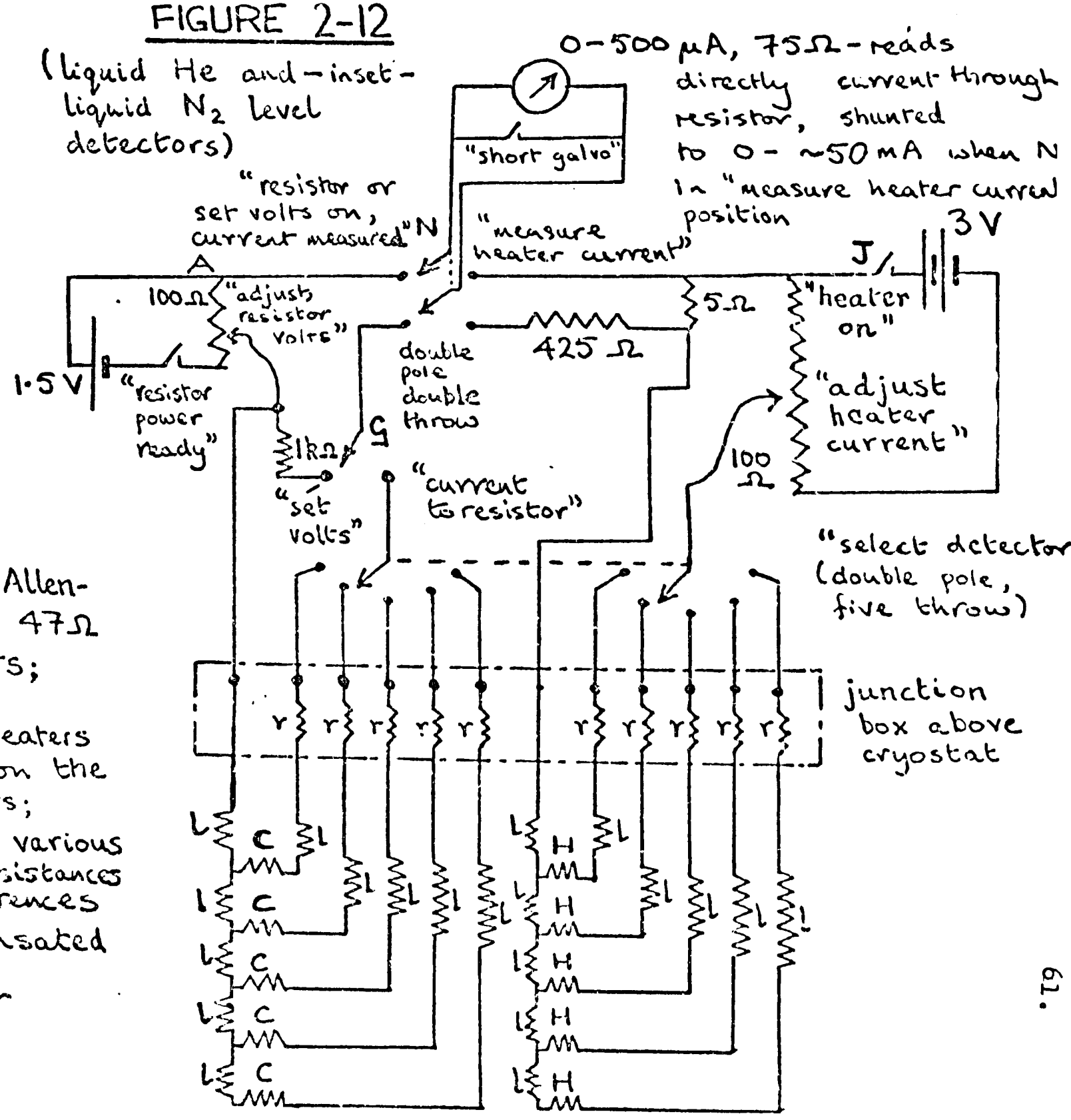

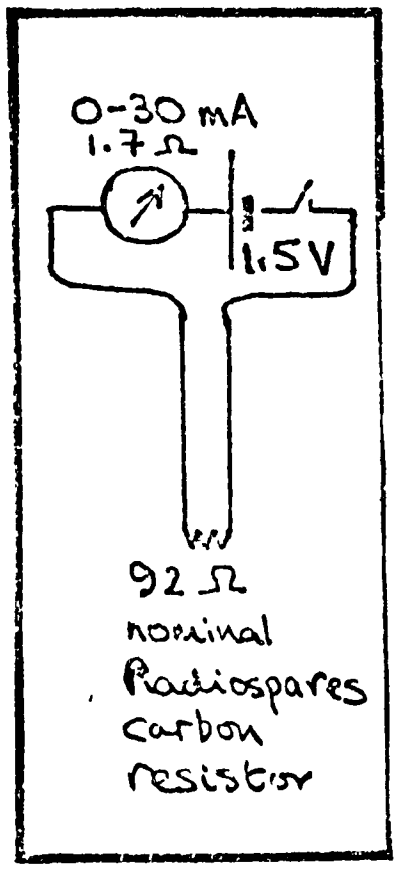

Cs are Allen-Bradley 47Ω resistors;
Hs are 25Ω heaters wound on the resistors;
Ls are various lead resistances whose differences are compensated by various resistors r

in liquid helium or rising helium gas at 4.2 K. By applying a 20 mA current through the Karma heater, however, liquid and gaseous helium can be distinguished. Typically, when this is done (by closing switch J in Figure 2-12), the resistor current will rise from 170 μA to 210 μA if the detector is immersed in liquid, but from 170 μA to 260 μA if it is in gas at the same temperature.

The five pumping tubes (stainless steel) passing upwards through the economiser can (stainless steel can 20.3 cm long by 12.7 cm diameter) are (see Plates 2-I and -II) each in two parts connected at brass couplings so as to facilitate assembly of the cryostat in the first instance, and also to allow removal of the lower part for substantial repairs, should these be necessary. In the upper portion of each tube is fixed a helical twist of metal, serving as a baffle to absorb room-temperature radiation coming from the parts of the tubes above the top of the economiser can leading to the vacuum lines.

Knurled knobs for operating the needle valve and the jaws via screw mechanisms emerge from tubes passing through the economiser can and containing the screw mechanisms (see Plate 2-II). The mechanism for the needle valve operates (without rotational movement) a long steel rod which ends in the needle, and that for the jaws tensions or releases a length of piano wire which is fastened, via a screw connector, to the bellows on the lid of the outermost chamber. Both mechanisms are provided with washers to make them substantially gas-tight.

The leads from the helium level detectors and from the epoxy-resin seals on the lid of the outermost chamber are all of 34 SWG manganin and pass to a 30-contact 37 mm glass-metal lead-through seal (obtained from Wesley-Coe of Scotland Road, Cambridge). This seal (situated at P in Figure 2-1 - see also Plates 2-I and 2-II) is

at the bottom end of a "double funnel" with a long connecting "spout" extending up through the economiser can. Varnished 40 SWG silk-covered wires pass from the contacts in the seal up the "spout" and out, via a polythene tube screened with copper gauze, to the junction box above the cryostat (these latter features are visible in Plate 2-II).

Following Clay (1965), who used a similar arrangement, the "double funnel" was filled with diphenyl ether (m.p. 26°) to avoid condensation on the leads from the air and to provide thermal contact between the leads and the liquid nitrogen in the economiser can. The use of diphenyl ether was regretted, however, for even slight warming of the apparatus when not in cryogenic use melted the diphenyl ether to a very mobile and obnoxious-smelling liquid, which found its way out of small leaks near the Wesley-Coe seal. In retrospect, it seems that paraffin wax (m.p. 47 - 65°) would have been much better, even though perhaps somewhat more difficult to introduce in the first place.

The dewar for the liquid helium (shown only in Figure 2-1) is, as already stated, of monax, a glass which is much less permeable to helium than pyrex. Repumping of the dewar nevertheless became desirable after about 300 hours' exposure to liquid helium. The dewar is silvered in the usual way. Various spacers (of polystyrene or of asbestos tape) are glued onto the monax to prevent direct banging of the monax against the inside of the stainless steel dewar. The dewar is almost 90 cm long and has a diameter at the upper end of almost 16 cm. Because of its "waisted" form, the volume of liquid in the dewar when filled so as just to cover the outermost chamber is only $2^1/2$ l. The total volume up to the level of the brass couplings is about 4 l. The dewar was made in the Clarendon Laboratory glassblowing

workshop.

The use, as shown in Figure 2-1, of a helium siphon fitted with an extension tube ensures that incoming helium emerges at the bottom of the monax dewar. This maximises the potentially very useful cooling effect of the rising cold gas [$\Delta H_{vap,m}(He^4, 4.2\ K) = 82.34\ J\ mol^{-1}$; $\Delta H_{lm}(He^4, g, 80\ K) - \Delta H_m(He^4, l, 4.2\ K) = 1684\ J\ mol^{-1}$]. The siphon fits into tube A in Figure 2-1 with an O-ring seal and can be removed once the liquid helium has been put into the cryostat.

The outer dewar (see Plate 2-III) is of thin-walled stainless steel, and was made in the Clarendon Laboratory engineering workshop. In accordance with Clarendon Laboratory practice, the dewar has a pumping valve and also a blow-off valve (to guard against any accident caused by nitrogen leaking into the vacuum space at a cracked weld) and the vacuum space contains "Brelite" powder.

For raising and lowering the dewars (which, with refrigerant(s) together weigh about 30 kg), a very simple hoist (see Plate 2-III) is used, which in fact works remarkably well. The dewars stand on a dural plate to which four pieces of nylon clothesline are attached at the corners. The lines pass over pulleys, and at the other end of each line is a cylindrical 10 kg lead weight running in a plastic drainpipe in each corner of the frame of the apparatus. The plate can be arrested in the "up" position (as in Plate 2-III) by means of a system of plates and rods, or at ground level by rods. Although the lead weights and the dewars are not in balance, the frictional forces at the pulleys are sufficiently great that the dewars can be gently raised or lowered provided they are guided by hand, with one person on each side of the apparatus.

Finally, a liquid nitrogen level detector is provided in the outer dewar, just below the lower part of the rubber of the Leiden

seal, so as to allow the operator to avoid cracking the rubber of the Leiden seal (it was not possible to look directly into the outer dewar). In liquid nitrogen the detector (a Radiospares nominal 92 Ω carbon resistor) has about 25% greater resistance than at room temperature, and the change is readily detected on the milliameter in the circuit shown in the inset of Figure 2-12 (page 61).

Section 2-9: calorimetric determinations

a. performing a calorimetric run

In the preceding Sections 2-3 to 2-8 the various parts of the new calorimeter have been described, and also the setting up of the cryostat part of the calorimeter in preparation for a run.

It being now imagined that such preparation, including electrical and leak testing, is complete, a run on the calorimeter will be described. First of all, the three "spaces" (as defined in Figure 2-1, page 22) and the helium-3 pot are all thoroughly pumped out with the fast diffusion pumps. (For this purpose the helium-3 pot and the innermost space were in practice connected in parallel at the vacuum line, since they were in any case connected by the leak previously mentioned at page 20.) The helium-4/nitrogen pot is pumped out with the 100 l/min rotary pump, the needle valve being of course closed.

The next step is to surround the cryostat with liquid nitrogen. Both the inner, monax dewar and the outer, stainless steel dewar are hoisted into position, liquid nitrogen being poured into the inner dewar (but not usefully into the outer), before and/or after hoisting. (The stainless steel dewar at this stage merely supports and protects the monax dewar.) After hoisting, tube A in Figure 2-1 (as yet unoccupied by the helium siphon) can be used for pouring in liquid nitrogen.

Helium exchange gas (previously purified by passing gas from a

cylinder over activated charcoal at 77 K) is admitted into the outermost and intermediate spaces to a pressure of a few cmHg and the jaws of the thermal switch are closed. Once the vigorous initial boil-off has ended, tube A is plugged with a rubber bung, the Leiden seal is put into position over the brass hood, and a plug of tissue paper is inserted into the end of the polyethylene tube attached to tube B in Figure 2-1, so as to allow escape of gas without the occurrence of any icing up in the cryostat.

When the vessel temperature is close to the liquid nitrogen boiling point, the exchange gas is pumped out of the outermost space, conveniently overnight. After this pumping, the economiser can is filled with liquid nitrogen and is not allowed to run dry during measurements for the reason given in the third paragraph of page 27. The helium-4/nitrogen pot is then filled with liquid nitrogen from the monax dewar by opening the needle valve with continued pumping on the pot until the liquid nitrogen in the pumping tube has been raised above the level of the top of the economiser can; this condition is detected by the liquefied air running down the outside wall of the tube.

The needle valve is closed again, and pumping on the pot is maintained. The temperatures of the intermediate chamber, innermost chamber (or shield), and vessel fall, the temperature of the vessel reaching the region of 50 K in a couple of hours, this temperature having presumably been already reached by the intermediate chamber and by the shield. The intermediate chamber maintains a temperature in this region for about 12 hours, during which time the nitrogen in the pot is presumably all pumped away. The lowest temperature obtainable in this way is just below 48 K. (Below the triple point of 65 K, the nitrogen under pumping must be <u>solid</u>.)

Once a suitably low temperature has been reached, the exchange gas is pumped out of the intermediate space; and, when the temperatures of the vessel and shield are equal as indicated by the thermocouple, the thermal switch is opened. Then a run of heat capacity determinations is begun, with the use of the method of intermittent electrical heating discussed in Section 2-1. In this temperature range (48 - 84 K), the heater on the shield is manually controlled so as to maintain a near-zero thermocouple signal during both drift and heating periods (adiabatic operation). When the vessel has reached internal equilibrium, the drifts in vessel temperature are undetectable provided that the shield is accurately controlled, except at the very bottom of the range with a sample of rather low heat capacity. Therefore, a drift is followed until the potentiometer measurements on the thermometer circuit are practically steady (usually from about 10 - 15 minutes after the end of a heating period, by which time equilibrium has been achieved), and the "steady" potentiometer measurements are averaged for the calculation of a single temperature which serves as T_A for the previous heating period and as T_F for the succeeding one. (The fact that drifts are undetectable above 50 K reflects the decrease of thermometer sensitivity with rising temperature - see Figure 2-3, page 31.) A further feature of operation in the nitrogen range is that the response of the thermocouples to heating of the vessel and shield is noticeably more sluggish than at lower temperatures, and this may explain why there appears to be a systematic error in the results obtained in this range (see Section 3-3d). Operation in the nitrogen range is shown schematically in Figure 2-13(g).

If there are no anomalies in the heat capacity between 48 K and

FIGURE 2-13

temperatures approximate;
innermost space under high vacuum throughout

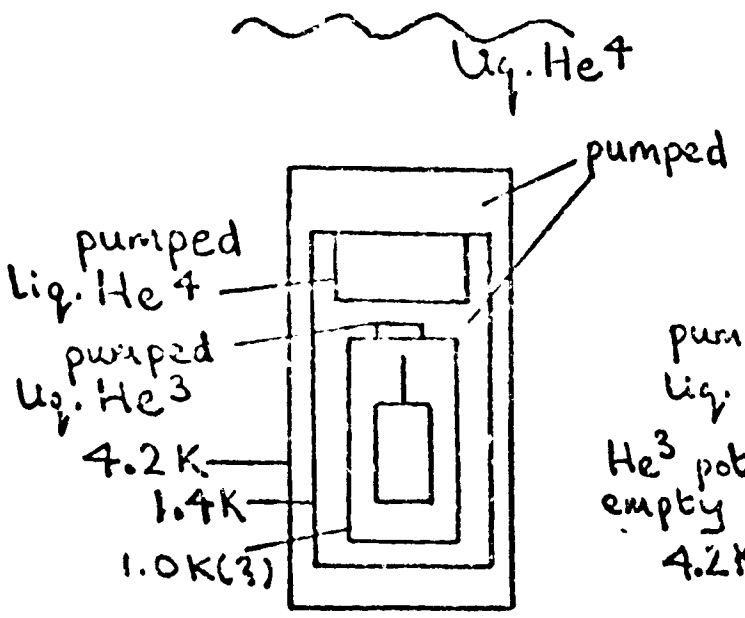

(a)

vessel temp. 1.0 K(?) - 1.4 K

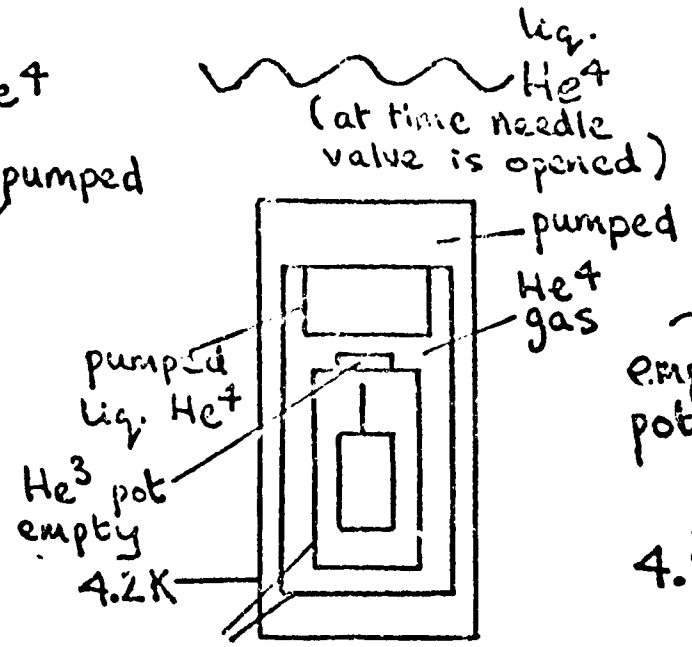

(b)

1.4 K - 4.2 K

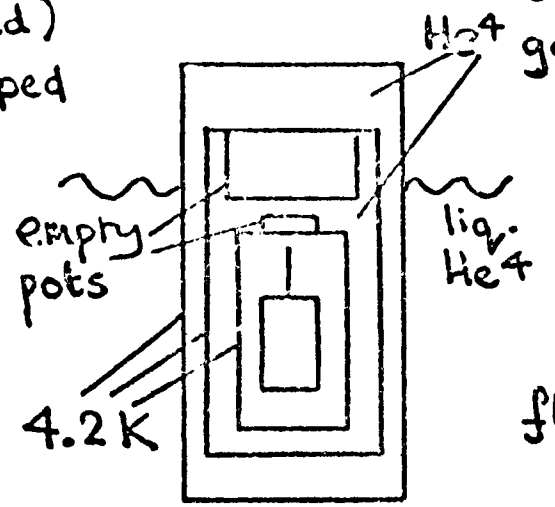

(c)

4.2K - 9K

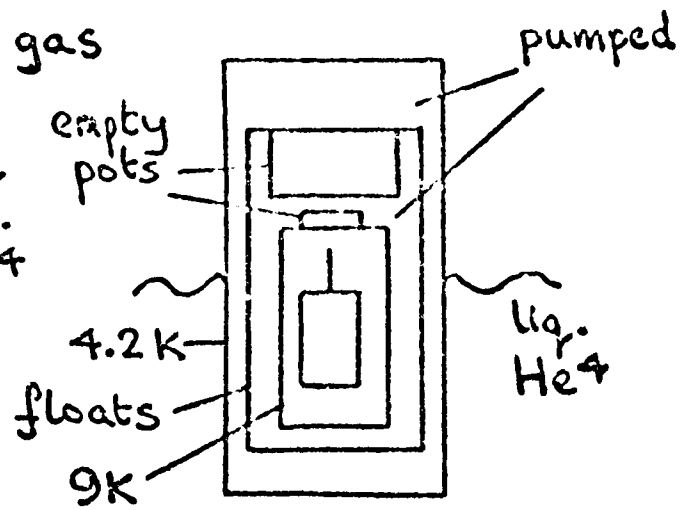

(d)

9K - 15K

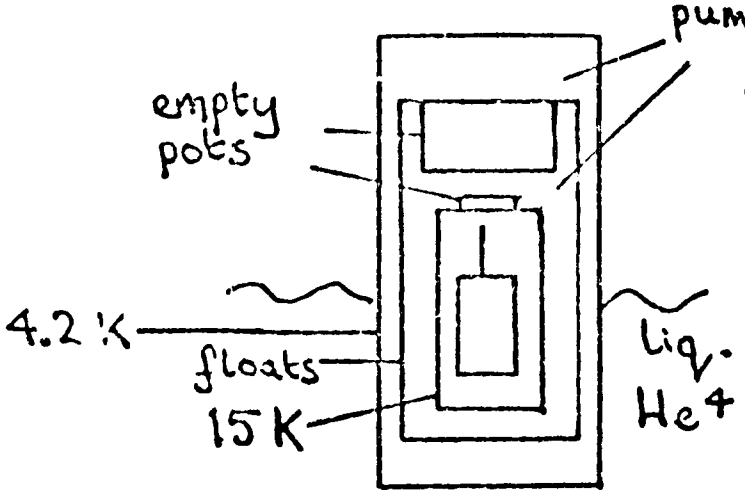

(e)

vessel temp. 15 K - 20 K

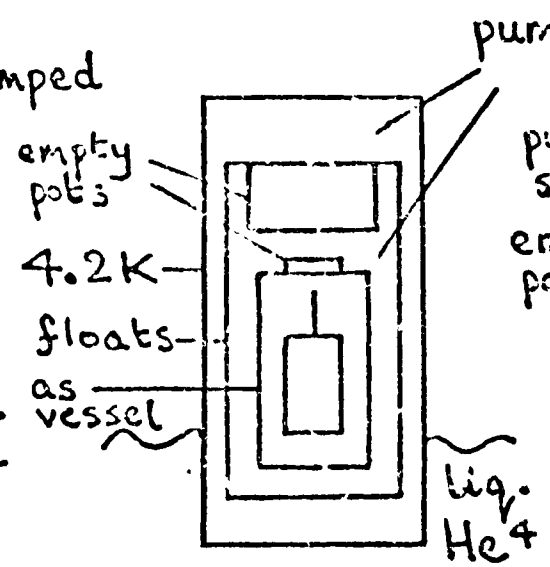

(f)

20 K - 50 K

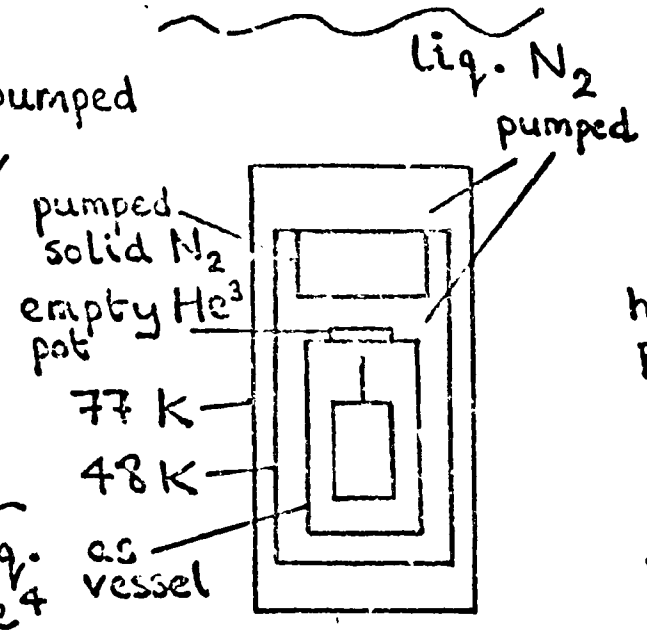

(g)

48 K - 84 K

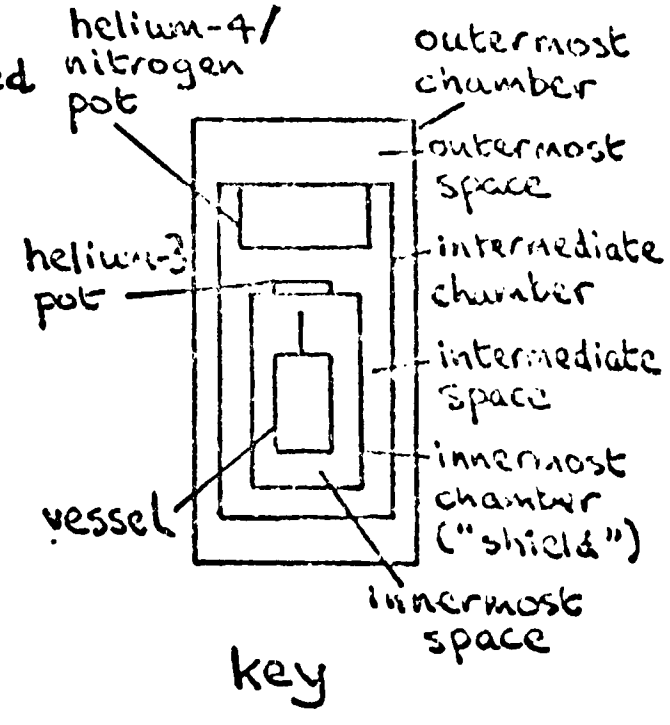

key

84 K, the pumped nitrogen lasts long enough for the whole range to be covered (in 3 K intervals) in a continuous run of about 12 hours' duration, if desired; but the cheapness of liquid nitrogen means that as many runs as desired can readily be performed. This is not the case with the determinations in the helium range, however, where the most must be made of the duration of helium under pumping and then of the helium in the monax dewar.

In a typical helium run, the procedure is as follows: -

On Thursday afternoon (say), by pumping on liquid nitrogen in the manner already described, vessel, innermost chamber (shield), and intermediate chamber are cooled to about 50 K, and the exchange gas is pumped out of the intermediate space and the thermal switch is opened. (The outermost and innermost space are already under pumping.) On Thursday evening, after the intermediate space has been thoroughly pumped out, exchange gas is introduced into the outermost space until the nitrogen in the helium-4/nitrogen pot has been pumped away, the intermediate chamber thus being brought to 77 K. The exchange gas in the outermost space is then pumped away overnight.

By Friday morning (say 10 a.m.), the outermost space has been thoroughly pumped out and the cryostat is ready for cooling in liquid helium. The innermost chamber and vessel have warmed somewhat overnight (to about 60 K), but even this extra precooling which has been achieved saves time and liquid helium.

Now the outer dewar is filled with liquid nitrogen and the helium siphon is inserted into the cryostat. Then, the following operations are performed in rapid succession: both dewars are lowered; the inner dewar is removed; the liquid nitrogen in it is tipped out; the empty dewar is replaced in the stainless steel dewar; the dewars

are raised up; and the Leiden seal is put into position. (Speed is necessary to minimise warming of the cryostat.) Helium is then passed over (first gas, then liquid) from a storage dewar of liquid helium, and shortly after this transfer is begun, the economiser can is filled with liquid nitrogen. During the transfer, exchange gas is introduced into the outermost and intermediate spaces and the thermal switch is closed.

The efficiency of the transfer depends on how quickly the dewars are lowered and raised when the liquid nitrogen is being tipped out of the monax dewar, and also on the timing of the introduction of exchange gas and of the closing of the thermal switch. In a well-managed transfer about 11 l of liquid helium are used to cool the cryostat and fill the monax dewar to about half-way between the lid of the outermost chamber and the bottom of the economiser can.

Once the monax dewar has been filled and all the chambers of the cryostat (including the vessel) are near 4.2 K, the outermost space is pumped out for about an hour and a half, by which time the pressure recorded on the Penning gauge in the pumping line is still of the order of 10^{-3} mmHg because of the slow pumping rates achievable on chambers maintained at such low temperatures.

Next, the needle valve is opened for half a minute or so, while pumping, partly throttled by the ball valve in the line, is maintained on the helium-4/nitrogen pot. This procedure apparently fills the helium-4/nitrogen pot with liquid helium without wasting excessive amounts of liquid helium in the monax dewar. With the needle valve closed, the ball valve is opened wide. The temperature of the vessel falls for about 1/2 hour with increasing rapidity (presumably as the thermal conductance of the switch connecting the shield and the vessel increases relative to the vessel heat capacity), and

then the temperature abruptly levels off at 1.4 - 1.5 K, this presumably being the temperature already reached by the shield and by the intermediate chamber. This temperature is maintained by the intermediate chamber for 7 - 8 hours and then, as the helium-4 runs out, the temperature of the intermediate chamber rises very rapidly back towards 4.2 K (compare the previous comments at page 55 on the very large heat leaks and on the need for a substantial volume of pumped helium-4).

During this period of 7 - 8 hours (from say 2.30 p.m. on Friday to 10 p.m.), a run is performed from 1.4 - 1.5 K to above 4.2 K. About ten individual determinations will suffice below 4.2 K if there is no heat capacity anomaly.

It should be remembered that for measurements to be successful in the 1.4 K to 20 K region, especially below 4.2 K, an excellent vacuum must be maintained in the innermost space, in fact a vacuum superior to that provided by a fast diffusion pump with a liquid nitrogen trap; in McCullough and Scott (1968a), a figure of 10^{-9} mmHg is given. (It is indeed for this reason that a thermal switch, rather than exchange gas, is used for the making and breaking of thermal contact between vessel and shield.) The golden rule, therefore, is never to admit helium gas into the innermost space once the apparatus has been assembled and is ready for cooling from room temperature. If this prohibition is observed, then when the innermost space is cooled to liquid helium temperatures, practically all the remaining gas is frozen out, since only a very small proportion of this is helium. The prohibition is extended to not using on the innermost space any pump or backing volume which has been in contact with helium at any time in the previous few hours. (In principle, in fact, if the innermost space is vacuum tight, there should be no

need to pump it at all during working below 4.2 K; though in practice pumping was generally maintained to remove the gas which was evidently being desorbed from the warmer upper parts of the apparatus.)

The determinations up to 4.2 K are performed in a continuous run with the shield at 1.4 - 1.5 K (see Figure 2-13(b)). The shield temperature, according to the carbon resistor on it, drifts gradually downwards during the first few hours of the run, presumably because of the improving vacuum in the outermost space, but each individual determination is performed practically isoperibolically.

It was observed in the run with bis(adiponitrile)copper(I) nitrate that the downward temperature drift rate of the vessel increased in magnitude from 0 when the vessel was at the same temperature as the shield (1.4 - 1.5 K) to about 5 mK min^{-1} when the vessel was at 2 K, but remained at about 5 mK min^{-1} for vessel temperatures from 2 K to 4.2 K.

The present author briefly investigated the possibility of controlling the shield temperature at temperatures between 1.4 - 1.5 K and 4.2 K by heating the shield with the intermediate space pumped and the intermediate chamber at 1.4 - 1.5 K; it appeared that it was difficult to pump out the intermediate space well enough to allow the shield to be thus controlled without the use of heater powers so large as to reduce very considerably the lifetime of the pumped liquid helium-4. Walker (1959) has described a simple manostat for the helium-4 pumping line by which such control of the shield could be achieved if desired; but it would appear from the above observations on the variation of drift rate with vessel temperature that very frequent changes of shield temperature (inconvenient because the after drift of one determination would no longer serve as the fore drift of the

next) would be needed to obtain worthwhile reductions in the drift rates.

Vibration

It is well known that vibration from external sources (e.g. rotary pumps) can be transmitted into an apparatus of the present type and cause heating of the sample-containing vessel when the thermal switch is open, as the vessel vibrates on the nylon suspension threads. Manchester (1959) reports an instance where a vibrational heating power of 2×10^{-5} J min^{-1} was developed in a suspended vessel in an unfavourably situated cryostat, and that measurements below 4.2 K were therefore practically impossible on samples of low heat capacity; Martin (1961) describes the most elaborate precautions (apparatus set in concrete, pumping tubes passing through sand) for avoiding the transmission of vibrational energy in a cryostat operating below 1.5 K. The lower the temperature (and therefore, generally, the smaller the specific heats), the more significant vibrational heating becomes.

In the present work, measurements below 4.2 K were made in a room in which two rotary pumps were working, one about four metres from the cryostat and the other (the 100 l/min pump for the He^4 pumping) very close to the cryostat but mounted on foam rubber and connected successively via a flexible rubber hose, a copper tube mounted on foam rubber, and a solid rubber hose to the pumping line. In the run on bis(adiponitrile)copper(I) nitrate (where the total heat capacity was rather low, so as to make the effect most noticeable, if present), it appeared that the self-heating due to vibration was several times less than that reported by Manchester (see above); and it may be relevant that the vessel had been suspended in the shield with the suspending nylon threads so tensioned that, when the spike was plucked, a pleasant musical note (roughly middle C) was produced, presumably having a frequency above normal background vibrations.

* * *

Returning now to our discussion of a typical run with liquid helium: -

By 10 p.m. on Friday, the vessel has been heated, in a continuous series of drifts and heats from 1.4 K to 4.2 K or higher, and the pumped helium-4 has either run out or else can now be deliberately boiled off by admitting exchange gas to the outermost space. With exchange gas in outermost and intermediate spaces, and the shield therefore at 4.2 K, determinations are made isoperibolically up to about 9 K (Figure 2-13(c)). At about 3 a.m. Saturday, these determinations are complete. The liquid helium level in the monax dewar is by now approaching half-way down the outermost chamber of the cryostat, having in fact passed the lid of the outermost chamber during the 1.4 - 4.2 K determinations, but is now falling very much more slowly than previously. Now the outermost and intermediate spaces are pumped out "overnight", ready for the next day's work.

From Saturday at 12 noon, more isoperibolic determinations are made, with both outermost and intermediate spaces under continued pumping, and the shield maintained at about 9 K using manual heater control and the carbon resistor on the shield for temperature measurement; the temperature of the intermediate chamber is simply allowed to "float". See Figure 2-13(d). Once the vessel has reached 15 K, the shield is heated to 15 K, and further isoperibolic determinations are carried out (Figure 2-13(e)).

When the vessel has reached about 20 K, adiabatic operation is commenced, using the thermocouples and manual shield control (Figure 2-13(f)).

At 20 K, the carbon resistance thermometer and thermocouple circuits are approximately equally sensitive to temperature changes of the shield, the former being the more sensitive below 20 K and the latter

above 20 K; but in view of the inherent advantages of adiabatic operation over isoperibolic (first ten lines, page 18) a rather lower temperature than 20 K for the isoperibolic - adiabatic changeover would seem at first sight to be desirable. Therefore, in one run adiabatic operation was attempted in the 10 - 20 K region, but it was found that precise adiabatic control was impossible, because large amounts of gas were desorbed (perhaps from the inner wall of the "floating" intermediate chamber) into the intermediate space as the shield was rapidly heated during heating periods. This desorption caused rapid variations of pressure in the intermediate space which prevented satisfactory control of the shield heater power, very large powers being required while desorption was occurring.

Once shield and vessel temperatures have been raised to 20 K, however, desorption into the intermediate space ceases to be a problem and the calorimeter can be satisfactorily operated adiabatically to 50 K (reached by about 7 a.m. Sunday morning). The liquid helium in the monax dewar does not go below the bottom of the outermost chamber until about 12 noon on Sunday, so that further determinations can be made if necessary.

* * *

Figure 2-13 shows schematically not only the way in which the calorimeter is used from 1.4 K to 84 K, but also in (a) the way in which it had been intended to use the calorimeter for operations below 1.4 K. (In fact, this was never done, because of the leak in the helium-3 pot, q.v.)

Section 2-9b: a typical calorimetric determination: calculation of mean total heat capacity (vessel + sample + solder etc.)

The following measurements were made in a helium run on bis(adiponitrile)copper(I) nitrate, during isoperibolic operation according to (d) in the scheme shown in Figure 2-13.

Throughout the determination, the temperature of the innermost chamber (shield) is manually controlled by means of the shield heater circuit (Figure 2-9) so that the resistance of the carbon resistor on the lid of the shield is maintained at 188 Ω (corresponding to a temperature of about 9 K), as measured with the circuit of Figure 2-11.

At the end of the previous heating period, the resistance of the dummy heater has been adjusted to agree with that of the vessel heater at the end of that period, in the manner described later. At the beginning of the present determination, the switch Z in the vessel heater circuit (Figure 2-7) is in the "dummy" position, while switch Y is in the "low power" position. The initial vessel temperature is rather above 10 K, and the current through the dummy heater has been adjusted to a value such that a heating of about 1.1 K will be achieved in 6 minutes.

Switch X (thermometer circuit, Figure 2-4) off.

"thermals"

p.d. on potentiometer circuit A (connected to heater circuit, Figure 2-7)	= + 3.8 μV
p.d. on potentiometer circuit D (connected to thermometer circuit, Figure 2-4)	= 0 μV
p.d. on potentiometer circuit E (connected to thermometer circuit, Figure 2-4)	= - 3.1 μV

Switch X on.

Temperature of 10 kΩ standard = 24.0°C.

Potentiometer standardised.

fore drift

time min				
0	p.d.	on circuit	D = 0. 206 780 V	
1				
2	"	"	"	E = 0. 004 401 3 V
3	"	"	"	E = 0. 004 401 0 V
4	"	"	"	E = 0. 004 401 4 V
5	"	"	"	E = 0. 004 401 0 V
6	"	"	"	E = 0. 004 402 5 V
7	"	"	"	E = 0. 004 403 0 V
8	"	"	"	D = 0. 206 776 V

	time min	
heating period	9	Switch Z on.
	10	p.d. on circuit A = 1. 352 417 V
	11	" " " C = 0. 719 274 V
	12	" " " A = 1. 352 351 V
	13	" " " C = 0. 719 286 V
	14	" " " A = 1. 352 310 V
	15	Switch Z off. Timer reads 360.358 sec; is reset to 0.000 sec.

Dummy heater adjusted so that p.d. on circuit C = 1. 352 310 V as nearly as possible.

Switch X off.

"thermals"
- p.d. on circuit A = + 3.0 μV (relevant only to next heating period)
- p.d. on circuit D = - 5.0 μV
- p.d. on circuit E = - 2.9 μV

Switch X on.

Temperature of 10 kΩ standard = 24.0°C.

Potentiometer standardised.

	time min		
"after-drift"	24	p.d.	on circuit D = 0. 206 768 V
	25 1/3	"	" " E = 0. 004 259 1 V
	26	"	" " E = 0. 004 259 6 V
	27 1/2	"	" " E = 0. 004 260 2 V
	29 1/2	"	" " E = 0. 004 261 4 V
	30	"	" " E = 0. 004 261 7 V
	31	"	" " E = 0. 004 262 0 V
	32	"	" " E = 0. 004 262 7 V
	33	"	" " E = 0. 004 263 2 V
	34	"	" " D = 0. 206 768 V
	35	Switch Z on (relevant only to next heating period).	

Calculation of the result is performed as follows: -

The drifts in the p.d. measurements on circuits D and E are extrapolated to the mid-point of the heating period (time = 12 minutes), and the extrapolated values are each corrected for the measured "thermals", and T_F and T_A are calculated from these extrapolated, "thermal"-corrected values, using the known resistance of the 10 kΩ resistor at the ambient temperature.

Fore-drift

p.d. on D extrapolated to t = 12 minutes	= 0. 206 774 V
p.d. on D extrapolated to t = 12 minutes and corrected for "thermals"	= 0. 206 774 V
p.d. on E extrapolated to t = 12 minutes	= 0. 004 405 5 V
p.d. on E extrapolated to t = 12 minutes and corrected for "thermals"	= 0. 004 408 6 V
Resistance of 10 kΩ resistor at 24.0°C	= 10037.28 Ω
R_F of thermometer = 10037.28 Ω x 0.004 4086/ 0. 206 774	= 214.003 Ω
Using function (3) as given in Tables 2-1 and 2-2, T_F uncorrected for thermometer deviation	= 9.8995 K
Thermometer deviation at apparent T of 9.8995	= 0.1567 K
T_F = 9.8995 K + 0.1567 K	= 10.0562 K

After-drift

p.d. on D extrapolated to t = 12 minutes	= 0. 206 768 V
p.d. on D extrapolated to t = 12 minutes and corrected for "thermals"	= 0. 206 773 V
p.d. on E extrapolated to t = 12 minutes	= 0. 004 252 6 V
p.d. on E extrapolated to t = 12 minutes and corrected for "thermals"	= 0. 004 255 5 V
Resistance of 10 kΩ resistor at 24.0°C	= 10037.28 Ω
R_A of thermometer = 10037.28 Ω x 0. 004 255 5/ 0. 206 773	= 206.573 Ω
Using function (3) as given in Tables 2-1 and 2-2, T_A uncorrected for thermometer deviation	= 11.2082 K
Thermometer deviation at apparent T of 11.2082 K	= - 0.0071 K
T_A = 11.2082 K + (-0.0071) K	= 11.2011 K

$$T_{MID} = (T_F + T_A)/2 = 10.6286 \text{ K}; \quad \Delta T = (T_A - T_F) = 1.1449 \text{ K}$$

Heat input

In equation 2-3 and 2-4, V_A (average, corrected for "thermals")	= 1. 352 355 V
V_C (average)	= 0. 719 280 V
$R_{1\,k\Omega\ ST}$	= 1000.103 Ω
Energy input, from equation 2-4 = (1. 352 355 x 0. 719 280 x 360.358/1000.103) J	= 0. 350 492 J
$\overline{C}_p$(10.0562 K, 11.2011 K) = 0. 350 492 J /1.1449	= 0. 30613 J K^{-1}
From equation 2-3, R_H = 1. 352 355 x 1000.103Ω/ 0. 719 280	= 1880.344 Ω

Final result

T_{MID} = 10.629 K, ΔT = 1.145 K, $\overline{C}_p$ = 0.3061 J K^{-1}, R_H = 1880.34 Ω

Section 2-9c: results on empty vessel

The results of heat capacity determinations on the empty vessel are given in Table 2-3. The three left-hand columns list the mean heat capacities $\overline{C}_p(T_F, T_A)$ as a function of T_{MID} and ΔT calculated in the manner illustrated in Section 2-9b. The weights of solder etc. are listed at head of the table.

The $\overline{C}_p(T_F, T_A)$ results were fitted to a series of polynomials, and from these polynomials an approximate value of d^2C_p/dT^2 calculated for each T_{MID}. C_p for each T_{MID} corrected for curvature was then calculated using the equation (Douglas et al, 1954)

$$C_p(\text{corrected}, T_{MID}) = \overline{C}_p(T_F, T_A) - \frac{(\Delta T)^2}{24} \frac{d^2C_p}{dT^2} \qquad \text{eq. 2-7}$$

A further correction was then applied to compensate for the heat capacity of the exchange gas included in the vessel, by assuming a molar heat capacity of $\frac{3}{2}$ R. The values listed in the right hand column of Table 2-3 include both the above-mentioned corrections: that is to say, each is the curvature-corrected heat capacity of the vessel at a temperature equal to T_{MID} in the left-hand column, the vessel having the weights of solder etc. indicated at the head of the Table but containing no exchange gas.

Smoothing these final C_p values yielded the polynomials listed in the first three rows of Table 2-4. Iteration of the curvature correction with these polynomials was found to have only an insignificant effect (< 0.01% in all cases) on the C_p's in the right hand column of Table 2-3. It will be noted that the low temperature function contains only a linear term and a cubic term in T, corresponding, respectively, to electronic and Debye lattice heat capacities.

The polynomials listed join without any discontinuity in C_p at the overlap temperatures indicated, and only small discontinuities in $\frac{dC_p}{dT}$.

TABLE 2-3

Mass of vessel before assembly (excluding the nylon loops (about 4 x 2 mg, but replaced frequently) for the heat capacity of which no correction was made) = 44. 654 27 g

Mass of cap before assembly = 0. 509 51 g

Mass of indium solder used in assembly = 0. 372 70 g

Mass of electrical solder used in assembly = 0. 028 27 g

Mass of silver tube used in assembly = 0. 170 22 g

Quantity of exchange gas used in vessel (gas used was He^4; contrast runs with samples, where He^3 was available and was used) = 2.82×10^{-5} mol

$\frac{T_{MID}}{K}$	$\frac{\Delta T}{K}$	$\bar{C}_p/JK^{-1}$ of empty vessel as measured	C_p/JK^{-1} of empty vessel corrected for curvature and exchange gas
5.146	0.595	0.01538	0.01500
5.664	0.519	0.01914	0.01877
6.171	0.734	0.02313	0.02273
6.998	1.126	0.03131	0.03082
7.891	0.898	0.04107	0.04062
8.508	0.936	0.05089	0.05044
9.456	1.262	0.06517	0.06462
10.567	1.228	0.08571	0.08515
11.488	1.678	0.1100	0.1092
13.137	1.762	0.1564	0.1556
15.128	2.804	0.2201	0.2184
17.697	2.237	0.3347	0.3334
19.931	2.070	0.4551	0.4540
22.366	2.777	0.6099	0.6081
25.223	2.841	0.8242	0.8225
28.063	2.791	1.068	1.066
30.628	2.282	1.306	1.305
33.829	3.998	1.631	1.630
37.841	4.027	2.063	2.062
41.925	4.143	2.499	2.499
46.023	4.053	2.922	2.921
49.795	3.492	3.390	3.390
50.177	3.351	3.465	3.464
53.371	3.037	3.818	3.818
56.300	2.820	4.112	4.112
59.699	3.978	4.494	4.494
62.219	2.455	4.717	4.717
63.538	3.692	4.842	4.842
64.618	2.342	4.945	4.945
67.109	3.450	5.174	5.175
70.849	4.031	5.501	5.502
74.247	3.835	5.785	5.786
78.016	3.704	6.074	6.075
81.665	3.594	6.269	6.271

Table 2-4

$C_{p,MT}/(J\ K^{-1})$ or $c_p/(J\ g^{-1}K^{-1}) = A_0 + \sum_{i=1}^{6} A_i\ (T/K)^i$,list of coefficients used.

value smoothed	range of T/K	A_0	A_1	A_2	A_3	A_4	A_5	A_6
$C_p/(J\ K^{-1})$ of empty vessel as listed in 4th col., Table 2-3	$\leq$ 8.1596	0	1.295576 x 10^{-3}	0	6.296870 x 10^{-5}	0	0	0
	>8.1596 $\leq$40.1194	-1.675077 x 10^{-2}	5.177631 x 10^{-3}	-3.300208 x 10^{-4}	8.452101 x 10^{-5}	-1.084644 x 10^{-6}	0	0
	>40.1194	-6.757933 x 10^{-1}	1.291002 x 10^{-2}	2.158021 x 10^{-3}	-1.560821 x 10^{-5}	0	0	0
$c_p/(J\ g^{-1}K^{-1})$ of silver	$\leq$ 10	-3.971903 x 10^{-7}	6.265298 x 10^{-6}	-1.972271 x 10^{-7}	1.512959 x 10^{-6}	2.438856 x 10^{-8}	0	0
	> 10	8.562812 x 10^{-3}	-1.661392 x 10^{-3}	8.368314 x 10^{-5}	2.294414 x 10^{-6}	-9.029002 x 10^{-8}	9.856187 x 10^{-10}	-3.628940 x 10^{-12}
$c_p/(J\ g^{-1}K^{-1})$ of indium solder	$\leq$ 10	-1.583952 x 10^{-4}	2.855526 x 10^{-4}	-1.550457 x 10^{-4}	3.823410 x 10^{-5}	-1.380942 x 10^{-6}	0	0
	> 10	-7.814516 x 10^{-3}	2.131507 x 10^{-4}	2.475783 x 10^{-4}	-8.753895 x 10^{-6}	1.374119 x 10^{-7}	-1.045666 x 10^{-9}	3.125103 x 10^{-12}
$c_p/(J\ g^{-1}K^{-1})$ of electrical solder	$\leq$ 10	1.108909 x 10^{-4}	-2.682860 x 10^{-4}	2.260501 x 10^{-4}	-7.265924 x 10^{-5}	1.174346 x 10^{-5}	-5.451569 x 10^{-7}	0
	> 10	-4.889275 x 10^{-3}	-8.297530 x 10^{-4}	3.315958 x 10^{-4}	-1.135468 x 10^{-5}	1.811491 x 10^{-7}	-1.428304 x 10^{-9}	4.470877 x 10^{-12}

Indium and electrical solder values calculated by Kopp's rule for compositions 49% Bi, 15% Sn, 18% Pb, 18% In and 60% Sn, 40% Pb respectively.

Section 2-9d: calculation of molar heat capacities

When measurements are made with a sample (amount n_{sample}) in the vessel, $\bar{C}_p$ values are obtained (calculated as illustrated in Section 2-9b). $\bar{C}_{p,m}$, the mean molar heat capacity over the temperature range of the determination is given by

$$\bar{C}_{p,m} = \frac{1}{n_{sample}} \left\{ \bar{C}_p(T_F, T_A) - \int_{T_F}^{T_A} dT \left(C_{p,MT} + C_{V,m,exch.gas}\, n_{exch.gas} + C_{p,elecsol}\, \Delta m_{elecsol} + C_{p,indsol}\, \Delta m_{indsol} + C_{p,Ag}\, \Delta m_{Ag} \right) \right\} \qquad \text{eq. 2-8}$$

$n_{exch.gas}$ is the number of moles of exchange gas used. $\Delta m_{elecsol}$, Δm_{indsol}, and Δm_{Ag} are the differences between the masses of electrical solder, indium solder, and silver used in assembly in the run with sample and those masses given at the head of Table 2-3 for the empty run. If (as is in practice always the case), the mass of the vessel before assembly excluding the loops is not the same as given at the head of Table 2-3, then the difference between the mass in the run with sample and the mass in the empty run is added to Δm_{indsol}.

$C_{V,m,exch.gas}$ for He^3 is taken as $\frac{3}{2}$ R. $C_{p,MT}$ is obtained from the polynomials given in Table 2-4 for the empty vessel.

$C_{p,elecsol}$, $C_{p,indsol}$, and $C_{p,Ag}$ are obtained from the respective polynomials also listed in Table 2-4; these polynomials were obtained by smoothing the heat capacity values for silver and Kopp's rule values for the solders. (Specific heats of the pure metals were obtained from Chemical Rubber Company (1974a).)

It will be noted that, for calculations of $\bar{C}_{p,m}$ below 5.1 K, $C_{p,MT}$ was an extrapolated value, since determinations on the empty calorimeter were not extended below this temperature because of lack of time; however, as will be seen in Chapter 4, the inaccuracy

involved in the extrapolation did not significantly affect the analysis of results in this temperature range in the case of the one compound where such analysis was important, and the results obtained closely agreed with those obtained independently by certain other workers (see Section 4-3b).

$\overline{C}_{p,m}(T_F, T_A)$ values may be curvature-corrected by the use of equation 2-7 (q.v.), $d^2C_{p,m}/dT^2$ being estimated in the same way as described in Section 2-9c for the empty vessel (i.e. from smoothed functions), or by any mathematically equivalent procedure (see e.g. McCullough and Scott, 1968b). However, any such procedure is based ultimately on the assumption (reasonable with the empty vessel) that C_p is a smooth function of T, and cannot always compensate for the use of excessively large "ΔT"s. Accordingly, curvature corrections are, to a variable extent, arbitrary, and "$\overline{C}_{p,m}(T_F, T_A)$"s are always listed in Chapters 3 to 5 and also the curvature-corrected "$C_{p,m}(T_{MID})$"s, where these have been computed.

The "Δm"s etc. of equation 2-8 are also listed, so as to allow recalculation of the determinations if the polynomials listed in Table 2-4 should be later superseded.

CHAPTER 3: BIS(ADIPONITRILE)COPPER(I) NITRATE

Bis(adiponitrile)copper(I) nitrate is one of a number of copper (I) complexes with organic nitriles which have previously been described.

Morgan (1923) carried out elegant experiments in which various complexes of this type were prepared and characterised, among them two complexes of copper(I) nitrate, namely the solids tetrakis(acetonitrile)copper(I) nitrate $CuNO_3.4CH_3CN$ and bis(succinonitrile)copper(I) nitrate $CuNO_3.2NC(CH_2)_2CN$. Relatively recently, there has been renewed interest in these compounds in connection with the dyeing of polyacrylonitrile fibres by the cuprous ion process (Rath et al, 1957, 1957a; Kinoshita et al, 1959, 1959a, 1959b), and this has led to the preparation of bis(glutaronitrile)copper(I) nitrate $CuNO_3.2NC(CH_2)_3CN$ and bis(adiponitrile)copper(I) nitrate $CuNO_3.2NC(CH_2)_4CN$.

Each of the abovementioned copper(I) nitrate complexes may be prepared, in solution, by treating a solution of silver nitrate in the appropriate nitrile with metallic copper, which displaces silver from the solution. By cooling the solution thus obtained, or else by removal of excess nitrile, the solid complex may be isolated. The acetonitrile complex is rapidly oxidised by air, but the dinitrile complexes are fairly air-stable.

The room-temperature crystal structures of the dinitrile complexes with copper(I) nitrate have been investigated by Kinoshita and his coworkers by single-crystal X-ray diffraction, who noted various points of interest. The room-temperature structure of bis(adiponitrile)copper (I) nitrate will be discussed in detail in Section 3-4. However, it should be mentioned here that the main concern in the present work is

with the nitrate ions in the bis(adiponitrile)copper(I) nitrate crystal, which were shown by the X-ray studies to be disordered in some way at room temperature, and that the precise way in which the nitrate ions are disordered is not apparent from the X-ray studies. The purpose of the heat capacity measurements on bis(adiponitrile)copper(I) nitrate reported in Sections 3-2 and 3-3 was to search for any heat capacity anomaly below room temperature which might be attributable to the ordering of the nitrate ions as the solid is cooled and which might indirectly provide further information concerning the precise way in which the nitrate ions are disordered at room temperature (compare page 14).

An anomaly was indeed found. The likely structures of the high-temperature disordered state and of the low-temperature relatively ordered state are discussed in Sections 3-4 and 3-5, both having regard to the nature of the heat capacity anomaly and having regard to energetic considerations.

Section 3-1: preparation and characterisation of calorimetric sample

According to Kinoshita et al (1959b) bis(adiponitrile)copper(I) nitrate can be prepared by the method of Rath et al (1957a), who prepared bis(glutaronitrile)copper(I) nitrate by adding an excess of copper powder to a 0.1 mol dm^{-3} solution of silver nitrate in the dinitrile at 60°C, filtering off the precipitated silver and excess copper, and cooling the filtrate to precipitate crystals of the product.

However, it was found in the present work that Rath et al's procedure, exactly copied, was unsuitable for bulk preparation of bis(adiponitrile)copper(I) nitrate, since it gave a product which was slightly contaminated with silver, as indicated by test-tube reactions;

this was so even though twice the stoichiometric amount of copper was used and the reaction was allowed to proceed for over three hours before the precipitated silver and excess copper were filtered off.

By using a lower silver nitrate concentration (0.08 mol dm^{-3}) and a reaction temperature of 60°- 70°C, however, it was possible to prepare silver-free bis(adiponitrile)copper(I) nitrate in bulk. It was found, during investigation of this preparation, that the solubility of bis(adiponitrile)copper(I) nitrate in adiponitrile at 60°- 70°C is approximately 0.08 mol dm^{-3} compared with approximately 0.05 mol dm^{-3} at room temperature (at 0°C it is much the same as at room temperature). Accordingly, if a silver nitrate concentration of substantially more than 0.08 mol dm^{-3} is used, for an upper working temperature of 60°- 70°C, bis(adiponitrile)copper(I) nitrate begins to precipitate even in the hot solution when a substantial amount of the silver nitrate is still unreacted; and it is suggested that the silver contamination in the product obtained by using 0.1 mol dm^{-3} of silver nitrate solution occurred because this precipitation of the product in the hot solution masked the copper, preventing the reaction from going to completion, so that significant amounts of silver(I) were left in solution.

The use of 0.1 mol dm^{-3} silver nitrate solution had in any case the further disadvantage that the bis(adiponitrile)copper(I) nitrate precipitate in the hot solution is finely divided and clogs the filter paper during the filtration step, so that the solution cools in the filter during its consequently slow passage therethrough, precipitating prematurely further bis(adiponitrile)copper(I) nitrate and thereby reducing the final yield.

The procedure employed in the bulk preparation, in three batches, of the calorimetric sample was therefore as follows: -

Koch-Light copper powder ($\geq$ 99.95%) was cleaned with .880 ammonia to remove superficial oxide, and was added, in three times the stoichiometric amount, to a 0.08 mol dm^{-3} solution of BDH AR silver nitrate ($\geq$ 99.9%) in Koch-Light adiponitrile ($\geq$99%) at 60°- 70°C. After $1^1/2$ hours at this temperature, the solution was filtered and the filtrate was allowed to cool to room temperature, when crystals of the product precipitated. These crystals were filtered off, washed with ethanol, and dried in air and over calcium chloride (batch 1). Because preliminary experiments had shown that hot solutions of bis(adiponitrile)copper(I) nitrate in adiponitrile underwent red discoloration in air, the reaction, the filtering of the solution, and the cooling of the filtrate were performed under nitrogen; however, some discoloration of the solution was nevertheless observed.

The procedure was repeated by using the mother liquor from which batch 1 had been obtained, by adding 0.03 mol dm^{-3} of silver nitrate to it and treating the solution so obtained (which, q.v., contained already 0.05 mol dm^{-3} of bis(adiponitrile)copper(I) nitrate) with three times the stoichiometric amount of copper calculated on the added silver nitrate. Otherwise the procedure was that used to obtain batch 1. The product will be referred to as batch 2.

Batch 3 was then prepared by a hybrid of the procedures used for batches 1 and 2, in which the mother liquor from the preparation of batch 2 was used together with fresh adiponitrile.

In the preparation of each of the three batches, from 0.6 to 0.75 dm^3 of solution was used and the yield was approximately 0.02 mol per dm^3 of solution.

The three batches were analysed for copper by electrodeposition and for carbon, nitrogen, and hydrogen with the laboratory analytical machine. The analytical results for the three batches were similar to one another: -

Batch:	1	2	3	Calculated
% Cu:	18.42	18.47	18.56	18.59
% C :	41.6	41.8	41.6	42.16
% N :	20.0	20.3	20.2	20.49
% H :	4.8	5.0	4.6	4.72

The product was in the form of shiny needles about 2 mm long. They were brownish, but only superficially, for they crushed to a white powder. The crystals were peculiarly easily crushed, squashing like wax rather than crumbling.

X-ray powder diffraction photographs on the ground crystals could be indexed on the basis of the unit cell deduced by Kinoshita et al (1959b). Table 3-1 lists the interplanar spacings obtained by measuring up the lines on a photograph taken with a Guinier camera, and compares them with calculated interplanar spacings.

An interesting, but initially rather perplexing, result was obtained when the first X-ray photograph of the prepared bis(adiponitrile)copper(I) nitrate was taken. This photograph, like the later photograph to which Table 3-1 relates, was taken with a Guinier camera, but unlike this later photograph was taken with a sample comprising a ground mixture of bis(adiponitrile)copper(I) nitrate and potassium chloride calibrant. The photograph so obtained (see Table 3-2) contained many lines which could not possibly be indexed on the unit cell of Kinoshita et al (1959b), and, furthermore, all the lines in the photograph which could be indexed on that unit cell were of relatively weak intensity; this indicated the presence in the sample of predominant quantities of one or more undesired phases, accompanied by, at most, only small quantities of bis(adiponitrile)-copper(I) nitrate (at least in the crystalline form described by

TABLE 3-1

Listing of X-ray powder diffraction lines obtained in a Guinier photograph of bis(adiponitrile)copper(I) nitrate.

Radiation: Cu Kα (λ = 1.54178 Å), Ni filter

Exposure: $6^1/2$ hours

Calibration: no calibrant, calibration constant taken as identical with that obtained in photograph with KCl (Table 3-2)

Assignments based on unit cell of Kinoshita et al (1959b):

a = 9.41 ± 0.02 Å
b = 13.73 ± 0.02 Å
c = 5.85 ± 0.01 Å

Space group Pnnn - D_{2h}^2

Extinctions - hk0 for (h + k) odd,
0kl for (k + l) odd,
h0l for (h + l) odd

int	d_{hkl}obs	d_{hkl}calc	hkl	int	d_{hkl}obs	d_{hkl}calc	hkl
MS	7.77	7.76	110	VVW	2.631	2.636	150
MS	6.87	6.87	020	VVW	2.558	2.564	321
MS	5.37	5.38	011	MW	2.502	2.506	241
VW	4.97	4.97	101	MW	2.480	2.486 2.484	051 202
VW	4.11	4.12	130	VVW	2.436	2.444	212
W	4.02	4.02	121	M	2.381	2.384	132
S	3.882	3.881	220	VW	2.349	2.353	400
S	3.595	3.605	031	MW	2.332	2.336	222
S	3.535	3.542	211	W	2.222	2.226 2.226	042 420
S	3.362	3.366	131	MW	2.196	2.198	251
M	3.230	3.234	221	VVW	2.176	2.183	232
VW	3.045	3.058	310	M	2.150	2.156 2.153	411 341
VW	2.855	2.861	231	M	2.110	2.114	312
W	2.821	2.820	141	MW	2.076	2.080 2.079	421 161
M	2.769	2.773 2.764	240 301	W	2.061	2.066 2.058	350 260
VVW	2.705	2.710	311	W	2.009	2.012	242
VVW	2.680	2.691	022				

int = intensity, S = strong, M = medium, W = weak, V = very

All d values are given in Å.

TABLE 3-2

Listing of X-ray powder diffraction lines obtained in a Guinier photograph of a mixture of bis(adiponitrile)copper(I) nitrate and potassium chloride.

Radiation: Cu Kα (λ = 1.54178 Å), Ni filter

Exposure: 6 hours

Calibrant: KCl (3.146 Å, 2.224 Å, 1.816 Å, 1.573 Å lines) used to obtain a mean calibration constant of 1 mm = 0.7136° in 2θ.

d_{hkl} exp. ("expected") is the calculated d_{hkl} for bis(adiponitrile)-copper(I) nitrate, but the intensity given in the assignment column is the observed intensity from Table 1; for KNO_3, the d_{hkl} exp. and intensity are from the American Society for Testing and Materials Powder Diffraction File 5-0377. See text for explanation of *.

intensity	d_{hkl} obs	d_{hkl} exp.	assignment
M	8.42		*
VW	7.74	7.76	110, $Cu(adip)_2NO_3$ (MS)
VW	7.14		*
VW	6.87	6.87	021, $Cu(adip)_2NO_3$ (MS)
W	5.38	5.38	011, $Cu(adip)_2NO_3$ (MS)
W	5.04		*
VW	4.65	4.66	110, KNO_3 (23)
M	4.50		*
M	4.17		*
W	3.868	3.881	220, $Cu(adip)_2NO_3$ (S)
W	3.781	3.78	111, KNO_3 (100)
VW	3.736	3.73	021, KNO_3 (56)
VW	3.599	3.605	031, $Cu(adip)_2NO_3$ (S)
MS	3.573		*
MS	3.563		*
W	3.538	3.542	211, $Cu(adip)_2NO_3$ (S)
VVW	3.424		*
VW	3.369	3.366	?131 $Cu(adip)_2NO_3$ (S)
W	3.360		
W	3.287		*
W	3.261		*
W	3.191		*
S	3.149	3.146	KCl
W	3.040	3.033	012, KNO_3 (55)

TABLE 3-2 (cont.)

intensity	d_{hkl} obs	d_{hkl} exp.	assignment
VW	2.909		*
W	2.768	2.763	102, KNO_3 (28)
W	2.707	2.707	200, KNO_3 (17)
W	2.668	2.662	130, KNO_3 (41)
W	2.649	2.647	112, KNO_3 (55)
W	2.635	2.632	022, KNO_3 (20)
VVW	2.614		*
W	2.543		*
W	2.523		*
W	2.484		
VW	2.417		
W	2.378		
VW	2.331		
W	2.251		*
S	2.225	2.224	KCl
W	2.193	2.192	221, KNO_3 (41)
W	2.163	2.159	041, KNO_3 (20)
VW	2.146		
VW	2.123		*
VW	2.101		
W	2.070		
W	2.053	2.050	132, KNO_3 (18)

S = strong, M = medium, W = weak, V = very

adip = $NC(CH_2)_4CN$

All d values are given in Å.

Kinoshita et al).

When it was later found that no such problem arose if the potassium chloride calibrant was omitted (Table 3-1, q.v.), it became clear that some reaction between the solid bis(adiponitrile)copper(I) nitrate and the solid potassium chloride had taken place, either before the ground mixture was put into the X-ray machine, or during the exposure (of 6 hours). Analysis of the lines in Table 3-2 strongly suggests that the ground bis(adiponitrile)copper(I) nitrate mixture did indeed still contain small quantities of bis(adiponitrile)-copper(I) nitrate, since all of the "S" and "MS" lines of Table 3-1 have a counterpart in Table 3-2, and, further, that potassium nitrate is formed in the reaction, since every one of the potassium nitrate lines having an intensity from 18 to 100 in the ASTM listing for this compound has a counterpart in Table 3-2.

It seems possible, therefore, that the reaction between the solids is simply

$$Cu\left[NC(CH_2)_4CN\right]_2NO_3 + KCl \rightarrow Cu\left[NC(CH_2)_4CN\right]_2Cl + KNO_3.$$

This cannot, however, be confirmed on the basis of Table 3-2 alone, since, as far as the present author is aware, bis(adiponitrile)-copper(I) chloride has never been prepared and characterised; and various other reactions are also possible. In Table 3-2, the lines marked * cannot reasonably be ascribed to potassium chloride, bis(adiponitrile)copper(I) nitrate, or potassium nitrate; they therefore characterise the other product(s) of the reaction in addition to potassium nitrate, and could be used as a starting point for further investigation.

Plate 3-I shows Debye-Scherrer X-ray powder diffraction photographs of potassium chloride, bis(adiponitrile)copper(I) nitrate, a bis(adiponitrile)copper(I) nitrate-potassium chloride mixture, and

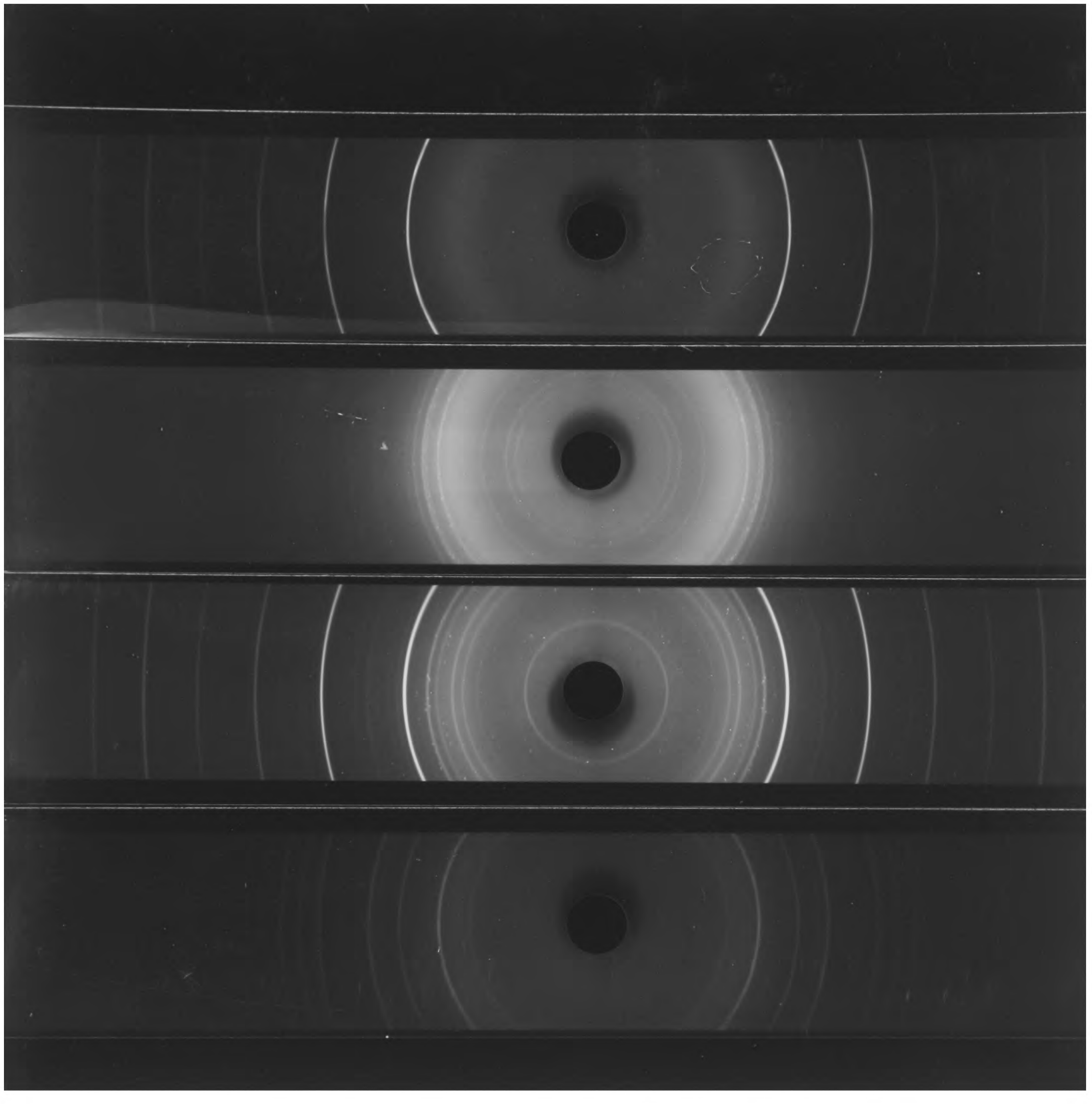

PLATE 3-I

Debye-Scherrer photographs:
Camera: 11.46 cm dia.
(1 mm = 1° in 2θ)
Film mounting: Straumanis method
Radiation: CuKα, Ni filter

(a)
KCl

(b)
$Cu(adip)_2NO_3$

Note especially that the innermost three, medium-intensity lines of (b) (7.76, 6.87, 5.38 Å) are almost invisible in (c); that the innermost, medium-intensity line in (c) (8.42 Å) does not occur in (b) or (a); that (c) contains weak-intensity counterparts to the three strongest "lines" in (d) (3.78/3.73 Å overlapping, 3.033 Å, and 2.662/2.647 Å/ ?others overlapping).

(c)
mixture of
$Cu(adip)_2NO_3$
and KCl

(d)
KNO_3

potassium nitrate, which (despite the relatively low resolution of the camera compared with a Guinier camera) illustrate the reaction between the solids.

Section 3-2: heat capacity results

Heat capacity determinations were first carried out, in collaboration with Dr S.H. Lee, formerly of this laboratory, in the adiabatic calorimeter constructed by Linford (1967), which for convenience will hereinafter be called the "Linford calorimeter". The charge in the sample-containing vessel consisted of 0.01412 mol, 0.01191 mol, and 0.01011 mol respectively of batches 1, 2, and 3 prepared as described in Section 3-1, making a total of 0.03613(9) mol ($C_{12}H_{16}N_5O_3Cu$ = 341.88(3); density for buoyancy correction taken as 1.51 g cm^{-3}). The results of these determinations are listed in Table 3-3.

After these determinations were complete, the crystals of the sample were unchanged in size and appearance and were reused for determinations in the new calorimeter described in Chapter 2.

The results in the new calorimeter are listed in Table 3-4, together with various weights, etc. as promised in Section 2-9d (page 83, last paragraph).

On being removed from the calorimeter, the crystals of the sample were again unchanged in size and appearance, and yielded X-ray powder diffraction photographs similar to those previously obtained.

The determinations in the two calorimeters took the sample through a range of temperature from about 1.5 K to over 300 K. The results from the two calorimeters overlapped for T_{MID}s in the 11 - 80 K region. The results below about 100 K are plotted in Figures 3-1 to 3-3.

TABLE 3-3

Results obtained in the Linford calorimeter.

T_{MID}/K	ΔT/K	$\overline{C_{p,m}}$/$JK^{-1}mol^{-1}$	% of total meas. C_p due to sample	notes
11.696	1.868	8.678	63	He
13.441	1.907	12.22	62	He
15.034	1.482	15.59	62	He
17.431	3.045	22.06	62	He
19.987	1.929	29.43	61	He
21.266	1.437	34.75	62	He
25.866	3.355	46.86	58	He
29.631	4.131	58.58	56	He
33.317	3.256	72.06	55	He
36.359	2.830	80.45	53	He
39.403	3.257	93.43	53	He
42.615	3.170	106.6	53	He
44.711	3.201	112.9	53	He
47.857	3.019	124.3	52	He
50.063	1.954	134.0	52	A He
52.802	2.230	132.7	50	A He
55.005	2.176	131.3	48	A He
57.142	2.088	135.3	48	A He
59.196	2.010	139.9	47	A He
60.285	4.849	143.2	47	He
65.055	4.674	155.9	47	He
70.083	5.445	157.9	45	He
75.633	5.604	168.8	45	He
80.484	4.092	178.8	45	He
83.063	6.340	185.8	46	N_2
89.232	6.003	192.0	45	N_2
95.113	5.761	202.1	45	N_2
100.856	6.904	212.1	45	N_2
107.625	6.652	218.4	45	N_2
109.459	6.598	220.7	45	N_2
115.940	6.390	226.7	45	N_2
127.730	6.055	244.5	46	N_2
133.717	5.936	246.6	45	N_2

TABLE 3-3 (cont.)

T_{MID}/K	ΔT/K	$\overline{C_{p,m}}$/JK^{-1}mol^{-1}	% of total meas. C_p due to sample	notes
139.592	5.816	252.4	45	N_2
145.361	5.707	258.7	45	N_2
151.021	5.606	263.9	46	N_2
156.575	5.501	270.8	46	N_2
162.052	5.440	274.2	46	N_2
168.894	5.446	278.9	46	N_2
174.288	5.345	287.3	46	N_2
182.014	5.279	290.5	46	N_2
187.287	5.242	296.1	47	N_2
192.497	5.164	302.6	47	N_2
202.134	5.087	308.5	47	N_2
207.220	5.040	313.6	47	N_2
212.258	4.979	318.1	48	N_2
217.229	4.958	321.9	48	N_2
222.177	4.900	329.9	48	N_2
232.493	4.807	336.1	49	N_2
237.287	4.767	339.9	49	N_2
241.239	3.113	343.2	49	N_2
237.185	4.440	339.6	49	CO_2
241.770	4.709	343.8	49	CO_2
247.681	4.593	350.5	49	CO_2
252.304	4.630	356.0	50	CO_2
256.919	4.572	363.1	50	CO_2
262.352	6.307	372.7	51	CO_2
269.209	5.961	383.2	51	CO_2
277.080	8.177	383.3	51	H_2O
285.195	7.958	388.7	51	H_2O
293.223	7.959	397.4	52	H_2O
302.760	8.432	404.4	52	H_2O

In "notes" column, He, N_2, CO_2, H_2O indicate respectively the use as refrigerant of liquid helium, liquid nitrogen, solid carbon dioxide/methanol, and ice/water under normal pressure. All the results with liquid helium refrigerant were obtained in a single run except for those marked A, which were obtained in a later run with smaller ΔTs in the anomalous region.

TABLE 3-4

Results obtained in the new calorimeter described in Chapter 2

Weights, etc. (see Section 2-9d for the meanings of the symbols):-

n_{sample} = 0.032 54(7 5)mol

$n_{exch.\ gas}$ = 7.03×10^{-6} mol of He^3

$\Delta m_{elecsol}$ = +0.127 20 g

Δm_{indsol} = −0.135 44 g

Δm_{Ag} = +0.007 05 g

($C_{12}H_{16}N_5O_3Cu$ = 341.88(3); density for buoyancy correction and calculation of $n_{exch.\ gas}$ taken as 1.51 g cm^{-3}.)

T_{MID}/K	ΔT/K	$\overline{C_{p,m}}$/$JK^{-1}mol^{-1}$	$C_{p,m}$/$JK^{-1}mol^{-1}$ (corrected for curvature)	% of total measured $\overline{C_p}$ due to sample	notes
1.665	0.273	0.02462	0.02455	24	A
1.914	0.335	0.03277	0.03265	26	A
2.090	0.291	0.04079	0.04069	28	A
2.218	0.458	0.04440	0.04414	28	A
2.538	0.346	0.05787	[0.05787]	30	A
2.866	0.480	0.09602	0.09519	37	A
3.105	0.318	0.1279	0.1275	41	A
3.376	0.430	0.1673	0.1665	44	A
3.711	0.465	0.2223	0.2213	47	A
4.070	0.482	0.3026	0.3012	49	A
4.446	0.626	0.4142	0.4115	54	A1
5.008	0.519	0.6201	0.6181	58	A1
5.536	0.586	0.8907	0.8878	61	A1
6.212	0.281	1.268	1.267	64	B
6.251	0.904	1.300	1.293	64	A1
6.702	0.787	1.655	1.648	66	B
7.010	0.699	1.877	1.871	67	A1
7.481	0.881	2.391	2.383	68	B
7.705	0.777	2.615	2.609	69	A1
8.341	0.940	3.275	3.265	69	B
9.235	0.974	4.292	4.280	69	B
10.142	0.970	5.699	5.687	70	B
10.629	1.145	6.680	6.662	71	B
11.746	1.305	8.589	8.562	71	B

TABLE 3-4 (cont.)

T_{MID}/K	ΔT/K	$\overline{C_{p,m}}$/$JK^{-1}mol^{-1}$	$C_{p,m}$/$JK^{-1}mol^{-1}$ (corrected for curvature)	% of total measured $\overline{C_p}$ due to sample	notes
12.892	1.306	11.50	11.50	72	B
14.151	1.398	14.29	14.29	71	B
15.552	1.557	17.14	17.14	70	B
17.376	2.269	21.94	21.94	69	B
19.599	2.161	28.62	28.62	68	B
21.877	2.395	35.47	35.47	67	B
24.608	3.052	43.66	43.66	65	B
27.767	3.263	53.80	53.80	63	B
30.894	2.987	63.97	63.97	61	B
33.925	3.076	74.43	74.43	60	B
37.204	3.482	85.71	85.71	58	B
40.588	3.286	97.57	97.57	57	B
43.832	3.203	109.5	109.5	57	B
46.207	1.547	118.2	118.2	56	B
47.699	1.437	129.1	[129.1]	57	B
49.321	1.605	134.2	[134.2]	57	C
50.890	1.533	139.9	[139.9]	56	C
52.618	1.924	135.9	[135.9]	54	C
54.655	2.149	134.9	[134.9]	53	C
56.757	2.057	139.3	[139.3]	52	C
58.784	1.997	140.7	[140.7]	51	C
60.961	2.356	148.9	[148.9]	51	C
63.249	2.204	161.9	[161.9]	52	C
65.927	3.153	155.4	[155.4]	50	C
70.739	6.471	165.0	165.0	49	C
76.129	4.308	172.7	172.7	49	C
80.344	4.122	180.8	180.8	49	C

Note:- These results were obtained in three separate, each essentially continuous runs, consisting of, respectively: determinations A and A1, made with liquid helium refrigerant according to, respectively, schemes (b) and (c) in Figure 2-13; determinations B, made with liquid helium refrigerant roughly according to schemes (c) to (f) in Figure 2-13; and determinations C, made with liquid nitrogen refrigerant according to scheme (g) in Figure 2-13.

The figures in the $C_{p,m}$/$JK^{-1}mol^{-1}$ column have been corrected for curvature except where they are given in square brackets, in which case $\overline{C_{p,m}}$/$JK^{-1}mol^{-1}$ is again given, generally because the form of the $\overline{C_{p,m}}$ - T plot prevented any worthwhile correction from being made.

FIGURE 3-1

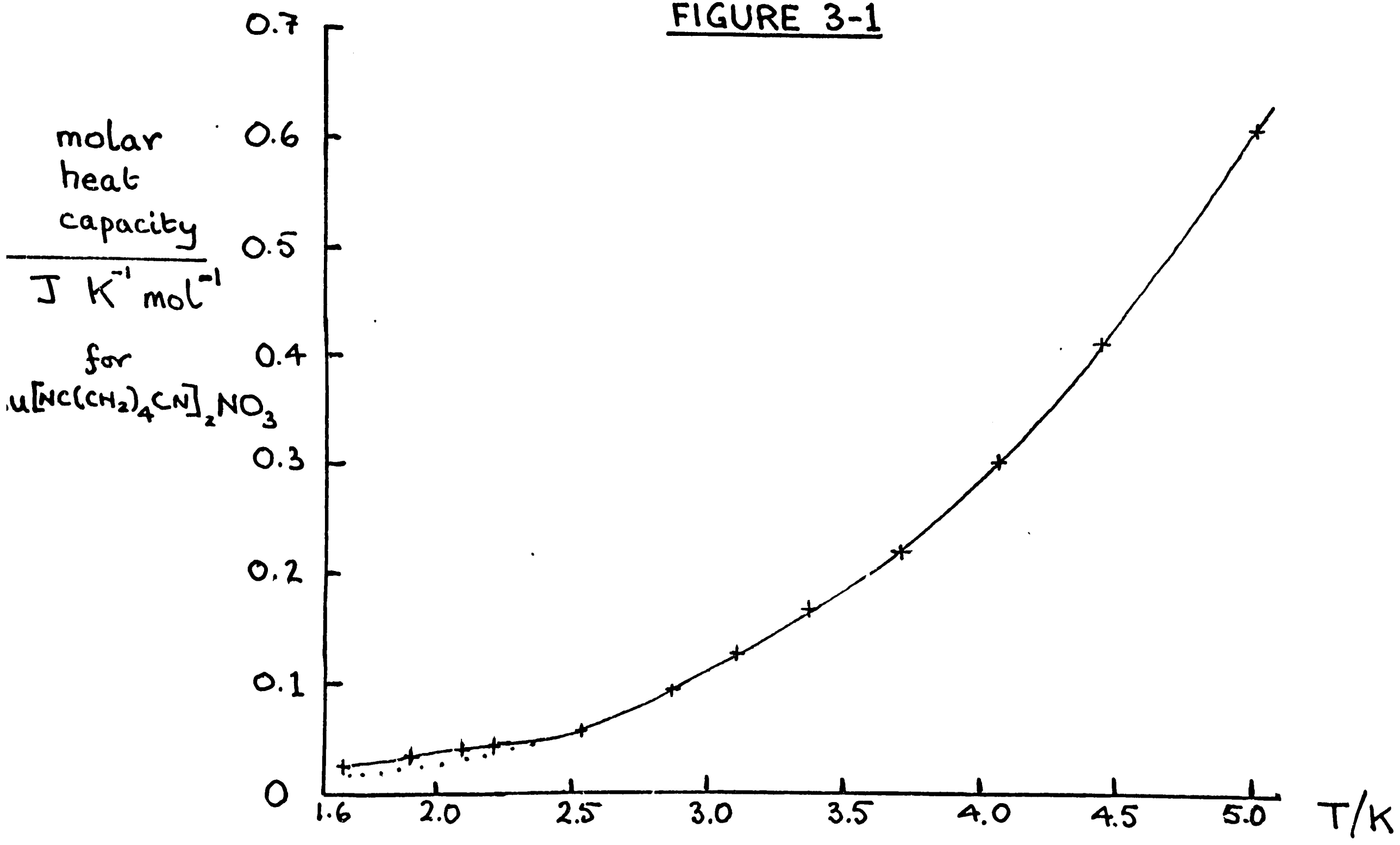
molar heat capacity / J K⁻¹ mol⁻¹ for U[NC(CH2)4CN]2NO3
0.7
0.6
0.5
0.4
0.3
0.2
0.1
0
1.6
2.0
2.5
3.0
3.5
4.0
4.5
5.0
T/K

FIGURE 3-2

⊗ : results in "Linford calorimeter" (Table 3-3)
\+ and curve: results in new calorimeter (Table 3-4)

To avoid congestion, only a sample of the results below 12 K are presented.

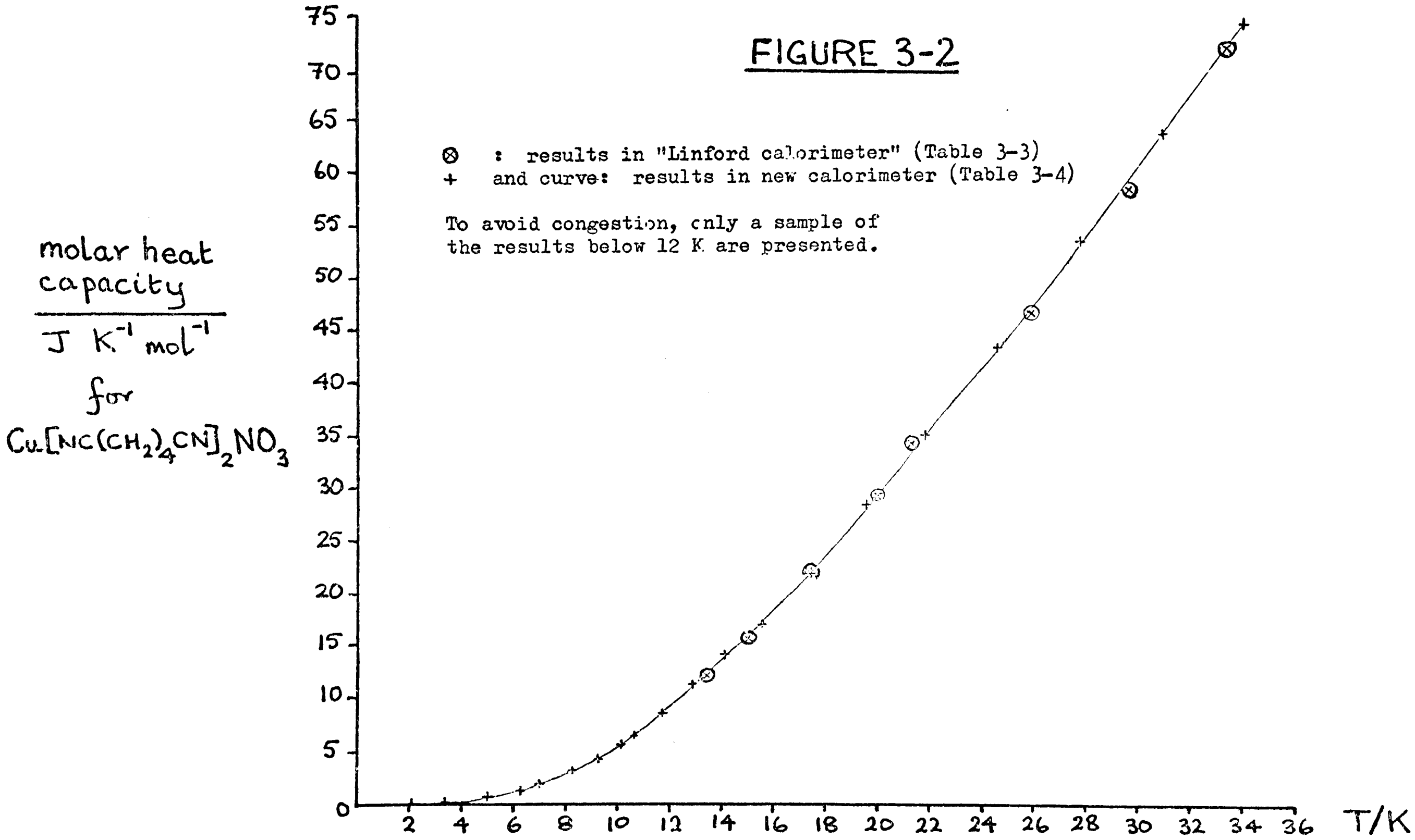

FIGURE 3-3

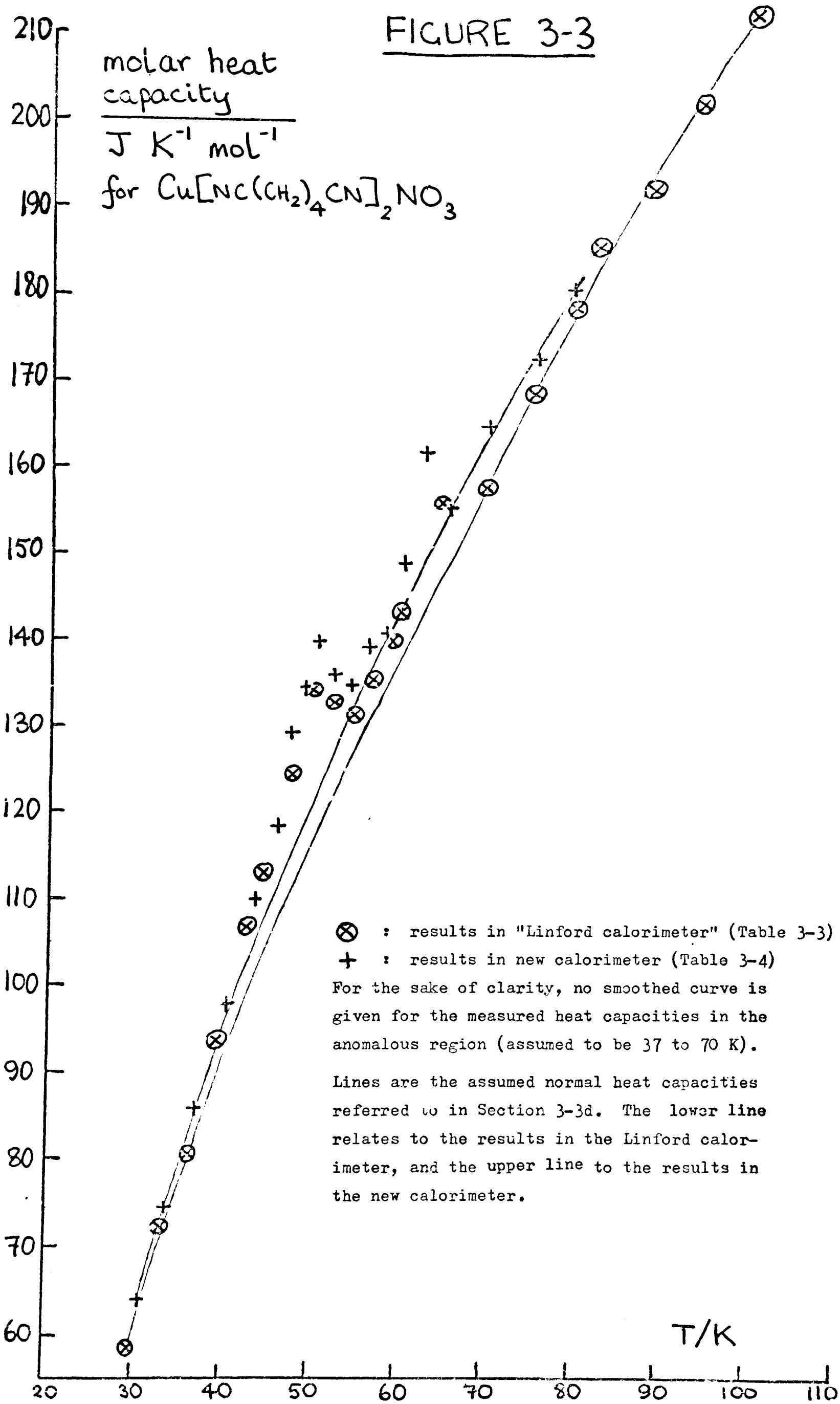
molar heat capacity / J K⁻¹ mol⁻¹
for Cu[NC(CH₂)₄CN]₂NO₃
210
200
190
180
170
160
150
140
130
120
110
100
90
80
70
60
T/K
20
30
40
50
60
70
80
90
100
110
⊗ : results in "Linford calorimeter" (Table 3-3)
+ : results in new calorimeter (Table 3-4)
For the sake of clarity, no smoothed curve is given for the measured heat capacities in the anomalous region (assumed to be 37 to 70 K).
Lines are the assumed normal heat capacities referred to in Section 3-3d. The lower line relates to the results in the Linford calorimeter, and the upper line to the results in the new calorimeter.

Section 3-3: description of heat capacity results; comparison of results in the two calorimeters

a. results below 4.2 K

The Linford calorimeter has no provision for the production of temperatures below 4.2 K. The only results in this range were, therefore, obtained with the new calorimeter described in Chapter 2. It was especially gratifying that warming due to vibration (see page 73) was small enough to permit operation down to vessel temperatures of about 1.5 K.

Since the heat capacity of the empty calorimeter used in calculating the results is extrapolated in this region (see Section 2-9d), and since the proportion of the total heat capacity due to the sample decreased markedly below 4.2 K (see Table 3-4), the absolute values of the molar heat capacity obtained may be subject to some error. However, regardless of whether there is such an error in the absolute values obtained, an anomaly, if present, should be readily detectable, since the heat capacity of the empty calorimeter is itself expected to decrease smoothly with decreasing temperature.

It is evident from Figure 3-1 that there is a marked change in slope of the $C_{p,m}$ - T plot at approximately 2.5 K, and that the values of $C_{p,m}$ below 2.5 K are unexpectedly high having regard to the values above 2.5 K, which rise smoothly with T. It is clear, however, that even if there is a genuine anomaly in the sample below 2.5 K, then the associated entropy change is small; for example, if the "normal" molar heat capacity is taken to follow the dotted curve shown in Figure 3-1 (which is based on a Debye T^3 extrapolation from the determination just above 2.5 K), the anomalous entropy gain in the region plotted is calculated to be only 2.7 mJ K^{-1} mol^{-1}, compared with R ln 2 = 5.76 J K^{-1} mol^{-1}.

In fact, it seems quite possible that the anomaly is spurious, being caused by the adsorption, on the sample or on the walls of the vessel, of a part of the He^3 exchange gas used within the vessel; for the enthalpy change associated with the "anomaly" is only 5.2 mJ mol^{-1}, while an enthalpy change of up to 9.7 mJ mol^{-1} could be explained by adsorption of He^3, if the heat of adsorption of the He^3 is assumed to be the same as the latent heat of vaporisation (which is 45 J mol^{-1} in the 1.6 - 2.6 K region, see Keller, 1969). Furthermore, Bloembergen and Miedema (1974) report a similar effect with the He^3 exchange gas. In fact, the effect observed by them was rather larger, presumably because they used higher pressures of exchange gas and a powdered sample.

Section 3-3b: results from 4.2 K to 11 K

The only reliable results in this region were obtained in the new calorimeter, and these indicate that the molar heat capacity continues to rise smoothly in this temperature range (see Figure 3-2).

In principle, the Linford calorimeter can be operated in this temperature range; but because there is no thermal switch in that calorimeter the only way of cooling the vessel and shield to 4.2 K reasonably rapidly involves admitting exchange gas into the space about the vessel. This exchange gas is difficult to pump away to a satisfactory degree (compare the paragraph bridging pages 71 and 72), and the results obtained are therefore unreliable (often spectacularly high).

Section 3-3c: results from 11 K to 30 K

The results from the two calorimeters are in good agreement over this range, both indicating a steady rise in the molar heat capacity. However, the Linford calorimeter results are somewhat more scattered about a smooth curve than are the results from the new calorimeter.

It is suggested that this relatively poor precision in the Linford calorimeter derives in part from the relatively poor insulation of the vessel from the shield in the Linford calorimeter, which in turn derives from the use of exchange gas to initially cool the vessel, q.v., and from the presence of copper electrical leads between the vessel and the shield (no copper leads were used between the vessel and the shield in the new calorimeter - see second new paragraph, page 44). These effects become less significant with rising temperature, for heat capacities generally rise more quickly than thermal conductivities. Further, the thermometer in the Linford calorimeter is a platinum resistance thermometer operated at a constant current of 3 mA, and is less precise at lower temperatures, in contrast with the germanium resistance thermometer used in the new calorimeter (see Figure 2-3, at page 31).

Section 3-3d: results from 30 K to 81 K

As shown in Figure 3-3, anomalous heat capacities were observed with both calorimeters in this range. In the new calorimeter, two heat capacity maxima were observed at values of T_{MID} near 51 K and 63 K respectively. The results in the Linford calorimeter are consistent with heat capacity maxima near these temperatures, if allowance is made for the different T_{MID}s and ΔTs which were employed with this calorimeter.

There is in the upper part of this range a clear systematic difference between molar heat capacities determined in the new calorimeter and those determined in the Linford calorimeter, the results on the new calorimeter being higher by up to about 3½ % if one ignores differences which may possibly arise from the differences in T_{MID}s and ΔTs. It is believed that the results in the Linford calorimeter, which has been thoroughly used and tested over many years,

are the more accurate. It has already been suggested (bottom of page 67) that this systematic error may be connected with the observed sluggishness of response of the thermocouples to heating of the vessel and the shield. The shield in the Linford calorimeter differs from that in the new calorimeter (which in any case was designed for best performance below 30 K) in being less massive and in being automatically rather than manually controlled; and perhaps these differences account at least partly for the Linford calorimeter's apparently superior accuracy in the upper part of this temperature range.

Nevertheless, despite the generally decreasing sensitivity of the germanium resistance thermometer of the new calorimeter in this range (see Figure 2-3 at page 31), the precision of the results in the new calorimeter (as opposed to their accuracy) appears to be fairly good, at least below 70 K; and the usefulness of the new calorimeter for determining the qualitative features of a $C_{p,m}$ - T plot (including a correct estimation of the position of heat capacity maxima) is considered to be confirmed by these results.

On inspection of large-scale plots of the results from each calorimeter, it was considered that a rough estimate of the anomalous contributions to the molar enthalpy and entropy of the substance could be made by assuming that the heat capacity as measured was normal both below 37 K and above 70 K. On this basis for each set of results a curve was drawn, freehand, to represent the normal contribution to $C_{p,m}$ in the 37 K - 70 K region. By graphical integration of the remainder of the measured $C_{p,m}$ (i.e. $C_{p,m,anom}$) with respect to T, $\Delta H_{m,anom}$, the anomalous contribution to the enthalpy, was estimated. By integration of $C_{p,m,anom}/T$ with respect to T, $\Delta S_{m,anom}$ was also estimated. The "normal" heat capacity contributions

assumed are shown, on a much reduced scale, in Figure 3-3. The values of $\Delta H_{m,anom}$ and $\Delta S_{m,anom}$ are given in Table 3-5.

Table 3-5: rough estimates of anomalous contributions to enthalpy and entropy between 37 K and 70 K

quantity measured \ calorimeter	Linford calorimeter	New calorimeter
$\Delta H_{m,anom}(< 55\ K)$ / J mol^{-1}	159	119
$\Delta H_{m,anom}(> 55\ K)$ / J mol^{-1}	84	50
$\Delta H_{m,anom}$(total) / J mol^{-1}	243	169
$\Delta S_{m,anom}(< 55\ K)$ / JK^{-1}mol^{-1}	3.33	2.43
$\Delta S_{m,anom}(> 55\ K)$ / JK^{-1}mol^{-1}	1.35	0.81
$\Delta S_{m,anom}$(total) / JK^{-1}mol^{-1}	4.68	3.24

Compare ΔS with R ln 2 = 5.76 J K^{-1} mol^{-1}
R ln 4 = 11.53 J K^{-1} mol^{-1}

The question of the significance of the values given in Table 3-5 will be discussed later, in Section 3-5; but it may be mentioned here that the difference between the values obtained from the results in the two calorimeters does not necessarily have any significance, in view of the rather arbitrary procedure by which they were calculated.

Section 3-3e: results from 81 K to 303 K

These results were obtained exclusively in the Linford calorimeter. In this range, the molar heat capacity was observed to rise fairly steadily, there being only one clear indication of anomalous

behaviour, in that there is a "hump" in the $C_{p,m}$ - T plot between 252 K and 285 K. It seems probable that there is a heat capacity maximum in the 266 K - 272 K region. No attempt was made to locate the position of this maximum more precisely. By assuming that the measured heat capacity was normal at 252 K and below and at 285 K and above, the "normal" contribution to the heat capacity in the 252 K - 285 K range was estimated by freehand drawing on a large-scale graph. The anomalous contribution to the molar enthalpy, $\Delta H_{m,anom}$ was then estimated as 135 J mol^{-1}, and the anomalous contribution to the entropy, $\Delta S_{m,anom}$ as 0.50 J K^{-1} mol^{-1} (compare R ln 2 = 5.76 J $K^{-1}mol^{-1}$).

In view of the small size of this anomaly, and the fact that it occurs near and below the melting point of adiponitrile (0 - 1°C according to Beilstein (1920), 2°C according to the manufacturers of the adiponitrile used in the present work, 1.9 to 4.4°C by the author's own measurements), it seems possible that the anomaly may have been caused solely by the presence in the sample of a small amount of occluded mother liquor (i.e. adiponitrile saturated with bis(adiponitrile)copper(I) nitrate). The amount of adiponitrile thereby occluded in the crystals was estimated by assuming that the anomalous heat corresponds to the latent heat of fusion of adiponitrile, and that, in turn, the molar entropy of fusion of adiponitrile (for which Landolt - Börnstein (1961) unfortunately gives no $\Delta H_{m,f}$) lies in or near the same range as various nitriles for which Landolt-Börnstein does give $\Delta H_{m,f}$ (namely HCN, CH_3CN, C_2H_5CN, $n\text{-}C_3H_7CN$, $n\text{-}C_4H_9CN$, $NC\text{-}C\equiv C\text{-}CN$, and $NC\text{-}C\equiv C\text{-}C\equiv C\text{-}CN$, all of which have $\Delta S_{m,f}$ between 16.9 J K^{-1} mol^{-1} and 52.8 J K^{-1} mol^{-1}). On this basis, the anomalous heat capacities observed between 252 K and 285 K could be explained by the presence of from 1 to 3 mol per cent (i.e. 0.3 - 1 weight per cent) of occluded adiponitrile in the calorimetric sample. At least

the lower end of this range is thought to be within the bounds of possibility.

Section 3-3f: summary

The molar heat capacity of bis(adiponitrile)copper(I) nitrate was determined between 1.67 K and 303 K, and heat capacity maxima were found at 51 K and 63 K. It seems likely that the heat capacity includes an anomalous contribution between about 37 K and 70 K, and the anomalous contribution to the molar entropy in this region was estimated to be between 1/2 R ln 2 and R ln 2. Other apparent heat capacity anomalies were small and very possibly not to be ascribed to changes occuring in the bis(adiponitrile)copper(I) nitrate crystal itself.

Section 3-4: room-temperature crystal structure of bis(adiponitrile)copper(I) nitrate

a) the cationic networks in the room-temperature structure

According to Kinoshita et al, 1959b, who carried out a single-crystal X-ray diffraction study, bis(adiponitrile)copper(I) nitrate contains discrete NO_3^- ions but no discrete $[Cu(NC(CH_2)_4CN)_2]^+$ ions. Instead, the crystal contains infinite three-dimensional polymeric ions $[Cu(NC(CH_2)_4CN)_2]_n^{n+}$.

The Cu atoms in one of these polymeric ions occupy the positions of C atoms in a distorted diamond lattice (see Figure 3-4); each Cu atom in the polymeric ion is at the centre of a non-regular tetrahedron at the corners of which are situated the four nearest Cu atoms of the ion. A $-NC(CH_2)_4CN-$ group lies roughly along the line between each Cu atom and each of its 4 Cu neighbours at the corners of the tetrahedron. The structure of the polymeric ion is, therefore, similar to that of the β -cristobalite form of SiO_2 (described, for

FIGURE 3-4

(schematic diagram of part of a $[Cu(NC(CH_2)_4CN)_2]^{n+}_n$ network)

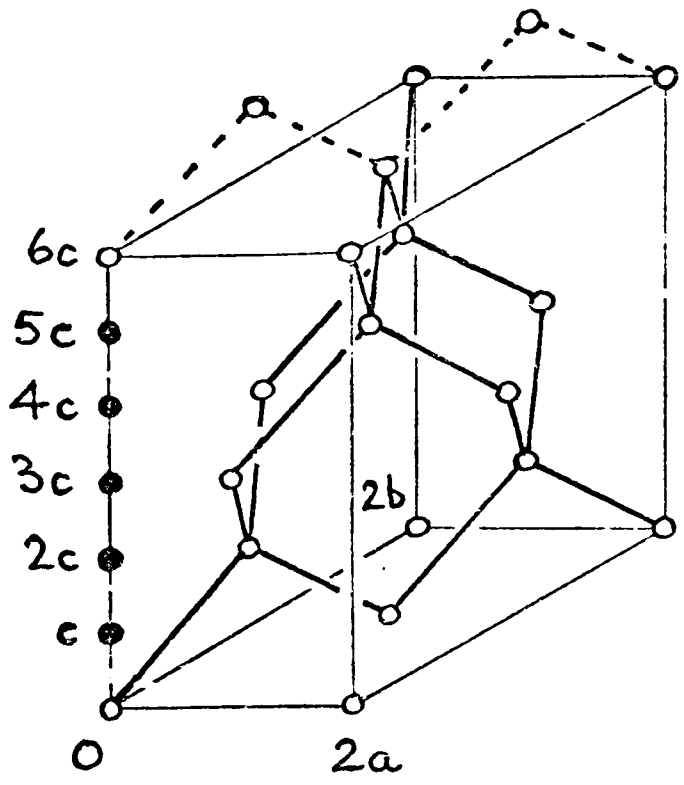

a, b, c are unit cell dimensions.

Box has dimensions 2a x 2b x 2c.

o = Cu belonging to the network shown

● = Cu belonging to other networks (only one shown for each)

——— = $-NC(CH_2)_4CN-$ within box

- - - - - = $-NC(CH_2)_4CN-$ outside box

example, in Addison, 1961), except that each Si is replaced by Cu and each O by $-NC(CH_2)_4CN-$, that the network is charged, and that the tetrahedral arrangement of Cu atoms is not regular.

The structure shown in Figure 3-4 is very open, because of the length of the adiponitrile ligands, and each Cu atom being 12.09 Å from its nearest Cu atom neighbours; and as a consequence of this, the crystal, most remarkably, contains <u>six</u> interpenetrating networks, only one of which is shown in Figure 3-4. To generate the full complement of polymeric networks in Figure 3-4, it would be necessary to draw in further networks starting from the Cu atoms shaded in black, each network being related to the previous one by a displacement <u>c</u>. There are no covalent bonds between networks.

Other structures comprising interpenetrating networks are known. Ag_2O and Cu_2O, which comprise <u>two</u> interpenetrating anti-β-cristobalite networks, are well known. Further examples have been listed by Thurn and Krebs (1969) and include Hittorff's phosphorus and modifications of ice.

The unit cell, with all atomic positions as determined by Kinoshita et al, is shown in Figure 3-5, in which the two projections are arranged so that the Figure may be read like an ergineering drawing in "first angle projection". The description by Kinoshita et al of the condition of the nitrate ions (central atoms N2 in Figure 3-5) is certainly an oversimplification (see Section 3-4b). This question being for now ignored, the structure can be described in more detail as follows:-

The unit cell shown contains two formula units of $Cu(NC(CH_2)_4CN)_2NO_3$. The Cu atoms lie in equivalent special positions (i.e. positions lying on symmetry axes, centres, and/or planes); a Cu atom shared between eight unit cells lies at each of the eight

FIGURE 3-5

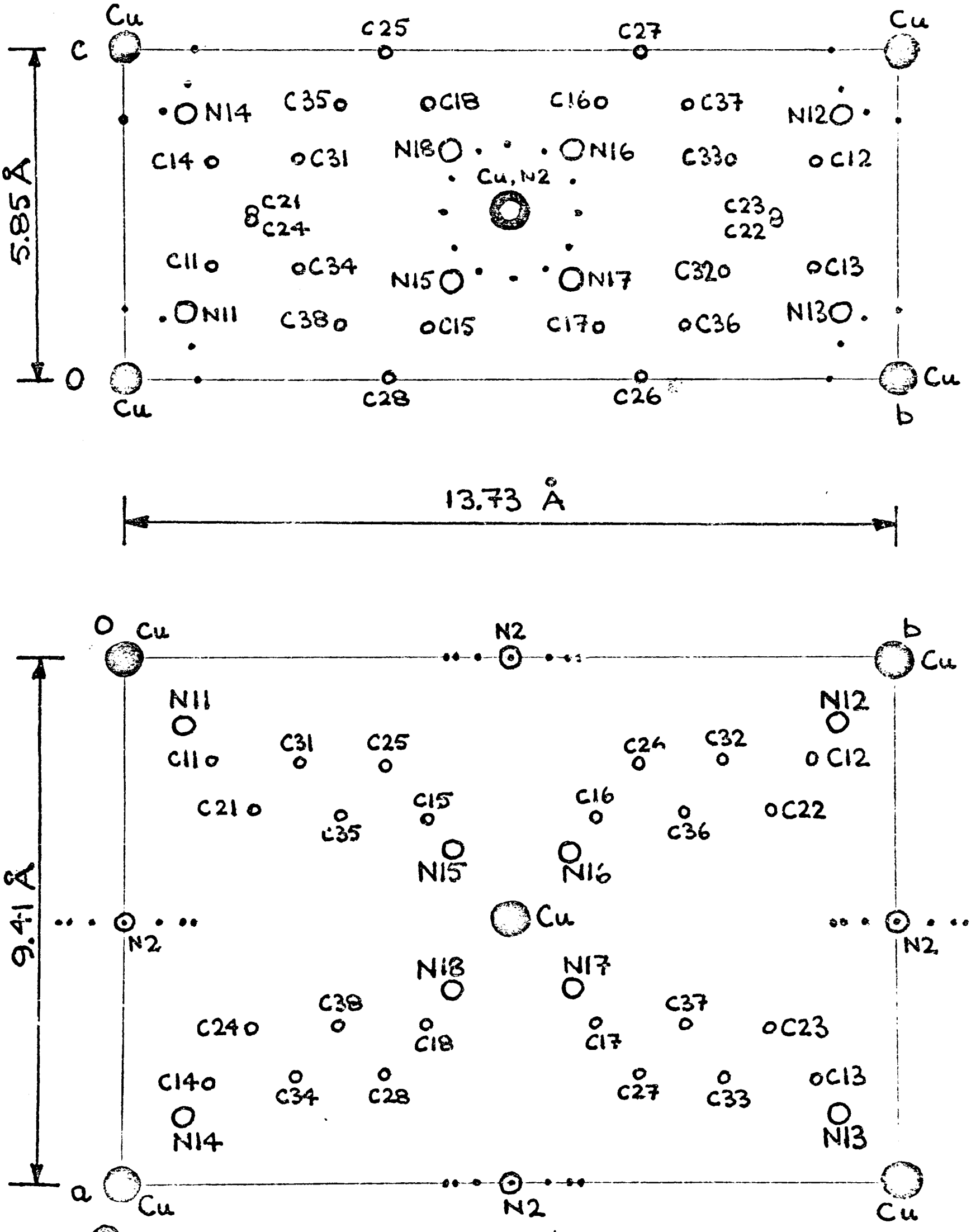

= Cu, O = N, o = C, • = 1/4 O.

N in NO_3^- are labelled N2.

N11 to N18 are the terminal N atoms of adiponitrile molecules; C11 to C18 are the C atoms of nitrile groups; C21 to C28 are the C atoms of α-methylene groups; C31 to C38 are the C atoms of β-methylene groups. N11 to N18, C11 to C18, etc. each constitute a set of eight equivalent general positions.

For a caveat on this structure, see third new paragraph, page 110.

cell corners, and one Cu atom lies in the body centre, giving two Cu atoms per unit cell. The C and N atoms of the adipcnitrile molecules lie in general positions. There are, within each unit cell, eight cyano group N atoms in equivalent positions (N11 to N18), eight cyano group C atoms in equivalent positions (C11 tc C18), eight α-methylene group C atoms in equivalent positions (C21 to C28), and eight β-methylene group C atoms in equivalent positions (C31 to C38).

It will be appreciated from Figure 3-4 that no single unit cell (such as shown in Figure 3-5) contains any single complete adiponitrile molecule. Thus, the atom N11 belonging to one end of an adiponitrile molecule coordinates the Cu atom at 0,0,0, and this molecule can be followed through C11, C21, C31, C35, C25 until it leaves the unit cell shown, and into the next unit cell in the c direction, where, via atoms C15 and N15 in that unit cell, it coordinates the Cu atom at the body centre of that unit cell - i.e. at 1/2, 1/2, 3/2 relative to the origin shown in Figure 3-5.

Preliminary note to the remaining sections of this chapter

These sections are concerned in part with the disordered arrangement of nitrate ions known to exist at room temperature. It will be shown that the statements by Kinoshita et al concerning the precise condition of the nitrate ions at room temperature are at best approximate, and may well be wrong in respect of the thermodynamically crucial question of the number of "orientations" among which the ions are disordered.

These sections (especially Section 3-4b and Section 3-5b) are concerned with describing the disordered state and the presumed order-disorder transition involving the nitrate ions, on the basis of what is certainly known of the crystal structure and on the basis of the ways in which the various species involved should interact. It would of course be highly satisfying to calculate these interactions theoretically and to predict for instance the temperature of the heat capacity anomaly and the form of the anomaly.

In the case of K_2SnCl_6 (see Morfee et al, 1960), a calculation of this general type met with some success. The first step was to calculate the interactions of $SnCl_6^{2-}$ with its environment without regard to cooperative $SnCl_6^{2-}$ interactions; this indicated two positions of equal energy for each $SnCl_6^{2-}$ ion. The second step was to perturb the model by including cooperative $SnCl_6^{2-}$ - $SnCl_6^{2-}$ interactions. The treatment here follows the same general plan.

However, in the case of K_2SnCl_6, it was apparently assumed from the start that the Sn atoms lay in the symmetry origin of the site in which the $SnCl_6^{2-}$ ions are situated (which assumption made for easy calculation); while it will be shown that in the present case a comparable assumption regarding the N atoms of the nitrate ions cannot be sustained (see the discussion of Table 3-7 following and see also

Appendix 3-III).* As a result of this and related difficulties, it was not possible, at least in the time available, to perform the extremely complicated ab initio calculations of the interaction of a nitrate ion with its environment that would properly be appropriate, although a combination of the results of a highly simplified calculation with other evidence (X-ray diffraction and heat capacity results) led to a tentative qualitative conclusion concerning the disordered state at 70 K. Unfortunately, the two parameters necessary to define the disordered state in question were not calculated, and the discussion of the nitrate - nitrate cooperative interactions in Section 3-5b therefore includes only an outline of the appropriate calculation (which outline, however, does have some points of intrinsic interest).

Now, bis(adiponitrile)copper(I) nitrate must be only one of many compounds (especially nitrates) in which this sort of complication must arise in any attempt to describe (let alone perform calculations on) the "orientationally" - disordered state, and therefore the arguments presented here concerning this complication should, after some adaptation, be of general applicability. Indeed, similar arguments were found to be of value in treating the order - disorder transition in TMMC (see page 172 and Appendix 4-III); in that case, the ions involved in the transition were tetramethylammonium ions.

---

*The use of quotation marks about "orientations" in the first paragraph of page 113 was in anticipation of this statement.

Section 3-4b: the nitrate ions at room temperature - proposal of Kinoshita et al, and further discussion

Kinoshita et al (1959b) indexed their X-ray reflections and explained the systematic extinctions on the basis of a unit cell of dimensions a = 9.41 Å, b = 13.73 Å, and c = 5.85 Å in the space group Pnnn - D_{2h}^2. The measured density indicates that there are two formula units of $Cu(NC(CH_2)_4CN)_2NO_3$ in the unit cell. It will now be shown that therefore the nitrate ions must be disordered*.

This unit cell has the following positions (see International Tables for X-Ray Crystallography, 1952):

8-fold general positions of symmetry 1 (C_1);

4-fold special positions of symmetry $\bar{1}$ (C_i or S_2) or 2(C_2); and

2-fold special positions of symmetry 222 (D_2) - four pairs only,

at 0,1/2,0 and 1/2,0,1/2 (2d); 0,0,1/2 and 1/2,1/2,0 (2c);

1/2,0,0 and 0,1/2,1/2 (2b); and 0,0,0 and 1/2,1/2, 1/2 (2a).

It is easy then to conceive ways in which 2 Cu atoms, 8 cyano N atoms, 8 cyano C atoms, 8 α-methylene C atoms, and 8 β-methylene C atoms can be fitted into the unit cell. A Cu atom can be placed at each of the 2a positions 0,0,0 and 1/2,1/2,1/2. The cyano N atoms and the carbon atoms of each type can be assigned to sets of eightfold positions. Such a structure has already been described with reference to Figure 3-5.

However, it is absolutely impossible to put 2 nitrate N atoms and 6 nitrate O atoms into the unit cell in the form of two discrete NO_3 groups, unless fractional atoms are permitted. Thus, if the two N atoms are assigned to a pair of twofold positions - say, the 2b sites 1/2,0,0 and 0,1/2,1/2 as in Figure 3-5 - it becomes necessary

*In the general discussion which follows, free rotation can be regarded as a limiting case of disorder, among an infinite number of positions.

to arrange 3 O atoms around each position without destroying its 222 symmetry. Now, quite generally, the only way of arranging 3 similar atoms about a position of 222 symmetry is to place one of the atoms at the point where the three mutually perpendicular twofold axes intersect, and to place the other two at equal but opposite distances from this point in one of the axes; but such an arrangement is absurd in the present case, for the N atom has already been assigned to the point where the three axes intersect.

This difficulty is overcome if it is supposed that the nitrate ions are disordered in some way. Disorder is formally represented for crystallographic purposes by the presence of fractional atoms in the crystal. Thus one structure which allows the 3 O atoms to be arranged about a 2b position occupied by N is that proposed by Kinoshita et al and shown in Figure 3-5. In this structure (shortly to be discussed critically), 1/4 O occupies each of twelve sites about the N atom. The physical significance of this structure (namely that proposed by Kinoshita et al) is indicated in column 2 of Table 3-6, for "Scheme 4". Each nitrate ion takes up, randomly, one of four positions I to IV. In each position N lies in the 2b position, and the whole ion lies in, or in a plane parallel to, the b c plane. (Disorder of this sort is often known as orientational disorder, since positions I to IV may be regarded as different orientations of the ion.) The probability that any ion will take up a particular orientation is 1/4. Orientations I and II are interconverted or else unaffected by any of the symmetry operations of the 2b position (namely twofold rotations in or parallel to the a, b, and c directions), and so are positions III and IV. Therefore, the X-ray diffraction experiment "sees" all nitrate ions as equivalent average species of 222 symmetry, as shown in Figure 3-5 or in column 3 of Table 3-6 for Scheme 4.

TABLE 3-6

COLUMN 1	COLUMN 2	COLUMN 3	COLUMN 4	COLUMN 5
SCHEME NO	NITRATE IONS ARE DISORDERED AMONG THESE POSITIONS (ORIENTATIONS) WITH PROBABILITY SHOWN IN BRACKETS. O = N AT A 2b SITE; ● = O. THE ENTIRE ION LIES IN OR PARALLEL TO THE b c PLANE.	EFFECTIVE SPECIES IN X-RAY DIFFRACTION ◍ = FRACTIONAL O ATOM (WEIGHT INDICATED)	GENERAL FORM OF POTENTIAL ENERGY - θ PLOT (NOT TO SCALE) 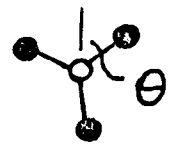	COMMENTS (ZERO-POINT ENERGIES IGNORED)
1	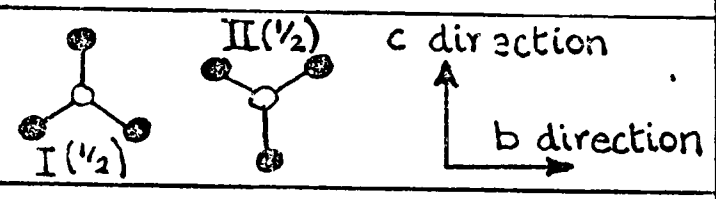	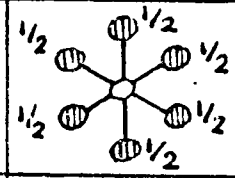	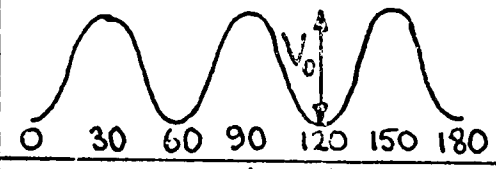	$V_0 >> kT$
2	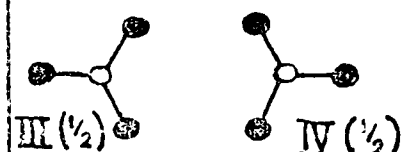	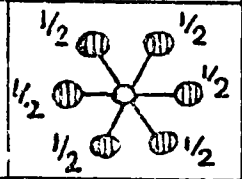	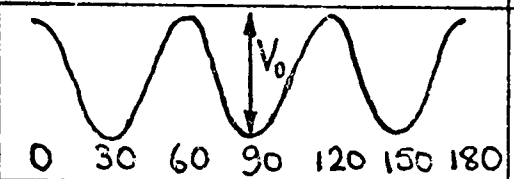	$V_0 >> kT$
3	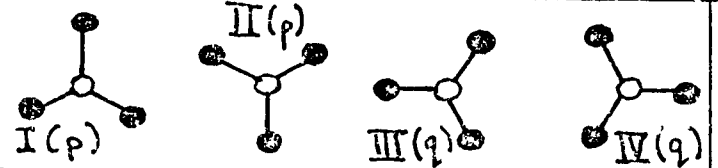	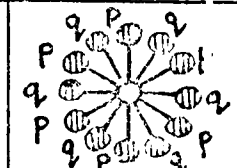	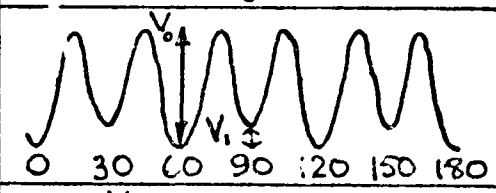	(p+q) x 2 = 1 $V_0 >> kT$, $(V_0 - V_1) >> kT$ p>q FOR V_1>0
4	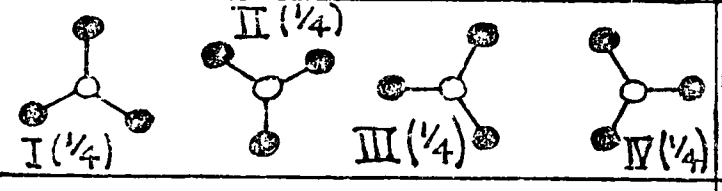	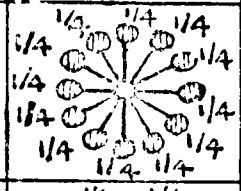	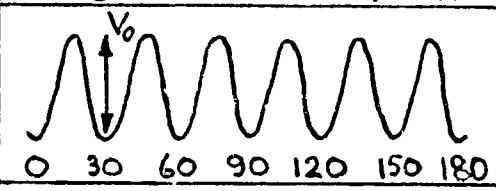	LIMITING CASE OF 3, WHERE $V_1 << kT$ CHOSEN BY KINOSHITA ET AL
5	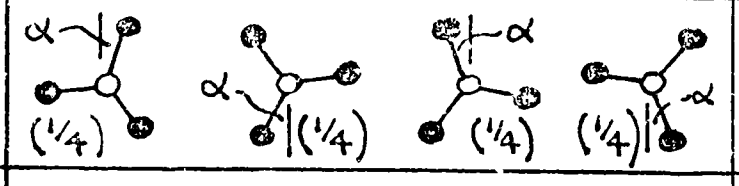	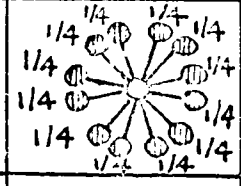	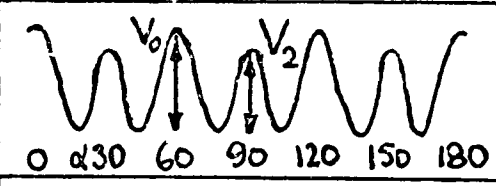	$V_0 >> kT$, $V_2 >> kT$
6	ALL ORIENTATIONS EQUALLY PROBABLE - FREE ROTATION OF ION	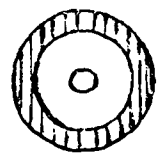 PROBABILITY OF FINDING AN O ATOM BETWEEN θ AND θ + dθ IS (3/360)x(dθ/°)	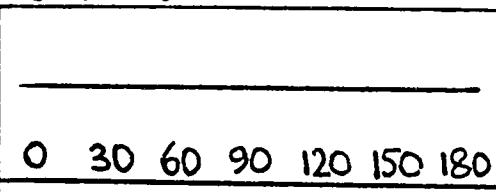	LIMITING CASE OF 1 TO 5, WHERE V_0, V_1, V_2 << kT

But while the conclusion that the nitrate ions must be disordered in some way follows from the observations of systematic extinctions, the selection of any particular scheme for this disordering (such as "Scheme 4") involves analysis of the relative intensities of observed reflections, and such analysis often does not permit certain elucidation of the fine details of structure. It appears, on a fair reading of the paper of Kinoshita et al, that the question of the disordering of the nitrate ions was rather a matter of such fine detail. They obtained this part of their proposed structure only after the general structure of the cationic networks had already emerged. They indicate that various disordered schemes were tested by trial calculations before they decided on "Scheme 4"; however, they do not state what other schemes were tested, nor whether Scheme 4 gave significantly better agreement with the observed intensities than did the other schemes.

This doubt concerning Scheme 4 is reinforced by the fact that even in simple nitrates (where there are fewer non-nitrate atoms to confuse the analysis of the X-ray results) thermodynamic work has in some cases failed to confirm the conclusions of X-ray crystallographers concerning the condition of the nitrate ions (see Newns and Staveley, 1966).

Some calculations illustrative of this point were made on the basis of a very simple energetic model of the bis(adiponitrile)copper(I) nitrate crystal. If cooperative nitrate - nitrate interactions are ignored and each nitrate ion is regular trigonal planar, rigid, and constrained to move only in the b c plane with N fixed at the 2b site in a constant field of 222 symmetry, then Scheme 4 can be interpreted in terms of a potential energy function for the rotating ion such as that shown in columns 4 and 5 of Table 3-6 for this Scheme. On this model, however, Schemes 1, 2, 3, 5, and 6 shown in Table 3-6 are

a priori at least as likely. Calculations of contributions to structure factors for various of these Schemes showed that some of them at least could well be difficult or impossible to distinguish by X-ray diffraction (see Appendix 3-I). However, from a thermodynamic point of view the Schemes differ greatly among themselves. Furthermore, an attempted calculation of the potential energy function of column 4 on the basis of atomic interactions (see Appendix 3-II) favoured a Scheme intermediate between Scheme 1 and Scheme 6; the calculated function was qualitatively like that given in column 4 for Scheme 1 but LV_o was only about 1 kJ/mol compared with RT at room temperature of about 2.5 kJ/mol.

However, these calculations are, strictly speaking, no more than illustrative. It is not to be supposed that Schemes 1 to 6 are the only likely schemes - or indeed that they are likely at all. Schemes for disordering the nitrate ions can be devised in which the N atoms as well as the O atoms are disordered while the positions taken up by the ions do not lie in any of the principal planes (see Table 3-7). Moreover, these schemes (which are unlikely to have been considered by Kinoshita et al in their trial calculations because of the number of continuously variable parameters needed to define them) are in fact more reasonable than the Schemes 1 to 6 of Table 3-6.

That this is the case is seen by considering a more realistic energetic model of the system than the previously used model (in which the nitrate ions were given only one degree of freedom). If it is assumed that the nitrate ions are regular trigonal planar, rigid, and free to move in any manner (with 6 degrees of freedom, in fact) in a constant field of 222 symmetry, then there is no symmetry reason to suppose that any potential energy minimum will correspond to a position in which the nitrate ion lies in one of the principal planes

TABLE 3-7

SCHEME NO	NITRATE IONS ARE DISORDERED AMONG THESE POSITIONS WITH PROBABILITY SHOWN IN BRACKETS
1'	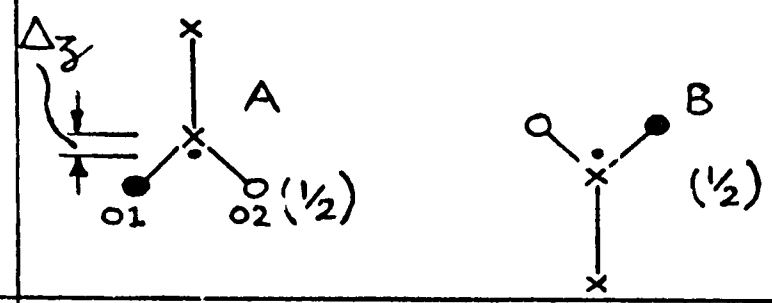
2'	
3'	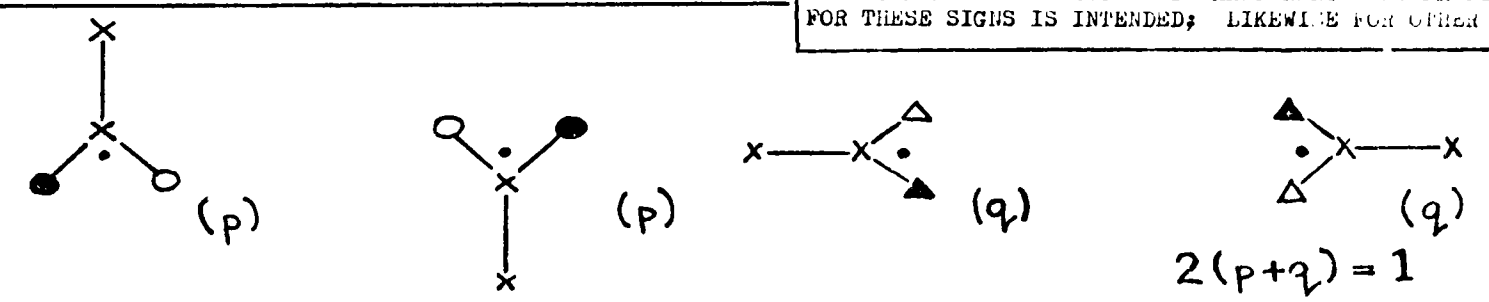
5'	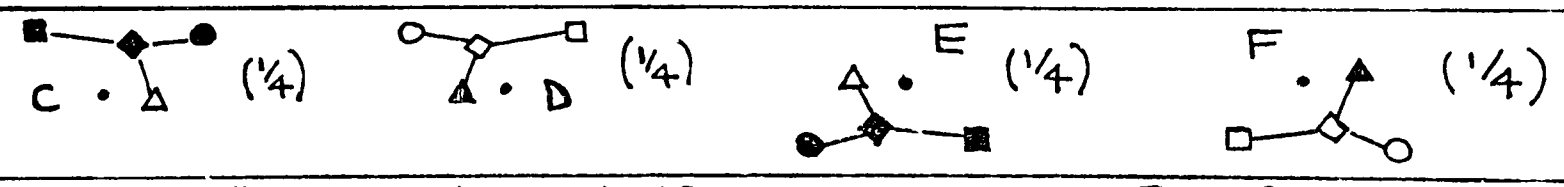
6'	FREE ROTATIONAL MOVEMENT WITH ONE OR MORE DEGREES OF FREEDOM AND OF 222 SYMMETRY
OTHERS INCLUDE	ANALOGUE OF 1' OR 2' IN WHICH ONE N–O BOND LIES IN TWOFOLD AXIS THROUGH 2b SITE PERPENDICULAR TO b c PLANE (N, HOWEVER, NOT LYING PRECISELY IN 2b SITE)

NOTES: c direction; b direction

FIGURES NOT NECESSARILY TO SCALE.

• REPRESENTS A 2b SITE IN THE PLANE OF THE PAPER.

× REPRESENTS AN ATOM IN THE PLANE OF THE PAPER, I.E. IN A PLANE THROUGH THE 2b SITE AND PERPENDICULAR TO a .

● , ▲ , ■ ,AND ◆ ARE ATOMS ABOVE THE PLANE OF THE PAPER AT VARIOUS DISPLACEMENTS.

○ , △ , □ ,AND ◇ ARE ATOMS AT EQUAL BUT OPPOSITE DISPLACEMENTS, I.E. BELOW THE PLANE OF THE PAPER.

POSITIONS A AND B OF SCHEME 1 ARE INTERCONVERTED OR ELSE UNAFFECTED BY ANY OF THE TWOFOLD ROTATIONS, SO THAT THE EFFECTIVE SPECIES IN X-RAY DIFFRACTION HAS 222 SYMMETRY; SIMILAR ARGUMENTS APPLY TO THE OTHER SCHEMES.

FOR SCHEME 1' THE CHOICE OF UPWARD DISPLACEMENT FOR O1 NOT O2 AND OF POSITIVE Δz IS ARBITRARY – NO PREFERENCE FOR THESE SIGNS IS INTENDED; LIKEWISE FOR OTHER SCHEMES.

and/or the N atom lies at the symmetry origin (see Appendix 3-III); accordingly, on this model, none of the structures of Table 3-6 can be precisely correct. (Perturbation of this model with cooperative NO_3 - NO_3 interactions will not alter this conclusion, but rather make the situation even more complicated.)

In contrast, Schemes 1', 2', 3', and 5' of Table 3-7 are consistent with this more realistic model. It is seen from these Schemes that disorder among 2 or 4 positions may still occur. If the potential energy barriers between these positions are small ($<< kT$) then rotation of the ion will occur (Scheme 6'). It is possible also to imagine disorder among any even number of positions. Thus, for instance, potential energy minima might occur for positions A and B of Table 3-7 and also for positions C to F. The depth of the minima for positions A and B could not be precisely the same as that for positions C to F, so that if all depths were $>> kT$ the positions A, B, C, D, E, and F would be taken up with probabilities r, r, s, s, s, and s, where $2r + 4s = 1$. However, as the number of potential energy minima imagined increases, so it becomes less likely that the potential energy of the ion will vary so rapidly with its position as to provide high energy barriers between minima, and therefore more likely that the ion will rotate with a considerable measure of freedom.

It is clear that the work of Kinoshita et al, alone, does not allow any progress beyond this point towards answering the thermodynamically important question - Among how many positions is the nitrate ion disordered, or else is it rotating with a greater or lesser measure of freedom?

On another point their work does provide some assistance. In their final electron density maps, while it is quite impossible to distinguish the oxygen atoms from one another, the nitrate ion is

clearly seen to lie in or parallel to the b c plane in the vicinity of the 2b positions. Further, calculations based on analogues of Schemes 1 to 6 in which the ions lie in or parallel to the a b or a c planes (see again Appendix 3-I) suggest that the observed X-ray intensities should be sensitive to the average orientation of the ions. Therefore, while (as we have seen) the ions cannot lie precisely in the plane of Table 3-7 in any of their permitted positions, it does seem reasonable to regard Schemes 1', 2', 3', and 5' with small displacements ●, ▲, ■, and ◆ as more likely than schemes, such as those indicated at the bottom of Table 3-7, which involve relatively large displacements out of the plane.

Section 3-5: interpretation of the heat capacity results

a. the anomaly at 37 -70 K and the nitrate ions

Order - disorder transitions in nitrates were discussed briefly on page 14, and have been reviewed, along with some transitions in other compounds containing polyatomic ions, by Newns and Staveley (1966). They consider a large number of transitions, some of which are first-order and the others of which are λ-transitions (for this term, see page 12). To a remarkable degree, the various values for the anomalous entropy gain per mole of polyatomic ions $\Delta S_{m,anom}$ "cluster" about the values R ln 2, R ln 3, and R ln 4. They suggest that in a high proportion of cases a $\Delta S_{m,anom}$ of approximately R ln n indicates a transition in which each ion undergoes an n-fold increase in the number of "orientations"* available to it (compare equation 1-6, page 14). From a theoretical point of view, this approach will be

*Newns and Staveley use the conventional word "orientations" (compare page 14); but it should be remembered that the positions available to each ion do not necessarily differ from one another in a purely orientational manner - see the comparative discussion of Tables 3-6 and 3-7 at pages 119 to 121.

valid only insofar as the entropy change due to any alteration in the lattice vibration spectrum which accompanies the change in the number of available ionic orientations is relatively small. The success of the approach of Newns and Staveley (including a more detailed analysis of several transitions in the light of information from other techniques) suggests that this is in fact the case. They point out, further, that the entropies of solid-solid transitions in the potassium and rubidium halides (where of course orientational disorder is impossible) are <u>small</u> (compare the calculation for sulphur on page 12), and that the vibrational contribution to $\Delta S_{m,anom}$ should in any case be less important the lower the temperature, by the third law of thermodynamics.

The $C_{p,m}$ - T plot for bis(adiponitrile)copper(I) nitrate displays two, possibly overlapping λ-type anomalies in the 37 K to 70 K region, and the total $\Delta S_{m,anom}$ over this range was estimated (see Section 3-3d) as between 1/2 R ln 2 (= R ln 1.414) and R ln 2. Unfortunately, this entropy change was obtained by the use of free-hand drawing to estimate the normal heat capacity; therefore it may be in considerable error, especially because of the rather wide anomalous temperature range (compare the comments at page 7). In particular it seems possible that the heat capacity contains a significant anomalous contribution even below 37 K, in which case the free-hand curves in Figure 3-3 have been drawn too high and the anomalous entropy change has been underestimated.

Suppose, then, that the correct value for the anomalous entropy change (which might be more nearly approached if a suitable comparison substance could be used) is R ln 2. Following the approach of Newns and Staveley, a reasonable (though not unique) explanation of the anomalies would be that at low temperatures practically all

nitrate ions are ordered while at 70 K and somewhat above they are disordered among two positions, for instance roughly according to Scheme 1' or Scheme 2' of Table 3-7. It has already been seen (see the last sentence of Section 3-4b, at page 122) that there is evidence that Schemes 1' and 2' for small displacements ● are more likely than any other schemes of disorder among two positions, at least at room temperature. Further, the fact that energetic calculations (performed with the use of room-temperature lattice parameters) favoured Scheme 1 over Scheme 2 (see page 119) - these schemes having certain similarities to Schemes 1' and 2' respectively - makes it reasonable to tentatively favour Scheme 1' for a temperature of 70 K or somewhat above. This conclusion is indeed a tentative one (for one thing, the possibility of substantial differences in structure at 70 K and room temperature has been ignored); but for the sake of definiteness it will be used in Section 3-5b as the starting point for treatment of the nitrate - nitrate interactions. In Section 3-5c the point just touched on, concerning changes that may occur between 70 K and room temperature, is dealt with.

Before we proceed with Sections 3-5b and 3-5c further possibilities for the 37 - 70 K anomaly will be considered, although on balance it is felt that these are less likely.

Suppose that the correct value of $\Delta S_{m,anom}$ is less than R ln 2. Then the above picture could be modified by supposing that in the low temperature state not all the ions are ordered. This would arise if the energy barrier to the movement of the ions were sufficiently high that the ordering process (though thermodynamically favoured) were not completed as the crystal were cooled. Two consequences of this would be the following:- (1) The transition would be to some degree time-dependent so that $C_{p,m}$ would depend correspondingly on the thermal

history of the sample. (There was no evidence for this in the present work, unless the difference between results in the two calorimeters is ascribed at least in part to such an effect.) (2) The disorder "frozen in" at low temperatures would cause a "residual entropy" at 0 K.

One possibility which can reasonably be eliminated is that the anomaly represents a change from an ordered (or even a disordered) arrangement of nitrate ions librating about their mean positions to an arrangement of freely rotating nitrate ions. The associated entropy change in this case would probably greatly exceed the observed value; the entropy of rotation of a nitrate ion about its 3-fold axis at 70 K is calculated (on eq. 27 - 56 of Lewis and Randall, 1965, taking n = 3 and r_{N-O} = 1.24 x 10^{-8} cm) to be 22.07 J $K^{-1}mol^{-1}$ = R ln 14.2.

It is conceivable that the anomaly has little to do with the nitrate ions, and derives largely from a change in the cationic networks. The observed entropy change is rather large for this, since there is no evidence that the cationic networks are disordered in configuration at room temperature, in which case the only entropy to be lost is vibrational. The structure is, admittedly, a very unusual one with its six interpenetrating cationic lattices, and therefore the usual "rules of thumb" may not apply. In the case of silver oxide (with two interpenetrating lattices - see page 110), well-formed crystals provide no heat capacity anomalies between 2 K and 300 K, while an anomaly was observed with a finely divided sample, apparently because of crystal defects (Gerkin and Pitzer, 1962; Gregor and Pitzer, 1962). Since in the present case the crystals were large and regular in appearance (see page 88), this tends to suggest that the observed anomaly does not derive from changes in the cationic networks.

Presumably heat capacity measurements on an isostructural halide would help to decide this point. However, it is not known whether such a compound exists; some relevant information is given on page 92.

Of course, the above uncertainties could very possibly be resolved by low temperature X-ray diffraction, say at 4.2 K and 77 K. Such low temperature diffraction should in any case yield rather precise structural parameters because the temperature factor B is much lower than at room temperature; however, facilities for it were not available either in Oxford or Harwell at the time of this work.

Section 3-5b: nitrate - nitrate interactions

Nitrate - nitrate interactions will now be considered, for the sake of definiteness, on the not unreasonable assumption (see page 124) that above 70 K the ions are disordered about the 2b sites roughly according to Scheme 1' of Table 3-7, displacement ● being small.

Figure 3-6 shows the lattice of 2b sites in bis(adiponitrile)-copper(I) nitrate at room temperature. The 2b sites lie in straight chains, adjacent sites being 5.85 Å apart. The chains run in the c direction. Each chain is surrounded by four similar chains at a perpendicular separation of 8.32 Å.

On the basis of Scheme 1' two nearest-neighbour ions (such as those associated with 2b sites L and M in Figure 3-6) have an equal probability (1/4) of taking up each of the four combinations of position shown in Figure 3-7(i), because the associated energies E_a, E_a, E_b, and E_c will be identical. This applies even at low temperatures, for the energetic model which gives rise to Scheme 1' is one in which each ion moves in a constant field of 222 symmetry (i.e. unaffected by the positions of the other nitrate ions).

One can make this model more realistic by supposing that the energy of a system including a mole of ions contains a major component

FIGURE 3-6

(i) perspective view showing 2b sites

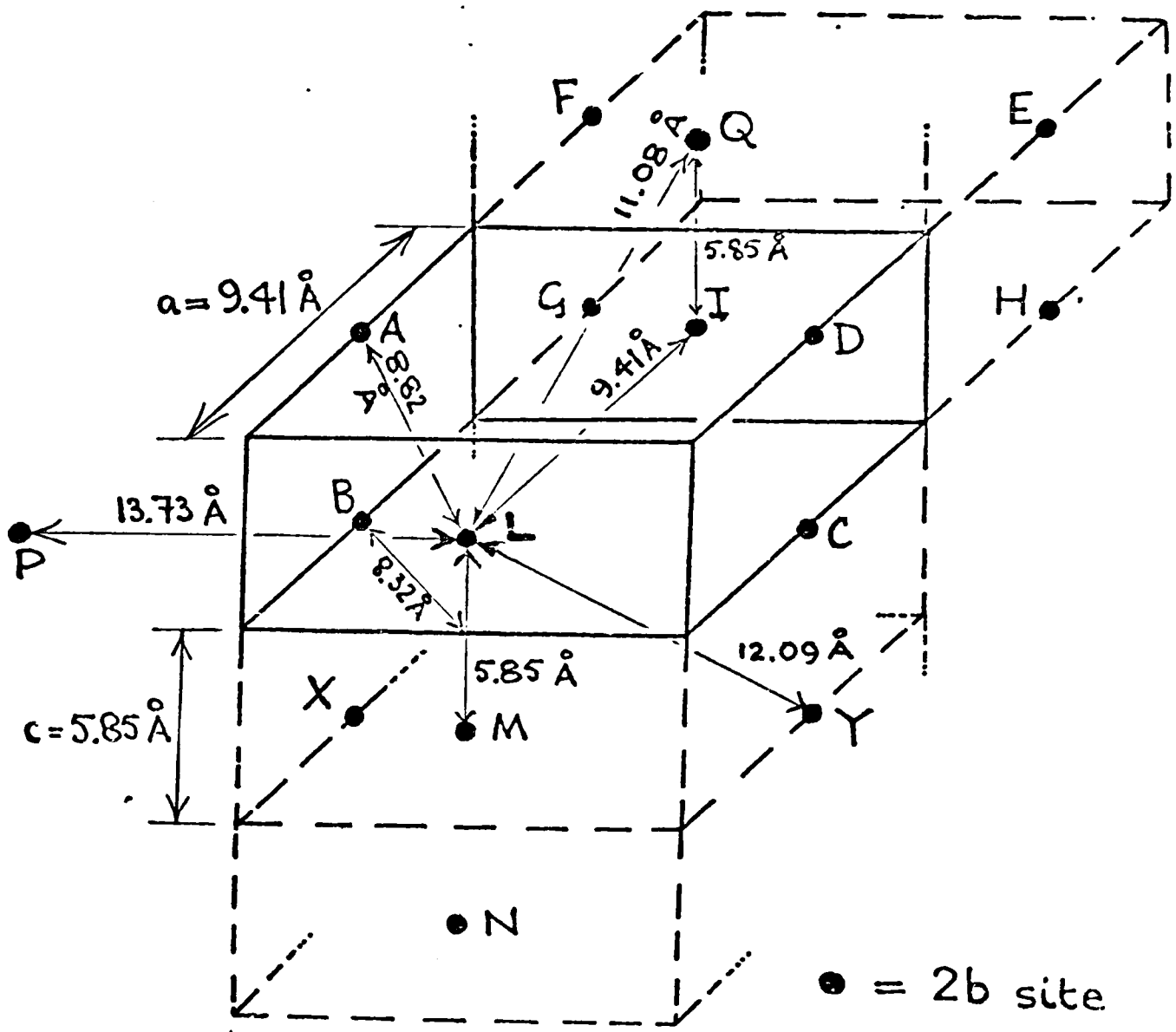

(ii) end view of chains of 2b sites

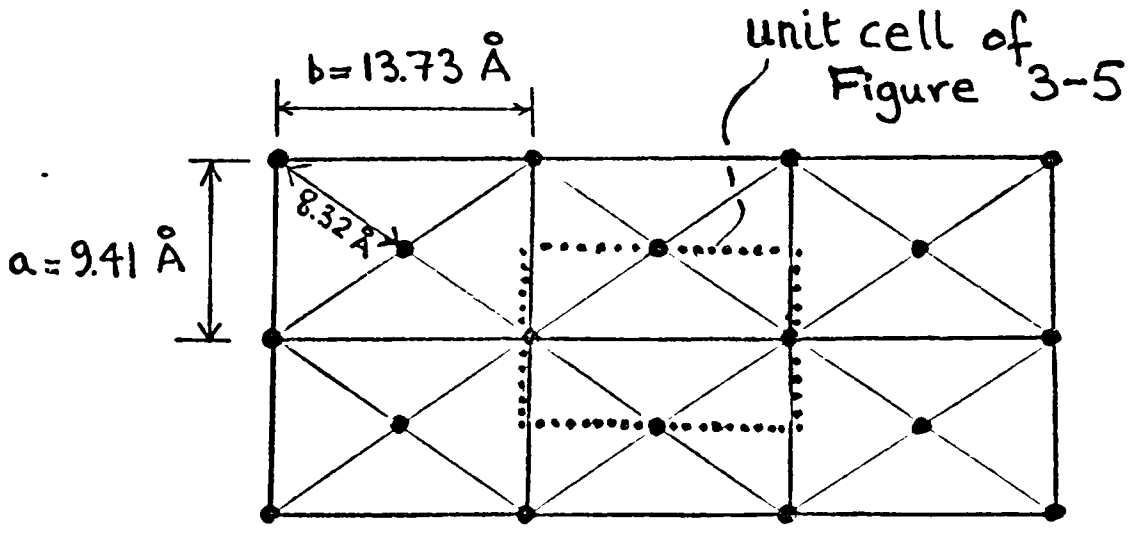

In (i) the unit cell of Figure 3-5 (page 111) is shown by continuous lines, and adjacent unit cells are shown by dashed lines. The 2b sites form a body-centred orthorhombic lattice (thus, for example, cuboid ABCDEFGH has site I at its body centre). Alternatively, the sites may be considered as lying in parallel chains (...ABX..., ...LMN..., ...DCY..., etc.) in which the separation between sites is 5.85 Å. The interchain distance is 8.32 Å. and the nearest distance between sites in adjacent chains is 8.82 Å.

(ii) shows the chains in end view.

FIGURE 3-7

(nitrate - nitrate interactions within the chains)

Symbols used are as in Table 3-7 (page 120)

Figures not necessarily to scale.

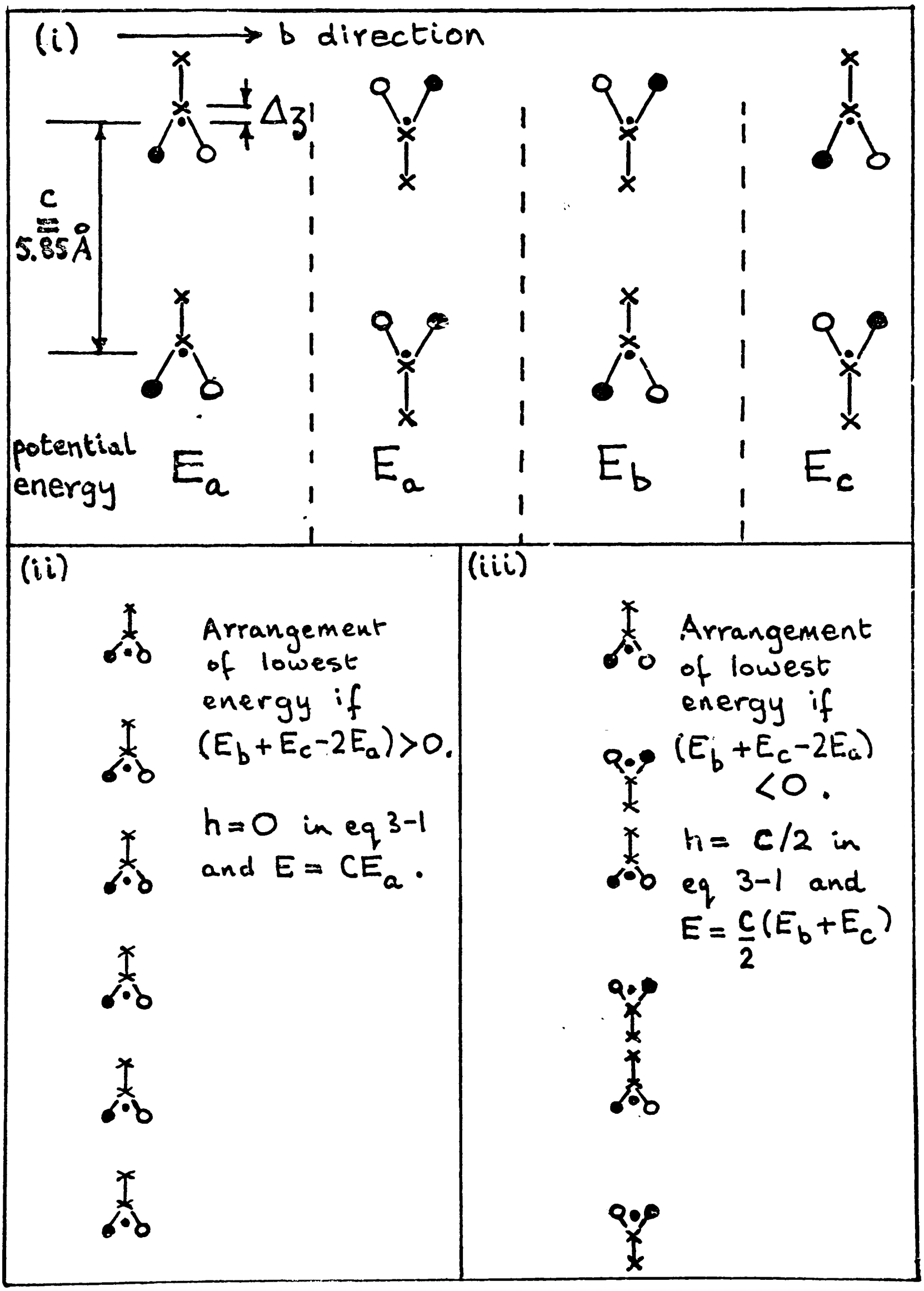

depending on the constant field of 222 symmetry and a minor component deriving from nearest-neighbour nitrate - nitrate interactions dependent on their relative positions. So long as this second component is minor, it is reasonable (following Morfee et al as briefly discussed at page 113, third paragraph) to ignore the changes in displacements Δz, O , and ● in Figure 3-7(i) which result from it; even if these changes are ignored, E_a, E_b, and E_c become different from one another and the associated probabilities of the respective combinations of position are no longer equal. These energies and the differences between them will (unless Δz in Figure 3-7(i) is very large) probably be predominantly electrostatic in origin. Were the displacements represented by Δz, O , and ● known, these energies could be estimated by assuming, say, a charge of -e/3 on each O atom of the nitrate ions.

Once one had got so far, an Ising treatment (similar to that described in Sato, 1970) would be possible. Consider a chain of ions along the c direction such as those near sites ...LMN... in Figure 3-6. Ignoring end effects, there must be equal numbers (say h) of E_b and E_c interactions. Thus, for a chain of C ions the energy

$$E = (C - 2h)E_a + h(E_b + E_c) = C E_a + h(E_b + E_c - 2E_a) \quad \text{eq. 3-1}$$

Clearly the arrangement of lowest energy E is that shown in Figure 3-7(ii) if $(E_b + E_c - 2E_a)$ is unfavourable and that in Figure 3-7(iii) if $(E_b + E_c - 2E_a)$ is favourable. The tendency to order towards these arrangements will be the greater, the greater is $|E_b + E_c - 2E_a|$; but the Ising treatment based on an equation such as eq. 3-1 shows that no heat capacity discontinuity will be observed in the system (compare the general observation in the sentence bridging pages 13 and 14). With decreasing temperature, short range order will increase, but no long range order will appear at any attainable temperature.

However, there will in fact be interactions between nitrate ions in different chains tending to order them relative to one another (e.g. by virtue of the interactions between the ion at L and the ions in other chains at 8.82 Å (A, B, C, D and four others), at 9.41 Å (I and one other), at 11.08 Å (Q and three others), at 12.09 Å (Y, X, and six others), at 13.73 Å (P and one other), and so on. These interchain interactions will probably be much weaker than the intrachain interactions because of the rapid fall-off with distance of interactions involving electrostatic multipoles.

Therefore, the further treatment of the system could be as of a one-dimensional Ising system subject to a molecular field representing the interchain interactions. This (see Sato, 1970a) does predict that an order-disorder transition will occur; in principle the critical temperature could be calculated if the interaction energies were known.

In Section 3-5a and in the present section so far, the fact that the anomaly is in two parts with one peak at 51 K and another at 63 K has not been commented on. This is a curious feature for which no explanation is here offered. Two-part anomalies have been observed in other compounds, but any analogy with the present compound seems rather doubtful. Thus, systems of linear chains of paramagnetic ions with strong intrachain interactions and weak interchain interactions (compare the above discussion of the interactions of the nitrate ions in the present case) give rise to two-part anomalies (see page 13 and Figure 1-2(d) at page 8); but the higher temperature part is much broader and generally accounts for a larger part of the entropy gain than in the present case. Lerbscher and Wulff (1970) and Lee and Wulff (1974) reported two-part transitions in $(NH_4)_2SbBr_6$ and Rb_2SbBr_6; but these compounds are unusual in that they contain two

anionic species ($SbBr_6^-$ and $SbBr_6^{3-}$) which, Mulff and his coworkers suggest, undergo independent orientational disordering as the crystal is heated.

Section 3-5c: changes occurring between 70 K and 300 K

It was seen in Section 3-5a and 3-5b that it is not unlikely that at 70 K the nitrate ions are disordered among two positions, according to Scheme 1' or Scheme 2' in Table 3-7. (Of these schemes, Scheme 1' was tentatively preferred, but this is not of concern here.) However, it cannot be assumed that the same applies at room temperature, even though no clear anomaly was observed between 70 K and 300 K; it will now be shown that, in particular, the heat capacity results are unlikely to show any clear indication of a further transition towards free rotation of the ions.

The picture of this disordered state at 70 K which has been developed in Sections 3-4b, 3-5a, and 3-5b has each nitrate ion vibrating in a potential well corresponding to one of the two positions, the form, depth, and position of this potential well being affected only to a small extent by the condition of the neighbouring ions. The part of the vibrational motion tending to take the ion into the other position over the energy barrier between the two positions will be referred to as "librational". As the temperature is raised, the ions will librate progressively more vigorously in these wells and will tend towards rotation, this rotation becoming progressively less restricted. The change will essentially be localised on each ion, and the associated heat capacity anomaly will therefore (compare pages 10 to 11) not be a sharp one.

How sharp such an anomaly can be is illustrated by calculating the heat capacity of a mole of nitrate ions each one of which librates and/or rotates in its own plane about its threefold axis, the potential

function having six minima of depth 600 K k, like that given for Scheme 1 or Scheme 2 of column 4 of Table 3-6. This should roughly reproduce the molar heat capacity of ions in a 222 environment if they tend towards rotation with approximately one degree of freedom (even though the 222 environment will make the librational and rotational motions rather complicated). The molar heat capacity curve obtained is shown in Figure 3-8. It is seen that for the barrier height chosen the motion of the ions at 300 K is already very substantially rotational in character, but that the rise and fall of the molar heat capacity associated with the onset of rotational motion is too gentle to distort the overall $C_{p,m}$ - T plot perceptibly having regard to the magnitude and rate of rise of the overall $C_{p,m}$ (Section 3-2). It is possible, however, that the presence of such a distortion would become evident if the heat capacity of a comparison substance such as bis(adiponitrile)copper(I) chloride were measured and subtracted from that of the nitrate (after correcting for the heat capacity due to the internal vibrations of the nitrate ions).

In their review on nitrates, Newns and Staveley (1966) state (at page 270): "It seems to us that the balance of evidence rules out free rotations in the literal sense, even in one degree of freedom, in any [one of the nitrates of Na, K, Rb, Cs, Ag, and Tl(I)] in any phase." It would, however, be unwise to eliminate the possibility of relatively free rotation at 300 K in the present case. In the simple nitrates to which Newns and Staveley refer, the electrostatic forces on the nitrate ions are probably far stronger than in bis(adiponitrile)copper(I) nitrate because of the relatively high density of charged species (both cations and other nitrate ions). The energy barrier to rotation may well, therefore, be much lower in bis(adiponitrile)copper(I) nitrate than in the simple nitrates.

In fact, differences of this general sort between relatively

FIGURE 3-8

$\frac{C_m}{J\ K^{-1}\ mol^{-1}}$ for NO_3^- capable of motion only about its threefold axis, the potential function being sinusoidal with periodicity $2\pi/6$ and barrier height 600 K k, as calculated by joint use of Table 27-8 and eq. (27-56) of Lewis and Randall (1965). N-O distance taken as 1.24 Å.

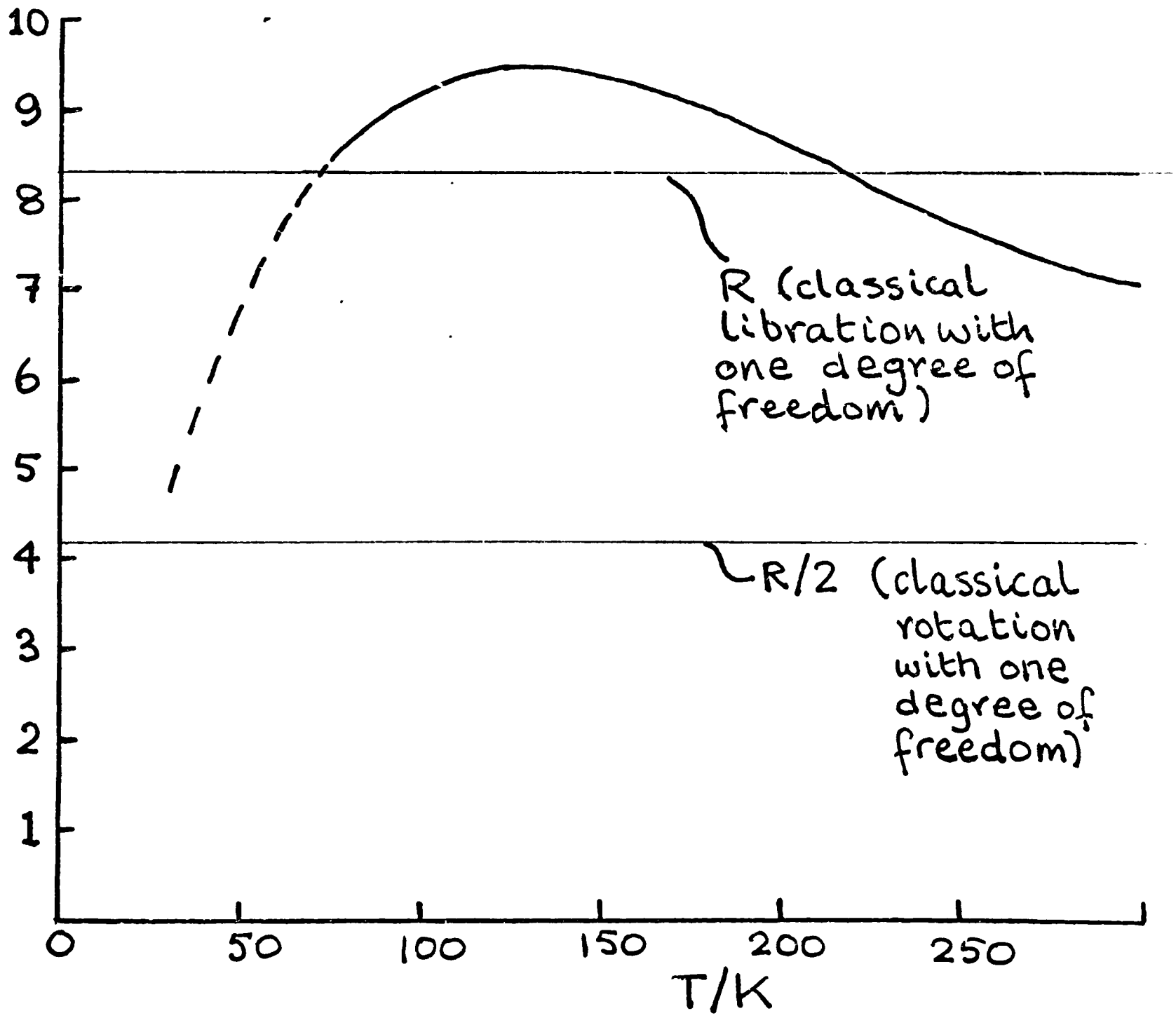

simple and relatively complex salts have been previously observed. Thus in the face centred high-temperature forms of NH_4Cl, NH_4Br, and NH_4I almost free rotation of the ammonium ion occurs, but only about one N - H bond, while in ammonium stannichloride and stannibromide at room temperature the ammonium ion is tending towards free rotation with three degrees of freedom (see Staveley, 1961).

CHAPTER 4: TETRAMETHYLAMMONIUM TRICHLOROMANGANATE(II), "TMMC"

Tetramethylammonium trichloromanganate(II), Me_4NMnCl_3 ($Me = CH_3$), is also known as tetramethylammonium manganese chloride; from this latter name derives the widely-used abbreviation "TMMC", which will also be used here. TMMC has attracted much attention over recent years. In contrast to the interest in bis(adiponitrile)copper(I) nitrate (Chapter 3) and the phthalocyanines (Chapter 5), the interest in TMMC has been purely academic.

Some of the studies on TMMC have dealt with its magnetic properties. It is a nearly one-dimensional antiferromagnet at low temperatures (the Mn^{2+} ions being strongly coupled within mutually parallel chains between which coupling is weak). The Néel temperature is at 0.84 K, despite the persistence of short range magnetic order for tens of kelvins beyond 0.84 K (compare the paragraph bridging pages 13 to 14).

Other studies have concentrated on the NMe_4^+ ions; these have suggested that whereas above 126 K the unit cell is hexagonal and the NMe_4^+ ions are disordered, below 126 K the unit cell is monoclinic and the NMe_4^+ ions are long-range ordered. Both this transition and the nature of the thermal motion of the NMe_4^+ ions in the high- and low-temperature forms have been investigated by various workers.

In 1972, Dr J.W. White of the Physical Chemistry Laboratory, Oxford pointed out to us in this laboratory that while many physical techniques had been used in these investigations (diffraction, magnetic resonance, bulk magnetic susceptibility measurements, spectroscopy, and neutron scattering), there was a need for heat capacity

measurements to be performed. (He and his coworkers had themselves been using inelastic neutron scattering to study TMMC.) The present author used the new calorimeter described in Chapter 2 to cover a range of T_{MID} from 1.53 K to 79.2 K (these results are given in Section 4-2), while Dr R.D. Worswick and Mr A.G. Dunn used the calorimeter constructed by Worswick (1972) - a calorimeter which is operated only above about 80 K - to extend the measurements up to about 300 K.

It turned out that other groups were engaged in rather similar investigations at about the same time, and these were reported in full after the present author's experiments were complete. Their results will be compared with the present author's results in Section 4-3.

The theoretical significance of the heat capacity results will be discussed in Section 4-4.

Section 4-1: preparation and characterisation of the calorimetric sample

Formally, TMMC is a double salt $Me_4NCl.MnCl_2$. Many workers have prepared TMMC by crystallisation (commonly evaporative crystallisation) from a solution of tetramethylammonium chloride and manganese(II) chloride in water or in dilute aqueous hydrochloric acid of 1 - 2 mol dm^{-3} concentration (e.g. Lawson, 1967; Dingle et al, 1969; Nagata and Tazuke, 1972; Hutchings et al, 1972; and Magnum and Utton, 1972). Dingle et al and Magnum and Utton recommended the use of an $MnCl_2$: Me_4NCl molar ratio slightly in excess of 1 : 1; presumably this was intended to avoid the formation of tetramethylammonium tetrachloromanganate(II), $2Me_4NCl.MnCl_2$ or $(Me_4N)_2MnCl_4$, which is known (e.g. from Lawson) to be obtainable from solutions in which the molar ratio

is 1:2.

For the present work some preparations were carried out in which $MnCl_2.4H_2O$ and Me_4NCl (both of Laboratory Reagent quality) were dissolved in the minimum amount of HCl of concentration 2 mol dm^{-3} in a molar ratio of 1.05:1. However, even with this 5% excess of $MnCl_2$, there was a tendency for $(Me_4N)_2MnCl_4$ to be formed. Thus, in one experiment, in which crystallisation was effected by cooling a solution from 100°C, green crystals of $(Me_4N)_2MnCl_4$ were at first precipitated, crystals of TMMC appearing only when the temperature dropped below 40°C. Eventually, there was no visible sign of the green crystals (these having presumably redissolved as the system equilibrated). However, an X-ray powder photograph of the product contained weak $(Me_4N)_2MnCl_4$ lines as well as the expected TMMC lines; this suggested that nuclei of metastable $(Me_4N)_2MnCl_4$ had been enclosed in the TMMC crystals. In another experiment with HCl of 2 mol dm^{-3} concentration, evaporative crystallisation at about 30°C also produced a product which gave weak $(Me_4N)_2MnCl_4$ lines in the X-ray powder photograph, perhaps because the temperature control had been insufficiently precise.

In these circumstances, the sample eventually preferred for the calorimetric work was one prepared with the use of concentrated aqueous HCl as solvent. Concentrated HCl had previously been used by Adams and Smardzewski (1971), who employed an $MnCl_2$:Me_4NCl molar ratio of 1:1, and by Mr N. Brown (private communication) of the Physical Chemistry Laboratory, who employed an excess of $MnCl_2$. At no point in any of the present experiments with concentrated HCl solvent was any formation of $(Me_4N)_2MnCl_4$ detected. The procedure used in the preparation of the calorimetric sample was as follows:-

$MnCl_2.4H_2O$ and Me_4NCl of Laboratory Reagent quality were dissolved

in the minimum quantity of concentrated aqueous HCl at 100°C, the $MnCl_2.4H_2O$ being in a molar excess of 5%. The solution was cooled slowly (over more than 24 hours) to room temperature. When this was done on a large enough scale to produce enough crystals to fill the calorimeter (well over 20 g), the crystals obtained were about 1 cm long (some much longer) and about 3 mm across, mostly rather beautiful specimens in the form of very clearly defined hexagonal prisms. The crystals were filtered off, washed with methanol, vacuum dried, and stored in a desiccator. (On humid days, they were observed to deliquesce rapidly - compare Nagata and Tazuke (1972), who found it necessary to coat the crystals in clock oil before performing epr measurements.) The analysis of the product was satisfactory:

	Mn	Cl	C	N	H
observed	23.2	45.2	20.4	5.7	5.1
calculated	23.33	45.17	20.41	5.95	5.14

An X-ray powder photograph of the product was taken. No lines indicating the presence of $(Me_4N)_2MnCl_4$ were observed, although there were still some weak lines which could not be indexed on the unit cell given by Morosin and Graeber (1967) for TMMC; see Table 4-1. These weak lines had in fact also been observed in the photographs of the products obtained with dilute HCl solvent in addition to the TMMC and $(Me_4N)_2MnCl_4$ lines; and it is possible that in both cases they are caused by the presence of a small amount of some phase formed by the reaction of atmospheric water and/or oxygen with the finely divided, hygroscopic sample during the X-ray exposure.

Since the preparation with concentrated HCl solvent had previously not been widely used, and since neither Adams and Smardzewski nor Brown had reported detailed characterisation of their samples, it

TABLE 4-1

Listing of X-ray powder diffraction lines obtained in a Debye-Scherrer photograph of the TMMC sample used in calorimetry.

Camera: 11.46 cm dia

Film mounting: Straumanis method

Calibration: none, each line x mm away from straight-through position taken to correspond to $2\theta = x^{\circ}$

Radiation: Cu Kα (λ = 1.54178 Å), Ni filter

Exposure: 16 hours

Assignments based on unit cell of Morosin and Graeber (1967):

a = 9.1510 Å
c = 6.4940 Å

Space group $P6_3/m$

Extinctions - 001 for 1 odd

int	d_{hkl}obs	d_{hkl}calc	hkl*	int	d_{hkl}obs	d_{hkl}calc	hkl
VVW	8.63	-	-	M	2.718	2.720	121
VS	7.94	7.925	010	M	2.648	2.648	112
VVW	7.37	-	-	M	2.509	2.512	022
MW	5.03	5.023	011	M	2.444	2.447	031
S	4.57	4.576	110	M	2.288	2.288	220
W	4.15	-	-	S	2.199	2.202	122
VW	3.95	3.963	020			2.198	130
W	3.74	3.740	111	W	2.082	2.082	131
S	3.38	3.383	021	MW	2.049	2.049	032
MW	3.25	3.247	002				
W	3.00	3.005	012				
		2.995	120				

int = intensity, S = strong, M = medium, W = weak, V = very

* In all cases except 002, there are unlisted non-equivalent reflections with identical values for d_{hkl}calc.

All d values given in Å.

was felt desirable to check for the presence of Me_3NH^+, $Me_2NH_2^+$, $MeNH_3^+$, or NH_4^+ ions in the sample. (It seemed, a priori, not impossible that smallish amounts of such ions, especially of Me_3NH^+, might be incorporated in the crystal in place of Me_4N^+ ions without noticeably affecting the X-ray diffraction pattern or the analysis for Mn, Cl, C, N, and H; moreover, such ions could conceivably be formed under the rather harsh conditions of the preparation by reactions such as $Me_4N^+ + HCl \xrightarrow{100^\circ C} Me_3NH^+ + MeCl\uparrow$.) These ions ($Me_3NH^+$ etc.) were estimated by heating about 1.7 g of the sample with concentrated NaOH solution at 130°C for 15 - 20 minutes, condensing the evolved vapours in water, and titrating the solution thus obtained with aqueous HCl of concentration 0.1 mol dm^{-3}. Only 0.1 cm^3 of the aqueous HCl was necessary to reach the end point; this indicated that 0.14 per cent of the Me_4N^+ at the very most had been replaced.

The above preparations were performed with much valuable assistance from Mr M. Gascoygne of the Laboratory Analytical Service. He also performed the chemical analyses.

Note on $(Me_4N)_2MnCl_4$

Small samples of $(Me_4N)_2MnCl_4$ were prepared for the purpose of preparing a comparison X-ray powder diffraction photograph.

The mother liquor from a TMMC preparation with concentrated HCl solvent was mixed with about half its volume of the ethyl alcohol, and then diethyl ether* was added until no more precipitation of the green $(Me_4N)_2MnCl_4$ was observed. The precipitate (rather powdery in form) was filtered off, washed with diethyl ether several times, and dried in a vacuum desiccator. A partial analysis was satisfactory -

*In the preparation of TMMC, it is important not to wash the TMMC crystals with diethyl ether, lest $(Me_4N)_2MnCl_4$ is formed in a similar way.

	Cl	C	N	H
obs.	41.1	27.8	8.2	7.3
calc.	41.10	27.85	8.12	7.01

A Debye-Scherrer X-ray powder diffraction photograph was taken. The low-angle lines (being the most useful for spotting the presence of this phase as an impurity in TMMC) are listed in Table 4-2. The positions of these lines are close to those calculated for $(Me_4N)_2ZnCl_4$, which is reported by Morosin and Graeber (1967) to be "isomorphous" with the Mn compound, and for which Wiesner et al (1967) give the lattice parameters.

TABLE 4-2

Listing of low angle lines for $(Me_4N)_2MnCl_4$ obtained in a Debye-Scherrer photograph.

Camera, film mounting etc. precisely as given at head of Table 4-1.

d_{hkl}calc values are obtained from the unit cell given by Wiesner et al (1967) for $(Me_4N)_2ZnCl_4$:

a = 12.276 Å
b = 13.998 Å
c = 15.541 Å

Space group Pnma

Extinctions - 0kl for (k + l) odd;
hk0 for h odd

int	d_{hkl}obs	d_{hkl}calc	hkl
M	7.86	7.787	011
		7.771	002
S	6.66	6.576	111
		6.566	102
M	6.17	6.138	200
MW	5.35	5.304	112
VW	5.09	5.071	210
M	4.86	4.821	211
		4.817	202
S	4.54	4.499	020
		4.490	013
S	4.00	3.959	203
S	3.92	3.894	022
		3.885	004

int = intensity, S = strong, M = medium, W = weak, V = very
All d values given in Å.

Section 4-2: heat capacity results

The results dealt with here are those obtained by the present author in the new calorimeter described in Chapter 2. For the relatively high temperature results mentioned on page 136, see Dunn (1974).

It has already been remarked (at page 138) that the TMMC sample was in the form of large hexagonal prisms, and that TMMC deliquesces on humid days. For these reasons the sample was introduced into the sample-containing vessel in a dry glove box, each crystal being dropped lengthwise through the filling port by means of forceps (the longest crystals having been first broken into shorter lengths). Once the vessel was full, it was removed from the glove box and was sealed up in the open laboratory (as described at page 39) as rapidly as possible.

The results obtained in the new calorimeter are listed in Table 4-3, together with various weights etc. as promised in Section 2-9d (page 83, last paragraph).

When the sample was removed from the calorimeter, the crystals were unchanged in size and appearance.

The results for T_{MID}s between 1.6 and 4 K could be reasonably reliably corrected for curvature, since they fitted fairly well an equation of the form $\overline{C_{p,m}} = aT + bT^2$ from which $d^2C_{p,m}/dT^2$ (see equation 2-7, page 79) could be calculated to a good approximation (as 2b). Table 4-4 gives $C_{p,m}$ (corrected for curvature) for the particular values of T in the 1.6 to 4 K range. b was taken as $0.045\ J\ K^{-3}\ mol^{-1}$. It will be seen that the effect of curvature-correction is very small in this case ($\leq 0.05\%$).

TABLE 4-3

Results obtained in the new calorimeter described in Chapter 2

Weights, etc. (see Section 2-9d for the meanings of the symbols):-

n_{sample} = 0.092 38(6 4)mol

$n_{exch.\ gas}$ = 1.045 x 10^{-5} mol of He^3

$\Delta m_{elecsol}$ = +0.129 87 g

Δm_{indsol} = −0.133 06 g

Δm_{Ag} = −0.005 72 g

($C_4H_{12}NMnCl_3$ = 235.446; density for buoyancy correction and calculation of $n_{exch.\ gas}$ taken as 1.679 g cm^{-3}.)

T_{MID}/K	ΔT/K	$\overline{C_{p,m}}$/$JK^{-1}mol^{-1}$	% of total measured $\overline{C_p}$ due to sample	notes
1.529	0.0242	0.2527	91	A
1.574	0.0629	0.2656	91	A
1.636	0.0609	0.2738	91	A
1.718	0.111	0.2959	91	A
1.870	0.205	0.3260	91	A
2.048	0.179	0.3748	91	A
2.233	0.215	0.4266	91	A
2.441	0.228	0.4980	92	A
2.675	0.263	0.5709	92	A
2.906	0.232	0.6462	92	A
3.131	0.265	0.7395	92	A
3.381	0.272	0.8394	92	A
3.630	0.264	0.9219	92	A
3.871	0.262	1.036	92	A
4.145	0.287	1.138	91	A1
4.497	0.414	1.294	91	A1
4.905	0.407	1.517	91	A1
5.352	0.498	1.758	91	A1
5.850	0.513	2.060	90	A1
6.055	0.565	2.185	90	B
6.593	0.535	2.621	90	B
7.230	0.760	3.126	90	B
8.127	1.065	4.047	89	B

TABLE 4-3 (cont.)

T_{MID}/K	ΔT/K	$\overline{C_{p,m}}$/$JK^{-1}mol^{-1}$	% of total measured $\overline{C_p}$ due to sample	notes
9.275	1.255	5.184	88	B
10.781	1.837	7.330	88	B
12.364	1.330	10.06	88	B
13.642	1.784	12.25	87	B1
13.894	1.728	12.66	86	B
15.512	1.960	15.02	85	B1
15.513	1.511	15.08	85	B
17.408	2.002	18.77	84	B
17.451	1.943	18.83	84	B1
19.514	2.211	23.24	83	B
21.789	2.338	27.82	82	B
24.238	2.561	32.74	80	B
26.970	2.903	38.09	78	B
29.942	3.042	44.09	77	B
33.415	3.903	50.74	75	B
36.688	2.644	57.01	73	B
38.644	1.270	60.24	72	B
39.887	1.216	62.50	72	B
41.082	1.174	64.13	71	B
44.100	4.862	69.45	70	B
48.254	3.447	76.91	69	B
49.183	2.425	78.47	69	C
51.544	2.296	82.16	68	C
54.190	2.996	86.04	67	C
57.089	2.803	91.02	67	C
60.183	3.386	95.01	66	C1
62.551	3.166	97.70	66	C1
65.797	3.326	102.7	65	C1
69.047	3.174	107.0	65	C1
72.396	3.524	112.4	65	C1
75.846	3.375	117.4	65	C1
79.156	3.246	122.2	65	C1

Key to notes:- Determinations marked A and A1 were performed with liquid helium refrigerant in an essentially continuous run roughly according, respectively, to schemes (b) and (c) in Figure 2-13 (page 68). Then the work was broken off for an overnight rest during which time the sample cooled by less than 0.4 K. Then determinations B were performed in a

TABLE 4-3 (cont.)

Key to notes (cont.):-

continuous run roughly according to schemes (c) to (f) in Figure 2-13, except that adiabatic shield operation was begun at a lower temperature, namely at about 10 K. This led to some difficulties in shield control for vessel temperatures around 15 K (compare page 75). Once the highest-temperature determination (T_{MID} = 48.254 K) had been completed, the vessel was recooled so as to recheck this region with isoperibolic shield operation (determinations B1). Determinations C and C1 comprise separate runs with liquid nitrogen refrigerant according to scheme (g) in Figure 2-13.

TABLE 4-4

Curvature-corrected heat capacities of TMMC between 1.6 K and 4 K.

T/K	$C_{p,m}$/J K^{-1} mol^{-1}
1.636	0.2738
1.718	0.2959
1.870	0.3258
2.048	0.3747
2.233	0.4264
2.441	0.4978
2.675	0.5707
2.906	0.6460
3.131	0.7392
3.381	0.8392
3.630	0.9217
3.871	1.036

Section 4-3: description of heat capacity results, including those obtained by Dunn and Worswick in this laboratory, and comparison with results obtained in other laboratories

a. general comments

It has already been noted (at page 136) that other laboratories were working on the heat capacity of TMMC at about the same time as this laboratory. It is an indication of the peculiar interest in TMMC that in all seven laboratories are now known to have been involved in such work - four in the USA, one in the Netherlands, one in Japan, and this laboratory. The temperature ranges over which measurements were performed in the various laboratories were not the same, and the results are not always reported fully and precisely in the literature.* This means that the various sets of results are not easy to compare with one another quantitatively; but there are no gross discrepancies. In particular, one can say that two heat capacity maxima have been amply confirmed - the one at 0.83 - 0.84 K and the other at 126.4 - 126.5 K. These temperatures correspond to the two transition temperatures (the Néel temperature and the monoclinic-hexagonal transition temperature respectively) referred to on page 135. Figures 4-1 to 4-4 present the results obtained in this laboratory, together with (in Figure 4-1) the very low temperature results (over the range 0.4 K to 1.5 K) of Vis et al (1974) to complete the overall picture.

More detailed comments follow.

Section 4-3b: results below 4 K

The most striking feature of the molar heat capacity in this region (see Figure 4-1) is that it is very large, even well above the temperature of the anomaly, on account of the magnetic contribution

*The work performed at the University of Missouri, USA and at the University of Wyoming, USA (see footnote 3 to Blacklock et al, 1974) has apparently not been published in full and is not specifically discussed below.

FIGURE 4-1

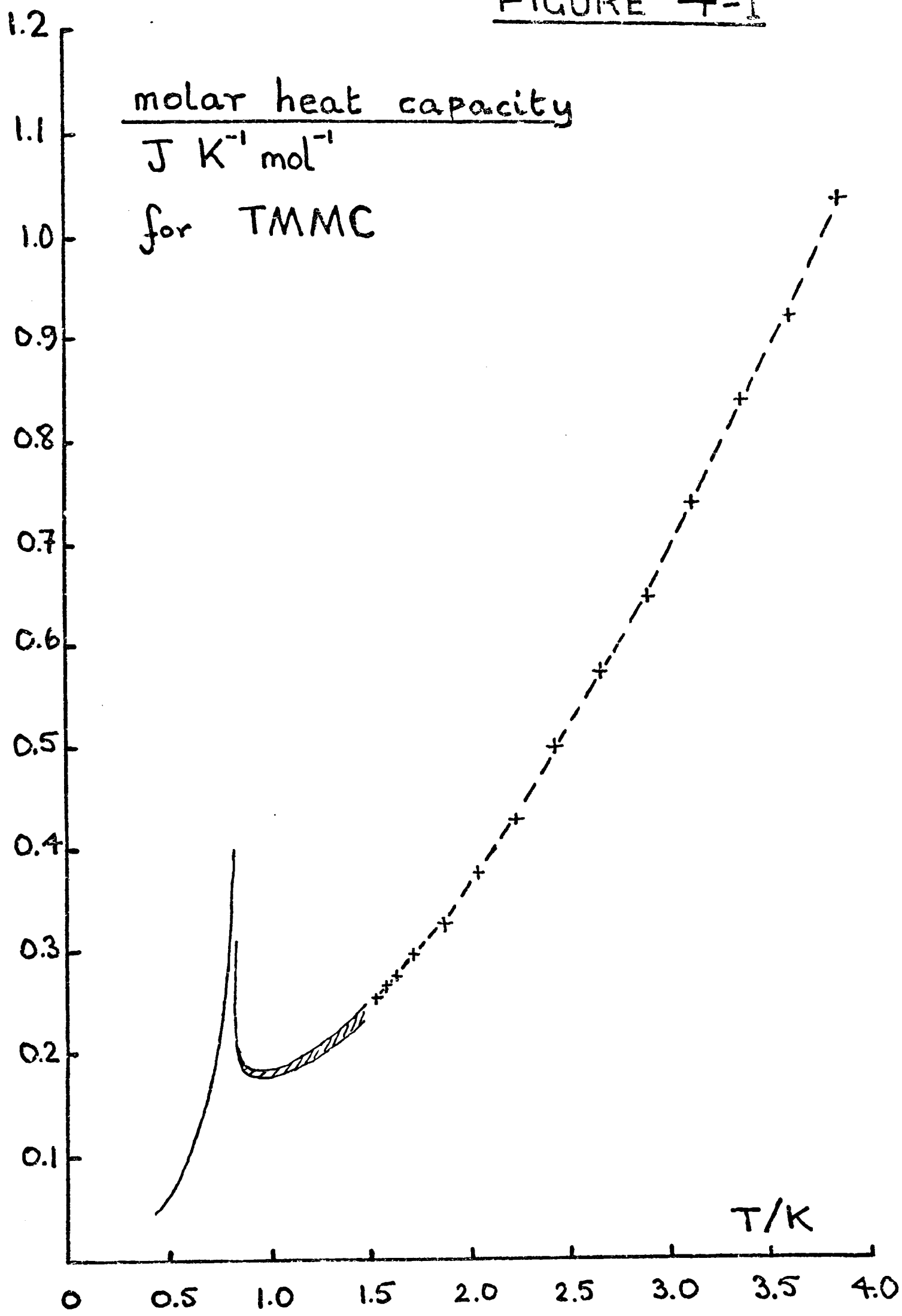

Continuous lines and shading represent the results below 1.5 K of Vis et al (1974) traced from their Fig. 2 (their results are not quoted numerically); there is a considerable spread above about 0.9 K. Crosses represent the results given in Table 4-4 except for the lowermost two, which represent the first two results given in Table 4-3.

FIGURE 4-2

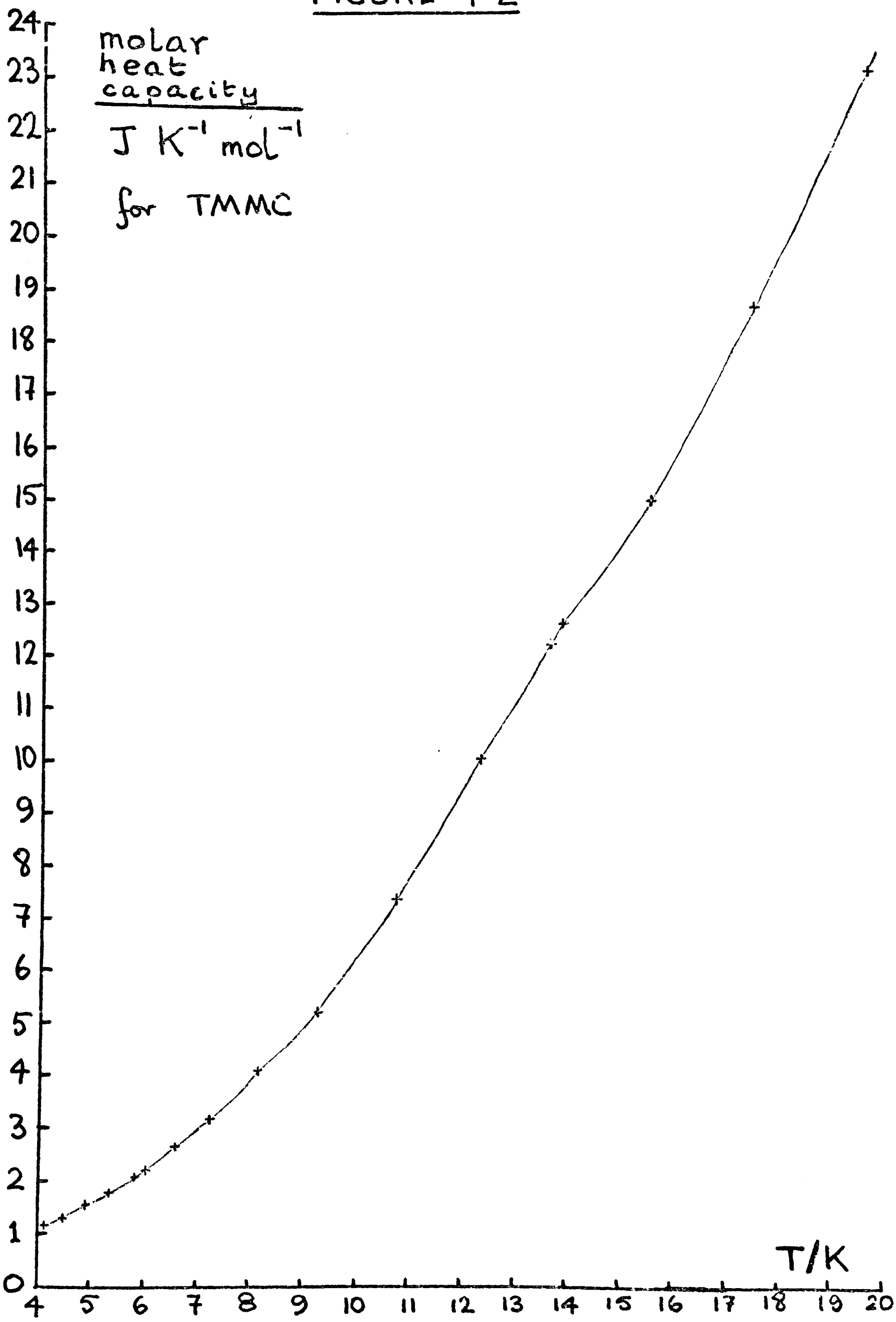

Crosses represent results in Table 4-3. The determinations for T_{MID} = 15.513 K and T_{MID} = 17.451 K are not represented, because the corresponding crosses would merge with those for T_{MID} = 15.512 K and 17.408 K respectively.

FIGURE 4-3

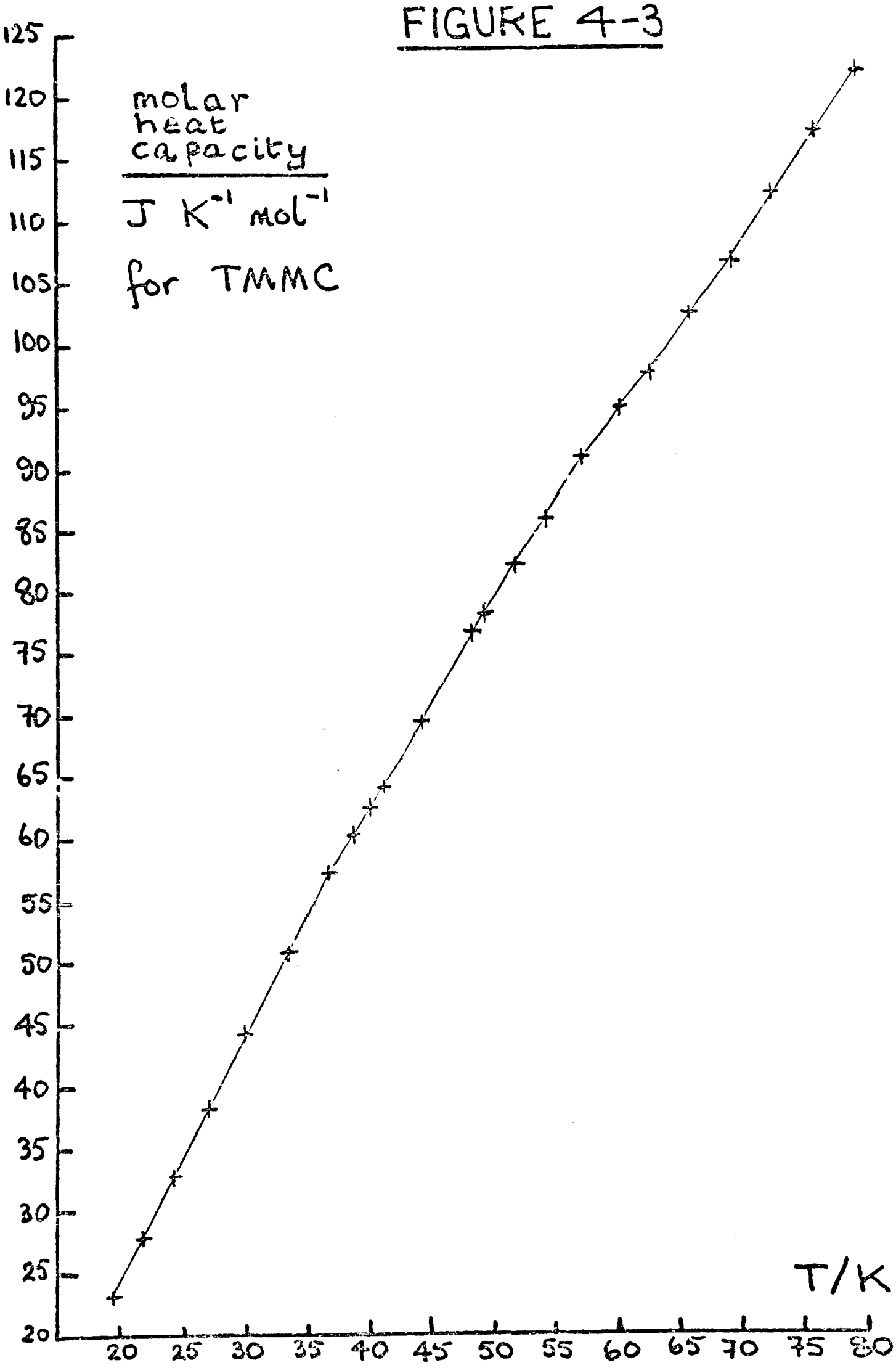

Crosses represent results in Table 4-3.

FIGURE 4-4

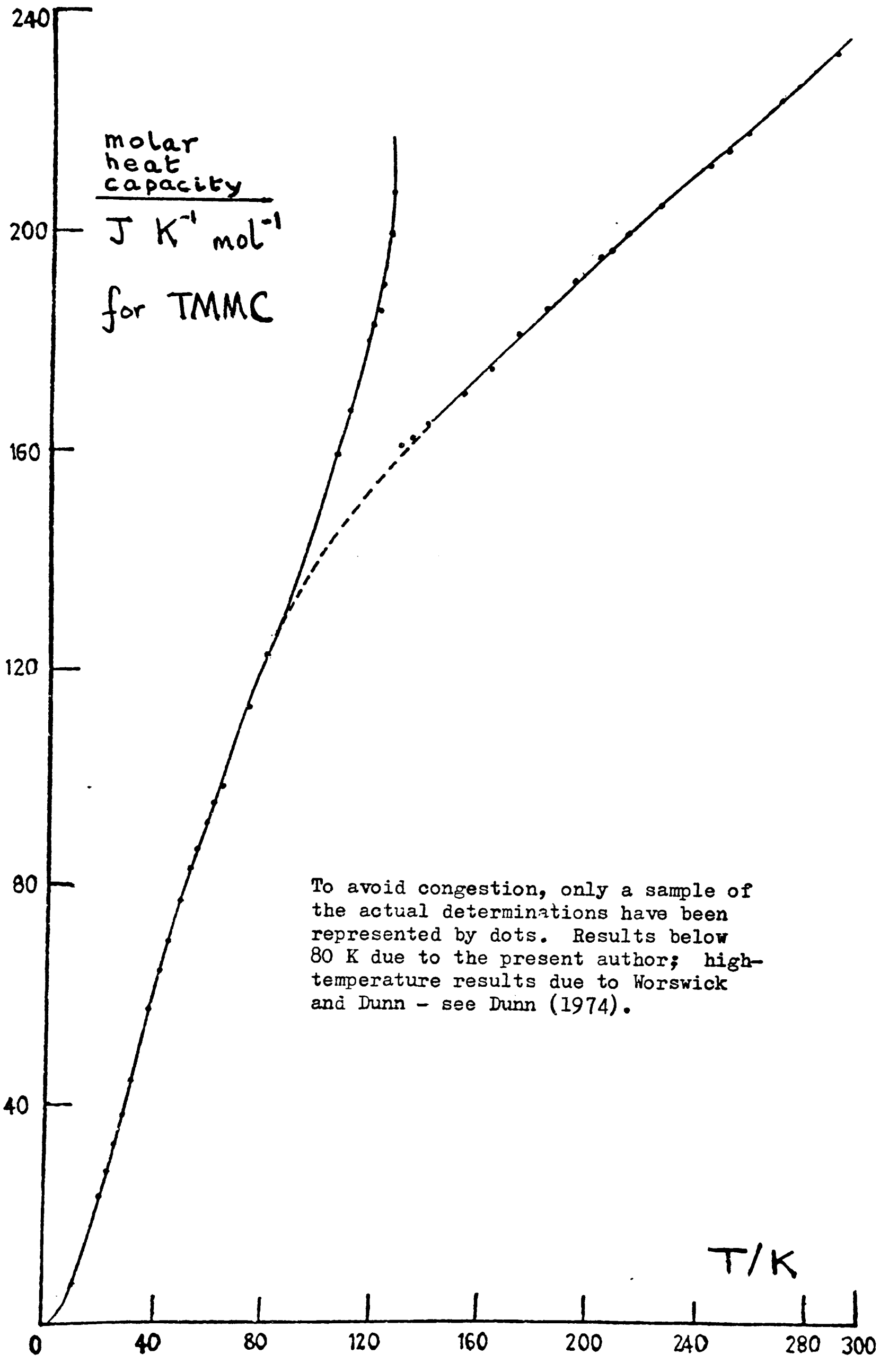
240
200
160
120
80
40
molar heat capacity
J K⁻¹ mol⁻¹
for TMMC
To avoid congestion, only a sample of the actual determinations have been represented by dots. Results below 80 K due to the present author; high-temperature results due to Worswick and Dunn - see Dunn (1974).
T/K
0
40
80
120
160
200
240
280
300

to the heat capacity. As a very crude comparison, it may be noted that at any temperature between 1.6 K and 2 K bis(adiponitrile)-copper(I) nitrate was observed (see Chapter 3) to have a molar heat capacity (presumably purely vibrational in origin) of only about 1/10 of the molar heat capacity of TMMC at the same temperature.

Below 4 K the heat capacity of the empty vessel used in the calculation of the molar heat capacities is an extrapolated value (compare the paragraph bridging pages 82 and 83 and the second paragraph on page 102). However, the proportion of the total measured $\overline{C_p}$ which is due to the sample itself is over 90%, so that an error of 20% in the heat capacity of the vessel (which analysis of the extrapolation shows to be very unlikely, even at 1.5 K) would cause an error of only 2% in the calculated molar heat capacity.

It is not possible to tell whether the heat capacities below 2.6 K include a contribution from He^3 adsorption (compare the apparent observation of such an effect with bis(adiponitrile)copper(I) nitrate as discussed in the first paragraph of page 103), since in this case the effect would probably raise $C_{p,m}$ only by 2% or less. A plot of $C_{p,m}/T$ against T (see the crosses + in Figure 4-5) shows that below 1.6 K there is an upward deviation of $C_{p,m}$ from an equation

$$C_{p,m} = aT + bT^2 \qquad \text{eq. 4-1}$$

which fits the results from 1.6 K to 4 K fairly well; such an upward deviation is in any case expected as the Néel temperature is approached from the high-temperature side (compare Figure 4-1), so that any contribution to this deviation from He^3 adsorption cannot be assessed.

The nature of the dependence of $C_{p,m}$ on T from 1.5 K to 4 K has attracted particular theoretical attention, and in this range reasonably full details of the experimental results have been published in four separate papers (Takeda, 1974; Dietz et al, 1974; Vis et al,

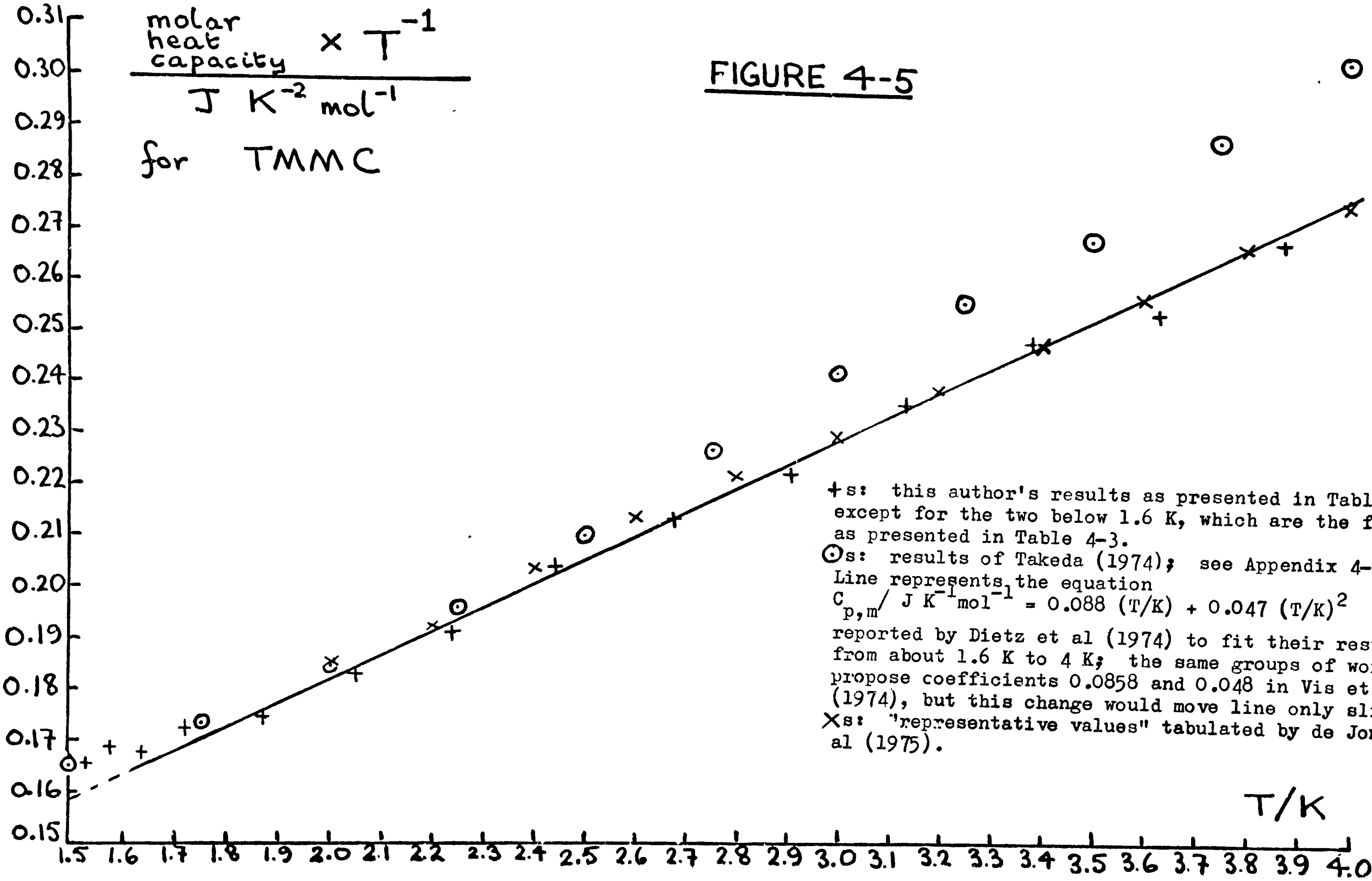

FIGURE 4-5

+s: this author's results as presented in Table 4-4, except for the two below 1.6 K, which are the first two as presented in Table 4-3.

⊙s: results of Takeda (1974); see Appendix 4-I.

Line represents the equation

$C_{p,m} / J\,K^{-1}\,mol^{-1} = 0.088\,(T/K) + 0.047\,(T/K)^2$

reported by Dietz et al (1974) to fit their results from about 1.6 K to 4 K; the same groups of workers propose coefficients 0.0858 and 0.048 in Vis et al (1974), but this change would move line only slightly.

×s: "representative values" tabulated by de Jonge et al (1975).

1974; and de Jonge et al, 1975). All these results and the present author's results are compared graphically in Figure 4-5. It is seen that the present author's results are reasonably consistent with all the results of the other workers except for those of Takeda. Takeda's heat capacities from 2.3 K to 4.0 K are higher than everyone else's; the discrepancy is greatest at 4.0 K, where it is about 9%.

Section 4-3c: results from 4 to 52 K

From 4 to 52 K, de Jonge et al's results are available for comparison. They report only "representative values" at regular temperature intervals, from which it is reasonable to suppose that some smoothing has been carried out. Since such a smoothing procedure may have been somewhat arbitrary, detailed comparison of the present author's results with the "representative values" is not necessarily meaningful. For example, the slight shoulders in Figure 4-2 around 14 K and in Figure 4-3 around 40 K are not apparent when these "representative values" of de Jonge et al are plotted out; but it may simply be that they too observed these features but smoothed them out. On large-scale plots, it was seen that the present author's results lay from about 3% below to about $1\frac{1}{2}$% above a smooth line through the "representative values". This suggests that while the breadth of the deviation may well result from the effect of de Jonge et al's smoothing, their results are probably systematically somewhat higher, by about 1%. Whether this discrepancy is due to the calorimetry, or whether it is due to the sample used, it is not possible to say; although it should be noted that de Jonge et al's sample consisted of small crystals obtained by evaporation of an aqueous solution whereas the author's sample (see Section 4-1) consisted of large crystals prepared from concentrated HCl solution, and that de Jonge et al do not refer to any special precautions to avoid pickup of moisture in the

handling of the sample (contrast pages 138 and 142 above).

Section 4-3d: results above 52 K

Above 52 K, the only known data with which this laboratory's results (i.e. the author's up to 80 K and those of Dunn and Worswick above 80 K*) can be compared are given in a very small-scale plot of Dietz et al (1974). So far as one can tell from this plot, there are no significant discrepancies between the results obtained in this laboratory and Dietz et al's results, at least below about 160 K.+ The slight shoulder at around 65 K (compare those at around 14 K and 40 K already mentioned) is not mentioned by Dietz et al, and it would not be visible in their plot. They do, however, specifically refer to a "broad peak at about 50 K" (perhaps "hump" would have been a more appropriate term); it will be seen that the plot in Figure 4-3 displays a rather marked net change in slope between 35 K and 70 K.

---

*It should be noted, for the sake of completeness, that Worswick and Dunn used a sample of TMMC prepared by cooling a solution of $MnCl_2$ and NMe_4Cl in aqueous HCl of 2 mol dm^{-3} concentration, and that their crystals were smaller than the author's (typically, 5 mm long and 1 mm across) - contrast Section 4-1.

+The heat capacity above 160 K is not of particular interest for the discussion of Section 4-4; and in any case the deviations, even if they are not a figment of Dietz et al's graph-plotting, do not exceed about 3% (their results being the higher).

Section 4-4: discussion

a. crystal structure of TMMC; change of structure at 126 K

Morosin and his coworkers (see Morosin and Graeber, 1967 and for confirmation* Peercy et al, 1973) have proposed, primarily on the basis of X-ray single-crystal work, a room-temperature structure for TMMC in which the unit cell is hexagonal (a = 9.1510Å, c = 6.4940Å) and the space group is $P6_3/m$. There follows here a description of the structure which they propose. Despite an enormous number of investigations of TMMC since 1967, it appears that no one has suggested that this structure is incorrect in any major respect;* and therefore this entire discussion section will be based on it. However, two caveats are necessary: firstly, the disordered arrangement of the NC_4 units here described is an oversimplification (even though it is based on Morosin and Graeber's final atomic positions); and secondly no H atom positions are specified. Both of these matters may be of significance in relation to the transition at 126 K and will be referred to again in Section 4-4f.

The Mn atoms and the Me_4N^+ ions lie in separate chains in or parallel to the c axis, as shown in Figure 4-6. The Mn atoms are incorporated in infinite $[n\ MnCl_3]^{n-}$ chains, in which all adjacent pairs of Mn atoms c/2 apart are bridged by three Cl atoms. A segment of such a chain is shown in Figure 4-7. The Mn atoms lie in positions of only $\bar{3}$ (S_6) symmetry, but their coordination by Cl is approximately octahedral, the distortion from octahedral corresponding to a lengthening along the chain. It is to be noted that the

*The importance of subsequent confirmation is that on the basis of Morosin and Graeber's original work a space group of $P6_3$ was possible although improbable. The choice of $P6_3$ as a space group would not affect the $[n\ MnCl_3]^{n-}$ chain structure shortly to be described, but it would permit ordered Me_4N^+ ions at room temperature.

FIGURE 4-6

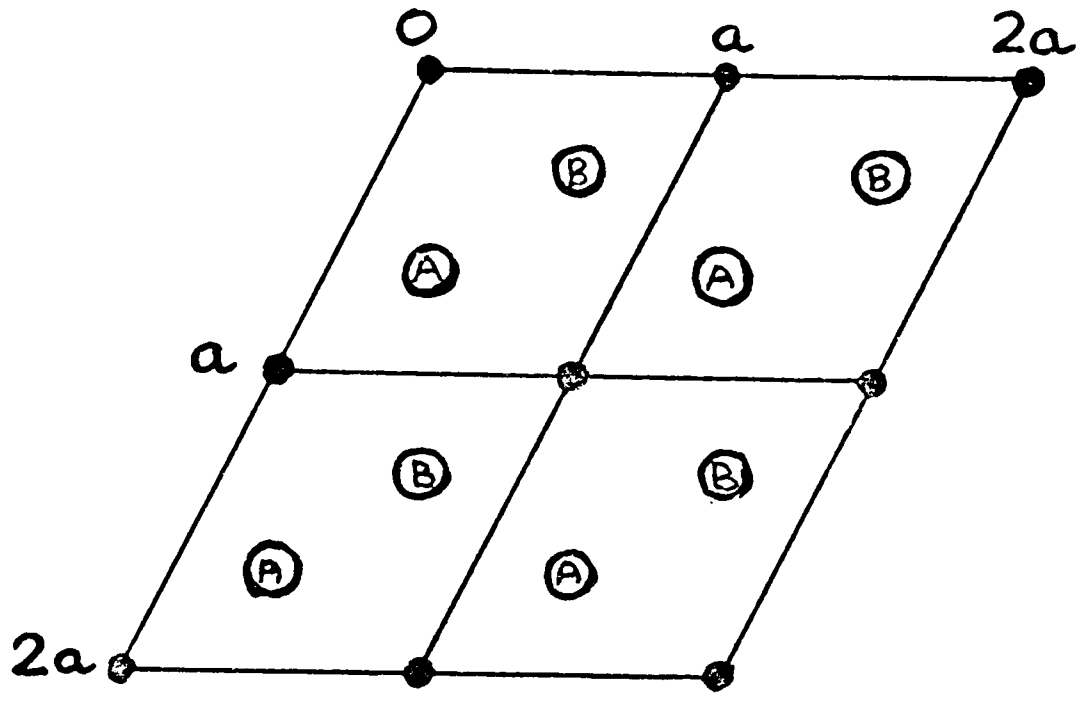

● = Mn atoms at z = 0, c/2, c, 3c/2, etc.

Ⓐ = N atoms at z = 3c/4, 7c/4, etc.

Ⓑ = N atoms at z = c/4, 5c/4, etc.

FIGURE 4-7

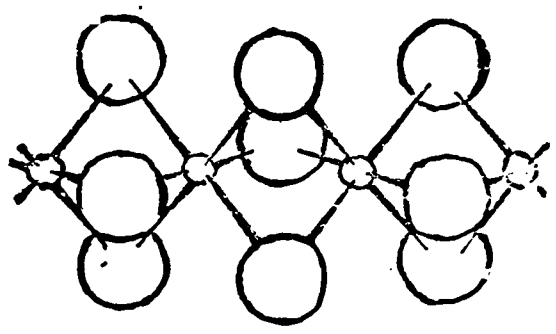

small circles Mn, large circles Cl

FIGURE 4-8

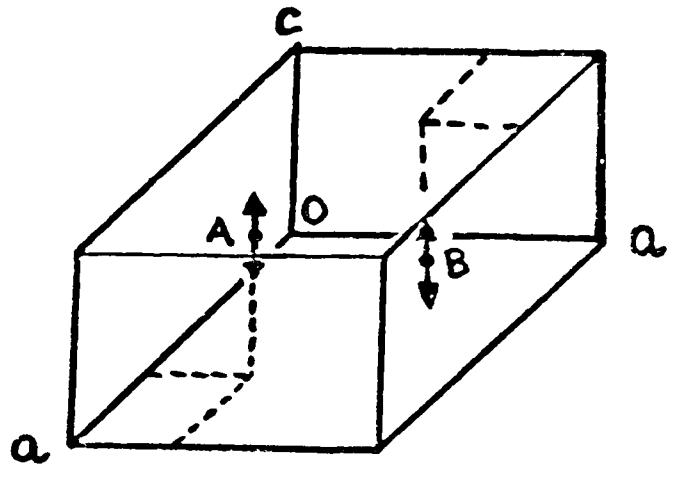

➡ represents an N–C bond; A, B refer to chains of N atoms indicated in Figure 4-6; two orientations for each ion of probability 1/2

description of the Mn atoms as lying along a "chain" can be taken rather literally. Not only are the Mn atoms connected by Cl atoms, but also the nearest neighbour Mn-Mn intrachain distance is only $c/2 = 3.25$ Å whereas adjacent chains are separated by $a = 9.15$ Å.

The use above of the word "chain" in relation to the Me_4N^+ ions is, however, purely a formalism. Within a "chain", the nearest-neighbour N-N distance is $c = 6.49$ Å, whereas the perpendicular interchain distance is $a/\sqrt{3} = 5.28$ Å and the nearest interchain N-N distance is $((a/\sqrt{3})^2 + (c/2)^2)^{1/2} = 6.20$ Å.

The (2/3, 1/3, 1/4) and (1/3, 2/3, 3/4) positions to which the N atoms are assigned have symmetry $\bar{6}$ (C_{3h}), the threefold axis being parallel to the c axis. By an argument similar to that used in relation to the nitrate ions of bis(adiponitrile)copper(I) nitrate at pages 115 to 116, it can be shown that the NMe_4^+ ions must be disordered. Figure 4-8 depicts the disordered arrangement according to Morosin and Graeber's final atomic positions. The ions take up with equal probability two orientations for which a threefold axis of the ion coincides with the threefold axis of the site, N being situated at the symmetry origin in each orientation, and each orientation of the ion being a mirror image of the other. Thus the X-ray experiment "sees" the ion as having $\bar{6}$ (C_{3h}) symmetry.

The structure is rather difficult to depict in its entirety in a single perspective view or by means of projections (hence the above stepwise description); but an attempt at such a depiction is reproduced from Hutchings et al (1972) as Figure 4-9.

Peercy et al (1973) studied the phase transition at 126 K by (inter alia) X-ray diffraction. They deduced that in the low-temperature phase the Me_4N^+ ions are ordered in the manner depicted in Figure 4-10. In Figure 4-11 is shown the variation with temperature

FIGURE 4-9

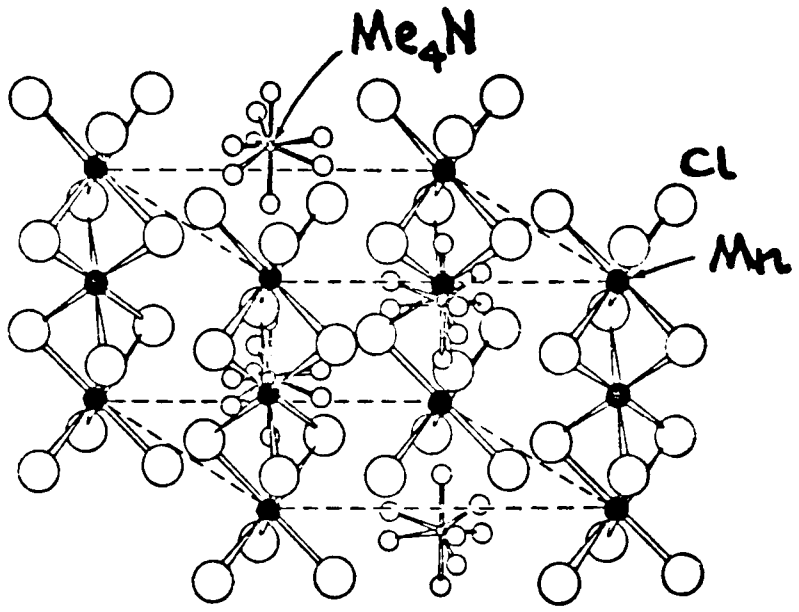

Me_4N represented by central N with weight 1 and Cs with weight 1/2; cell viewed with 120° angle in foreground left.

FIGURE 4-10

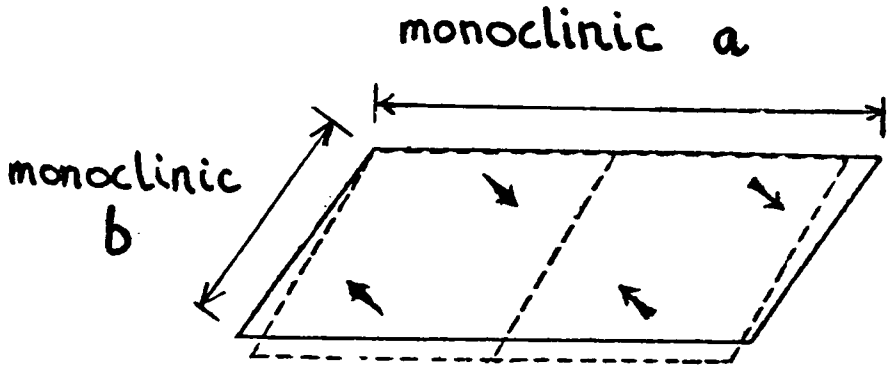

Dashed lines - two room-temp. hexagonal cells; solid lines - low-temp. monoclinic ($P2_1/a$) cell, distortions much exaggerated. $P2_1/a$ glide operation relates Me_4Ns (each at general site) in a manner similar to that indicated by arrows. Fat/thin tail indicates tipping towards/away from observer.

FIGURE 4-11

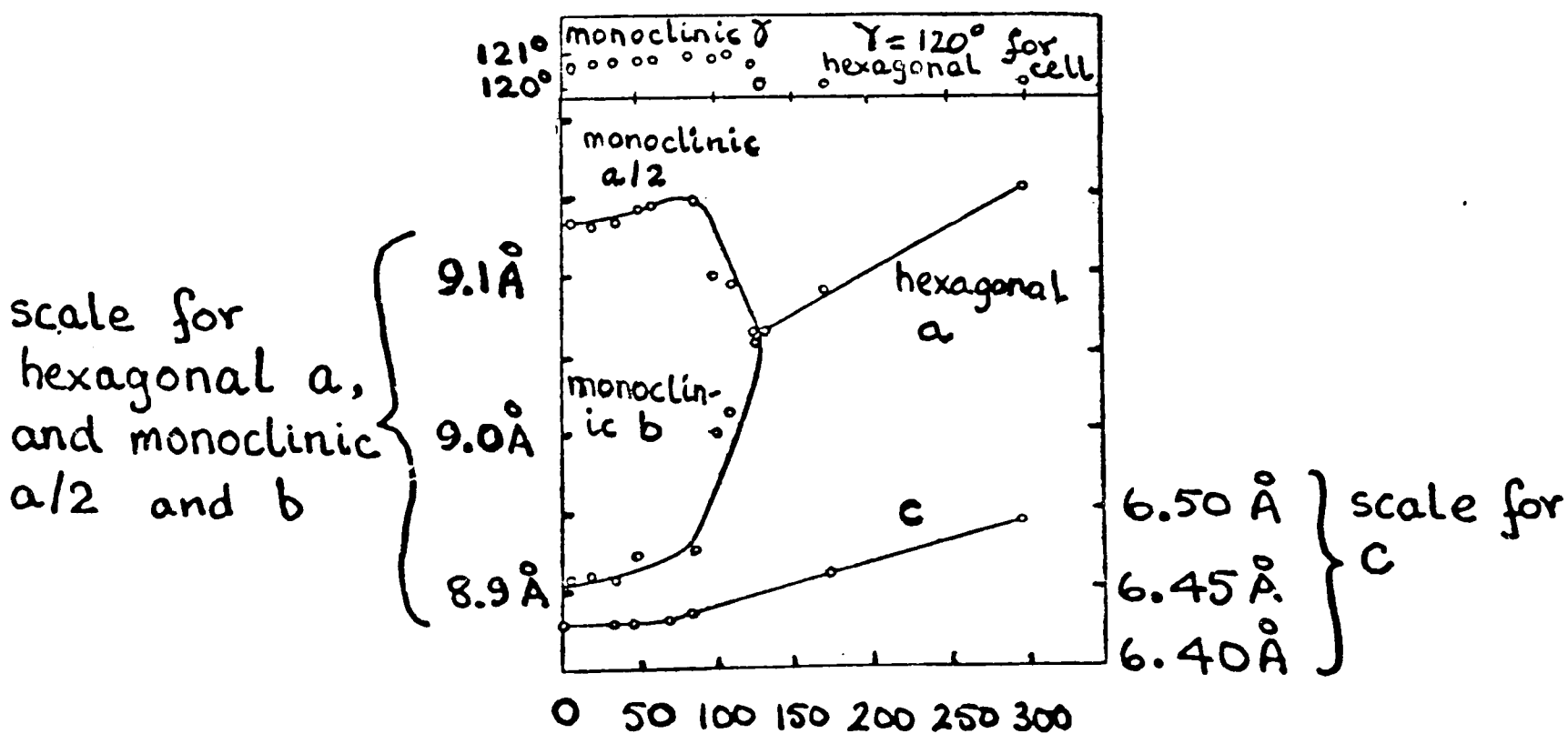

of the lattice parameters. As the crystal is cooled through 126 K, the Me_4N^+ ions order in such a way that one of the new, monoclinic unit cell axes is approximately twice the hexagonal cell's a - "approximately", because at the same time the mutual arrangement of the $[n\ MnCl_3]^{n-}$ chains and Me_4N^+ chains changes slightly but rather abruptly. However, the distance between adjacent Mn atoms in any $[n\ MnCl_3]^{n-}$ chain changes apparently quite continuously as the temperature is lowered. This is important, since it means that the 1-d character of the magnetic properties (see Section 4-4b) is almost unaffected by the transition.

Section 4-4b: magnetic properties of TMMC

From the above description of the $[n\ MnCl_3]^{n-}$ chains, it is reasonable to suppose that there will be a strong antiferromagnetic interaction between adjacent Mn^{2+} ions (of spin 5/2) via Cl^- bridges by the superexchange mechanism (compare Dekker, 1958a, where MnO is specifically discussed). Between the chains, however, either in the low-temperature (<126 K) or the high-temperature (>126 K) form only very feeble Mn^{2+} - Mn^{2+} interactions can be expected, whether these are direct or of the superexchange type via the Me_4N^+ ions. It is expected therefore that TMMC will behave as a 1-d antiferromagnet except at the rather low temperatures at which these interchain interactions will become significant.

Dingle et al (1969) confirmed these expectations. They observed a broad maximum in the magnetic susceptibility (both $\chi_{\parallel}$ and $\chi_{\perp}$) about 50 K. This broadness contrasts with the relative sharpness at the changes of $\chi_{\parallel}$ and $\chi_{\perp}$ at T_N of a simple (i.e. essentially 3-d) antiferromagnet such as $MnCl_2.4H_2O$ (see, for example, the plot in Domb and Miedema, 1964a). Qualitatively, this broadness results from the fundamental impossibility of a discontinuity associated with the

disruption of 1-d order (which cannot be long-range - see page 13, last three lines).

Now, the Heisenberg model of a linear system of N spins in zero magnetic field uses the Hamiltonian

$$\hat{H} = -2J \sum_{i=1}^{N-1} (\hat{\vec{S}}_i \cdot \hat{\vec{S}}_{i+1}) \qquad \text{eq. 4-2}$$

For a ferromagnet, J is positive and for an antiferromagnet J is negative. The subscript i refers to the ith spin in the line.

Dingle et al found that the susceptibility of TMMC above 40 K could be explained on the Heisenberg model for J = -6.3 K k.*

Dingle et al and later Walker at al (1972) and Magnum and Utton (1972)+ measured the Néel temperature of 0.84 K, below which 3-d long-range order exists. This Neel temperature would, in a simple antiferromagnet, indicate a value for |J| very much smaller than 6.3 K k, as is readily seen from the following comparison of TMMC with three simple Mn^{2+} antiferromagnets:-

salt	T_N/K	J/(K k)	
$MnCl_2.4H_2O$	1.62	-0.058	information taken from Domb and Miedema (1964b)
$MnBr_2.4H_2O$	2.14	-0.088	
MnF_2	67	-2.0	
TMMC	0.84	-6.3	

The ratio $kT_N/|J|$ for TMMC is many times smaller than for the simple antiferromagnets. In general terms, the smallness of the parameter $kT_N/|J|S^2$ - in which the S^2 term is intended to allow comparison between systems differing in the ionic spins involved - has been used as a measure of the approximation of a system to 1-d antiferromagnetism.

---

*Dingle et al in fact give J a positive value, but only on account of a different (less usual) sign convention.

+These later references are cited as further authority in view of Dingle et al's concern that, possibly, their results were in error because of the presence of $(Me_4N)_2MnCl_4$ in their sample (compare Section 4-1 above).

On this basis Dingle et al commented that, to that date, TMMC was the "closest physical approximation...to a linear-chain quasi-Heisenberg antiferromagnet", and this is essentially the reason why TMMC has been so intensively studied.

As for the orientational nature of the 1-d antiferromagnetism, the fact that below about 50 K* χ measured with a magnetic field along the c axis exceeds that measured with the field perpendicular to it indicates that as the temperature is reduced the spins "condense" normal to the c axis. This behaviour indicates, in fact, that the Heisenberg Hamiltonian of equation 4-2 (page 160) is not completely satisfactory. In order to explain the existence of a preferred spin direction it is necessary to include "anisotropic" terms in the Hamiltonian, such as terms corresponding to magnetic dipole-dipole interactions.

Section 4-4c: magnetic heat capacity and magnetic entropy below 4 K

From equation 1-5 (page 12) it follows that the molar magnetic entropy gain for TMMC as the crystal is heated from near 0 K, where a 3-d ordered arrangement prevails, to a temperature where each magnetic moment takes up its orientation practically independently of the others is R ln (2 x 5/2 + 1) = R ln 6 = 14.90 J K^{-1} mol^{-1}. While as we have already noted (paragraph bridging pages 146 and 151) the heat capacity below 4 K is much larger than one would expect for a compound without an anomalous heat capacity contribution, only a small proportion of the R ln 6 magnetic entropy gain is achieved below 4 K - indeed, even the total molar calorimetric entropy at 4 K appears to be only 0.78 J $K^{-1}mol^{-1}$, i.e. about 5% of R ln 6 (see Appendix 4-II).

Now, in view of the strong intrachain and weak interchain

---

*This temperature is dependent on the field strength.

interactions in TMMC discussed in Section 4-4b, one expects that at, say, 4 K the different chains will be almost completely disordered relative to one another but that each chain will contain long segments of aligned spins despite the absence of long-range order in the chains; and the abovementioned calorimetric entropy at 4 K is consistent with this expectation.

The region from about 1.6 K to 4 K (or somewhat above) is nevertheless of especial importance in that if one can separate out the magnetic contribution to the heat capacity from the vibrational contribution, then this can be compared with the low temperature limiting behaviour of theoretical models of 1-d antiferromagnets. (The temperature range below 1.6 K is not usable in this way because of the effect of the interchain interactions.) Interestingly, while Dietz et al (1974) and de Jonge et al (1975) report very similar values for the total $C_{p,m}$ (both sets of values agreeing well with the present author's results - see especially Figure 4-5, page 152)*, they separate the heat capacity into vibrational and magnetic contributions in quite different ways.

Dietz et al fitted their results to the equation (cf. page 151 and Figure 4-5, page 152) -

$$C_{p,m}/\mathrm{J\ K^{-1}mol^{-1}} = 0.088\ (T/K) + 0.047\ (T/K)^2 \qquad \text{eq. 4-3}$$

- and, tentatively at least, treated the linear term as the magnetic contribution and the quadratic term as the vibrational contribution. This separation is at first sight not unreasonable in that spin-wave theory (see e.g. Gopal, 1966a for a general description of the theory) for a linear antiferromagnet predicts a linear dependence of $C_{p,m}$

*In the following discussion, no consideration will be given to the very minor effects on interpretation which would result from using the present author's experimental values instead of Dietz et al's or de Jonge et al's.

on T.* To explain the quadratic nature of the vibrational term (which contrasts with the more usual Debye cubic term in accordance with equation 1-3, page 7), Dietz et al refer to the known "important low-frequency librational motions" of the Me_4N^+ ions. The separation of the heat capacity proposed by Dietz et al is depicted in Figure 4-12.

The separation proposed by de Jonge et al is shown in Figure 4-13. This separation is based (as we shall see) on the use of "TMCC", Me_4NCdCl_3, as a comparison compound and for this reason is expected to be much more nearly correct than Dietz et al's separation. The general size of the error in Dietz et al's analysis is immediately apparent from a comparison of Figures 4-12 and 4-13; in fact, Dietz et al have overestimated the vibrational contribution to the heat capacity by a factor of about 10 at 2 K and by a factor of about 3 at 4 K.

With the advantage of hindsight, one can criticise Dietz et al's (albeit tentative) acceptance of $0.047\ (T/K)^2\ J\ K^{-1}mol^{-1}$ as the vibrational contribution, even without any knowledge of the heat capacity of TMCC. This "vibrational contribution" is curiously high compared with various other materials which contain per mole rather similar numbers of light and heavy atoms and of librating species and whose heat capacities are mostly vibrational in origin in this temperature range:-

Substance	T/K	$\frac{C_{p,m}}{JK^{-1}mol^{-1}}$	$0.047(T/K)^2$	Reference for first three columns
$Cu(adip)_2NO_3$	2	0.04	0.19	Chapter 3
$(CH_3)_2NH_2CuCl_3$	2.5	0.04	0.29	Clay et al (1969)
$(CH_3NH_3)_2CdCl_4$	2	0.06	0.19	Bloembergen and Miedema (1974)

*In the low-temperature limit, so does the Heisenberg model (q.v.) as will be seen on page 166; but Dietz et al do not consider this model.

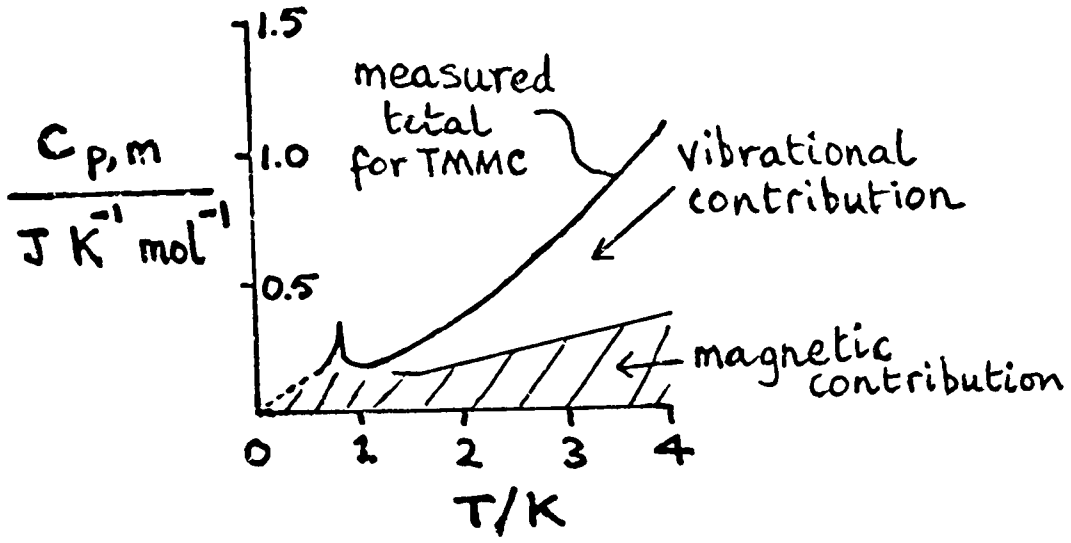

FIGURE 4-12 : separation of heat capacity proposed by Dietz et al

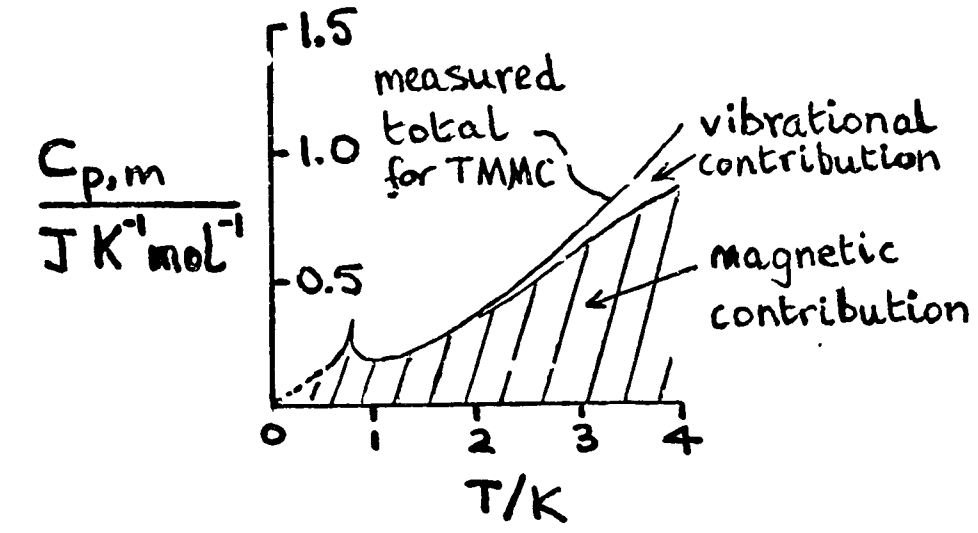

FIGURE 4-13 : separation of heat capacity proposed by de Jonge et al

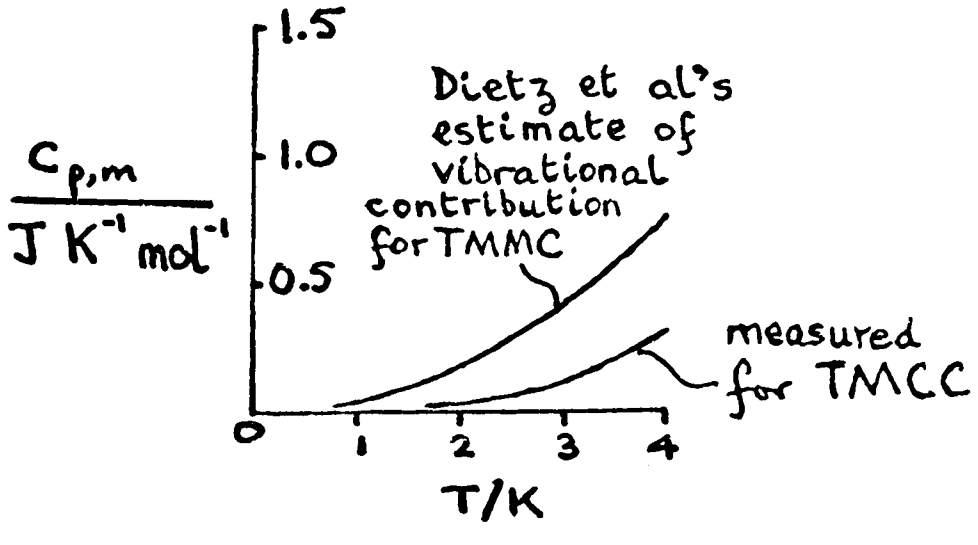

FIGURE 4-14

Furthermore, the librations to which Dietz et al refer to explain the quadratic nature of vibrational term in the heat capacity would appear to have much too high a frequency to influence noticeably their estimated vibrational heat capacity below 4 K. Lassier et al (1973) reported a librational motion at a wave number of 32 cm^{-1} in the inelastic neutron scattering spectrum, but no lower-frequency peaks. The well-known equation for the heat capacity of a quantised simple harmonic oscillator (see e.g. Lewis and Randall, 1965a), indicates that L librational modes of wave number 32 cm^{-1} would contribute only about 0.4 $\mu J\ K^{-1}mol^{-1}$ at 2 K and about 0.01 $J\ K^{-1}mol^{-1}$ at 4 K, compared with 0.047 $(T/K)^2\ J\ K^{-1}mol^{-1}$ at these temperatures of 0.19 $J\ K^{-1}mol^{-1}$ and 0.75 $J\ K^{-1}mol^{-1}$.

De Jonge et al estimated the vibrational heat capacity in this temperature range by the procedure of Stout and Catalano (1955) - that is to say, they assumed that the vibrational heat capacity of TMMC is related to the measured heat capacity of TMCC (presumably purely vibrational in origin) by the equation

$$C_{p,m}^{TMMC,vib}(T) = C_{p,m}^{TMCC}(T/Q) \qquad \text{eq. 4-4}$$

The "scaling factor" Q was taken as 1.08, on the basis of comparisons between the TMMC and TMCC heat capacity curves up to 50 K. While the precise value of Q used could perhaps be questioned,* there can be little doubt that it should be greater than 1, because of the greater mass of the Cd atom compared with the Mn atom. In other words, the heat capacity of TMCC can be regarded as an upper-limit estimate for that of TMMC. Even this upper-limit estimate makes the gross inaccuracy of Dietz et al's vibrational term immediately apparent (see Figure 4-14).

*For instance, it might be objected that in its low temperature form (<118 K) TMCC is not isomorphous with TMMC, as is strictly desirable. However, TMCC is isomorphous with TMMC at higher temperatures, and the difference in the low-temperature form relates apparently only to the precise way in which the Me_4N^+ ions are ordered (see Peercy et al, 1973).

As for the magnetic contribution shown in Figure 4-13, de Jonge et al found that this conforms to a low temperature limiting equation for a Heisenberg (see page 160) S = 5/2 antiferromagnet as calculated by de Neef and his coworkers (the de Neef work was then partly unpublished - see especially de Neef, 1976 for fuller details). The equation is

$$C_{p,m}^{magnetic} = b_1 |kT/J| + b_2 |kT/J|^2 + b_3 |kT/J|^3 \qquad \text{eq. 4-5}$$

This equation becomes practically linear in the low-temperature limit. However, the values of the bs and Js found by fitting the magnetic heat capacity to equation 4-5 indicate that linearity is <u>not</u> practically achieved above 2 K; this contrasts with Dietz et al's assumption that the magnetic heat capacity is linearly proportional to temperature (pages 162 to 163).

The bs found by de Jonge et al are consistent with those predicted by the de Neef theory. Furthermore, the value of J found (-6.7 K k) compares well with the values found by other techniques such as magnetic susceptibility measurements (see page 160).

<u>Section 4-4d: overall development of magnetic ertropy</u>

De Jonge et al (1975) succeeded also in separating the magnetic heat capacity from the vibrational heat capacity from 4 K to 50 K. Their technique in this range was to use a then unpublished theory for the lattice heat capacity of low-dimensional systems (since published in Kopinga et al, 1976), according to which the lattice heat capacity can be expressed as a function of temperature and three characteristic temperatures. They checked the validity of this theory by showing that the measured heat capacity of TMCC could be fitted to it very well. Then they used this theory in combination with the de Neef theory of the 1-d Heisenberg antiferromagnet as it applies to higher temperature ranges; if both theories are correct, then the

heat capacity should be adequately represented by a four-parameter equation, the four parameters being the previously-mentioned three characteristic temperatures and J. De Jonge et al found that such fitting could be carried out very satisfactorily. For the best fit, J was -6.7 K k, in agreement with that found from the relatively low-temperature heat capacity (see Section 4-4c), and the three characteristic temperatures were 6.8, 7.0, and 9.7 % greater than those which had already been found for TMCC. The average of these three increases was about 8%; this was the origin of the value 1.08 for the scaling factor Q used in analysing the low-temperature results (page 165).

Figures 4-15 and 4-16 are plots of magnetic entropy and heat capacity against temperature as calculated by de Neef for J = -6.7 K k and (from 2 to 52 K) as confirmed by de Jonge et al. A significant feature of the de Neef theory is that even at 82 K (i.e. near the upper temperature limit of the present author's measurements) the magnetic heat capacity is still almost 4 J $K^{-1}mol^{-1}$, and about 16% of the R ln 6 entropy is still to be gained.

At 117 K, the magnetic heat capacity is still over 2 J $K^{-1}mol^{-1}$ and decreasing only rather slowly; a rough estimate from de Neef's graphs indicates that at 117 K about 8% of the magnetic entropy is still to be gained. It follows that a significant part of the tail of magnetic anomaly overlaps with the anomalous contribution due to the disordering of the Me_4N^+ ions on the low-temperature side of the 126 K transition (see Figure 4-4, page 150). Therefore it is unlikely that the de Neef theory can be experimentally checked for TMMC at these higher temperatures.

The present author, before the publication of heat capacity results on TMCC or of the theoretical work, attempted a rough-and-ready

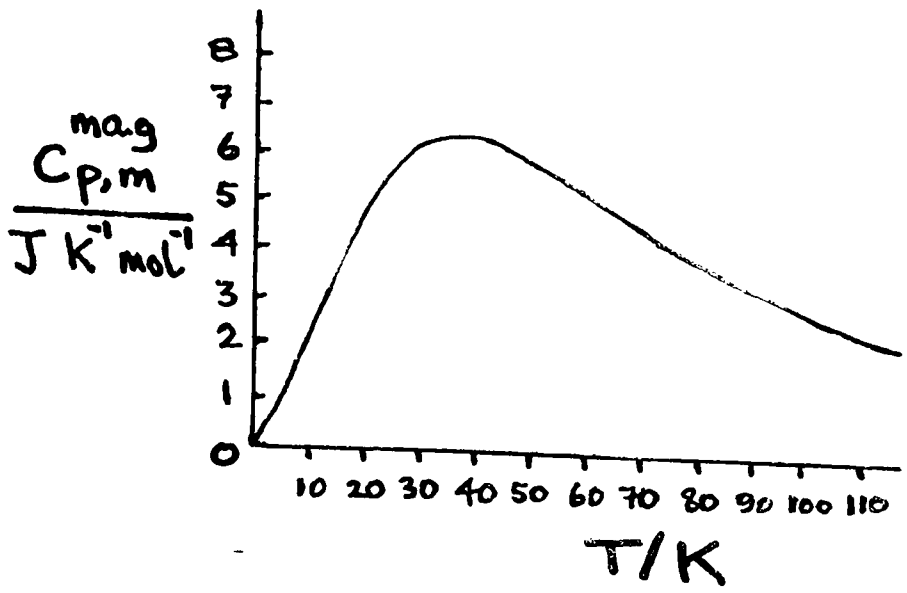

FIGURE 4-15

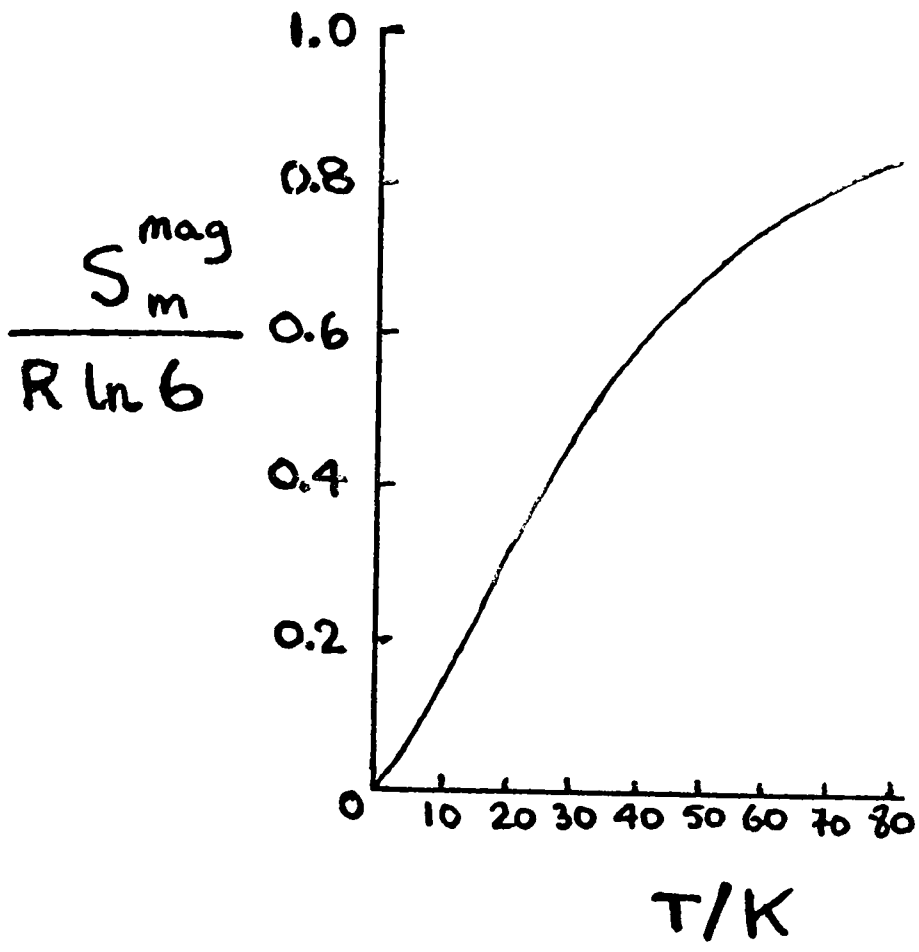

FIGURE 4-16

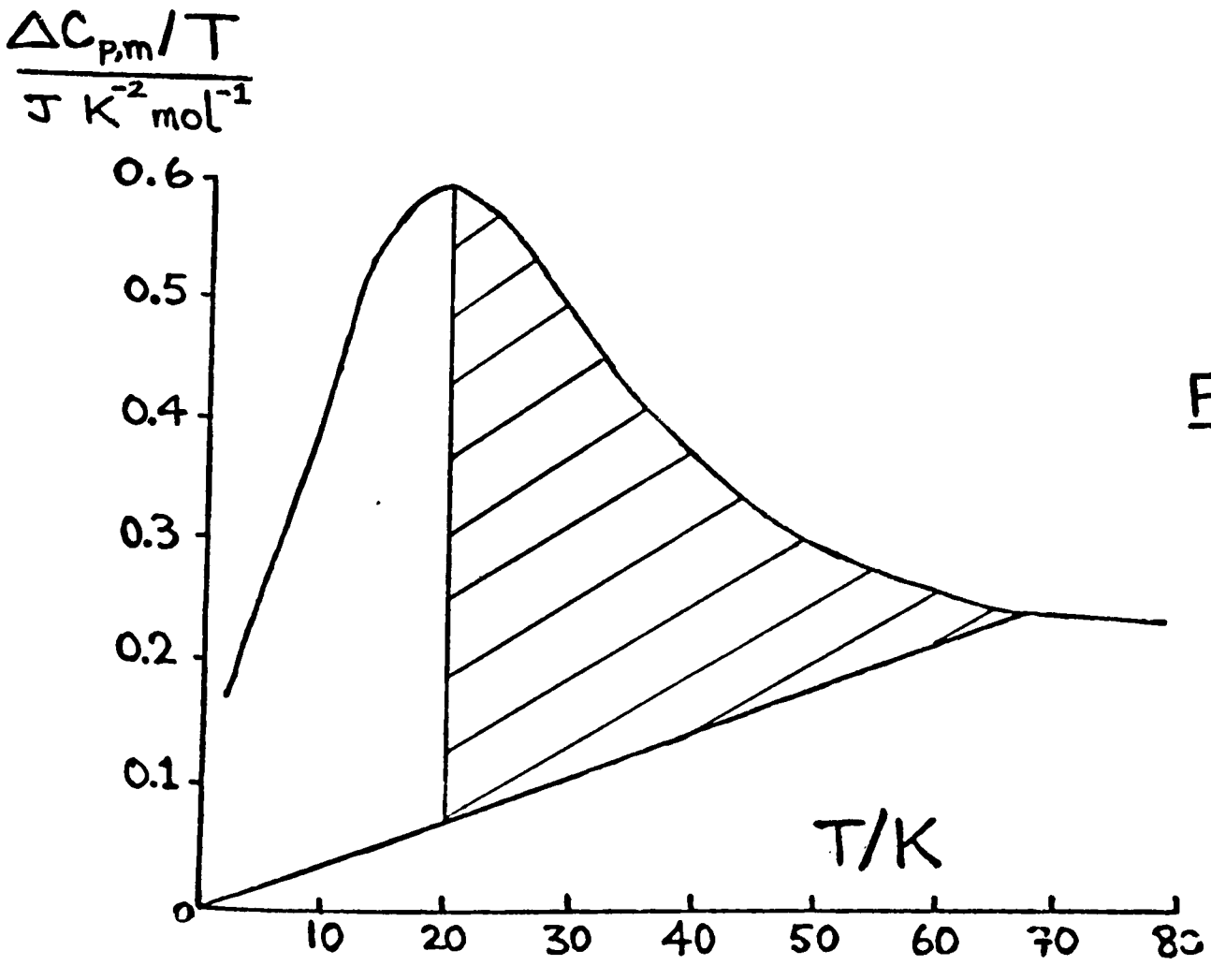

FIGURE 4-17

analysis of the results which is of some interest in that, despite its serious and immediately evident imperfections, it at least gave qualitatively correct results. The analysis involved evaluating

$$\Delta C_{p,m}/T = \frac{1}{T} \times \left\{ C_{p,m}(\mathrm{TMMC}) - C_{p,m}(\mathrm{Me_4NCl}) - C_{p,m}(\mathrm{MnCl_2}) \right\}$$

and plotting this against T up to 80 K. For $C_{p,m}(\mathrm{Me_4NCl})$ above 5 K the smoothed values given by Chang and Westrum (1962) were used (the first-order transition at 75.75 K being ignored); for $C_{p,m}(\mathrm{MnCl_2})$ above 10 K those of Chisholm and Stout (1962) were used; and below 5 and 10 K respectively T^3 extrapolations were used.

The result of this procedure (heavily smoothed) is shown in Figure 4-17. While it was too much to hope that $C_{p,m}(\mathrm{MnCl_2}) + C_{p,m}(\mathrm{Me_4NCl})$ would be a very good approximation to the vibrational heat capacity of TMMC, it was felt at the time that the maximum rate of magnetic entropy gain was achieved somewhat below 20 K as indicated by the pronounced maximum in $\Delta C_{p,m}/T$, and further that, say, the size of the area shaded (corresponding to about 10 J $K^{-1}mol^{-1}$ compared with R ln 6 = 14.9 J $K^{-1}mol^{-1}$) was a rough indication of the (very substantial) magnetic entropy gain between 20 K and 66 K.

Section 4-4e: "shoulders" near 14 K, 40 K, and 65 K; Magnum and Utton's "transition" at 39 K

These "shoulders" were previously referred to in Section 4-3. Although they were not very marked, the precision of the results as judged from large-scale plots suggests that they are genuine. De Neef's theory (see Figure 4-15) suggests that the shoulders cannot be adequately accounted for by the variation in the magnetic heat capacity. It therefore seems quite likely that they reflect some complexity in the vibrational frequency spectrum (compare the paragraph bridging pages 3 and 5). The librational motions of the Me_4N^+ ions are a possible cause of such complexity. If they are essentially uncoupled with the Debye-like vibrations of the lattice, then one can

imagine the total vibrational heat capacity as the sum of a Debye-type heat capacity and several quantised simple harmonic oscillator heat capacities. These latter heat capacities will have a marked shoulder at a temperature of approximately 0.5 $h\nu/k$ (see Seitz, 1940). If one then crudely identifies these shoulders with the shoulders in the overall heat capacity, one concludes that, very approximately, the motions in question have wave numbers of 20, 55, and 90 cm^{-1}. These figures bear no obvious relation to the lowest-frequency vibrations observed by Lassier et al (1973) in inelastic neutron scattering experiments or to those observed by Adams and Smardzewski (1971) and Peercy et al (1973) with infra-red and Raman spectroscopy, but they are of the same general magnitude.

Magnum and Utton (1972) observed a marked change in the pmr spectrum near 39 K. They suggested that the orientations of the Me_4N^+ ions are different below 39 K from those in the 39 to 50 K region. (Above 50 K, the pmr spectrum becomes a single unstructured line, so that no firm conclusions can be drawn.) Peercy et al (1973) specifically searched for evidence of such a further structural transition by X-ray diffraction and by Raman spectroscopy, but concluded that no such transition occurs.

It was thought possible that if after all the 39 K transition is genuine, then there might be a small "latent heat" near 39 K (small, because the transition would presumably be between one ordered structure and another). Therefore, smaller ΔTs than usual were used in the 39 K region in the heat capacity determinations (see page 144 and Figure 4-3, page 149). Nevertheless, no "latent heat" was detected.

Section 4-4f: order-disorder transition at 126 K

For the sake of completeness it may be mentioned that Worswick

and Dunn found that the heat capacity was a maximum at 126.5 K (compare Dietz et al, 1974 who quote 126.4 K), the transition possibly ending in an isothermal manner.

By combining the present author's results with Worswick and Dunn's it was possible to estimate a "normal" heat capacity by freehand drawing, as shown by the dashed line in Figure 4-4 (page 150). The anomalous molar entropy gain was calculated as 8.51 J $K^{-1}mol^{-1}$, of which about one-third is acquired between 124 K and 127 K. It is believed that the estimate of the total entropy gain is if anything conservative, for two reasons: firstly, it would appear from Figure 4-11 (page 158) that rapid changes of two lattice parameters continue down at least to the lower temperature at which the dashed curve meets the actual heat capacity curve in Figure 4-4; and secondly, any systematic error in the 50 to 80 K results of the author's is likely to make them too high (see Section 3-3d).

On the basis of the description of the 126 K transition given in Section 4-4a, an anomalous entropy change of R ln 2 (5.76 J $K^{-1}mol^{-1}$) is to be expected, if one follows Newns and Staveley's approach discussed at pages 122 to 123. The fact that a conservative estimate of 8.51 J $K^{-1}mol^{-1}$ has been reached suggests that the caveats at page 155 concerning the room-temperature structure may be important.

The first caveat concerned the specified disordered arrangement of NC_4 units. Morosin and Graeber (1967) specifically point out:

> The anisotropic thermal parameters for the carbon atoms are quite large and imply small disordering of the $[N(CH_3)_4]^+$ ions about the central nitrogen atom [in addition to the orientational disordering shown in Figure 4-8, page 156]. The oscillation of the tetrahedral ion is such as to tip the carbon on the threefold axis away from the axis....[The] large thermal parameters for the carbon atoms result from disordering rather than from large thermal motion.

The implications of this statement are not made clear by Morosin

and Graeber, and a similar statement in Peercy et al (1973) is not amplified. The operations of the $\bar{6}(C_{3h})$ point group on an Me_4N^+ ion in a position in which there is no coincidence between an N-C bond and the 3 (C_3) axis generate five further ionic positions; and therefore Morosin and Graeber appear to be suggesting disorder among six positions at room temperature. If this is in fact the case, then the estimated anomalous entropy gain is less than 60% of what is expected (i.e. of R ln 6 = 14.90 J $K^{-1}mol^{-1}$), presumably because the "normal" curve in Figure 4-4 has been drawn too high.

However, the present author has some doubt whether the large thermal parameters for the C atoms are significant. These were obtained when Morosin and Graeber refined a structure in which the N atoms were already fixed at the symmetry origins of the $\bar{6}$ sites (i.e. at 2/3, 1/3, 1/4 and 1/3, 2/3, 3/4). By using arguments (see Appendix 4-III) analogous to those which were used in Chapter 3 with respect to an NO_3^- ion in a 222 site, it can be shown that for Me_4N^+ in a $\bar{6}$ site a disordered structure in which the N atoms are not themselves disordered cannot be precisely correct. In performing their refinement thus, Morosin and Graeber fixed a parameter which they should have allowed to vary; the fact that they then obtained an unusual value for other parameters which they did allow to vary is therefore not necessarily significant.

The second caveat at page 155 concerned the positions of the H atoms in the room-temperature structure. The fact that these positions are not specified at all by Morosin and Graeber is scarcely surprising; H atom positions cannot be determined by the X-ray method at room temperature in a crystal containing large numbers of relatively highly diffracting atoms. It is, therefore, possible that there may be further disorder in the room temperature crystal arising from the positions

of the H atoms (or, to express it differently, from the orientations taken up by the CH_3 groups with respect to rotation about the N-C bonds), and that this disorder might be frozen out, at least partly, somewhere between room temperature and 0 K.

Now, the potential energy function for rotation of the CH_3 groups about the N-C bonds will contain a contribution from internal interactions within the ion comparable to those which inhibit internal rotation in the ethane molecule, and also a contribution from interactions with the $[nMnCl_3]^{n-}$ chains. This latter contribution may well be quite large, as is indicated by the C - Cl distances for the structure described in Section 4-4a. In that structure, there are C-Cl distances of between 3.6 and 3.8 Å, while the van der Waals radii of CH_3 and Cl^- are 2.0 and 1.8 Å. The potential energy functions for rotation of the methyl groups can therefore be reasonably expected to undergo a considerable change at 126 K when the NC_4 tetrahedra reorient themselves and the relative positions of the Me_4N^+ ions and the $[nMnCl_3]^{n-}$ chains undergo changes. The conclusion one can thus reach is that if there is disorder in the H atoms at room temperature, any ordering process as the crystal is cooled is likely to be linked with the ordering of the NC_4 tetrahedra. This immediately provides another possible explanation of the excess of the anomalous entropy gain over R ln 2, namely that the H atoms become ordered as the crystal is cooled, but that the process occurs at least partly in the same temperature range in which the NC_4 tetrahedra order, so as not to give rise to any distinguishable second anomaly.

A priori, it might be hoped that neutron diffraction on deuterated TMMC would throw some light on this possibility. The change of lattice parameters around 128 K for fully-deuterated TMMC was reported by Hutchings et al (1972), who however did not carry out a full study.

Their results do not correspond to those obtained by X-ray diffraction of undeuterated TMMC (Figure 4-11, page 158), except in respect of c and γ, as shown by the following table (which compares lattice parameters, say, 10 K on either side of the transition).

X-ray diffraction on undeuterated TMMC	neutron diffraction on fully deuterated TMMC
monoclinic a rather more than twice hexagonal a	monoclinic a almost the same as hexagonal a
monoclinic b rather less than hexagonal a	monoclinic b rather less than four times hexagonal a
monoclinic c about the same as hexagonal c	
monoclinic γ rather in excess of 120°	

The situation is evidently very complicated, and there appears to be no attempt in the literature to comment on or explain these differences. However, low temperature X-ray work and heat capacity measurements on deuterated TMMC might well clarify the situation greatly.

CHAPTER FIVE: PHTHALOCYANINES

Since the observation in 1928 of a dark blue insoluble compound (later identified as ferrous phthalocyanine) in an iron vessel used for the preparation of phthalimide, a large number of phthalocyanine compounds have been prepared and studied. Phthalocyanine compounds are of considerable commercial importance, especially copper phthalocyanine and its derivatives as pigments and dyes for plastics, paints, printing inks, and textiles.

The characteristic feature of the molecule of a phthalocyanine compound is the presence of a divalent unit $C_{32}H_{16}N_8$ (commonly abbreviated as "Pc") which consists, formally, of four isoindole molecules joined together in a ring, with loss each of three H atoms, via four additional N atoms. The structural formulae of the molecules of the three compounds (PcCu, PcNi, and PcH_2) with which this work is concerned are given in Figure 5-1. These molecules persist in the solid state, at least in the (well-defined) β-modifications.

Other types of phthalocyanines are represented by $PcLi_2$ and PcAlCl.

Many metal phthalocyanines may be prepared directly from phthalonitrile (or a closely related compound such as o-cyanobenzamide) - for example by the reaction

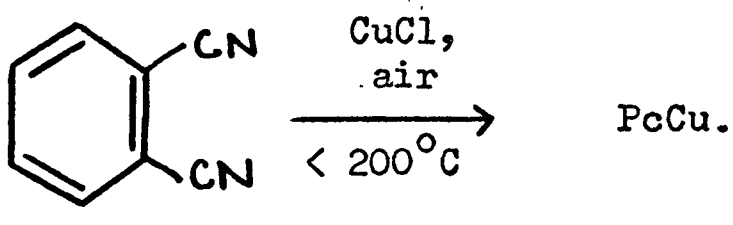

PcCu.

Metal-free phthalocyanine, PcH_2, may be prepared by demetallation of certain metal phthalocyanines, or directly -

FIGURE 5-1

(a)

copper phthalocyanine ("PcCu") for M=Cu;
nickel phthalocyanine ("PcNi") for M=Ni

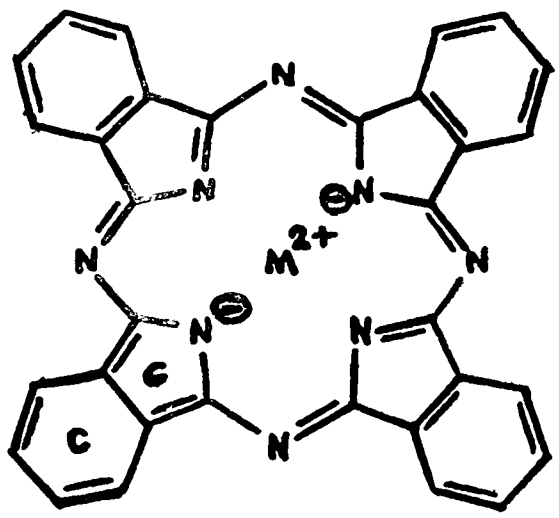

(b)

metal-free phthalocyanine ("PcH_2")

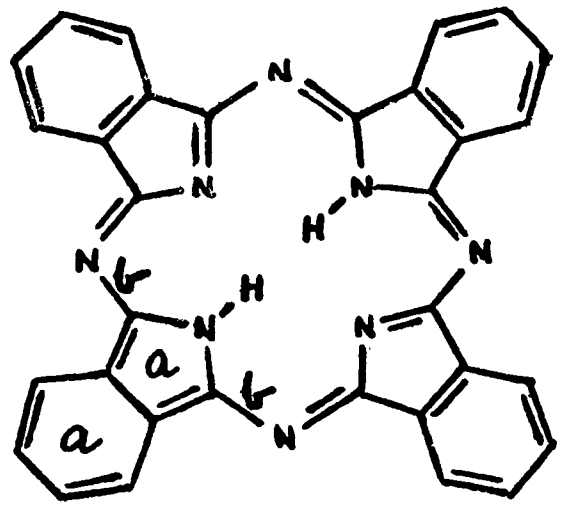

Caveat: see Section 5-4a for a discussion of the inadequacy of these formulae.

aa, bb, cc are reference letters used in Section 5-4a.

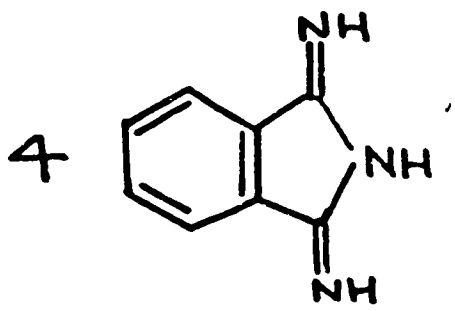

Polymorphism is common among the phthalocyanines, the polymorphs apparently differing in the ways in which the molecules are arranged relative to one another in the solid. However, many form a well-defined, stable "β-modification". The three materials with which the present work is concerned are the β-modifications of PcH_2, PcCu, and PcNi. Room-temperature X-ray diffraction studies have shown that the three crystals have the same space group, namely $P2_1/a$ (C_{2h}^5), and also closely similar lattice parameters and structures. The dimensions of the three (monoclinic) unit cells as quoted by Lever (1965) are -

	a/Å	b/Å	c/Å	β/°
β - PcH_2	19.85	4.72	14.8	122.2
β - PcCu	19.6	4.79	14.6	120.6
β - PcNi	19.9	4.71	14.9	121.9

Further general information is given in the reviews by Lever (1965) and Moser and Thomas (1963).

The immediate background to the present work is that about ten years ago Dr R.M. Clay of this laboratory measured heat capacities of β-PcCu and β-PcNi from about 5 K to about 80 K. He obtained rather complex results which will be discussed in detail later (Sections 5-2b onwards). The origin of the effects he observed was obscure, and therefore it was thought pertinent for the present author to determine the heat capacity of β-PcH_2 for comparison with those of β-PcCu and β-PcNi. It was hoped that comparison of the results for β-PcH_2 with those for the other two compounds would make more evident any heat capacity effects in those other compounds which were

associated with the presence of the transition metal ions (such as - see Section 1-3 - magnetic ordering effects or Schottky anomalies).*

Section 5-1: preparation and characterisation of β-PcH_2; further checks or comments on Dr Clay's samples of β-PcCu and β-PcNi

In 1967, this laboratory was supplied with unanalysed laboratory-prepared samples of PcCu, PcNi, and PcH_2 by Messrs Imperial Chemical Industries Limited. The PcCu and PcNi samples, without further purification or treatment, were used at that time for Dr Clay's calorimetric work; the PcH_2 sample was now (1973) used as the starting material for the preparation of the present calorimetric sample, and the PcCu and PcNi samples were rechecked. There was no evidence that any of the samples had deteriorated in the previous years (the phthalocyanine compounds generally are of remarkable stability).

The 1967 PcH_2 sample (which was a deep blue dull dust) was analysed for C, N, and H by the laboratory analytical service (see Appendix 5-I for a caveat on these analyses), with satisfactory results:-

	C	N	H
obs	74.6	21.9	3.5
calc $C_{32}H_{18}N_8$	74.70	21.78	3.53

However, this analysis could conceivably conceal the presence of impurities having similar C and N contents (such as phthalonitrile).

Some fresh commercial materials were considered as possible calorimetric samples, namely a free sample of ICI PcH_2 and a sample of PcZn bought from Eastman Kodak. In contrast with the 1967 PcH_2, they both gave unsatisfactory analyses, and the PcZn actually contained impurities visible to the naked eye. These samples were therefore rejected in favour of the reasonably pure 1967 PcH_2. This was

*The above account is included for the sake of historical accuracy. It will be seen in Section 5-4 that neither of these effects is likely to be of significance (evidence on this has accumulated since the present experimental work was performed), and that analysis of the results led in somewhat unexpected directions.

a pity, for the quantity of the latter was rather small; a larger sample would have made for more accurate calorimetry, especially above 30 K, where the contribution of the sample to the total measured heat capacity was less than 40 per cent (see Section 5-2a). Further, β-PcZn would itself have been a valuable comparison substance for β-PcCu and β-PcNi.

An X-ray powder photograph of the 1967 PcH_2 was taken (see Plate 5-I(a)). The lines observed were weak and rather fuzzy, indicating that the sample was not highly crystalline. This conformed with the dull dust-like appearance of the sample. Furthermore, the positions of the observed lines indicated that the sample contained little, if any, of the desired β-modification.

Karasek and Decius (1952) state that German scientists discovered (during World War II) that an α-β phase transition occurs for metal-free and copper phthalocyanine above 200°C, "α" being one of the less stable, less well-characterised modifications. Accordingly, a method of converting the sample into the desired β-modification by heating in vacuo was investigated and used. The calorimetric sample consisted of three batches of β-modification prepared as follows:-

> From 2 to 5 g of the 1967 sample of metal-free phthalocyanine was put into a 10 cm-long alumina boat, which was then inserted into a silica furnace tube about 50 cm long. The tube was connected to a vacuum line and enclosed by an electric furnace. The tube was evacuated (very carefully because of the dustlike nature of the sample) with a rotary pump and liquid nitrogen trap. The tube was then isolated from the pump and trap. The furnace was made to warm up slowly, over about four hours, during which time the tube was periodically reconnected to the pump and trap to remove any vapours evolved. Then the furnace

PLATE 5-I

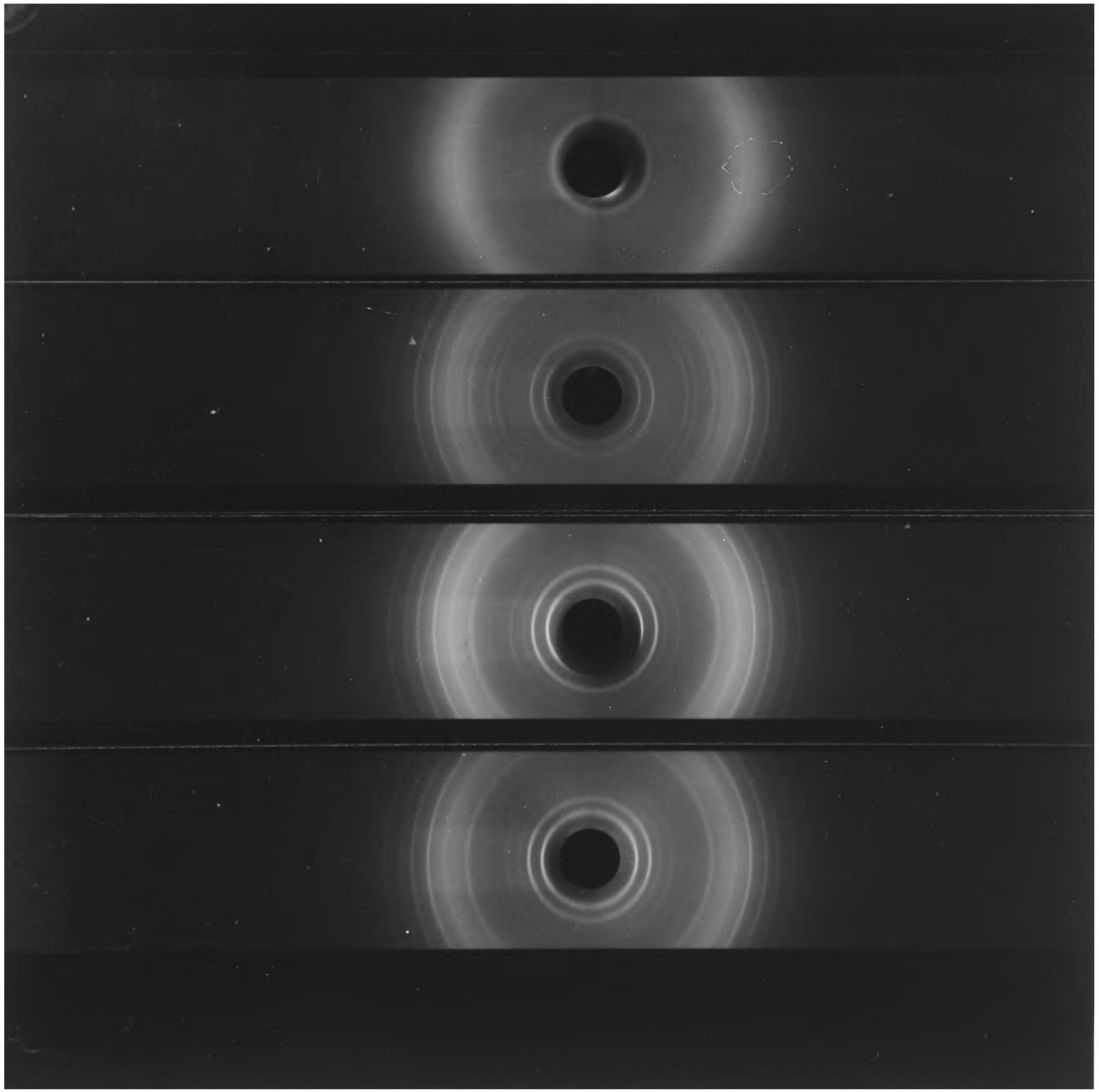

(a)
PcH_2, before heat treatment

(b)
PcH_2, after heat treatment at 310°C - 385°C approx. in vacuo (β-phase)

(c)
β-PcCu

(d)
β-PcNi

Debye-Scherrer photographs.
Camera: 11.46 cm dia.
Line x mm away from straight-through position corresponds to $2\theta = x^{\circ}$.
Film mounting: Straumanis method.
Radiation: CuKα, Ni filter.

Note that the innermost four lines visible in (b) all have counterparts in (c) and (d) but with greatly changed relative intensities. Note that the third and fourth innermost lines of (c) and (d) (200 and $20\bar{2}$ reflections) should in principle occur in (b), but are in fact too weak to be seen.

current was controlled automatically so as to maintain, for a period of at least four hours, a temperature which, measured immediately outside the silica tube, was within the range 310°C to 385°C over the whole length of the boat, the maximum temperature being in the middle of the boat. The furnace was allowed to cool, and the silica tube was removed from the furnace. In what had been the cooler parts of the tube to either side of the boat, there were successive zones of purple, blue, brown, yellow, and white deposits on the silica. The first two zones were presumably of sublimed phthalocyanine and the other zones may have been of sublimed, perhaps decomposed, impurities. The loss in weight of the sample during this treatment was about five per cent.

Each of the three batches thus prepared were noticeably more crystalline in appearance than the starting material, the individual particles (although still very small) being lustrous rather than dull. X-ray powder diffraction photography (see Plate 5-I(b)) showed that a phase change had indeed occurred in each batch. Samples taken from different parts of the boat gave identical diffraction patterns. The diffraction lines were measured up; they agreed with the results for β-PcH_2 of Karasek and Decius (1952), who also used a powder diffraction method, and they could be indexed on the unit cell determined by single crystal work (and given at page 177). See Table 5-1.

The analyses of the three batches were satisfactory:-

Batch no.	C	N	H
1 obs	74.5	21.9	3.6
2 obs	74.5	21.9	3.6
3 obs	74.5	22.0	3.5
calc $C_{32}H_{18}N_8$	74.70	21.78	3.53

TABLE 5-1

Listing of lines in X-ray powder diffraction photograph of β-PcH_2 and their assignment.

Camera: 11.46 cm dia

Film mounting: Straumanis method

Calibration: none, each line x mm away from straight-through position taken to correspond to $2\theta = x^{\circ}$

Radiation: Cu Kα (λ = 1.54178 Å), Ni filter

Exposure: 17 hours

present photograph		powder diffraction data of Karasek and Decius (1952)		calculated on basis of the unit cell dimensions given at page 177+			
intensity	d_{hkl}/Å	intensity*	d_{hkl}/Å	d_{hkl}/Å	h	k	l
VS	12.5	VS	12.4	12.52	0	0	1
VS	9.80	S	9.78	9.80	2	0	$\bar{1}$
M	6.29	VS	6.24	6.26	0	0	2
M	5.73	S	5.69	5.71	2	0	1
MS	4.89	S	4.91	4.93	2	0	$\bar{3}$
				4.90	4	0	2
MW	4.54	W	4.54	4.54	1	1	0
W	4.31	W	4.32	4.33	4	0	$\bar{3}$
MW	4.13	W	4.16	4.17	0	0	3
				4.11	2	1	0
VW	3.95	VW	3.96	3.96	1	1	$\bar{2}$
				3.94	2	1	2
VS	3.72	M	3.76	3.77	0	1	2
				3.73	3	1	2
S	3.39	M	3.41	3.41	2	1	$\bar{3}$
				3.40	4	1	2
				3.38	4	1	1
M	3.19	MW	3.18	3.19	4	1	$\bar{3}$
				3.19	3	1	1
VW	3.11	-	-	3.11	6	0	$\bar{1}$
M	2.95	MW	2.95	2.95	5	1	$\bar{1}$
				2.95	4	0	5
				2.95	5	1	3

S = strong, M = medium, W = weak, V = very

*The intensities are not given in this form by Karasek and Decius; the values given were estimated by the present author from their diffractometer trace.

+Extinctions for $P2_1/a$ (b axis unique) are h0l for h odd
0k0 for k odd

Finally, some further checks were made on the samples of PcCu and PcNi which Dr Clay had used.

The β-PcCu had been analysed for Cu in 1967 by a $KI/Na_2S_2O_3$ method. The results of two determinations were 10.52% Cu and 10.62% Cu, compared with the theoretical value of 11.03% Cu for $C_{32}H_{16}N_8Cu$. In 1973, an atomic absorption method gave results of 10.51% and 10.56%, in good agreement with the earlier results.

C, N, H analysis gave the following results:

	C	N	H
obs	66.2	20.1	2.8
calc $C_{32}H_{16}N_8Cu$	66.71	19.46	2.80

The copper analysis suggests the presence of some non-copper-containing contaminant. ICI suggested that this could possibly be phthalonitrile.* The C, N, H analysis suggests a contaminant with a lower C : N ratio than phthalonitrile.

Dr Clay's PcNi sample had been analysed in 1967 for Ni with EDTA and bromopyrogallol red. Two determinations gave respectively 10.00% Ni and 10.22% Ni, compared with 10.28% Ni calculated for $C_{32}H_{16}N_8Ni$. No further analyses were now performed.

As for the modification of the PcCu and PcNi samples, it was first noted that the PcNi was in the form of lustrous small deep purple crystals, while the PcCu was deep blue and more dust-like. Dr Clay had demonstrated that the samples were β-phase by recording their infra-red spectra in nujol mulls and comparing these spectra with those reported by Ebert and Gottlieb (1952). By way of a further (and more reliable) check, the X-ray powder diffraction patterns

---

*This was no more than a suggestion, for the relevant records were not available.

were now recorded - see Plate 5-I(c) and (d). The patterns of the β-PcCu and β-PcNi samples are strikingly similar to one another, as one would expect in view of the close similarity of the reported lattice parameters (see page 177), and in view of the close similarity of the diffracting powers of Cu and Ni. The positions of the lines correspond to those in β-PcH_2, which has similar lattice parameters, but the relative intensities of the lines are very different, because of the large diffracting power of Cu or Ni compared with 2H.

Section 5-2: heat capacity results

a. results in the new calorimeter on β-PcH_2

The three batches of β-phase metal-free phthalocyanine ("β-PcH_2") prepared as described in Section 5-1 were loaded into the new calorimeter described in Chapter 2. The sample was so light and fine that it required extreme care to evacuate the vessel without sucking it into the vacuum line.

The heat capacity results are listed in Table 5-2 below. No useful measurements were made in the 1.4 K to 2.8 K region because of erratic drifts, the vessel warming (once the thermal switch was opened) despite being surrounded by a shield at about 1.4 K. This was probably due to the vibration discussed at page 73, and contrasts with the satisfactory performance in the run on bis(adiponitrile)copper(I) nitrate. The vessel in the present case had not been strung up so tightly, so that it vibrated with relatively low frequency. Even at 2.4 K, the vessel was warming at almost 10 mK min^{-1}, corresponding to an excess of the vibrational power generation over heat loss by conduction of about 5×10^{-5} J min^{-1}. From 3.5 K to 4.5 K the drifts were negative (with the shield at 1.4 K), but still somewhat erratic. Above 4.5 K no such effect was observable, but the equilibrium times

TABLE 5-2

Heat capacity results with β-PcH_2 in the new calorimeter

Weights, etc. (see Section 2-9d for the meanings of the symbols):-

n_{sample} = 0.016 95(1 1)mol

$n_{exch.\ gas}$ = 1.450×10^{-5} mol of He^3

$\Delta m_{elecsol}$ = +0.169 17 g

Δm_{indsol} = −0.119 82 g

Δm_{Ag} = −0.036 42 g

($C_{32}H_{18}N_8$ = 514.55(2); density for buoyancy correction and calculation of $n_{exch.\ gas}$ taken as 1.44 g cm^{-3}.)

T_{MID}/K	ΔT/K	$\overline{C_{p,m}}$/$JK^{-1}mol^{-1}$	% of total measured C_p due to sample	notes
2.931	0.267	0.133	29	A*
3.277	0.284	0.235	38	A*
3.606	0.335	0.241	34	A*
3.916	0.367	0.242	31	A*
4.194	0.358	0.402	40	A*
4.538	0.486	0.691	50	A^+
5.065	0.713	0.933	51	A^+
5.798	0.993	1.494	56	A^+
6.994	0.845	2.587	59	Al^+
7.986	1.261	3.837	60	Al^+
9.288	1.463	5.444	59	Al
10.792	1.681	7.881	59	Al
12.364	1.578	10.98	58	Al
13.860	1.562	13.59	56	Al
15.672	2.306	15.64	52	Al
17.849	2.103	19.95	50	Al
19.932	2.152	24.19	47	Al
22.298	2.762	28.84	45	Al
24.597	2.129	33.86	43	Al
27.145	2.968	38.94	40	Al
29.830	2.416	45.21	38	Al
32.435	2.803	51.33	37	Al
35.309	2.945	58.21	36	Al

TABLE 5-2 (cont.)

T_{MID}/K	ΔT/K	$\overline{C_{p,m}}$/$JK^{-1}mol^{-1}$	% of total measured $\overline{C_p}$ due to sample	notes
38.244	2.926	65.37	34	A1
41.258	3.101	71.72	33	A1
44.553	3.488	81.04	33	A1
48.082	3.570	87.95	32	A1
50.165	4.633	94.29	32	B
51.565	3.396	98.62	32	A1
54.064	3.163	103.0	31	B
57.315	3.340	110.1	31	B
60.737	3.503	117.3	30	B
64.316	3.662	123.7	30	B
68.059	3.824	131.1	30	B
71.863	3.786	139.9	30	B
75.032	2.551	147.1	30	B
79.897	7.179	159.5	30	B

Determinations B were made with liquid nitrogen refrigerant according to scheme (g) in Figure 2-13, page 68.

Determinations A were performed with liquid helium refrigerant roughly according to scheme (b) in Figure 2-13; and determinations A1 were made with the same charge of liquid helium refrigerant after an overnight stand, roughly according to schemes (c) to (f) in Figure 2-13. Between the last of determinations B and the beginning of determinations A (about 36 hours) the temperature of the sample did not rise above about 83 K, and the minimum temperature reached by the sample before determinations A was about 1.5 K.

* indicates determinations of doubtful accuracy because of vibration.

+ indicates determinations where equilibrium time after heating period was long (> 15 minutes).

No curvature corrections were made, because either the accuracy of the determinations or the form of the $\overline{C_{p,m}}$ - T plot made such corrections not worthwhile.

were curiously long (15 - 30 minutes) over the temperature range 4.5 K to 9 K.

Therefore, the accuracy of the results below 9 K may be below that of which the apparatus was capable in more favourable circumstances, either because of the erratic drifts (below 4.5 K), or because of the long extrapolations (necessary from 4.5 K to 9 K). While the difficulty below 4.5 K was a matter of operating procedure, that from 4.5 K to 9 K may have been intrinsic to the sample, and will be discussed in Section 5-3e.

Section 5-2b: Dr Clay's results on β-PcCu and β-PcNi

The results obtained by Dr Clay on β-PcCu and β-PcNi have not been previously published in any form, and are given in Tables 5-3 and 5-4 respectively. The calorimeter he used is described in Clay (1965); it should be noted that the germanium resistance thermometer was identical with that in the new calorimeter.

Perhaps the most remarkable feature of Dr Clay's work was his discovery that first-order (or partly first-order) transitions appear to occur in β-PcCu. These manifested themselves (for reasons described more fully later) in determinations in which, after the heat input, the sample began to cool and eventually finished at a lower temperature than that prevailing before the heat input. The ΔT values and, formally, the $\overline{C_{p,m}}$ values are then negative, and are recorded as such in Table 5-3 so as to give an idea of the energies involved and of the observed temperature drops. Equilibrium times after such points were long (15 - 30 minutes). If such negative $\overline{C_{p,m}}$ values are ignored, $\overline{C_{p,m}}$ rises fairly smoothly with T (see Figures 5-2, 5-4, and 5-5 at pages 195, 197, and 198).

Dr Clay observed no negative $\overline{C_{p,m}}$ values in his first liquid He run (4.2 - 20 K for him, as he used liquid H_2 for 20 - 84 K), but

TABLE 5-3

Dr Clay's results on β-PcCu

/Private communication; units converted, and results with negative $\overline{C}_{p,m}$ values recalculated./

Calorimetric sample: 0.02576 mol. Exchange gas He^4.

T_{MID}/K	ΔT/K	$\overline{C}_{p,m}$/$JK^{-1}mol^{-1}$	refrigerant (and run number if repeated)
21.12	1.387	26.32	H_2
22.66	1.697	29.20	H_2
24.70	2.397	33.26	H_2
26.92	2.048	37.99	H_2
29.48	3.063	43.51	H_2
32.51	2.998	50.00	H_2
35.59	3.189	56.82	H_2
38.82	3.259	63.81	H_2
42.57	4.245	71.25	H_2
46.79	4.202	80.83	H_2
50.91	4.071	89.29	H_2
55.58	5.269	100.3	H_2
60.59	4.749	110.4	H_2
65.79	5.638	119.5	H_2
71.17	5.132	129.9	H_2
76.37	5.267	140.4	H_2
81.48	4.956	150.0	H_2
5.13	0.573	1.125	He(1)
5.67	0.660	1.498	He(1)
6.29	0.761	2.096	He(1)
7.06	0.908	2.937	He(1)
8.00	1.107	4.171	He(1)
9.15	1.384	5.519	He(1)
10.54	1.597	7.740	He(1)
12.12	1.692	10.71	He(1)
13.56	1.327	13.43	He(1)
15.10	1.873	15.52	He(1)
17.19	2.394	19.16	He(1)
19.62	2.568	24.02	He(1)
22.15	2.619	28.58	He(1)

TABLE 5-3 (cont.)

T_{MID}/K	ΔT/K	$\overline{C_{p,m}}$/$JK^{-1}mol^{-1}$	refrigerant (and run number if repeated)
4.66	0.443	0.841	He(2)
5.30	0.977	1.276	He(2)
6.18	1.117	1.974	He(2)
7.19	1.522	2.954	He(2)
8.13	1.094	4.154	He(2)
9.20	1.781	5.52	He(2)
10.27	1.313	7.57	He(2)
11.21	1.562	9.37	He(2)
11.16	-0.238	-112.7	He(2)
12.00	2.334	10.88	He(2)
14.37	2.611	14.73	He(2)
15.01	-0.931	-79.64	He(2)
16.10	3.513	17.15	He(2)
19.26	2.868	23.26	He(2)
8.85	2.036	5.02	He(3)
10.44	1.779	6.99	He(3)
9.97	-1.295	-22.09	He(3)
10.62	2.820	8.03	He(3)
12.86	1.819	12.26	He(3)
13.16	-0.942	-85.06	He(3) [combination of two determinations]
14.03	2.874	13.97	He(3)
16.77	2.748	18.37	He(3)
18.55	0.938	21.76	He(3)

Dr Clay used adiabatic shield control when liquid H_2 was the refrigerant, but left the shield at 4.2 K when liquid ^{2}He was used as the refrigerant. The determinations are listed above in chronological order; beyond this, details of thermal history of the sample are not available.

TABLE 5-4

Dr Clay's results on β-PcNi

[Private communication; units converted.]

Calorimetric sample: 0.01964 mol. Exchange gas He^4.

T_{MID}/K	ΔT/K	$\overline{C_{p,m}}$/$JK^{-1}mol^{-1}$	refrigerant (and run number if repeated)
21.35	1.908	29.16	H_2
23.21	1.813	32.55	H_2
25.08	1.925	36.40	H_2
27.04	2.009	40.46	H_2
29.64	3.189	45.98	H_2
32.84	3.213	52.80	H_2
35.95	3.001	59.60	H_2
38.89	2.872	65.56	H_2
42.29	3.915	71.96	H_2
46.19	3.894	81.09	H_2
50.11	3.947	88.37	H_2
54.61	5.052	99.41	H_2
59.69	5.101	108.4	H_2
64.80	5.114	116.7	H_2
69.88	5.043	127.6	H_2
74.96	5.136	136.4	H_2
80.17	5.266	143.9	H_2
4.49	0.446	1.029	He(1)
4.91	0.450	1.351	He(1)
5.36	0.584	1.753	He(1)
5.90	0.663	2.259	He(1)
6.60	0.949	3.134	He(1)
7.47	0.979	4.088	He(1)
8.31	1.013	5.15	He(1)
9.18	1.044	6.19	He(1)
10.15	1.214	7.87	He(1)
11.26	1.308	10.13	He(1)
12.37	1.209	12.76	He(1)
13.75	1.694	15.69	He(1)
15.38	1.676	17.74	He(1)
17.21	2.103	21.51	He(1)

TABLE 5-4 (cont.)

T_{MID}/K	ΔT/K	$\overline{C_{p,m}}$/$JK^{-1}mol^{-1}$	refrigerant (and run number if repeated)
19.24	2.059	25.61	He(1)
21.33	2.265	29.33	He(1)
4.75	1.027	1.276	He(2)
5.76	1.118	2.184	He(2)
6.74	1.046	3.301	He(2)
7.86	1.454	4.81	He(2)
9.13	1.409	6.28	He(2)
10.53	1.725	9.12	He(2)
12.14	1.718	12.22	He(2)
13.62	1.399	15.15	He(2)
14.99	1.484	17.20	He(2)
16.73	2.169	20.13	He(2)
18.73	2.003	24.69	He(2)
20.73	2.158	28.12	He(2)

Dr Clay used adiabatic shield control when liquid H_2 was used as the refrigerant, but left the shield at 4.1 K when liquid He was used as the refrigerant. The measurements are listed above in chronological order; beyond this, details of the thermal history of the sample are not available.

observed two such values in each of his second and third runs, though at different temperatures.

Negative $\overline{C_{p,m}}$ values are consistent with the occurrence of a first-order phase transition at which there is superheating. (Superheating is very often associated with a first-order phase transition, but not with a wholly gradual transition.) The $\overline{C_{p,m}}$ values to either side of the negative values are apparently not abnormally high, and therefore it can be reasonably supposed that, at the end of the determination giving the negative $\overline{C_{p,m}}$ value, all of the sample is in the high temperature form. In that case, the enthalpy change associated with the transition from the low to the high temperature form, ΔH_m, is given by

$$\overline{C_{p,m}} \times \Delta T = \Delta H_m + \overline{C_{p,m}}' \times \Delta T$$

where $\overline{C_{p,m}}$ and ΔT have the signs given in Table 5-3 and $\overline{C_{p,m}}'$ is the "normal" value of $\overline{C_{p,m}}$ at T_{MID} obtained by smoothing the adjacent "normal" values.

The final extrapolated temperature ($T_{MID} + \Delta T/2$, where ΔT is negative) will probably be greater than the equilibrium transition temperature*, and therefore the molar entropy change for the transition ΔS_m is at least $\Delta H_m/(T_{MID} + \Delta T/2)$.

Estimates of ΔH_m and ΔS_m thus calculated are given in Table 5-5. In view of the long extrapolations necessary in the calculation of the negative $\overline{C_{p,m}}$ values, these estimates are crude; but it is quite clear that the anomalies observed in the $\overline{C_{p,m}}$ of β-PcCu are quite massive in entropy terms.

---

*That this is the case can be seen if the various possible temperature-time plots are drawn, it being remembered that the shield is at lower temperature than the vessel at all times, and further that the actual process of conversion of low to high temperature form can occur only at or above the equilibrium transition temperature. (There is implicit in this approach, however, the approximation that the temperature over the sample and vessel is uniform.)

TABLE 5-5

"Transitions" in β-PcCu

run	(T + ΔT/2)/K	$\frac{\Delta H_m}{J\ mol^{-1}}$	$\frac{\Delta S_m}{JK^{-1}mol^{-1}}$	
He(2)	11.04	29.0	> 2.63	> 8.69
He(2)	14.54	88.6	> 6.09	
He(3)	9.32	37.6	> 4.03	> 11.29
He(3)	12.69	92.1	> 7.26	

Compare R ln 2 = 5.76 J $K^{-1}mol^{-1}$
R ln 3 = 9.13 J $K^{-1}mol^{-1}$
R ln 4 =11.52 J $K^{-1}mol^{-1}$

* * *

The results for β-PcNi included no negative $\overline{C_{p,m}}$ values, and no exceptionally long equilibrium times were observed.

Section 5-2c: numerical and graphical comparison of results for β-PcH_2, β-PcCu, and β-PcNi

The heat capacities of the three solids can be compared directly in Table 5-6, which gives smoothed values for various temperatures. In the case of β-PcCu the negative $\overline{C_{p,m}}$ values were excluded from the smoothing. Experimental and smoothed results are also presented graphically in Figures 5-2 to 5-5.

TABLE 5-6

Smoothed heat capacity results for β-PcCu, β-PcNi, and β-PcH_2.

T/K	molar heat capacity/J $K^{-1}mol^{-1}$ (smoothed) β-PcCu	β-PcNi	β-PcH_2
5	1.042	1.423	0.929
6	1.799	2.402	1.619
7	2.753	3.523	2.584
8	3.891	4.73	3.85
9	5.31	6.07	5.06
10	7.03	7.66	6.54
11	8.83	9.54	8.23
12	10.75	11.92	10.21
13	12.47	13.97	12.10
14	14.06	15.73	13.74
15	15.52	17.20	14.89
16	17.11	18.83	16.20
17	18.87	20.96	18.17
18	20.71	23.10	20.10
19	22.59	25.15	22.20
20	24.52	26.99	24.22
22	28.20	30.33	28.36
24	32.13	34.14	32.46
26	36.07	38.28	36.63
28	40.29	42.51	41.00
30	44.56	46.69	45.48
35	55.44	57.32	57.42
40	66.11	67.57	69.40
45	76.99	78.24	81.60
50	87.86	88.70	93.80
55	98.74	98.95	105.64
60	108.78	108.78	115.62
65	118.6	118.0	125.3
70	128.1	127.0	135.7
75	137.6	135.9	147.5
80	147.0	144.8	159.6

FIGURE 5-2

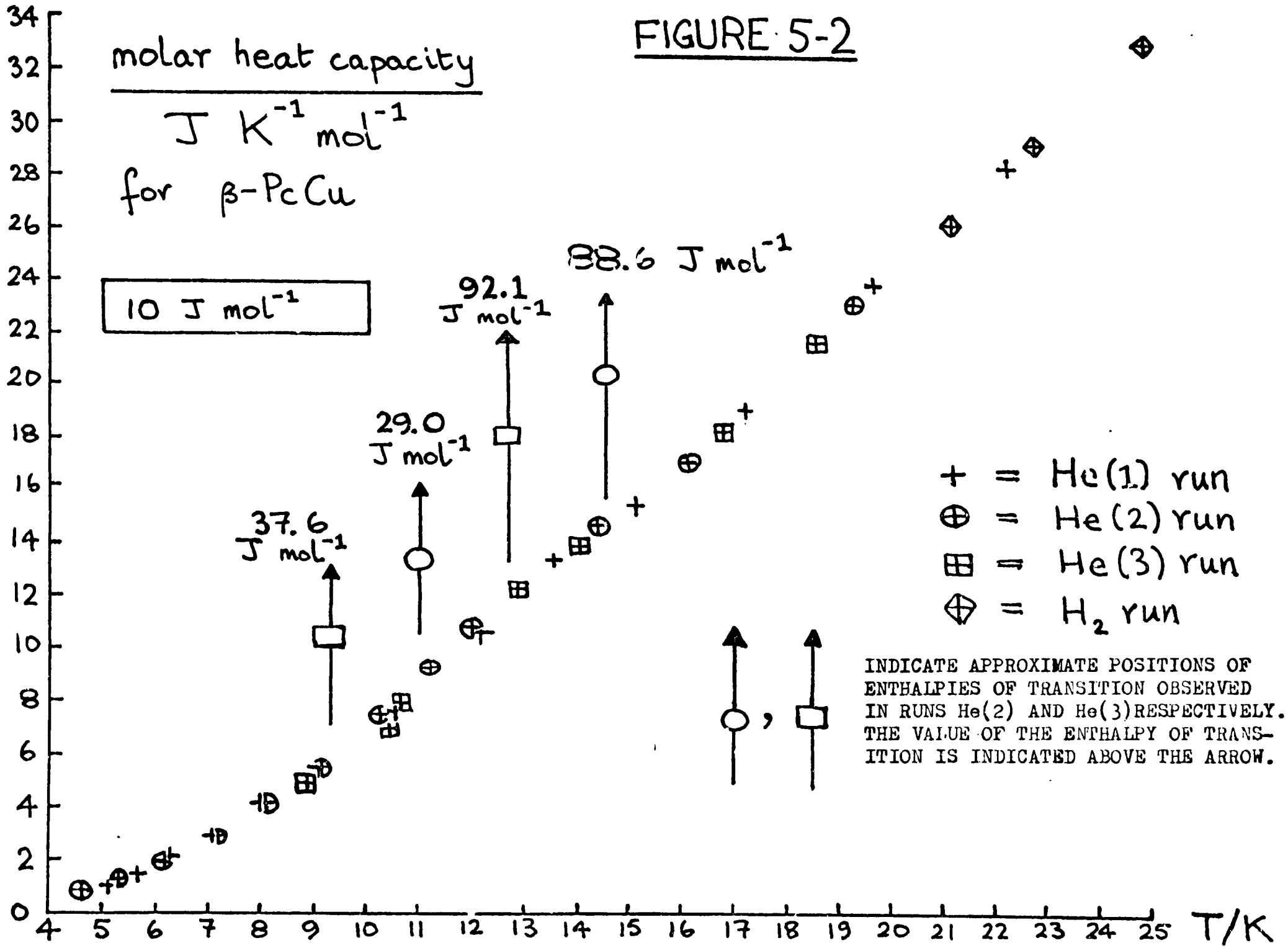
molar heat capacity
J K⁻¹ mol⁻¹
for β-PcCu
10 J mol⁻¹
92.1 J mol⁻¹
38.6 J mol⁻¹
29.0 J mol⁻¹
37.6 J mol⁻¹
+ = He(1) run
⊕ = He(2) run
⊞ = He(3) run
⊕ = H₂ run
INDICATE APPROXIMATE POSITIONS OF ENTHALPIES OF TRANSITION OBSERVED IN RUNS He(2) AND He(3) RESPECTIVELY. THE VALUE OF THE ENTHALPY OF TRANSITION IS INDICATED ABOVE THE ARROW.
T/K

FIGURE 5-3

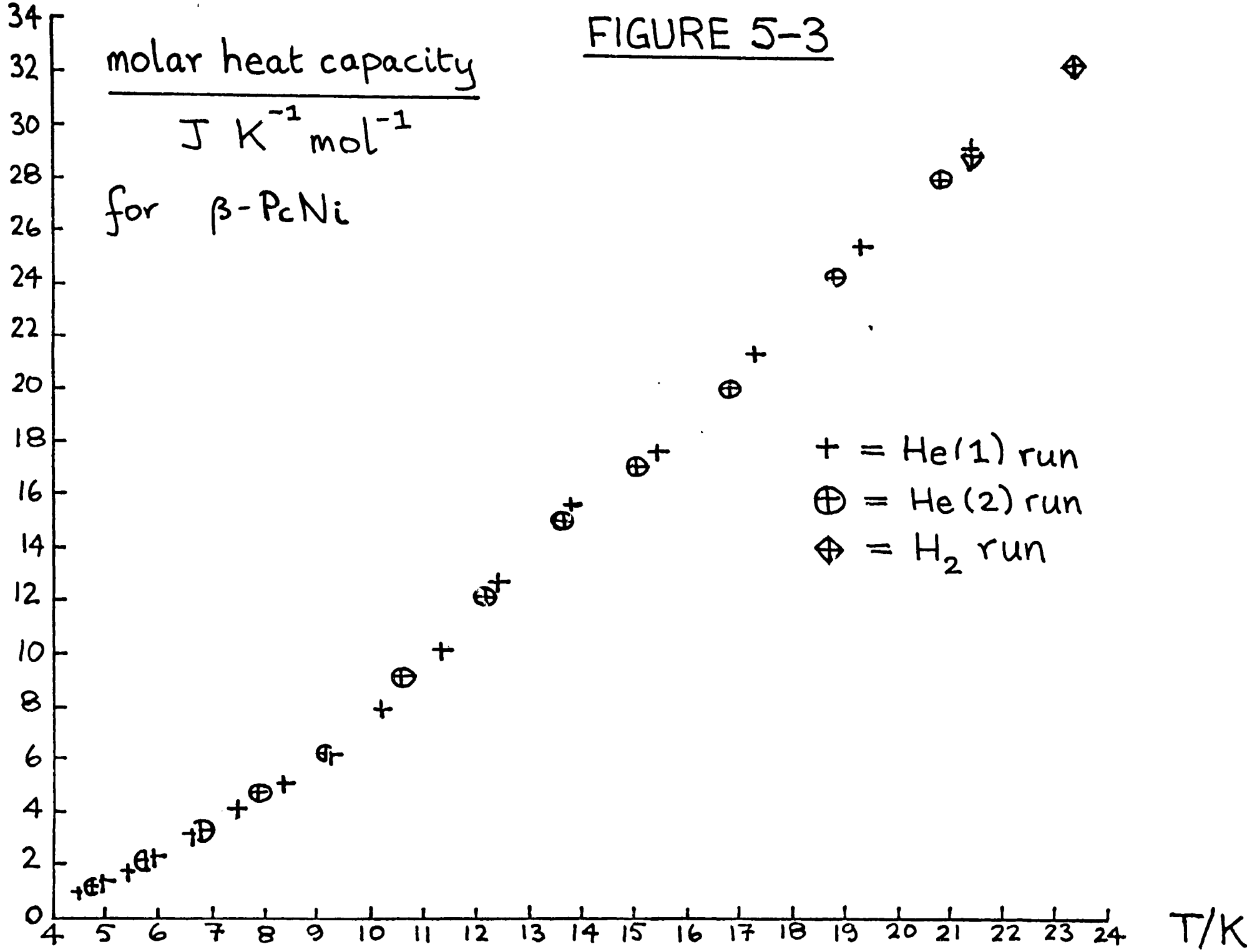
molar heat capacity
J K⁻¹ mol⁻¹
for β-PcNi
+ = He(1) run
⊕ = He(2) run
⊕ = H₂ run
T/K
0
2
4
6
8
10
12
14
16
18
20
22
24
26
28
30
32
34
4
5
6
7
8
9
10
11
12
13
14
15
16
17
18
19
20
21
22
23
24

FIGURE 5-4

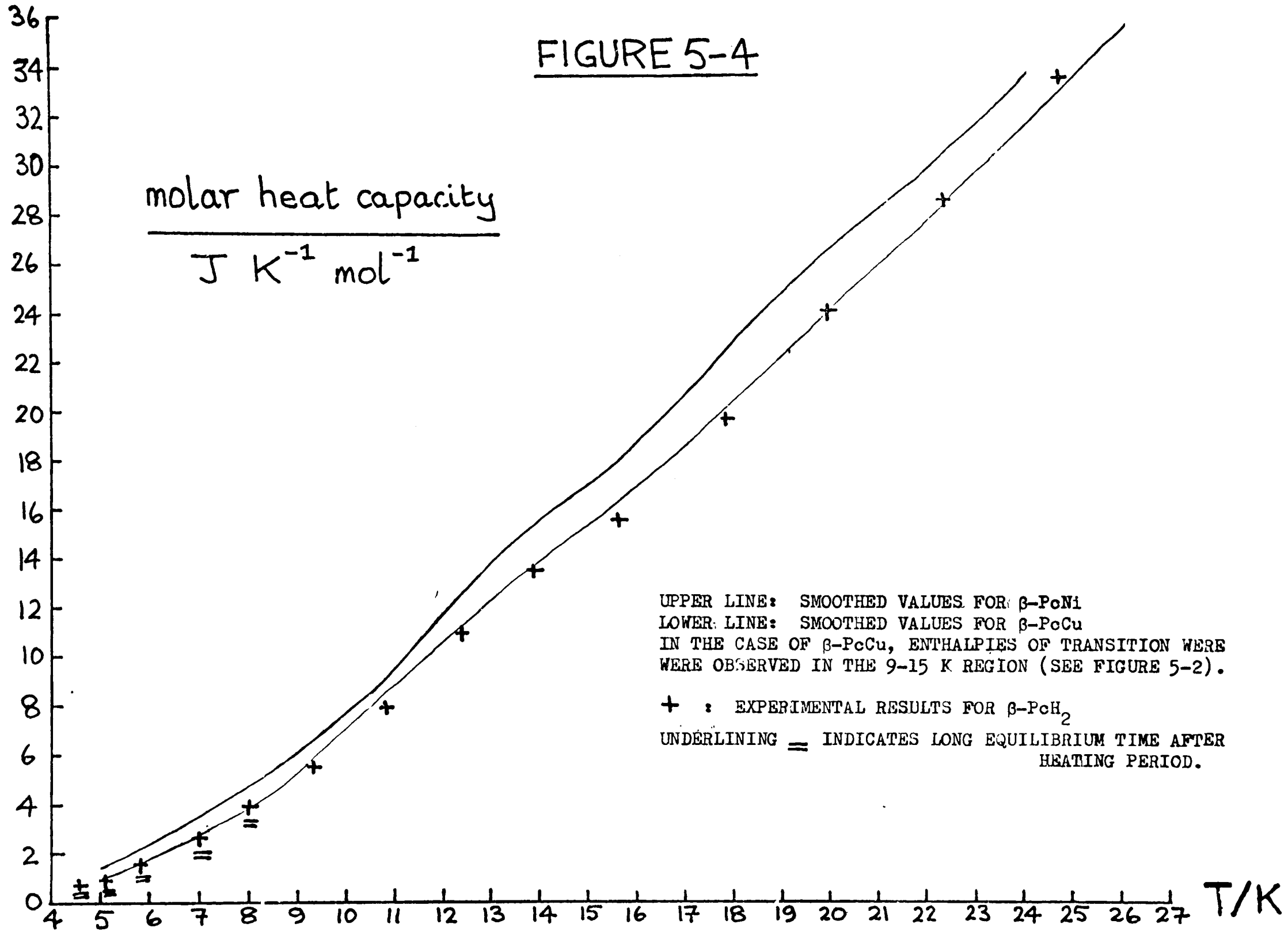
molar heat capacity
J K⁻¹ mol⁻¹
T/K
UPPER LINE: SMOOTHED VALUES FOR β-PcNi
LOWER LINE: SMOOTHED VALUES FOR β-PcCu
IN THE CASE OF β-PcCu, ENTHALPIES OF TRANSITION WERE WERE OBSERVED IN THE 9-15 K REGION (SEE FIGURE 5-2).
+ : EXPERIMENTAL RESULTS FOR β-PcH2
UNDERLINING = INDICATES LONG EQUILIBRIUM TIME AFTER HEATING PERIOD.

FIGURE 5-5

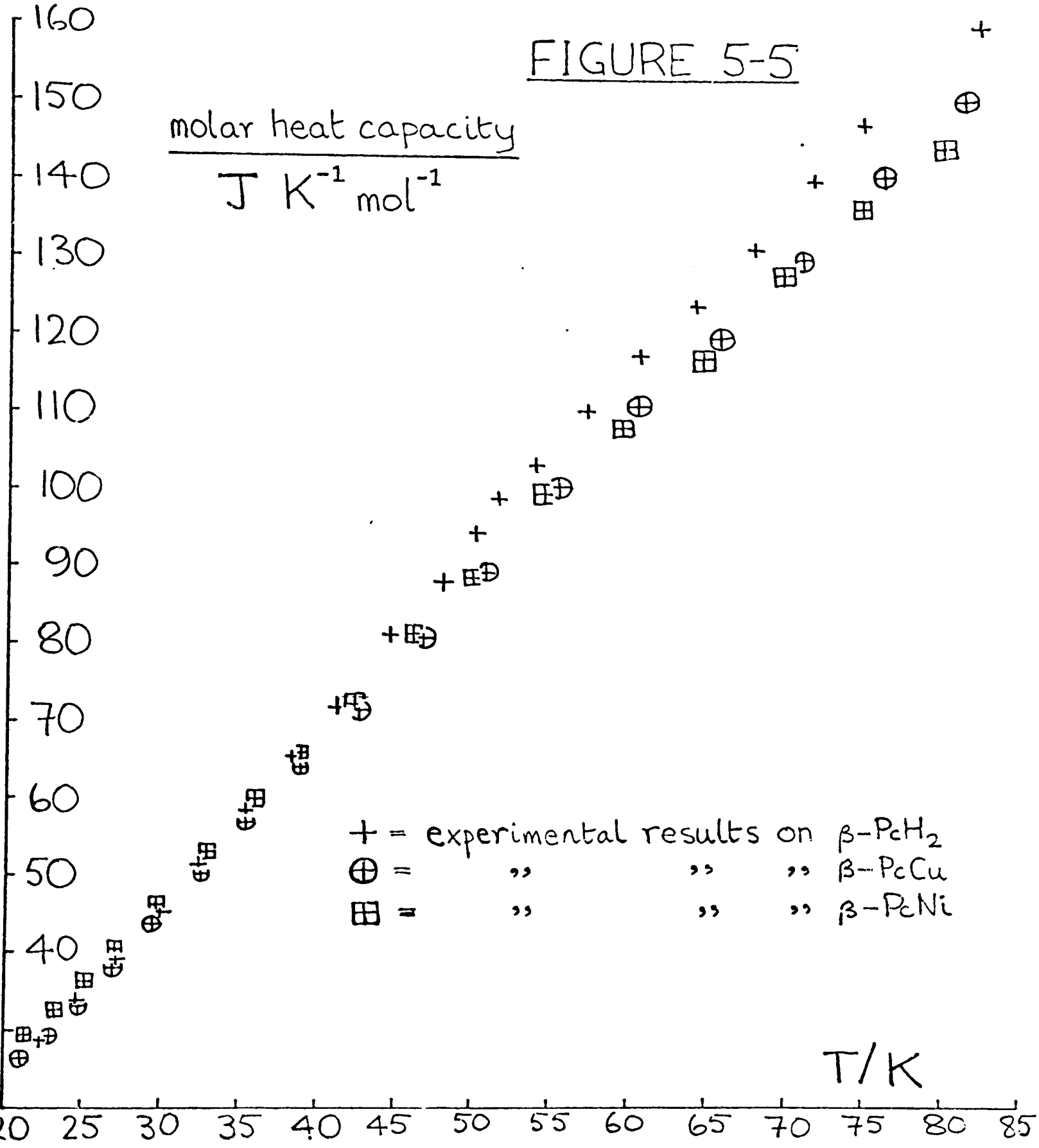
molar heat capacity
J K⁻¹ mol⁻¹
160
150
140
130
120
110
100
90
80
70
60
50
40
+ = experimental results on β-PcH2
⊕ = " " " β-PcCu
⊞ = " " " β-PcNi
T/K
20 25 30 35 40 45 50 55 60 65 70 75 80 85

Preliminary note to the remainder of this chapter

Section 5-3 will set out in a mainly descriptive (rather than interpretative) manner the features of the heat capacity results for the three materials (β-PcCu, β-PcNi, and β-PcH_2) which one would hope eventually to "explain" - i.e. to correlate with what is known, from other work on these materials, of their structure and other properties.

Section 5-4a will provide detailed information on the structures of the three materials as a preliminary to Sections 5-4b to 5-4e, which will deal with various factors which, a priori, seem to be of possible relevance to an explanation of the heat capacity features. It may as well be stated now, at the outset, that the present author does not claim to have positively identified all the factors which are in fact of relevance. However, it will be seen that it is possible to eliminate some factors from further consideration with fair certainty, even on the evidence presently available. Some tentative but more positive suggestions are made, and it is hoped that these could at least stimulate further work.

Much of the discussion will relate to the materials β-PcCu and β-PcNi, the heat capacities of which were determined (see Section 5-2b), not by the present author, but by Dr R.M. Clay in 1967; the present author's heat capacity determinations on β-PcH_2 were always intended to provide a comparison rather than to provide results of intrinsic interest. However, it should be stated that the discussion of the β-PcCu and β-PcNi results is essentially original; in particular, Dr Clay was unable (in the time available to him and with the state of knowledge of these compounds in 1967) to provide an explanation of his results which could be re-used here.

Section 5-3: mainly descriptive comments on the heat capacity results

a. results below 25 K, general comments

Figure 5-4 (page 197) displays the very marked differences between the heat capacities of the three materials in the temperature range below 25 K.

If one compares the β-PcCu and β-PcNi results, it is particularly noticeable that the heat capacity of β-PcCu lies very substantially lower than that of β-PcNi, but that, superimposed upon this lower heat capacity curve, there are latent heats which are not always observed but which are very large though of varying size. (These latent heats will be further discussed in Section 5-3d.)

The heat capacity - temperature plot for β-PcNi displays two broad "humps" centred, respectively, at about 13 K and at about 19 K, whereas only one such hump occurs for β-PcCu, centred at about 12 K.

On the other hand, the heat capacities of β-PcH_2 and β-PcCu are (the latent heats of the latter apart) rather similar in form below 25 K in that they each display a single hump centred at about 12 K. However, the heat capacity of β-PcCu is somewhat higher that that of β-PcH_2 below about 21 K, while the β-PcH_2 heat capacity is the higher above about 21 K.

Section 5-3b: trial of the Debye T^3 law at low temperatures

The Debye model predicts that, at low enough temperatures, a material having a purely vibrational heat capacity will have a heat capacity proportional to the cube of the absolute temperature (see pages 6 to 7). Therefore, $C_{p,m}/T^3$ was calculated for every available determination below 13 K except for those affected by vibration in the case of β-PcH_2 and those directly affected by the latent heats in the case of β-PcCu. The results are plotted in Figure 5-6.

FIGURE 5-6

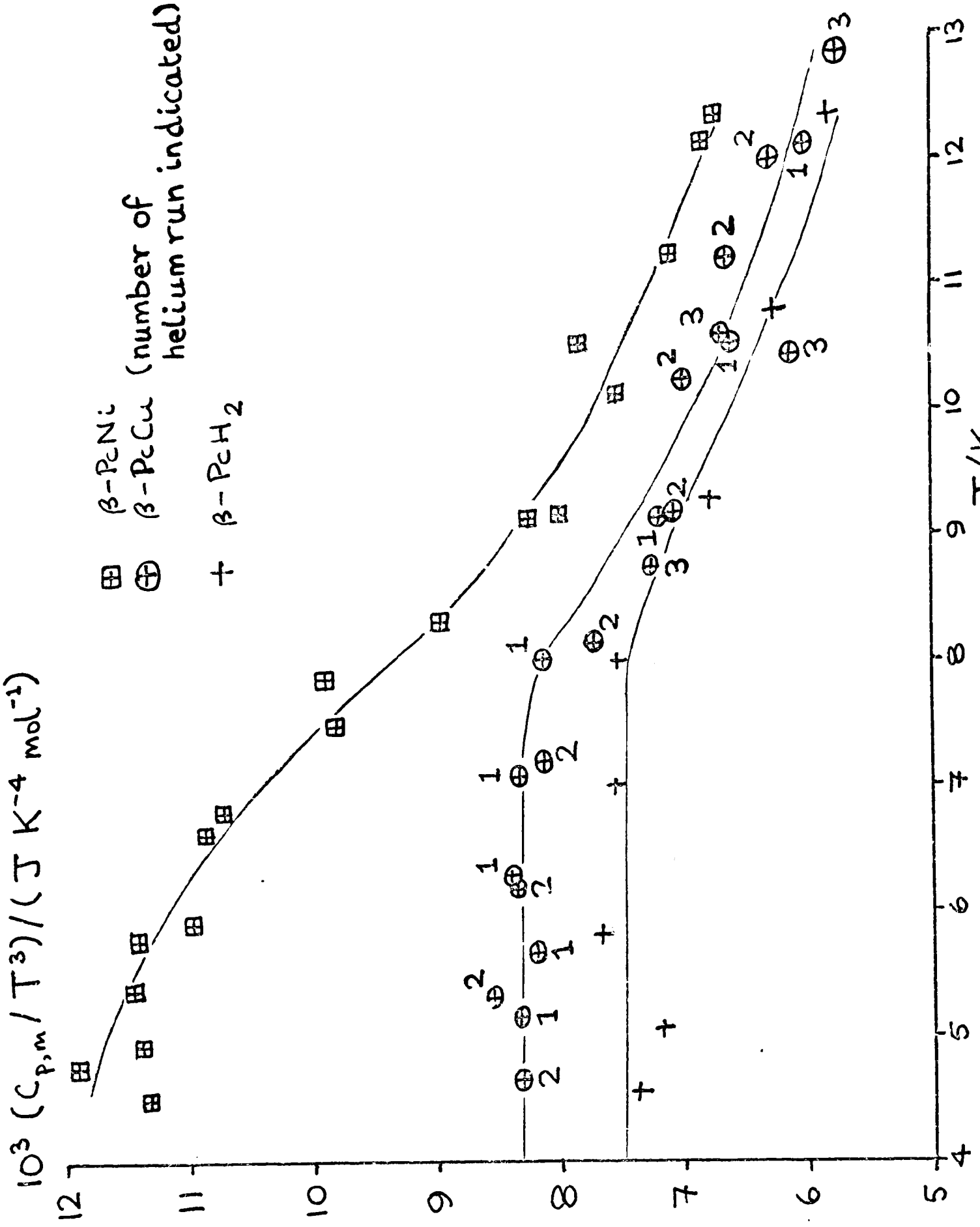
⊞ β-PcNi
⊕ β-PcCu (number of helium run indicated)
+ β-PcH2
10³ (Cp,m / T³)/(J K⁻⁴ mol⁻¹)
T/K
12
11
10
9
8
7
6
5
4
13

Section 5-3c: development of entropy

Figure 5-7 plots the difference between $(\partial S_m/\partial T)_p$ for β-PcNi and $(\partial S_m/\partial T)_p$ for β-PcCu (calculated simply as (1/T) x the difference in molar heat capacities) as a function of T. It is seen that while the two heat capacities are equal at 60 K, the entropy gain between 5 and 60 K calculated for β-PcCu is very different from that calculated for β-PcNi, regardless of whether the results from the first, second, or third helium run are used in the calculation for β-PcCu. In these three cases, the gain for β-PcCu is calculated to be, respectively, R ln 1.5 less than for β-PcNi, at least R ln 1.9 greater, and at least R ln 2.6 greater.

Figure 5-8 plots as a function of temperature the difference between $(\partial S_m/\partial T)_p$ for β-PcCu and $(\partial S_m/\partial T)_p$ for β-PcH_2, and also the difference between $(\partial S_m/\partial T)_p$ for β-PcNi and $(\partial S_m/\partial T)_p$ for β-PcH_2. It is observed that the entropy gains of β-PcH_2 and β-PcNi are approximately the same at 65 K. It may be that the marked downward turn of the plots above 65 K reflects at least in part the apparent tendency (previously noted at pages 104-5) of the new calorimeter described in Chapter 2 to give high results towards the upper end of its operating range.

Section 5-3d: the variation in the latent heats in β-PcCu

The fact that Dr Clay observed no latent heats in his first helium run and large but varying latent heats in his second and third runs (see Table 5-5, page 193) is readily explained if one supposes that β-PcCu undergoes two first-order phase transitions in the region of 9 - 13 K if it is heated or cooled sufficiently slowly, but that over-rapid cooling to 4 K can result in a supercooled high-temperature form. One imagines that in Dr Clay's first run such supercooling was total. In order to explain the relative sizes of the latent heats in the second and third runs, one must suppose that partial supercooling occurred

FIGURE 5-7

$$\frac{\left(\frac{\partial S_m(\beta\text{-PcNi})}{\partial T}\right)_p - \left(\frac{\partial S_m(\beta\text{-PcCu})}{\partial T}\right)_p}{\text{J K}^{-2}\text{ mol}^{-1}}$$

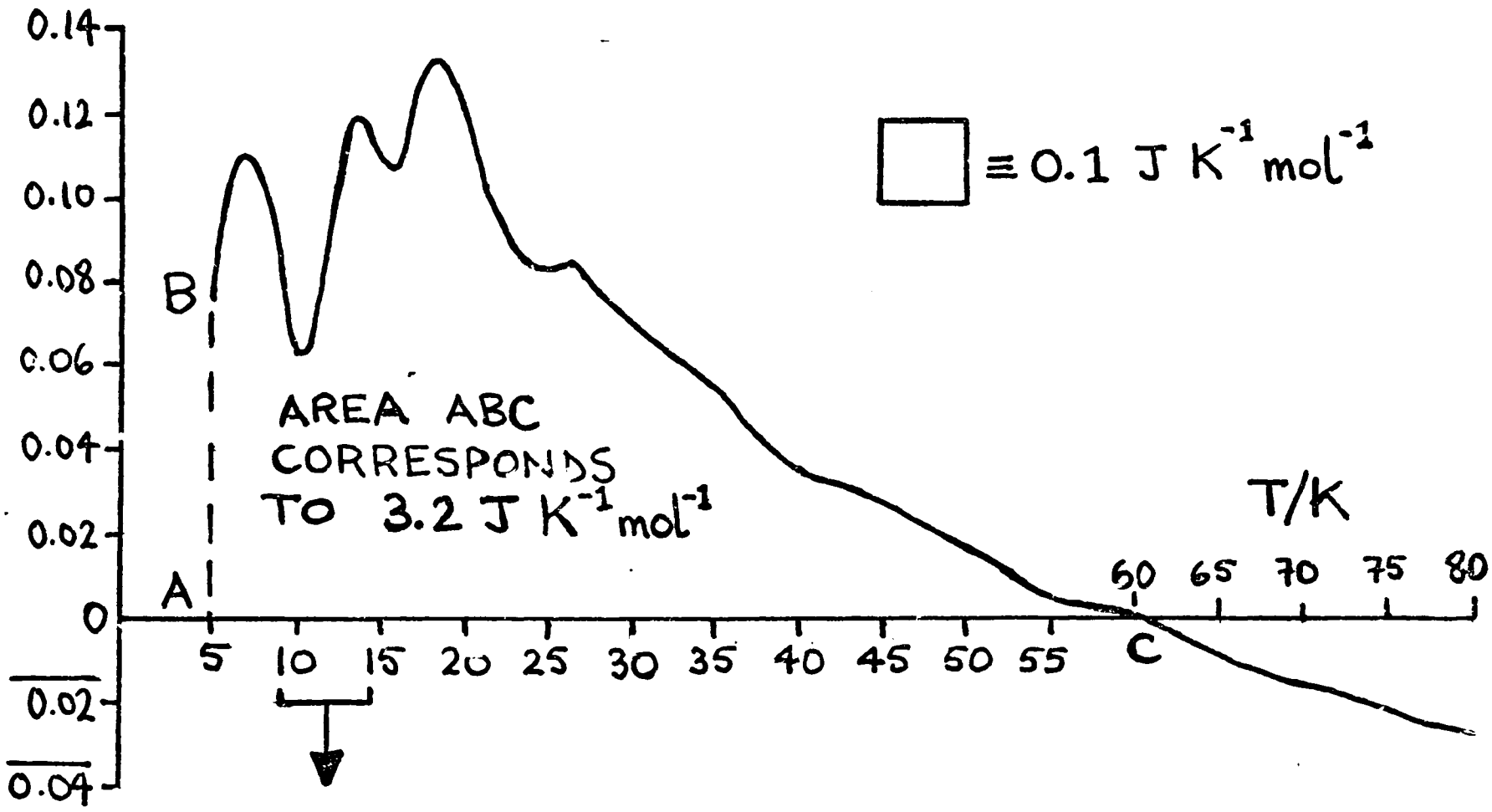

Large negative areas
in this temperature
region corresponding
to the entropies of
transition observed in helium
runs 2 and 3 on β-PcCu;
total of entropies of
transition > 8.7 J $K^{-1}mol^{-1}$
in run 2 and > 11.3 J $K^{-1}mol^{-1}$
in run 3

(No transitions observed in run 1)

Compare R ln 1.5 = 3.37 J $K^{-1}mol^{-1}$
R ln 2 = 5.76 J $K^{-1}mol^{-1}$
R ln 3 = 9.13 J $K^{-1}mol^{-1}$
R ln 4 = 11.52 J $K^{-1}mol^{-1}$

FIGURE 5-8

$$\frac{\left(\frac{\partial S_m(\beta\text{-}PcM)}{\partial T}\right)_p - \left(\frac{\partial S_m(\beta\text{-}PcH_2)}{\partial T}\right)_p}{J\ K^{-2}\ mol^{-1}}$$

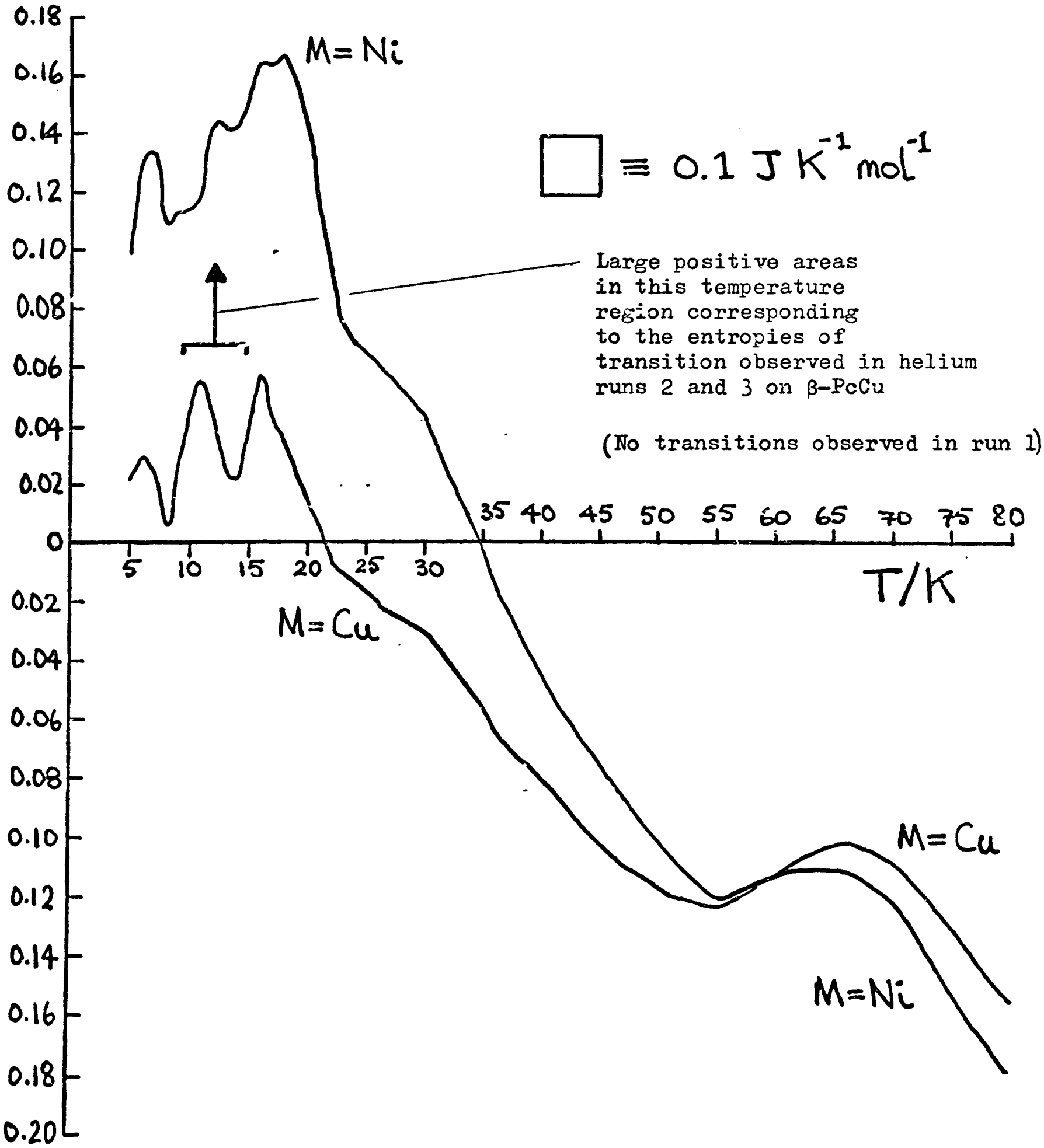

in the cool-down of the second run and that relatively little supercooling (possibly none) occurred in the third.

If in fact no supercooling occurred in the cool-down of the third run, then one can identify the true total entropy change in the two transitions with that observed in the third run; if some supercooling occurred in the cool-down even of the third run, then the true entropy change is even greater. On referring again to Table 5-5, it is seen that the total molar entropy gain in the two transitions must, on the above argument, be not less than approximately R ln 4.

It may be noted that supercooling, like the superheating which was relatively directly observed (page 192, first new paragraph), is quite commonly associated with first-order solid-state transitions.

Section 5-3e: equilibrium times of β-PcH_2 between 4.5 and 9 K

Peculiarly long equilibrium times of the β-PcH_2 sample were observed in the 4.5 to 9 K region (see Section 5-2a, pages 184-187). However, unlike the long equilibrium times observed by Dr Clay in his work on β-PcCu (Section 5-2b at page 187) these were not associated with any latent heats, and occurred at relatively low temperatures. The Debye law dependence of the heat capacity (see Figure 5-6, page 201) - albeit only approximately confirmed because of the small number of measurements and their presumably low precision on account of the long extrapolations - suggests that the long equilibrium times are not associated with anomalous behaviour.

In principle, the long equilibrium times might reflect adsorption of a major part of the He^3 exchange gas below 9 K. He^3 adsorption was previously observed, apparently, with bis(adiponitrile)copper(I) nitrate (see Section 3-3a, pages 102-103), but only at temperatures well below 4 K; one would have therefore to assume that the metal-free phthalocyanine sample had a peculiarly high adsorptive power

for He^3, for example because of its much greater surface area (on surface areas, see pages 181 and 88). At present, however, one cannot decide whether such an explanation is correct, and the possibility cannot be eliminated that the long equilibrium times reflect some intrinsic property of the sample.

Section 5-4: theoretical discussion of the heat capacity results

a. structures of β-PcCu, β-PcNi, and β-PcH_2 at room temperature

It was pointed out at page 175 that these materials are molecular crystals; a structural formula for each molecule was given in Figure 5-1 (page 176). X-ray or neutron diffraction has indicated (see Figure 5-9) that in each case all the atoms of the molecule lie approximately in a single plane. Further, not only the C-C bonds of the benzene rings but also the C-N bonds of the innermost ring of C and N atoms have bond lengths intermediate between those expected for single and double bonds. The molecules are therefore seen to have aromatic character not confined to the benzene rings; the valence bond structures of Figure 5-1 are very inadequate,* and it is necessary to describe the structure in terms of resonance among various valence bond structures or else by a molecular orbital method (Berezin, 1965; Schaffer et al, 1973; and Malter, 1976). Berezin points out that if one treats the bonds such as C(1) - C(2), C(7) - C(8), etc. in Figure 5-9(a) as single (σ) bonds, then the Pc^{2-} unit contains five separate aromatic rings, each obeying the Hückel 4n + 2 rule

*The inadequacy is a matter of symmetry as well as of precise bond lengths. The valence bond structures of Figure 5-1 are inconsistent with the $\bar{1}$ symmetry indicated by the diffraction results (to be further discussed shortly); note especially the o-quinonoid structure in isoindole units aa and cc. In the case of PcH_2 at least, there is the interesting further point that the isoindole unit in question would be relatively free to rotate out of the plane of the others about single bonds bb, if the structures of Figure 5-1 were correct. (See Robertson, 1935.)

FIGURE 5-9

(a) molecule in β-PcCu, after Brown (1968)

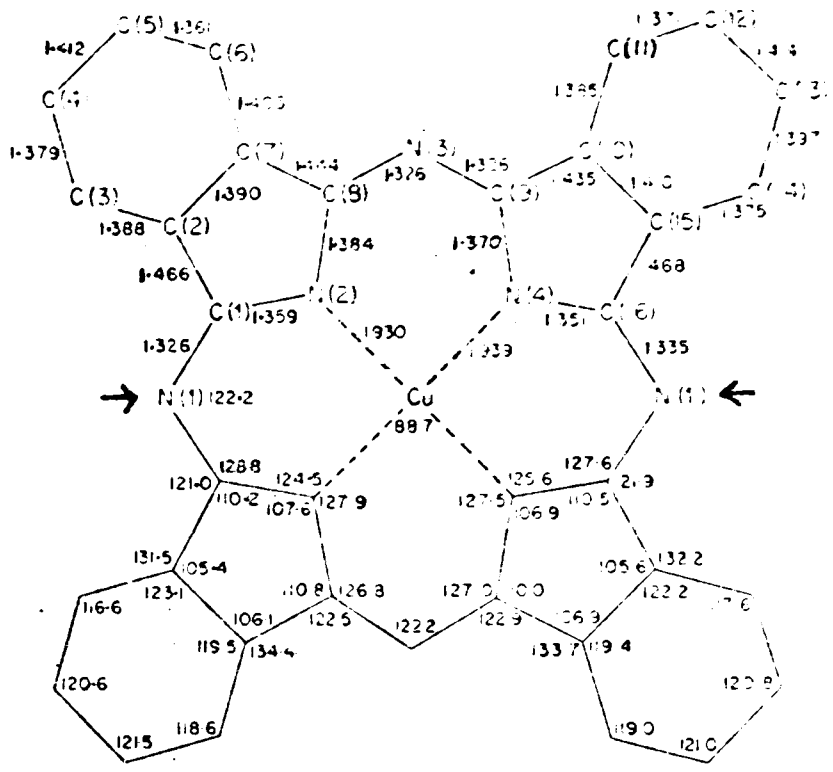

(b) molecule in β-PcNi, after Robertson and Woodward (1937)

• = C ; o = N

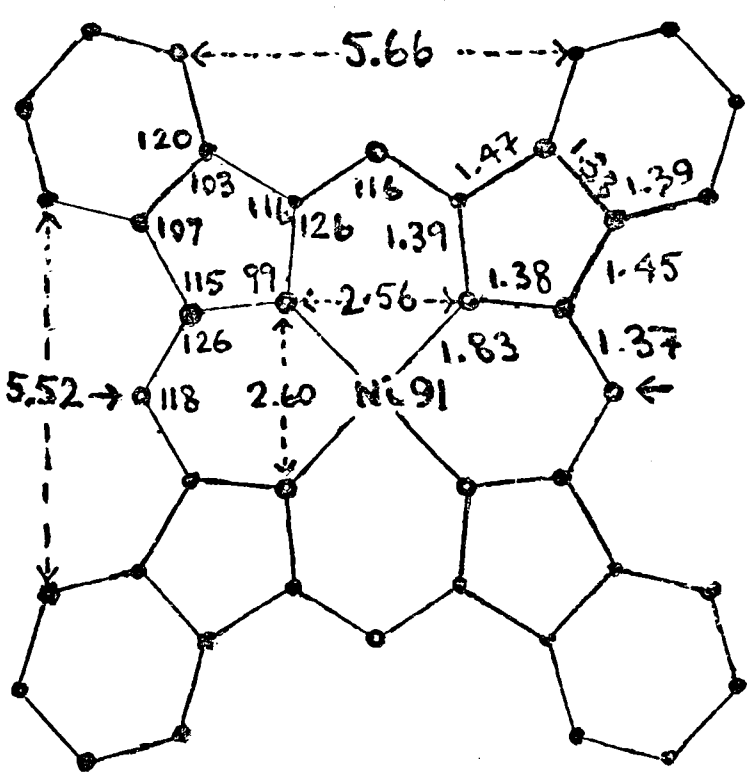

(c) molecule in β-PcH_2, after Hoskins et al (1969)

*, *, +, + are positions occupied by H/2

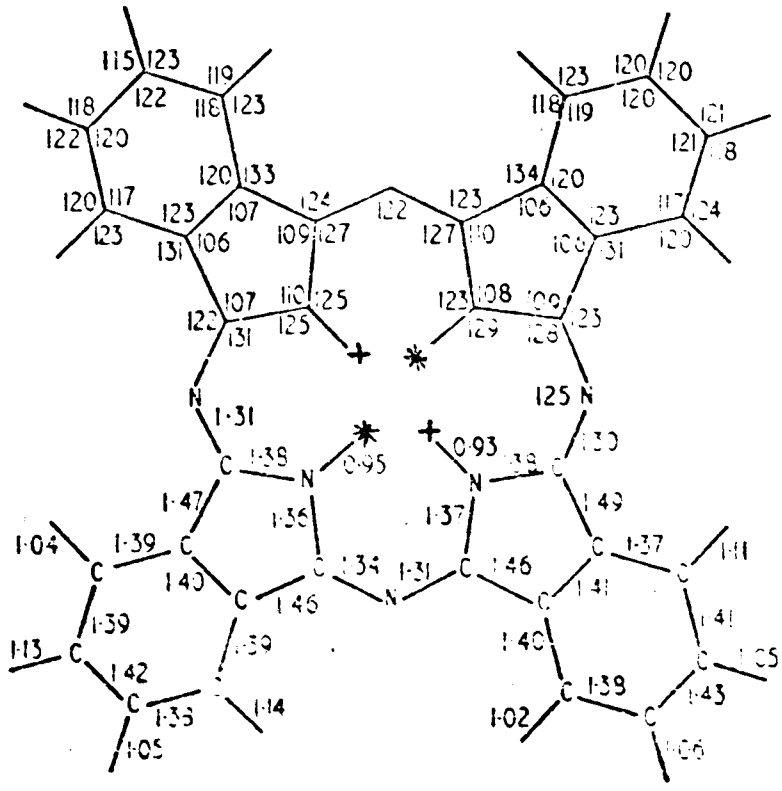

(four benzene rings with n = 1, and one ring of alternating C and N atoms with n = 4).

The arrangement of the molecules in the unit cell is shown in Figure 5-10; although this figure relates strictly only to β-PcCu, it is qualitatively correct for the other two compounds. There are two molecules in each unit cell.

In the cases of β-PcCu and β-PcNi the coordination of the ion is of importance. In the space group $P2_1/a$ (C_{2h}^5), the special positions all have the symmetry $\bar{1}$ (C_i) and are twofold. The metal ions are therefore assigned to one set of such special positions, so as to give two metal ions in the unit cell.* The $\bar{1}$ symmetry requires, quite strictly, that the metal ion and all four isoindole N atoms (i.e. the four nearest neighbours of the metal ion, at 1.83 - 1.94 Å) should lie in a common plane. In fact, the N atoms are found to lie approximately at the corners of a square at the centre of which lies the metal ion. For this reason, the symmetry labels usually given to the electronic energy states of the molecule (even in the crystal) are those appropriate to 4/mmm (D_{4h}) symmetry.

This approximation (that the metal ion has an environment of 4/mmm symmetry) holds even if one considers the nearest-neighbour N atoms in adjacent molecules. The normal to the plane of the metal ion and the four N atoms through the metal ion passes approximately through one of the bridging N atoms which are marked with an arrow in Figure 5-9(a) or 5-9(b) in each of the two nearest molecules along the ± b direction. The distance of these N atoms from the ion is 3.28 Å in β-PcCu (see Figure 5-10(ii)) and about 3.38 Å in β-PcNi. Therefore, the metal ion can be considered to be coordinated by an

*The possibility of positional disordering of these atoms is here ignored.

FIGURE 5-10

(arrangement of molecules in crystal of β-PcCu, after Brown, 1968)

(i) diagrammatic projection on (010)

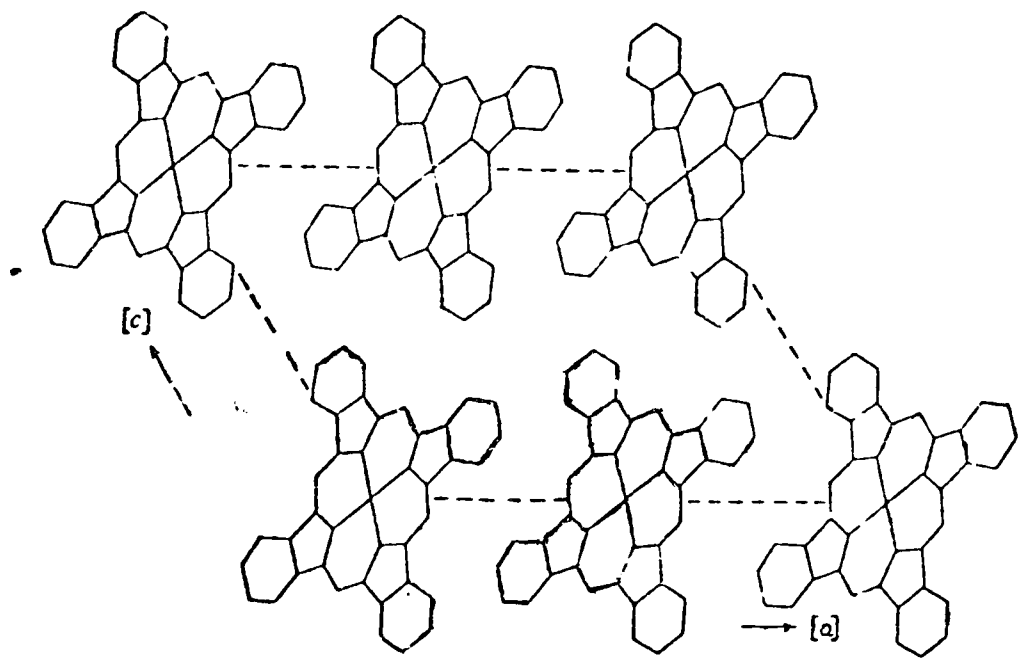

(ii) diagrammatic projection on (001) showing relative orientations of the phthalocyanine rings

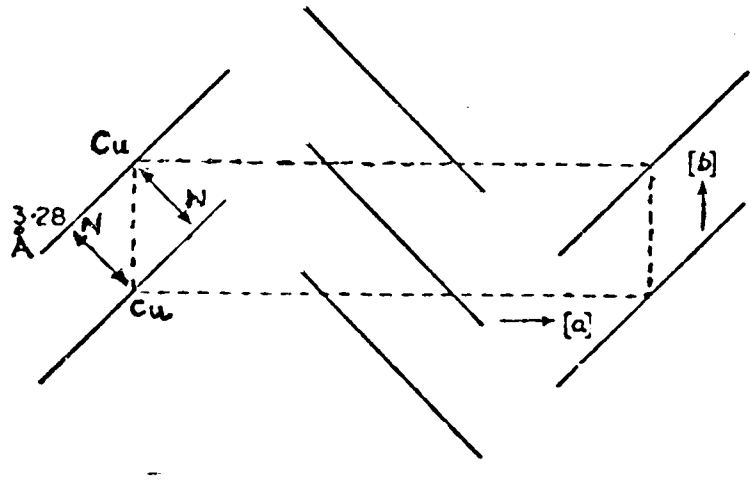

Note:- (ii) of Brown appears to be highly simplified, although adequate for present purposes. See Figure 5 in Robertson (1936).

octahedron of N atoms which has been elongated along one axis. Such coordination is very common in Cu(II) compounds generally; and in the present case the interaction between the Cu ion and the two more remote N atoms is sufficiently strong for these N atoms to be significantly displaced out of the plane in which all the other atoms of its molecule appear (within experimental error) to lie. The displacement is about 0.066 Å towards the Cu ion in the adjacent molecule which the N atom coordinates.

The case of β-PcH_2 is more complex. Robertson (1935, 1936) used X-ray diffraction to establish qualitatively all the features shown in Figure 5-9(c) except for the position of the central H atoms. There are two such H atoms but four N atoms to which they could conceivably be bonded. The four N atoms lie at the corners of a parallelogram (approximating to a square) of which the centre is a position of $\bar{1}$ symmetry. It might therefore be reasonably supposed that the two H atoms lie in the plane of the other atoms bound to opposite (not adjacent) N atoms, for instance at positions * and * in Figure 5-9(c) - compare also Figure 5-1(b).

However, when Hoskins et al (1969) studied β-PcH_2 by neutron diffraction, they confidently placed four half-hydrogen atoms at the positions *, *, +, and + in Figure 5-9(c). All atoms of the molecule were found to be coplanar within experimental error.

This is an interesting case of disorder which contrasts with the nitrate ion disorder in bis(adiponitrile)copper(I) nitrate and the Me_4N^+ ion disorder in TMMC. In those cases the observed symmetry of the site of the species in question required disorder to exist (see pages 115-116 and 157 respectively). In this case, ordered structures are just as consistent with the $\bar{1}$ site symmetry as the disordered structure.*

*Another case where disorder exists although not required by the site symmetry is K_2SnCl_6 (see page 113).

Hoskins et al do not attempt to describe their structure in concrete physical terms. One possible explanation of their structure is that the crystal contains equal numbers of molecules with the H atoms at * and * and of molecules with the H atoms at + and +, the two sorts of molecules being randomly distributed.

Section 5-4b: vibrational contributions to the heat capacities

In Section 5-4a it was seen that β-PcCu and β-PcNi are isostructural at room temperature. If they are approximately isostructural at lower temperatures also, then the vibrational heat capacity contribution to the heat capacity at such temperatures is expected to be almost the same in each material, for the substitution of Cu by Ni (of very similar mass) should only have a slight effect on the frequency spectrum (for this term, see page 3). If one were to apply the scaling procedure of Stout and Catalano (see page 165) to the two materials, one would expect a scaling factor Q very close indeed to unity.

It was also seen in Section 5-4a that β-PcH_2 has a structure very similar to those of β-PcCu and β-PcNi; the central metal atom is replaced by two central H atoms but the molecular shape and molecular stacking are changed relatively slightly. If a close structural relationship exists also at low temperatures, then one can reasonably expect that the frequency spectrum of β-PcH_2 will differ from that of β-PcCu or β-PcNi in that the modes of the metal phtalaocyanines associated with metal atom vibrations will be replaced by a larger number of relatively high frequency modes associated with vibration of the relatively numerous and relatively light H atoms. From the form of the heat capacity - temperature relationship for quantised simple harmonic oscillators (see Lewis and Randall, 1965a) it then follows that β-PcH_2 should have a lower heat capacity than

β-PcCu and β-PcNi at low temperatures, and that it should have a higher heat capacity than β-PcCu and β-PcNi at relatively high temperatures.

The extent to which the observed heat capacities of the three compounds deviate from the predictions of the previous two paragraphs is a measure of (a) how dissimilar the structures are at low temperatures and/or (b) the size of any non-vibrational contributions to the heat capacity.

From the observed behaviour of the heat capacities below 25 K (see Section 5-3a) one can conclude that at every temperature up to at least 25 K there is -

(i) a substantial structural difference between the β-PcNi sample and the β-PcCu sample (regardless of whether the latter is in a high- or low-temperature form and of whether that form is stable or metastable at the temperature in question),* and/or

(ii) a non-vibrational contribution to the β-PcNi heat capacity.

Consider now the results below 8 K as discussed in Section 5-3b and especially as presented in Figure 5-6 (page 201). Supercooled β-PcCu (run 1) and partly converted β-PcCu (run 2) appear to have very similar heat capacities below 8 K which obey the Debye T^3 law with about the same proportionality constant. β-PcH_2 also apparently obeys a T^3 law below 8 K, although with a proportionality constant about 10% lower. These observations are consistent with the above predictions, and they make it seem likely that the heat capacity is essentially vibrational in the forms of β-PcCu and in β-PcH_2.

In this low-temperature region at least, there is a reasonable expectation that further purely calorimetric work could allow one to

---

*For what is here intended by the reference to "forms", see Section 5-3d.

distinguish between possibilities (i) and (ii) above. Thus, if the work on all three materials were extended below 4 K, and one found that the T^3 behaviour of β-PcCu and β-PcH_2 was preserved (ordinates in Figure 5-6 approximately equal to 8.3 and 7.5 respectively) while the ordinate for β-PcNi levelled off at, say, 12, then possibility (i) would be seen to be the case. If on the other hand the ordinate for β-PcNi went through a pronounced maximum at, say, 3 K and levelled out at 8.3 below, say, 2 K, then possibility (ii) would be seen to be the case.

Section 5-4c: the possibilities of magnetic ordering and/or Schottky anomalies

In respect of the following, the present author must gratefully acknowledge valuable conversations and correspondence with Dr A.K. Gregson, formerly of the Inorganic Chemistry Laboratory, and now of the University of New England, Armidale, NSW, Australia, and especially the communication of Dr Gregson's unpublished results.

The possibility of magnetic ordering is always worth considering in transition metal compounds. In the present cases, however, it seems not to be of relevance.

β-PcNi - and also, not surprisingly, β-PcH_2 - display no temperature-dependent paramagnetism* at room temperature (see Barraclough et al, 1971), so that no magnetic ordering is expected as these materials are cooled. This behaviour of β-PcNi is explained in terms of the Ni^{2+} (d^8) ion having a low- (for a d^8 ion, zero-) spin configuration in a square planar ligand field. Similar behaviour occurs in other square planar Ni^{2+} complexes such as Ni(dimethylglyoxime)$_2$ - see for example Figgis (1966).

In β-PcCu, however, the Cu^{2+} (d^9) ion has a spin of 1/2, and

*β-PcNi displays temperature-dependent paramagnetism, and therefore it would not be quite correct to describe it as simply diamagnetic.

temperature-dependent paramagnetism is displayed (see Martin and Mitra, 1970 and Gregson et al, 1976). In principle, magnetic ordering should occur at sufficiently low temperatures; but Dr Gregson has recently (private communication, September 1978) completed susceptibility measurements at 4.2 K in fields from 20 to 1400 Oe, and finds that β-PcCu is a "near-perfect paramagnet" even at 4.2 K. One does not expect, therefore, that there will be significant magnetic contributions to the heat capacity in the temperature range in which the heat capacity was measured (4 - 82 K).

The "humps" in the heat capacity curves referred to in Section 5-3a (page 200) are somewhat reminiscent of Schottky anomalies, which were described from page 9, second new paragraph to page 10, four lines from below. The only further information on these anomalies which is needed at present is that the maximum in a Schottky heat capacity occurs at a temperature of about* 0.4 ϵ/k where ϵ is the energy gap between the ground and the first excited electronic states (see Rosenberg, 1963a) Therefore, if one identifies the centre of one of the "humps" (all in the 12 - 19 K region) with the heat capacity maximum of a Schottky anomaly, an ϵ of from 30 K k to 50 K k is indicated. In the (strictly speaking, inaccurate) language of spectroscopists ϵ is from 20 to 35 cm^{-1}.

The question is now whether the ground and first excited electronic states in one or more of the three molecules PcH_2, PcCu, and PcNi are separated by an ϵ of this magnitude.

The abovementioned magnetic properties of β-PcH_2 and β-PcNi indicate that only a singlet ground state is significantly populated at room temperature, so that no ϵ of this size is possible.

---

*The precise numerical factor depends on the ratio g_1/g_0 (for symbols see page 9).

In the case of PcCu, the ground state is $^2B_{1g}$,* according to epr on PcCu diluted in β-PcH_2 single crystals, to magnetic anisotropy measurements on β-PcCu single crystals, and to molecular orbital calculations+ (see, respectively, Harrison and Assour, 1964; Martin and Mitra, 1970 and Gregson et al, 1976; and Schaffer et al, 1973). The epr work was apparently performed at room temperature (no temperature is specified by Harrison and Assour), and the magnetic anisotropy measurements were performed from 80 K to 300 K. If even at 300 K the molecules are still almost all in the $^2B_{1g}$ state, then the next highest state must be very much higher in energy than 30 K k (∈ appropriate to a Schottky anomaly causing the hump in the heat capacity of β-PcCu).

For the sake of completeness, the energy level scheme proposed by Martin and Mitra and by Gregson et al is depicted in Figure 5-11. The ground state corresponds to a hole in the $d_{x^2-y^2}$ orbital of the Cu^{2+} ion.

It might be thought that the $^2B_{1g}$ ground state could itself be split into two singlets, separated by a gap of about the right size to cause a Schottky anomaly in the region of 12 K. Kramers' theorem is relevant here. The theorem "implies that all complicated ligand-field splitting, spin-orbit coupling, and electron spin-spin interactions in transition metal ions can never remove the degeneracy of a state with spin S = 1/2" (this formulation is taken from Carrington and McLachlan, 1967). A "Kramers' doublet" <u>can</u> be split by interaction of one paramagnetic ion with the magnetic dipole of another or with

---

*This symmetry label, like those used subsequently, is a D_{4h} symmetry label - compare page 208.

+It will be noted that uv and visible spectroscopy are not included in the above list. This is because the rather weak parity-forbidden d-d transitions are obscured by extremely strong change-transfer transitions (compare the commercial use of copper phthalocyanine and its derivatives as pigments and dyestuffs referred to at page 175).

FIGURE 5-11

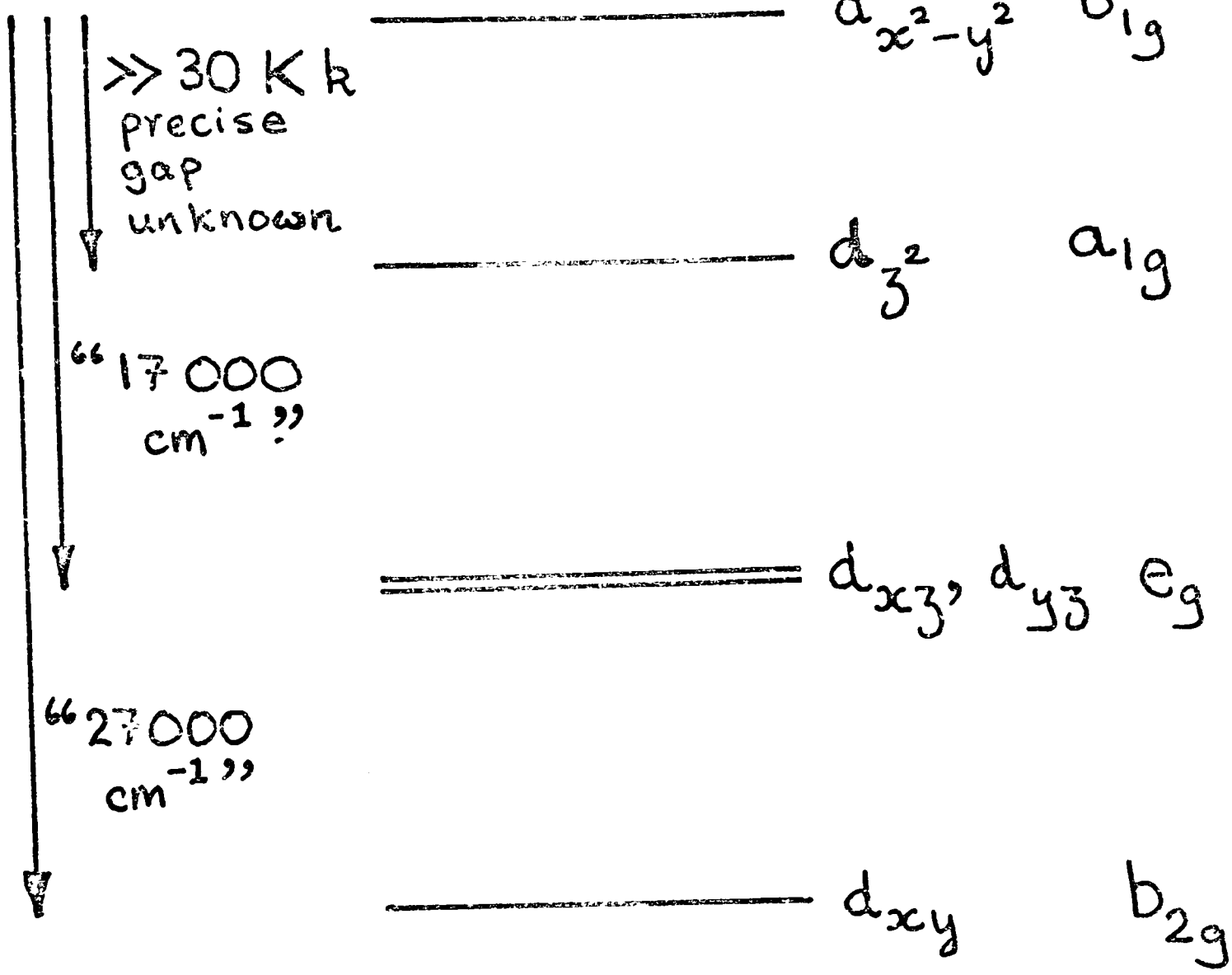
$d_{x^2-y^2}$ b_{1g}
≫ 30 K k
precise
gap
unknown
d_{z^2} a_{1g}
"17000
cm^{-1}"
d_{xz}, d_{yz} e_g
"27000
cm^{-1}"
d_{xy} b_{2g}

nuclear spin or quadruple moments; but such effects lead (see Rosenberg, 1963b) to splittings two or more orders of magnitude less than 30 K k. Confirmation of the latter proposition in the present case is provided by the epr results of Harrison and Assour.

In conclusion, it may be said that the evidence from non-thermodynamic studies is strongly against any explanation of the heat capacity results which involves magnetic ordering or Schottky anomalies.

Section 5-4d: the possibility of positional disordering of the metal ions

It was already noted at pages 210-11 that the hydrogen atoms in β-PcH_2 are disordered at room temperature, even though such disorder is not actually required by the symmetry of the site on which the phthalocyanine molecule is centred. It is an interesting speculation that perhaps the Cu^{2+} or Ni^{2+} ion in the metal phthalocyanines may be likewise "unnecessarily" disordered. In the case of β-PcCu, such disordering (if it occurred at high temperature and were "frozen out" as the crystal was cooled) could readily account for an entropy change of R ln 4 (compare page 205, first new paragraph) in the two first-order transitions, as will now be explained.*

Suppose that the potential energy of a Cu^{2+} ion moving in the field of the four isoindole N atoms is not a minimum for a position in the centre of the square (strictly, parallelogram) of which the corners are the N atoms (see Section 5-4a for structural details). Then there will be four minima because of the approximate fourfold

---

*The discussion which follows is the first detailed discussion in this thesis of the possibility of an anomaly due to positional ordering effects; however, the arguments are broadly analogous to those presented (albeit in a more complex case) in Sections 3-4b to 3-5c. An anomaly involving positional disordering of a somewhat similar type to the above occurs in KH_2PO_4 (see Staveley, 1972).

symmetry. One might have, for instance, the potential energy function sketched in Figure 5-12 (the positions of the minima are not to be taken seriously, but their number would almost certainly be four).

For an appropriate choice of energies and positions of the minima, one would on this model have at, say, 20 K each Cu^{2+} ion taking up randomly one of the four positions almost independently of the positions taken up by the other Cu^{2+} ions. The energy barrier to movement of an ion from one position to another could be small enough to allow the Cu^{2+} ions to order under some cooperative interaction between the molecules as the crystal is cooled to 8 K (at least provided the cooling is slow). For complete ordering the loss in configurational entropy is R ln 4, since 4 is the number of positions occupied at high temperature. The approach of Newns and Staveley (see pages 122 to 123) leads us to identify this entropy change with the sum of the entropies of the first-order transitions, which identification is consistent with the estimate at page 205.

The above speculation is not necessarily inconsistent with the work of Brown (1968), from whose paper Figure 5-9(a) (page 207) is taken. Disordering of the type proposed could well be very difficult to distinguish from thermal vibration about the central position by X-ray diffraction. In any case it is conceivable that at room temperature kT is so great compared with the difference in energies of, say, contours 1 and 4 in Figure 5-12 that the motion of the Cu^{2+} ion could reasonably accurately be described as thermal vibration about the central position.

No explanation will be attempted here of why the ordering should occur in <u>two</u> first-order transitions. However, it will be recollected from Chapter 3 (pages 130 to 131) that such "split" anomalies are known.

FIGURE 5-12

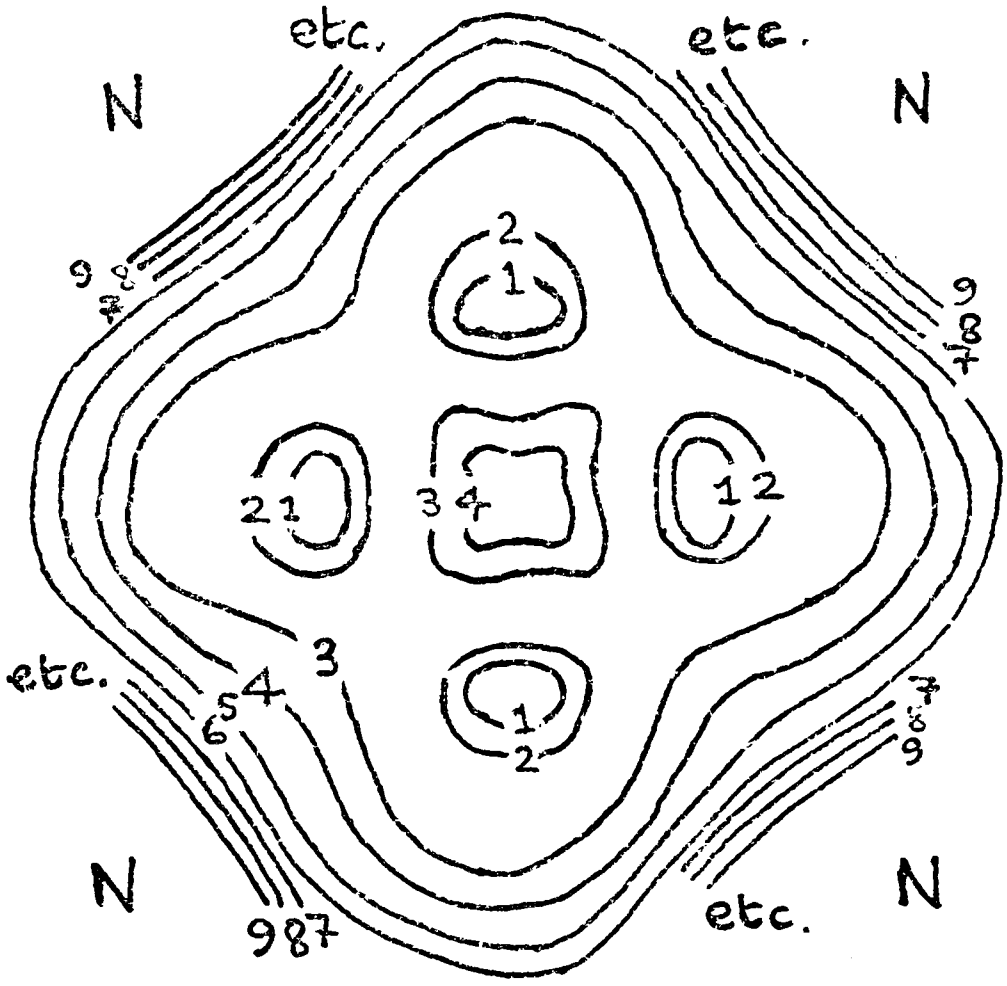

The above plots potential energy as a function of the Cu^{2+} ion position in the plane of the four isoindole N atoms shown. 1, 2, 3,....9 are contour lines of increasing (unfavourable) energy at arbitrary intervals.

However, it is necessary if the above speculation is to be defended to suggest how the cooperative interactions between the molecules (necessary for ordering to occur) might arise. One known interaction between the molecules is that referred to at page 210 between the Cu^{2+} ions and the two remoter N atoms in the coordinating tetragonally-distorted octahedron.

There is at present no evidence for a similar effect in β-PcNi; but the probable absence of strong cooperative interactions would suggest that even if the Ni^{2+} ions were positionally disordered at high temperature, then the temperature at which ordering would occur would be much lower than for β-PcCu, or else the disorder would be "frozen in".

Section 5-4c: further problems

If one is to understand properly the structural processes occurring in the crystals of β-PcH_2, β-PcCu, and β-PcNi below 80 K and to begin to test speculative proposals such as that presented in Section 5-4d, diffraction studies of these materials at, say, 4 K and 77 K are highly desirable. Such studies are, of course, desirable as a matter of general principle; but the need for them has been increased by the recent suggestions from East European workers that all three materials undergo phase transitions somewhat below room temperature (see Dudreva and Grande, 1974 and Füstöss-Wégner, 1978). It is an indication of the difficulty of working with these materials that transitions at such accessible temperatures should apparently have passed unnoticed previously, despite the enormous amount of work published on them as a result of their commercial importance.

Dudreva and Grande do not explain the transitions, although they (but curiously not Füstöss-Wégner) reject the possibility that the low-temperature state is ferroelectric.

Heat capacity results on all three materials between 80 K and 300 K would also be valuable, since any anomalies observed might well be crucial to understanding the processes occurring below 80 K. (Füstöss-Wégner reports heat capacities on β-PcH_2 from 255 K to 420 K.)

The transitions reported by the East Europeans are rather slow, taking several hours to complete just below the transition temperature. However, the rate increases greatly as the temperature is lowered further. This latter fact makes it seem improbable that the samples of which the present author or Dr Clay measured the heat capacity were supercooled or partially supercooled with respect to the East Europeans' transitions, but the possibility should be borne in mind when future work is attempted. (No special care was taken in cooling the samples from room temperature to 77 K either by the present author or presumably by Dr Clay, for all our experimental work was done before Dudreva and Grande's paper appeared.)

Finally, the rather mundane observation should be made that Dr Clay's sample of β-PcCu was of poorer purity and/or crystalline quality than the author's sample of β-PcH_2 and than Dr Clay's sample of β-PcNi (see Section 5-1). Therefore, it is conceivable that some of the effects in β-PcCu discussed in preceding sections may have been peculiar to Dr Clay's sample; repetition of his work with a better sample would be valuable in view of the remarkable nature of his results.

APPENDIX 3-I (SEE PAGES 119 AND 122): CALCULATION OF STRUCTURE AMPLITUDES FOR SCHEMES 1, 2, 4, AND 6 OF TABLE 3-6 (PAGE 117)

The principle of the X-ray method for determination of crystal structure is the observation of the intensity of a large number of reflections, the calculation from the intensities of observed structure amplitudes from those reflections, and the comparison of the observed structure amplitudes with those calculated for various trial structures. Therefore, whether the Schemes of Table 3-6 are distinguishable from one another depends on whether the calculated structure amplitudes differ substantially from scheme to scheme for the observed reflections.

In the space group Pnnn - D_{2h}^{2}, for the h00, 0k0, and 001 reflections (which are the only ones considered here, but which should give a fair overall picture), the contributions of the O atoms to the structure factor are separable from those of the C, H, and N atoms and are given by the equations

$$F_{h00}^{oxygen} = \exp(-B(1/2d_{h00})^2) \sum nwf \cos 2\pi hx$$

(h even only, extinction for odd h)

$$F_{0k0}^{oxygen} = \exp(-B(1/2d_{0k0})^2) \sum nwf \cos 2\pi ky$$

(k even only, extinction for odd k)

$$F_{001}^{oxygen} = \exp(-B(1/2d_{001})^2) \sum nwf \cos 2\pi lz$$

(l even only, extinction for odd l)

In these equations (derived from those in International Tables for X-ray Crystallography, 1952a), the summation is over sets of equivalent sites. Each set consists of n sites each occupied by an O atom with weighting w, and the reduced coordinates of any one of the

sites are x, y, z relative to the origin shown in Figure 3-5 (page 111). d_{hkl} is the spacing between adjacent reflecting planes, and f is the atomic scattering factor of oxygen (f itself being a function of d_{hkl}). For Scheme 6 the number of sets of sites is infinite, and the equations become (compare Palin and Powell, 1947)

$$F_{h00}^{oxygen} = 6\ f\ J_o(Z)\ \cos 2\pi h x_{N2}$$

$$F_{0k0}^{oxygen} = 6\ f\ J_o(Z)\ \cos 2\pi h y_{N2}$$

$$F_{001}^{oxygen} = 6\ f\ J_o(Z)\ \cos 2\pi l z_{N2}$$

where x_{N2}, y_{N2}, z_{N2} are the reduced coordinates of one of the nitrate N atoms (1/2, 0, 0 or 0, 1/2, 1/2), J_o is the zeroth order Bessel function of Z, and $Z = \frac{2\pi r(N-O)}{d_{hkl}}$

in which r(N-O) is the N-O internuclear distance in the nitrate ion.

The structural parameters for Schemes 1, 2, 4, and 6 are given in Table 3-I-1. In the Table, the parameters for Scheme 4 are those of Kinoshita et al (1959b), and those for the other Schemes are modelled on those of Kinoshita et al. It is evident that each of these schemes gives the same F_{h00}^{oxygen} for all h. For each of the 0k0 and 001 reflections observed by Kinoshita et al F^{oxygen} was calculated on the basis of Schemes 1, 2, 4, and 6 and of Schemes according to which ions lie in or parallel to the a b or a c planes. The results of these calculations are given in Table 3-I-2. In the calculations values for f were taken from International Tables for X-ray Crystallography, 1962, and the value of B used (3.0 Å^2) was that of Kinoshita et al.

The difference between the values for Schemes 4 and 6 given in Table 3-I-2 are no more than 0.3 for any reflection. The structure amplitudes observed by Kinoshita et al are quoted to the nearest

TABLE 3-I-1: structural parameters used in structure amplitude calculations

Scheme	Atom	n	Wyckoff notation	(w)	x	y	z
4 (Kinoshita et al)	O1	4	j	(1/4)	0.000	0.410	0.500
	O2	4	l	(1/4)	0.000	0.500	0.288
	O3	8	m	(1/4)	0.000	0.455	0.317
	O4	8	m	(1/4)	0.000	0.422	0.394
1	O2	4	l	(1/2)	0.000	0.500	0.288
	O4	8	m	(1/2)	0.000	0.422	0.394
2	O1	4	j	(1/2)	0.000	0.410	0.500
	O3	8	m	(1/2)	0.000	0.455	0.317
6	N2	2	b	(1)	0.000	0.500	0.500
	r(N-O) = 1.24 Å; x for Os = 0.000						

TABLE 3-I-2: calculated contributions (F^{oxygen}) of O atoms to structure amplitudes for all 0k0 and 00l reflections observed by Kinoshita et al

scheme / reflection h k l	1	2	4	6	ion in or // to a b plane	ion in or // to a c plane
0 2 0	31.5	31.6	31.5	31.5	*	44.8 +
0 4 0	3.0	2.6	2.8	2.7	*	36.9 +
0 6 0	-8.9	-11.3	-10.1	-10.1	*	27.7 +
0 8 0	-2.8	-9.5	-6.1	-6.1	*	19.5 +
0 10 0	6.2	-4.9	0.6	0.7	*	13.5 +
0 12 0	8.8	-3.3	2.8	2.7	*	9.3 +
0 14 0	5.6	-3.0	1.3	1.2	*	6.2 +
0 16 0	1.5	-1.9	-0.2	-0.5	*	4.3 +
0 0 2	-4.7	-3.7	-4.2	-4.3	33.7 +	*
0 0 4	-6.0	3.9	-1.1	-1.0	15.1 +	*
0 0 6	-3.0	5.4	1.2	1.1	6.1 +	*

* not calculated, as depends on how the nitrate ion is orientationally disordered within the plane specified

\+ value independent of how the nitrate ion is disordered within the plane specified

integer; therefore, Schemes 4 and 6 are indistinguishable on the basis of observations of this precision. The difference in the values for, say, Schemes 1 and 4 are greater, but this does not necessarily mean that they are distinguishable, for the reasons that (1) the agreement between observed and calculated structure amplitudes reported by Kinoshita et al for these reflections is by no means perfect (there being a discrepancy of up to 5), (2) a refinement of all atomic parameters on the basis of Scheme 1 might lead to an improved agreement between observed and calculated amplitudes, and (3) the correction for thermal vibration (by factor B) has been performed rather arbitrarily.

It is also evident from Table 3-I-2 that schemes in which the plane of the ion is different give very different calculated contributions to the structure amplitude.

APPENDIX 3-II (SEE PAGE 119): CALCULATION OF THE POTENTIAL ENERGY FUNCTION OF COLUMN 4 OF TABLE 3-6 (PAGE 117).

The interaction energy between the O atoms of the nitrate ion and the environment was calculated as a function of θ as defined at the bottom of column 4 of Table 3-6, for various sets of equivalent species in the vicinity of the nitrate ion. The results of the calculations, and the basis on which they were performed, are indicated in Table 3-II-1. According to these calculations the effect of non-cooperative electrostatic forces on the relative energy of the various orientations of the ion is rather small, but the effect associated with a Lennard-Jones interaction with the set of four nearby C2 methylene groups is relatively strong. (For a nitrate group at 0, 1/2, 1/2 these are (in Figure 3-5, page 111) the groups at the sites C25 and C26 and at the sites corresponding to C27 and C28 in the next unit cell in the -a direction. These sites are 4.14 Å from 0, 1/2, 1/2.) This interaction was much stronger than the others considered, taken singly or together, and gave an LV_o of approximately 1 kJ/mol as quoted on page 119.

TABLE 3-II-1

Calculations of the interaction between all three O atoms of NO_3 with N at 0, 1/2, 1/2 treated as -	- and the following surrounding atoms or groups (described either with reduced coordinates or with respect to Figure 3-5) -	- treated as -	indicates that L x (energy of orientation with $\theta = 0^o$ - energy of orientation with $\theta = 30^o$) is:
point charges of -0.33e	NO_3 at 0, 1/2, -1/2; 0, 1/2, 3/2	point charges of -e	+39 J/mol
"	NO_3 at 0, 3/2, 3/2; 0, 3/2, -1/2; 0, -1/2, 3/2; 0, -1/2, -1/2	"	+0.1 J/mol
"	NO_3 at 1, 1/2, 3/2; 1, 1/2, -1/2; -1, 1/2, 3/2; -1, 1/2, -3/2	"	+0.02 J/mol
"	NO_3 at 1/2, 0, 0; 1/2, 0, 1; 1/2, 1, 0; 1/2, 1, 1; -1/2, 0, 0; -1/2, 0, 1; -1/2, 1, 0; -1/2, 1, 1	"	+2 J/mol
"	Cu at 1/2, 1/2, 1/2; -1/2, 1/2, 1/2	point charges of +e	0
"	Cu at 0, 0, 0; 0, 0, 1; 0, 1, 0; 0, 0, 1	"	-11 J/mol
"	Cu at 1/2, 1/2, 3/2; 1/2, 1/2, -1/2; -1/2, 1/2, 3/2; -1/2, 1/2, -1/2	"	-3 J/mol
Ne atoms	Nitrile N atoms at N15, N16; N17, N18 in next cell in -a direction	Ne atoms	-0.2 J/mol
point charges of -0.33e	"	point charges of -0.71e	-1 J/mol
"	"	point charges of -0.31e	-0.4 J/mol

TABLE 3-II-1 cont.

Ne atoms	Nitrile C atoms at C15, C16; C17, C18 in next cell in -a direction	Ne atoms	-18 J/mol
point charges of -0.33e	"	point charges of 0.71e	44 J/mol
Ne atoms	CH_2 groups at C25, C26; C27, C28 in next cell in -a direction	CH_4 molecules	-1024 J/mol
point charges of -0.33e	"	point charges of 0.31e	75 J/mol
Ne atoms	CH_2 groups at C31, C32; C33, C34 in next cell in -a direction	CH_4 molecules	-42 J/mol

Notes:

1. In all cases, energy was calculated at 1° intervals and its variation was found to be monotonic from $\theta = 0$ to $\theta = 30^\circ$.
2. Positions of O atoms were calculated assuming r(N-O) = 1.24 Å; positions of other atoms were taken directly from Kinoshita et al, 1959b.
3. Ne - Ne and Ne - CH_4 interactions calculated from the Lennard-Jones equation

$$V = 4\,\varepsilon\,[(\sigma/r)^{12} - (\sigma/r)^{6}]\,.$$

For Ne - Ne ε was taken as 34.9 Kk and σ as 2.78 Å. For Ne - CH_4 ε and σ were taken respectively as the geometric and arithmetic means of the values for Ne - Ne and CH_4 - CH_4; for this purpose ε for CH_4 - CH_4 was taken as 148.2 Kk and σ as 3.817 Å. See Hirschfelder at al (1954).
4. Electrostatic charges on N1, C1, and C2 are estimates based on the dipole moment of CH_3CN.

APPENDIX 3-III

This appendix is to demonstrate the proposition made in the paragraph bridging pages 119 and 121, and also that made in the first sentence of the first new paragraph of page 121. For the sake of definiteness, the discussion here will use Scheme 1' in Table 3-7 (page 120) as an example.

If one takes the potential energy of the ion as $U(q_1, q_2, \ldots q_6)$, where the q_i $(i = 1,2,\ldots 6)$ are the six coordinates which must be specified to define the position of the ion completely, then an essential requirement for a potential energy minimum is that $\left(\frac{\partial U}{\partial q_i}\right)_{q_j \neq q_i} = 0$ for all i.

In position A given in Figure 3-7 for Scheme 1', the coincidence of one twofold axis of the ion with one twofold axis of the site means that $\left(\frac{\partial U}{\partial q_i}\right)_{q_j \neq q_i} = 0$ for four of the six q_i. (This can be shown by pictorially depicting the effect of, and considering the effect on U of, equal and opposite displacements in each of the q_i of an ion in position A.) It will be noted that to completely define a position such as A, two continuously variable parameters have still to be specified, and therefore there will be at least one pair of values of these parameters for which the other two partial differential coefficients are also zero. In this respect, values of these two parameters which correspond to the N atom lying in the symmetry origin and/or the σ_h' plane of the ion intersecting two of the twofold axes of the site (for instance the pair of parameters defining position I in Table 3-6, page 117) are in no way distinguished from the rest; for when such values are chosen there is no additional

coincidence between identical symmetry elements of ion and site.

The propositions in the text follow directly.

APPENDIX 4-I (SEE FIGURE 4-5, PAGE 152)

Professor F. Haseda of Osaka University, Japan kindly provided us with the original graph of which Figure 1 in Takeda (1974) is a much-reduced copy. The following heat capacities were read off this original and converted into J K^{-1} mol^{-1}, R being taken as 8.3143 J mol^{-1} K^{-1}, and were used in the plotting of Takeda's results in Figure 4-5.

T/K	$C_{p,m}/JK^{-1}mol^{-1}$
1.50	0.247
1.75	0.303
2.00	0.368
2.25	0.443
2.50	0.526
2.75	0.624
3.00	0.725
3.25	0.831
3.50	0.940
3.75	1.075
4.00	1.209

(Precision is about 2% for T = 1.50 K, about $^{1}/_{2}$% for T = 4 K.)

APPENDIX 4-II (SEE PAGE 161): CALCULATION OF TOTAL ENTROPY GAIN UP TO 4 K IN TIMC

Vis et al (1974) at page 1767 estimate $\int_{0\ K}^{1.5\ K}(C_{p,m}/T)\ dT$ to be 0.226 J $K^{-1}mol^{-1}$; note that this figure includes the entropy associated with the pronounced anomaly at 0.84 K, and that the heat capacity is extrapolated below 0.43 K.

The entropy gain from 1.5 K to 4 K can be calculated from Figure 4-5 (page 152) as 0.550 J $K^{-1}mol^{-1}$. Therefore the total entropy gain up to 4 K is (0.226 + 0.550) J $K^{-1}mol^{-1}$ = 0.776 J $K^{-1}mol^{-1}$.

APPENDIX 4-III (SEE PAGE 172)

The $C_{3h}(\bar{6})$ site has two symmetry elements, namely a $C_3(3)$ axis and a mirror plane perpendicular thereto. The NC_4 unit, of symmetry $T_d(\bar{4}\ 3\ m)$, has C_3 axes along the N-C bonds but no mirror plane perpendicular to any of these axes. It follows that in any position for which the N atom and one C atom of the ion both lie in the C_3 axis of the site, coincidence of one and only one symmetry element of ion and site occurs. Among the set of such positions, therefore, those in which N lies at the symmetry origin are not distinguished from the rest in respect of the likelihood that all the $\left(\frac{\partial U}{\partial q_i}\right)_{q_j \neq q_i}$ will be zero. (Compare Appendix 3-III.) This leads directly to the proposition in the text.

APPENDIX 5-I: C, H, N ANALYSES IN SECTION 5-1

It became evident, when samples of PcH_2 were analysed (supposedly containing only C, H, and N) that the calibration of the laboratory analytical machine was not satisfactory. To investigate this difficulty, a sample of BDH Laboratory Reagent azobenzene $C_6H_5N = NC_6H_5$ was analysed. The results of three determinations were -

	C	N	H	total
(1)	78.91	15.31	5.52	99.74
(2)	79.57	15.34	5.44	100.35
(3)	79.99	15.34	5.67	101.00
calc $C_{12}H_{10}N_2$	79.10	15.37	5.53	100.00

The values in the total column indicate the inconstancy of the calibration. However, if the values for each determination are scaled so as to give a total of 100.00 in each case, then agreement with the calculated percentages is satisfactory:-

	C	N	H	total
(1), scaled	79.12	15.35	5.53	100.00
(2), scaled	79.29	15.29	5.42	100.00
(3), scaled	79.20	15.19	5.61	100.00
average of scaled values	79.2	15.3	5.5	100.0
calc $C_{12}H_{10}N_2$	79.10	15.37	5.53	100.00

The analytical results given for PcH_2 in Section 5-1 have been calculated in this way. No such scaling was performed with the PcCu results reported there.

REFERENCES

D.M. Adams and R.R. Smardzewski, Inorg.Chem., 10, 1127 (1971)..137,170

H.E. Addison, Structural Principles of Inorganic Compounds, p. 62, Longmans (1961).....110

E. Ambler and H.H. Plumb, Rev.Sci.Instr., 31, 656 (1960)..... 37

C.G. Barraclough, R.L. Martin, and Mitra, J.Chem.Phys., 55, 1426 (1971).....213

Beilsteins Handbuch der organischen Chemie, 4. Auflage, Band II, p. 653, Springer, Berlin (1920).....107

B.D. Berezin, Russ.J.Phys.Chem., 39, 165 (1965).....206

K. Blacklock, H.F. Linebarger, H.W. White, K.H. Lee, and S. Holt, J.Chem.Phys., 61, 5279 (1974).....146 fn

B.S. Blaisse, A.H. Cooke, and R.A. Hull, Physica, 6, 231 (1939).... 55

P. Bloembergen and A.R. Miedema, Physica, 75, 205 (1974).....103, 163

C.J. Brown, J.Chem.Soc. (A), 2488 (1968).....207, 209, 218

A. Carrington and A.D. McLachlan, Introduction to Magnetic Resonance, p. 152, Harper International Edition, New York (1967).....215

E. Catalano and J.W. Stout, J.Chem.Phys., 23, 1284 (1955)..... 39

S.-S. Chang and E.F. Westrum, Jr, J.Chem.Phys., 36, 2420 (1962)....169

Chemical Rubber Company, Handbook of Chemistry and Physics, 55th edition, p. E-10 (1974)..... 44

Chemical Rubber Company, op. cit., p. B-146 (1974a)..... 82

R.C. Chisholm and J.W. Stout, J.Chem.Phys., 36, 972 (1962).....169

R.M. Clay, D.Phil. thesis, Oxford (1965).....19, 30, 32, 63, 187

R.M. Clay, C.E. Dyball, and L.A.K. Staveley, paper presented at the First International Conference on Calorimetry and Thermodynamics, Warsaw (1969).....163

J.H. Colwell, J.Chem.Phys., 51, 3820 (1969)..... 44

J.H. Colwell, B.W. Magnum, and D.B. Utton, Phys.Rev., 181, 842 (1969) 40

R.S. Craig, C.W. Massena, and R.N. Mallya, J.Appl.Phys., 36, 108 (1965)..... 54

W.J.M. de Jonge, C.H.W. Swüste, K. Kopinga, and K. Takeda, Phys. Rev. B, 12, 5858 (1975).....152, 153, 162, 166

T. de Neef, Phys.Rev.B, 13, 4141 (1976).....166

A.J. Dekker, Solid State Physics, pp. 44-45, Macmillan, London (1958)..... 6

A.J. Dekker, op. cit., pp. 488-490 (1958a).....159

R.E. Dietz, L.R. Walker, F.S.L. Hsu, W.H. Haemmerle, B. Vis, C.K. Chau, and H. Weinstock, Solid State Commun., 15, 1185 (1974) 151, 152, 154, 162, 171

R. Dingle, M.E. Lines, and S.L. Holt, Phys.Rev., 187, 643 (1969) 136, 159

C. Domb and A.R. Miedema, Progr.Low Temperature Phys., III, 296 (1964)..... 14

C. Domb and A.R. Miedema, ibid., at p. 324 (1964a).....159

C. Domb and A.R. Miedema, ibid., at p. 323 (1964b).....160

T.B. Douglas, G.T. Furakawa, R.E. McCoskey, and A.F. Ball, J.Res.Nat. Bur.Stand., 53, 141 (1954)..... 79

B. Dudreva and S. Grande, Ferroelectrics, 8, 407 (1974).....220

A.C. Dunn, Part II thesis, Oxford (1974).....142, 150

C.E. Dyball, Part II thesis, Oxford (1966).....30, 32

C.E. Dyball, op. cit., at p. 16 (1966a)..... 38

A.A. Ebert and H.O. Gottlieb, J.Amer.Chem.Soc., 74, 2806 (1952)....183

M.H. Edlow and H.H. Plumb, Adv.Cryogenic Eng., 6, 542 (1961)..... 29

B.N. Figgis, Introduction to Ligand Fields, p. 318, Interscience, New York (1966).....213

G.T. Furakawa, M.L. Reilly, and W.G. Saba, Rev.Sci.Instr., 35, 113 (1964)..... 40

M. Füstöss-Wégner, Thermochimica Acta, 23, 93 (1978).....220

R.E. Gerkin and K.S. Pitzer, J.Amer.Chem.Soc., 84, 2662 (1962).....125

D.H.J. Goodall, UKAEA Research Group, Culham, Nr Abingdon, Berks, unclassified document (approved for sale) CLM-R 47, September 1965 (C/7 IMG)..... 57

E.S.R. Gopal, Specific Heats at Low Temperatures, p. 158-161, Plenum, New York (1966).....5 fn, 6

E.S.R. Gopal, op. cit., pp. 87-93 (1966a).....162

L.V. Gregor and K.S. Pitzer, J.Amer.Chem.Soc., 84, 2664 (1962).....125

A.K. Gregson, R.L. Martin, and S. Mitra, J.Chem.Soc. Dalton, 1458 (1976).....214, 215

S.E. Harrison and J.M. Assour, J.Chem.Phys., 40, 365 (1964).....215

R.W. Hill in Experimental Cryophysics, edited by F.E. Hoare, L.C. Jackson, and N. Kurti, pp. 264-274 at p. 266, Butterworths (1961) 15

J.O. Hirschfelder, C.F. Curtiss, and R.B. Bird, Molecular Theory of Gases and Liquids, Wiley, New York (1954).....229

B.F. Hoskins, S.A. Mason, and J.C.B. White, Chem.Comm., 554 (1969) 207, 210

M.T. Hutchings, G. Shirane, R.J. Birgenau, and S.L. Holt, Phys.Rev.B, 5, 1999 (1972).....136, 157, 173

International Tables for X-Ray Crystallography, Vol. I, Symmetry Groups, p. 134, Kynoch Press, Birmingham, England (1952).....115

International Tables for X-Ray Crystallography, Vol. I, Symmetry Groups, p. 400, Kynoch Press, Birmingham, England (1952a).....222

International Tables for X-Ray Crystallography, Vol. III, Physical and Chemical Tables, Kynoch Press, Birmingham, England (1962)....223

E.W. Karasek and J.C. Decius, J.Amer.Chem.Soc., 74, 4716 (1952) 179, 182

W.R. Keller, Helium-3 and Helium-4, Plenum, New York, p. 112 (1969) 103

Y. Kinoshita, I. Matsubura, and Y. Saito, Bull.Chem.Soc. Japan, 32, 741 (1959)..... 84

Y. Kinoshita, I. Matsubura, and Y. Saito, Bull.Chem.Soc. Japan, 32, 1205 (1959a)..... 84

Y. Kinoshita, I. Matsubura, T. Higuchi, and Y. Saito, Bull.Chem.Soc. Japan, 32, 1221 (1959b).....84, 88, 89, 108, 115, 223

K. Kopinga, P. van der Leeden, and W.J.M. de Jonge, Phys.Rev.B, 14, 1519 (1976).....166

O. Kubaschewski, E.Ll. Evans, and C.B. Alcock, Metallurgical Thermochemistry, 4th edition, p. 382, Pergamon (1967)..... 12

J.E. Kunzler, T.H. Geballe, and G.W. Hill, Rev.Sci.Instr., 28, 96 (1957)..... 29

Landolt-Börnstein Zahlenwerte und Funktionen, 6. Auflage, II. Band, 4. Teil, 349-355, Springer, Berlin (1961).....107

B. Lassier, C. Brot, and J.W. White, Journal de Physique, 34, 473 (1973).....165, 170

K.E. Lawson, J.Chem.Phys., 47, 3627 (1967).....136

A.J. Leadbetter and K.E. Wycherley, J.Chem.Thermodyn., 2, 855 (1970) 54

S.H. Lee and C.A. Wulff, J.Chem.Thermodyn., 6, 85 (1974).....130

J.A. Lerbscher and C.A. Wulff, J.Chem.Thermodyn., 2, 717 (1970)....130

A.B.P. Lever, Adv.Inorg.Radiochem., 7, 27 (1965).....177

G.N. Lewis and M. Randall, Thermodynamics, revised by K.S. Pitzer and L. Brewer, 2nd edition, International Student Edition, pp. 438-443, McGraw-Hill (1965).....125, 133

G.N. Lewis and M. Randall, op. cit., eq. 27-42 at p. 430 (1965a) 165, 211

P. Lindenfeld in Temperature - Its Measurement and Control in Science and Industry, Vol. 3, Part 1, edited by C.M. Herzfeld, p. 399, Rheinhold (1962)..... 34

R.G. Linford, D.Phil. thesis, Oxford (1967).....18, 94

J.P. McCullough and D.W. Scott, editors, Experimental Thermodynamics, Vol. I, Calorimetry of Non-Reacting Systems, p. 264, Butterworths (1968)..... 39

J.P. McCullough and D.W. Scott, op. cit., p. 272 (1968a)..... 71

J.P. McCullough and D.W. Scott, op. cit., p. 268 (1968b)..... 83

B.W. Magnum and D.B. Utton, Phys.Rev.B, 6, 2790 (1972)...136, 160, 170

H. Malter, Physica Status Solidi B, 74, 627 (1976).....206

F.D. Manchester, Canad.J.Phys., 37, 989 (1959).....53, 54, 73

D.L. Martin, Proc.Roy.Soc., A263, 378 (1961)..... 73

R.L. Martin and S. Mitra, Inorg.Chem., 9, 182 (1970).....214, 215

R.G.S. Morfee, L.A.K Staveley, S.T. Walters, and D.L. Wigley, J.Phys. Chem. Solids, 13, 132, at p. 143 (1960).....113, 210 fn

H.H. Morgan, J.Chem.Soc., 2901 (1923)..... 84

B. Morosin and E.J. Graeber, Acta Cryst., 23, 766 (1967) 138, 139, 141, 155, 171

F.H. Moser and A.L. Thomas, Amer.Chem.Soc. Monograph No. 157, Phthalocyanine Compounds (1963).....177

K. Nagata and Y. Tazuke, J.Phys.Soc. Japan, 32, 337 (1972)....136, 138

D.M. Newns and L.A.K. Staveley, Chem.Rev., 66, 267 (1966) 118, 122, 132, 171, 218

D.E. Palin and H.M. Powell, J.Chem.Soc., 208 (1947).....223

P.S. Peercy, B. Morosin, and G.A. Samara, Phys.Rev.B, 8, 3378 (1973) .....155, 157, 165 fn, 170, 172

A.B. Pippard, Elements of Classical Thermodynamics, 2nd corrected reprint, pp. 136-140, Cambridge (1964)..... 12

H. Rath, H. Rehm, H. Rummler, and E. Specht, Melliand Textilberichte, 38, 431 (1957)..... 84

H. Rath, H. Rehm, H. Rummler, and E. Specht, Melliand Textilberichte, 38, 538 (1957a)..... 84

J.M. Robertson, J.Chem.Soc., 615 (1935).....206 fn, 210

J.M. Robertson, J.Chem.Soc., 1195 (1936).....207, 209, 210

J.M. Robertson and I. Woodward, J.Chem.Soc., 219 (1937).....207

H.M. Rosenberg, Low Temperature Solid State Physics, pp. 28-29, Oxford (1963)..... 10

H.M. Rosenberg, op. cit., pp. 23-27 (1963a).....214

H.M. Rosenberg, op. cit., pp. 307-309 (1963b).....217

R.S. Rusby, National Physical Laboratory Report (1971).....30, 32

G.S. Rushbrooke, Introduction to Statistical Mechanics, pp. 149-153, Oxford (1949)..... 11

E. Sanders and D.F. Windenberg, Trans.Amer.Soc.Mech.Eng., 53, 207 (1931)..... 59

H. Sato in Physical Chemistry, an Advanced Treatise, edited by H. Eyring, D. Henderson, and W. Jost, Vol. X, pp. 579 et seq., at pp. 587 to 591 (1970).....129

H. Sato, ibid., at pp. 711-713 (1970a).....130

A.M. Schaffer, M. Goutermann, and E.R. Davidson, Theor.Chim. Acta, 30, 9 (1973).....206, 215

F. Seitz, Modern Theory of Solids, p. 104, McGraw-Hill, New York and London (1940).....170

L.A.K. Staveley, J.Phys.Chem. Solids, 18, 46 (1961).....11, 134

L.A.K. Staveley, Técnica (Lisbon), 414, 173 at Section G (1972) .....217 fn

J.W. Stout and E. Catalano, J.Chem.Phys., 23, 2013 (1955).....165, 211

K. Takeda, Phys. Letters, 47A, 335 (1974).....151, 152, 232

H.N.V. Temperley, Changes of State, pp. 22-24, Cleaver-Hume, London (1956)..... 11

H. Thurn and H. Krebs, Acta Cryst.B, 25, 125 (1969).....110

B. Vis, C.K. Chau, H. Weinstock, and R.E. Dietz, Solid State Comm., 15, 1765 (1974).....146, 147, 151, 152, 233

E.J. Walker, Rev.Sci.Instr., 30, 834 (1959)..... 72

L.R. Walker, R.E. Dietz, K. Andres, and S. Darack, Solid State Comm., 11, 593 (1972).....160

E.D. West and D.C. Ginnings, J.Res.Nat.Bur.Stand., 60, 309 (1958).. 45

G.K. White, Experimental Techniques in Low-Temperature Physics, 2nd edition, p. 324, Oxford (1968)..... 45

J.R. Wiesner, R.C. Srivastava, C.H.L. Kennard, M. DiVaira, and E.C. Lingafelter, Acta Cryst., 23, 565 (1967).....141

R.D. Worswick, D.Phil. thesis, Oxford (1972).....18, 136

ABSTRACT

The thesis as a whole is concerned with disorder in inorganic crystalline solids as revealed by heat capacity "anomalies". Chapter 1 is a general discussion of the definition, quantitative analysis, and causes of heat capacity anomalies. Chapter 2 describes the construction of a new calorimeter for the determination of heat capacities of solids from 1.5 to 84 K. Chapters 3, 4, and 5 are concerned with heat capacity results obtained in this and other calorimeters on, respectively, bis(adiponitrile)copper(I) nitrate, tetramethylammonium trichloromanganate(II), and β-modification metal-free, copper(II), and nickel(II) phthalocyanines. In the first two cases, the approximate temperature range covered was 1.5 - 300 K, and in the case of the phthalocyanine compounds from rather under 5 K to 80 K. The abbreviation "TMMC" will be used below for tetramethylammonium trichloromanganate(II), and "Pc" for the divalent phthalocyanine group $C_{32}H_{16}N_8$.

* * * * *

The central assembly of the calorimetric cryostat comprised three demountable, concentric cylindrical chambers made of copper, the innermost of which served as a calorimetric shield. Thermal contact between adjacent pairs of chambers could be made and broken by, respectively, the admission of He^4 exchange gas into the intervening space and evacuation of that space. The outermost chamber was cooled in liquid He^4 or liquid N_2 refrigerant contained in a dewar. The temperature of the intermediate chamber could, if desired, be reduced by admitting refrigerant from the dewar, via a needle valve, into a 70 cm^3 pot attached to that chamber, and then pumping on the refrigerant in the pot. With N_2 refrigerant, temperatures of about 48 K could be thus generated; and with He^4 refrigerant, temperatures of 1.4 - 1.5 K.

The innermost chamber also had an electrical heater and a 5 cm^3 pumping pot for He^3 (though the latter was in fact never used).

The sample-containing vessel, of volume 25 cm^3, was suspended in the evacuated innermost chamber or shield by nylon thread. Thermal contact between the vessel and the shield could be made and broken by means of a mechanical thermal switch. The vessel carried a 1900 Ω Karma heater and a germanium resistance thermometer. Heat capacity determinations were made by the method of intermittent electrical heating. Above 20 K, adiabatic shield operation was preferred; for this, thermocouples on the shield and the vessel were provided. Below 20 K, isoperibolic shield operation was preferred, and for this a carbon resistance thermometer was provided on the shield.

* * * * *

The heat capacity of bis(adiponitrile)copper(I) nitrate appeared to be somewhat anomalous below 2.5 K, but it is quite possible that the anomaly reflected only the adsorption of the He^3 exchange gas used within the vessel. The heat capacity was apparently anomalous in the 252 - 285 K region, but this anomaly was small enough to be reasonably accounted for by the presence of a small amount of occluded mother liquor in the crystals.

The heat capacity also had not-very-pronounced heat capacity maxima near 51 and 63 K. An anomalous entropy gain of between 1/2 R ln 2 and R ln 2 over the 37 - 70 K range was estimated. A reasonable (though not unique) explanation of this is that at low temperatures the nitrate ions are ordered while, at 70 K and somewhat above, the nitrate ions are disordered among <u>two</u> positions for each ion. It is pointed out, however, that a further change towards rotation of the ions might occur between 70 and 300 K without any immediately evident effect on the heat capacity.

The X-ray diffraction results of Kinoshita et al[1] had already indicated that the nitrate ions were not ordered at room temperature; but it is shown (by consideration of structure factors and the potential field on the nitrate ions) that their particular scheme for disordering of the nitrate ions at room temperature (which scheme specifies <u>four</u>fold orientational disordering) is of doubtful reliability.

There is presented, in outline, a theoretical treatment of the presumed order-disorder transition. The nitrate ions lie in parallel infinite linear chains, and the distance between a nitrate ion and either of its two near neighbours in a chain is considerably smaller than the distance between the ion and its nearest neighbours in other chains. It is probable that cooperative nitrate - nitrate interactions are predominantly electrostatic in origin, and it is likely that they are much stronger within the chains than between the chains.

* * * * *

The results obtained on TMMC agree reasonably well with those subsequently reported over various temperature ranges by Dietz et al[2], Vis et al[3], and de Jonge et al[4]. Below 4 K, these workers and the present author obtained results disagreeing with those of Takeda[5], whose reported heat capacities seem to be too high.

The advanced theoretical treatment by de Jonge et al of the vibrational and magnetic contributions to the heat capacity below 50 K is shown to be consistent with simpler theory based on direct comparisons of the heat capacity with heat capacities of other compounds. The theoretical treatment by Dietz et al of the vibrational and magnetic contributions to the heat capacity below 4 K is shown to be inconsis-

---

1. Y. Kinoshita, I. Matsubura, T. Higuchi, and Y. Saito, Bull. Chem. Soc. Japan, <u>32</u>, 1221 (1959).
2. R.E. Dietz, L.R. Walker, F.S.U. Hsu, W.H. Haemmerle, B. Vis, C.K. Chau, and H. Weinstock, Solid State Commun., <u>15</u>, 1185 (1974).
3. B. Vis, C.K. Chau, H. Weinstock, and R.E. Dietz, <u>ibid.</u>, 1765.
4. W.J.M. de Jonge, C.H.W. Swüste, K. Kopinga, and K. Takeda, Phys. Rev. B, <u>12</u>, 5858 (1975).
5. K. Takeda, Phys. Letters, <u>47A</u>, 335 (1974).

tent with simple theory, as it is with that of de Jonge et al.

Appropriate treatment of the heat capacity results reveals the development of the magnetic entropy gain of R ln 6 expected for a change from an ordered antiferromagnetic system of Mn^{2+} ions (S = 5/2) to a paramagnetic state. Well over 95% of this entropy gain arises above T_N (0.84 K), the rate of development of magnetic entropy being a maximum rather below 20 K. This behaviour reflects the persistence of short-range 1-d order for tens of kelvins above T_N, T_N being the temperature at which long-range 3-d order breaks down. Such persistence of 1-d order had already been indicated by other techniques, especially magnetic susceptibility measurements[6, 7, 8]; it is ascribed to strong coupling of the Mn^{2+} ions by superexchange within infinite parallel linear $[n \cdot MnCl_3]^{n-}$ chains in the crystal and very weak coupling between the chains. In this respect TMMC is of outstanding theoretical interest; at least at the date of reference 6, TMMC was reputedly "the closest physical approximation...to a linear-chain quasi-Heisenberg antiferromagnet".

The anomalous entropy change associated with the monoclinic - hexagonal transition at 126 K is estimated as R ln 2.8, of which about 1/3 occurs between 124 and 127 K. X-ray diffraction [9, 10] had already shown that the transition involved disordering of the Me_4N^+ ions, although the precise disordered structure was somewhat unclear. It is suggested that the anomalous entropy gain can be explained if the NC_4 tetrahedra become twofold disordered and the H atoms also undergo some disordering.

* * * * *

It appears that β-PcCu has two first-order phase transitions with

6. R. Dingle, M.E. Lines, and S.L. Holt, Phys.Rev., 187, 643 (1969).
7. L.R. Walker, R.E. Dietz, K. Andres, and S. Darack, Solid State Comm., 11, 593 (1972).
8. B.W. Magnum and D.B. Utton, Phys. Rev. B, 6, 2790 (1972).
9. B. Morosin and E.J. Graeber, Acta Cryst., 23, 766 (1967).
10. P.S. Peercy, B. Morosin, and G.A. Samara, Phys.Rev. B, 8, 3378 (1973).

equilibrium transition temperatures at about 9 - 13 K. The observation of these transitions is made difficult by marked supercooling and superheating. The total entropy change in the two transitions is estimated as not less than approximately R ln 4.

At any temperature where β-PcCu and β-PcNi are approximately isostructural (as they are known to be at room temperature[11, 12]), theory predicts that there should be very similar vibrational contributions to their heat capacities. Below 25 K the heat capacity of β-PcNi is in fact markedly higher than that of β-PcCu (the latent heats in the latter apart); this suggests that in this temperature range (i) β-PcNi is not isostructural with either the high- or the low-temperature form of β-PcCu and/or (ii) there is a non-vibrational contribution to its heat capacity. This view is supported by the fact that below 8 K the heat capacities of β-PcCu and β-PcH_2 (which are approximately isostructural at room temperature[11, 13]) appear to obey the Debye T^3 law, which is the low-temperature limiting behaviour for a purely vibrational heat capacity, whereas that of β-PcNi does not.

A survey of evidence from other techniques shows that neither Schottky nor magnetic anomalies are likely to contribute to the heat capacities in any of the three phthalocyanine materials. It is suggested that perhaps the transitions in β-PcCu involve disordering of the Cu^{2+} ions among four positions in the plane of each molecule. However, this suggestion is speculative, and a reasonably certain theoretical account of the heat capacity results described here will probably not be possible until further work (both calorimetric and crystallographic) is performed; precise suggestions regarding such further work are made.

---

11. C.J. Brown, J.Chem.Soc. (A), 2488 (1968).
12. J.M. Robertson and I. Woodward, J.Chem.Soc., 219 (1937).
13. B.F. Hoskins, S.A. Mason, and J.C.B. White, Chem.Comm., 554 (1969).

ASLIB ABSTRACT

Title: Thermodynamic Studies of Disorder in Inorganic Crystalline Solids
Candidate: Michael Jewess of New College, Oxford
Degree for which thesis submitted: Doctor of Philosophy
Term of submission: Michaelmas 1978

A calorimeter was constructed for the determination of heat capacities of solids from 1.5 to 84 K. Results from this and other calorimeters are discussed, on bis(adiponitrile)copper(I) nitrate and tetramethylammonium trichloromanganate(II) ("TMMC") from 1.5 to 300 K, and on β-modification metal-free, copper(II), and nickel(II) phthalocyanines from under 5 to 80 K.

Bis(adiponitrile)copper(I) nitrate has not-very-pronounced heat capacity maxima at 51 and 63 K. The total molar anomalous entropy change is estimated as between 1/2 Rln2 and Rln2. A previous assertion by X-ray crystallographers (Bull.Chem.Soc. Japan, 32, 1221 (1959)) that the nitrate ions are disordered among four orientations at room temperature is not supported by these results or by consideration of structure factors or of the potential field on the nitrate ions.

The TMMC heat capacity results are consistent with those given in Solid State Comm., 15, 1185 (1974) and Phys.Rev. B, 12, 5858 (1975). The anomalous molar entropy change associated with the monoclinic - hexagonal transition at 126 K is estimated as Rln2.8, of which 1/3 occurs between 124 and 127 K; it is suggested that the NC_4 tetrahedra undergo twofold disordering and that the H atoms also undergo some disordering.

The heat capacities of the copper and nickel phthalocyanines are surprisingly different from each other, especially below 25 K, where the former is markedly lower except for two first-order transitions at about 9 - 13 K with a total molar entropy change of not less than approximately Rln4. Magnetic and Schottky anomalies are, apparently, not involved in either material; perhaps the transitions in copper phthalocyanine involve disordering of the copper ions among four positions in the plane of each molecule. Below 8 K, the heat capacities of copper and metal-free (but not nickel) phthalocyanine apparently obey the T^3 law.